Generalized Fluid System Simulation Program, Version 5.0—Educational

A.K. Majumdar
Marshall Space Flight Center, Huntsville, Alabama

The NASA STI Program…in Profile

Since its founding, NASA has been dedicated to the advancement of aeronautics and space science. The NASA Scientific and Technical Information (STI) Program Office plays a key part in helping NASA maintain this important role.

The NASA STI Program Office is operated by Langley Research Center, the lead center for NASA's scientific and technical information. The NASA STI Program Office provides access to the NASA STI Database, the largest collection of aeronautical and space science STI in the world. The Program Office is also NASA's institutional mechanism for disseminating the results of its research and development activities. These results are published by NASA in the NASA STI Report Series, which includes the following report types:

- TECHNICAL PUBLICATION. Reports of completed research or a major significant phase of research that present the results of NASA programs and include extensive data or theoretical analysis. Includes compilations of significant scientific and technical data and information deemed to be of continuing reference value. NASA's counterpart of peer-reviewed formal professional papers but has less stringent limitations on manuscript length and extent of graphic presentations.

- TECHNICAL MEMORANDUM. Scientific and technical findings that are preliminary or of specialized interest, e.g., quick release reports, working papers, and bibliographies that contain minimal annotation. Does not contain extensive analysis.

- CONTRACTOR REPORT. Scientific and technical findings by NASA-sponsored contractors and grantees.

- CONFERENCE PUBLICATION. Collected papers from scientific and technical conferences, symposia, seminars, or other meetings sponsored or cosponsored by NASA.

- SPECIAL PUBLICATION. Scientific, technical, or historical information from NASA programs, projects, and mission, often concerned with subjects having substantial public interest.

- TECHNICAL TRANSLATION. English-language translations of foreign scientific and technical material pertinent to NASA's mission.

Specialized services that complement the STI Program Office's diverse offerings include creating custom thesauri, building customized databases, organizing and publishing research results…even providing videos.

For more information about the NASA STI Program Office, see the following:

- Access the NASA STI program home page at <http://www.sti.nasa.gov>

- E-mail your question via the Internet to <help@sti.nasa.gov>

- Fax your question to the NASA STI Help Desk at 443–757–5803

- Phone the NASA STI Help Desk at 443–757–5802

- Write to:
  NASA STI Help Desk
  NASA Center for AeroSpace Information
  7115 Standard Drive
  Hanover, MD 21076–1320
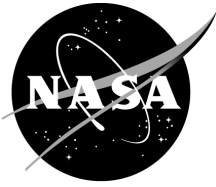
Generalized Fluid System Simulation Program, Version 5.0—Educational

A.K. Majumdar
Marshall Space Flight Center, Huntsville, Alabama

National Aeronautics and
Space Administration

Marshall Space Flight Center • Huntsville, Alabama 35812

Acknowledgments

Available from:

NASA Center for AeroSpace Information
7115 Standard Drive
Hanover, MD 21076–1320
443–757–5802

This report is also available in electronic form at
<https://www2.sti.nasa.gov/login/wt/>

PREFACE

The motivation to develop a general purpose computer program to compute pressure and flow distribution in a complex fluid network came from the need to calculate the axial load on the bearings in a turbopump. During the early years of space shuttle main engine development, several specific purpose codes were developed to model the turbopumps. However, it was difficult to use those codes for a new design without making extensive changes in the original code. Such efforts often turn out to be time consuming and inefficient. To satisfy the need to model these turbopumps in an efficient and timely manner, development of the Generalized Fluid System Simulation Program (GFSSP) was started at NASA Marshall Space Flight Center (MSFC) in March 1994. The objective was to develop a general fluid flow system solver capable of handling phase change, compressibility, and mixture thermodynamics. Emphasis was given to construct a user-friendly program using a modular structured code. The intent of this effort was that an engineer with an undergraduate background in fluid mechanics and thermodynamics should be able to rapidly develop a reliable model. The interest in modular code development was intended to facilitate future modifications to the program.

The code development was carried out in several phases. At the end of each phase, a workshop was held where the latest version of the code was released to MSFC engineers for testing, verification, and feedback. The steady state version of GFSSP (version 1.4) was first released in October 1996. This version is also commercially available through the Open Channel Foundation. The unsteady version was released in October 1997 (version 2.0). A graphical user interface (GUI) for GFSSP was developed and was part of Version 3.0 that was released in November 1999. GFSSP (version 3.0) won the NASA Software of the Year award in 2001. Fluid transient (water hammer) capability was added in version 4.0 that was released in March 2003. The main highlight of this version (version 5.0) is its capability to handle conjugate heat transfer.

This Technical Memorandum (TM) provides a detailed discussion of the mathematical formulation, computer program, GUI, and includes a number of example problems. Section 1 provides an introduction and overview of the code. The mathematical formulation, which includes the description of governing equations and the solution procedure to solve these equations, is described in section 2. The program structure is discussed in section 3. Section 4 describes GFSSP's GUI, which is called VTASC (visual thermofluid dynamic analyzer for systems and components). Several example problems are described in section 5. The new user may skip sections 2 and 3 initially, but will benefit from these sections after gaining some experience with the code.

This TM has been prepared for the educational version of GFSSP for distribution to accredited United States universities who have signed an agreement with MSFC for use in their educational curriculum. This version has been limited to developing models using only 30 or fewer nodes without any provision of user subroutines.

TABLE OF CONTENTS

TABLE OF CONTENTS (Continued)

TABLE OF CONTENTS (Continued)

TABLE OF CONTENTS (Continued)

LIST OF FIGURES

LIST OF FIGURES (Continued)

LIST OF TABLES

LIST OF ACRONYMS

CFD	computational fluid dynamics
FVM	finite volume method
GFSSP	Generalized Fluid System Simulation Program
GUI	graphical user interface
LOX	liquid oxygen
MOC	method of characteristics
MSFC	Marshall Space Flight Center
SASS	simultaneous adjustment with successive substitution
SIMPLE	semi-implicit pressure linked equation
SP	solver and property
TM	Technical Memorandum
TPA	turbopump assembly
US	user subroutine
VTASC	visual thermofluid dynamic analyzer for systems and components

NOMENCLATURE

A	area (in^2)
A_0	pump characteristic curve coefficient
a	length (in)
B_0	pump characteristic curve coefficient
b	length (in)
C	heat capacity (Btu/s-°R)
C_c	convergence criterion
C_L	flow coefficient
C_p	specific heat (Btu/lb °F)
C_v	flow coefficient for a valve
c	clearance (in)
$c_{i,k}$	mass concentration of kth specie at ith node
D	diameter (in)
f	Darcy friction factor
G	bound mass (lb/ft^2-s)
g	gravitational acceleration (ft/s^2); specific heat ratio
g_c	conversion constant (= 32.174 lb-ft/lb$_f$-s^2)
h	enthalpy (Btu/lb)
h_{ij}	heat transfer coefficient (Btu/ft^2-s-°R)
J	mechanical equivalent of heat (778 ft-lb$_f$/Btu)
K, K_1	nondimensional head loss factor
K_e	exit loss coefficient
K_f	flow resistance coefficient (lb$_f$-s^2/(lb-ft)^2)
K_{rot}	nondimensional rotating flow resistance coefficient

K_i	inlet loss coefficient
k	thermal conductivity (Btu/ft-s-°R)
k_v	empirical factor
L	length (in)
L_Ω	resistance of the Joule-Thompson device
M	molecular weight
m	resident mass (lb)
$\dot{m}$	mass flow rate (lb/s)
m_p	pitch (in)
N	revolutions per minute (rpm); number of iterations
N_B	number of branches
N_E	number of equations
N_N	number of nodes
Nu	Nusselt number
n	number of teeth
P	pump power (hp)
Po	Poiseuille number
Pr	Prandtl number
p	pressure (lb_f /in^2)
$Q, \dot{q}$	heat source (Btu/s)
R	gas constant (lb_f-ft/lb-°R)
Re	Reynolds number (Re = $\rho u D / m$)
r	radius (in)
S	momentum source (lb_f)
$\dot{S}$	entropy generation (Btu/s-°R)
s	entropy (Btu/lb-°R)

NOMENCLATURE (Continued)

T	fluid temperature (°F)
T_s	solid temperature (°F)
u	velocity (ft/s)
V	volume (in^3)
V_f	viscosity correction factor
v	specific volume (ft^3/lb)
w	Joule-Thomson device flow rate (lbm/hr)
x	quality and mass fraction
x_k	molar concentrations
z	compressibility factor

Greek

α	multiplier for Labyrinth seal resistance; under-relaxation parameter
β	ratio of orifice diameter to inside pipe diameter
γ	specific heat
Δh	head loss (ft)
$\Delta \tau$	time step (s)
δ	distances between velocity locations (ft)
δ_{ij}	distance between two solid nodes (ft)
ε	absolute roughness (in), heat exchanger effectiveness, Labyrinth seal carryover factor
ε/D	relative roughness
ε_{ij}	emissivity
θ	angle between branch flow velocity vector and gravity vector (deg); angle between neighboring branches for computing shear (deg)
θ_r	time required to drain pressurized propellant tank (s)

η	efficiency
μ	viscosity (lb/ft-s)
ν	kinematic viscosity (ft^2/s)
ρ	density (lb/ft^3)
$\bar{\rho}$	molar density (lb-mol/ft^3)
σ	Stefan-Boltzman constant (= 4.7611×10^{-13} Btu/ft^2-R^4-s)
τ	time (s)
ω	angular velocity (rad/s)

Subscript

amb	ambient
B	back
c	cold
cr	critical
Dis	discharge
eff	effective
F	front
f	liquid
g	vapor
gen	generation
h	hot
Im	impeller
i	node; inner
ij	branch

NOMENCLATURE (Continued)

o	outer
or	orifice
rot	rotational
S	solid
s	entropy
trans	transverse
Turb	turbine
u	upstream branch

TECHNICAL MEMORANDUM

GENERALIZED FLUID SYSTEM SIMULATION PROGRAM,
VERSION 5.0—EDUCATIONAL

1. INTRODUCTION

The need for a generalized computer program for thermofluid analysis in a flow network has been felt for a long time in Aerospace Industries. Designers of thermofluid systems often need to know pressures, temperatures, flow rates, concentrations, and heat transfer rates at different parts of a flow circuit for steady state or transient conditions. Such applications occur in propulsion systems for tank pressurization, internal flow analysis of rocket engine turbopumps, chilldown of cryogenic tanks and transfer lines, and many other applications of gas-liquid systems involving fluid transients and conjugate heat and mass transfer. Computer resource requirements to perform time-dependent, three-dimensional Navier-Stokes computational fluid dynamic (CFD) analysis of such systems are prohibitive and therefore are not practical. A possible recourse is to construct a fluid network consisting of a group of flow branches such as pipes and ducts that are joined together at a number of nodes. They can range from simple systems consisting of a few nodes and branches to very complex networks containing many flow branches simulating valves, orifices, bends, pumps, and turbines. In the analysis of existing or proposed networks, node pressures, temperatures, and concentrations at the system boundaries are usually known. The problem is to determine all internal nodal pressures, temperatures, concentrations, and branch flow rates. Such schemes are known as Network Flow Analysis methods and they use mostly empirical information to model fluid friction and heat transfer. For example, an accurate prediction of axial thrust in a liquid rocket engine turbopump requires the modeling of fluid flow in a very complex network. Such a network involves the flow of cryogenic fluid through extremely narrow passages, flow between rotating and stationary surfaces, phase changes, mixing of fluids, and heat transfer. Propellant feed system designers are often required to analyze pressurization or blowdown processes in flow circuits consisting of many series and parallel flow branches containing various pipe fittings and valves using cryogenic fluids. The designers of a fluid system are also required to know the maximum pressure in the pipeline after sudden valve closure or opening.

Available commercial codes are generally suitable for steady state, single-phase, incompressible flow. Because of the proprietary nature of such codes, it is not possible to extend their capability to satisfy the above-mentioned needs. In the past, specific purpose codes were developed to model the space shuttle main engine (SSME) turbopump. However, it was difficult to use those codes for a new design without making extensive changes in the original code. Such efforts often turn out to be time consuming and inefficient. Therefore, the Generalized Fluid System Simulation Program (GFSSP)[1] has been developed at NASA Marshall Space Flight Center (MSFC) as a general fluid flow system solver capable of handling phase changes, compressibility, mixture thermodynamics, and transient operations. It also includes the capability to model external body forces such as gravity and centrifugal effects in a complex flow network. The objective of the present effort

is to develop (1) a robust and efficient numerical algorithm to solve a system of equations describing a flow network containing phase changes, mixing, and rotation and (2) to implement the algorithm in a structured, easy-to-use computer program.

This program requires that the flow network be resolved into nodes and branches. The program's preprocessor allows the user to interactively develop a fluid network simulation consisting of fluid nodes and branches, solid nodes, and conductors. In each branch, the momentum equation is solved to obtain the flow rate in that branch. At each fluid node, the conservation of mass, energy, and species equations are solved to obtain the pressures, temperatures, and species concentrations at that node. At each solid node, the energy conservation equation is solved to calculate temperature of the solid.

This Technical Memorandum (TM) documents the mathematical formulation, computer program, and graphical user interface (GUI). Use of the code is illustrated by 12 example problems. It also documents the verification and validation effort conducted by code developers and users. This section also presents an overview of the subsequent sections to provide users with a global perspective of the code.

1.1 Network Flow Analysis Methods

The oldest method for systematically solving a problem consisting of steady flow in a pipe network is the Hardy Cross method.[2] Not only is this method suited for hand calculations, but it has also been widely employed for use in computer-generated solutions. But as computers allowed much larger networks to be analyzed, it became apparent that the convergence of the Hardy Cross method might be very slow or even fail to provide a solution in some cases. The main reason for this numerical difficulty is that the Hardy Cross method does not solve the system of equations simultaneously. It considers a portion of the flow network to determine the continuity and momentum errors. The head loss and the flow rates are corrected and then it proceeds to an adjacent portion of the circuit. This process is continued until the whole circuit is completed. This sequence of operations is repeated until the continuity and momentum errors are minimized. It is evident that the Hardy Cross method belongs in the category of successive substitution methods and it is likely that it may encounter convergence difficulties for large circuits. In later years, the Newton-Raphson method has been utilized to solve large networks.[3] The Newton-Raphson method solves all the governing equations simultaneously and is numerically more stable and reliable than successive substitution methods.

The network analysis method[4] has been widely used in thermal analysis codes (SINDA/G[5] and SINDA/FLUINT[6]) using an electric analog. The partial differential equation of heat conduction is discretized into finite difference form expressing temperature of a node in terms of temperatures of neighboring nodes and ambient nodes. The set of finite difference equations is solved to calculate temperature of the solid nodes and heat fluxes between the nodes. There have been some limited applications of thermal network analysis methods to model fluid flows. Such attempts did not go far because of the inability of heat conduction equations to handle the nonlinear fluid inertia term. There has been limited success in modeling compressible and two-phase flows by such methods.

At MSFC, another system analysis code, ROCETS, is routinely used for simulating flow in rocket engines.[7] ROCETS has a very flexible architecture where users develop the system model by integrating component modules such as pumps, turbines, and valves. The user can also build any model of specific components to integrate into the system model. ROCETS solves the system of equation by a modified Newton-Raphson method.[8]

The finite volume method (FVM) has been widely used in solving Navier-Stokes equations in CFD.[9] The FVM divides the flow domain into a discrete number of control volumes and determines the conservation equations for mass, momentum, energy, and species for each control volume. Simultaneous solutions of these conservation equations provide the pressure, velocity components, temperature, and concentrations representative of the discrete control volumes. The numerical method is called 'pressure based' if the pressures are calculated from the mass conservation equation and density from the equation of state. On the other hand, a 'density based' numerical method uses mass conservation equation to calculate density of the fluid and pressure from the equation of state. GFSSP uses a pressure-based FVM as the foundation of its numerical scheme.

1.1.1 Network Definitions

GFSSP constructs a fluid network using fluid and solid nodes. The fluid circuit is constructed with boundary nodes, internal nodes, and branches (fig. 1) while the solid circuit is constructed with solid nodes, ambient nodes, and conductors. The solid and fluid nodes are connected with solid-fluid conductors. Users must specify conditions such as pressure, temperature, and concentration of species at the boundary nodes. These variables are calculated at the internal nodes by solving conservation equations of mass, energy, and species in conjunction with the thermodynamic equation of state. Each internal node is a control volume where there is inflow and outflow of mass, energy, and species at the boundaries of the control volume. The internal node also has resident mass, energy, and concentration. The momentum conservation equation is expressed in flow rates and is solved in branches. At the solid node, the energy conservation equation for solid is solved to compute temperature of the solid node. Figure 1 shows a schematic and GFSSP flow circuit of a counterflow heat exchanger. Hot nitrogen gas is flowing through a pipe, colder nitrogen is flowing counter to the hot stream in the annulus pipe, and heat transfer occurs through metal tubes. The problem considered is to calculate flow rates and temperature distributions in both streams.

1.2 Units and Sign Conventions

GFSSP uses British gravitational units (commonly known as engineering units). Table 1 describes the units of variables used in the code. The units in the second column are the units that appear in the input and output data files. Users must specify the values in these units in their model. The units that are listed in the third column are internal to the code and used during the solution of the equations. GFSSP uses standard sign conventions for mass and heat transfer. Mass and heat input to a node is considered positive. Similarly, mass and heat output from a node is considered negative.
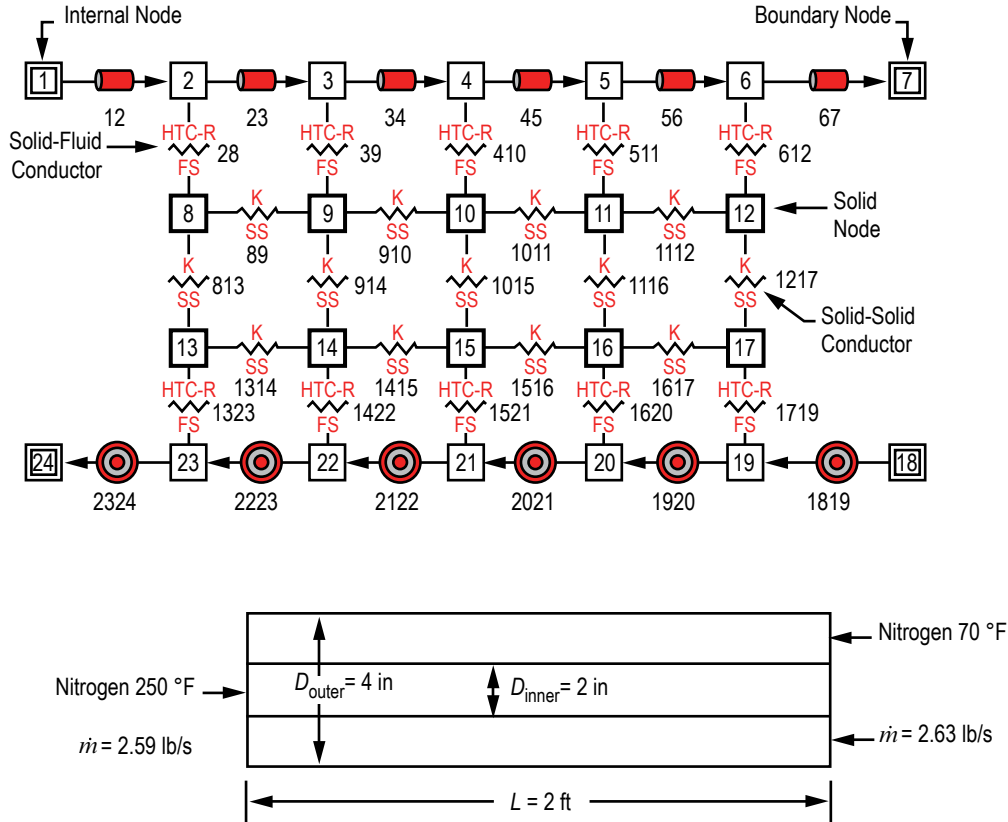
Figure 1. A typical flow network consists of fluid node, solid node, flow branches, and conductors.

Table 1. Units of variables in input/output and solver module.

Variables	Input/Output	Solver Module
Length	inches	feet
Area	inches^2	feet^2
Pressure	psia	psf
Temperature	°F	R
Mass injection	lbm/s	lbm/s
Heat source	Btu/s or Btu/lbm	Btu/s or Btu/lbm

1.3 Data Structure

GFSSP has a unique data structure (fig. 2) that allows constructing all possible arrangements of a flow network with no limit on the number of elements. The elements of a flow network are boundary nodes, internal nodes, and branches. For conjugate heat transfer problems, there are three additional elements—solid node, ambient node, and conductor. The relationship between a fluid node and a branch as well as a solid node and conductor is defined by a set of relational geometric properties. For example, the relational geometric properties of a node are number and name of branches connected to it. With the help of these properties, it is possible to define any
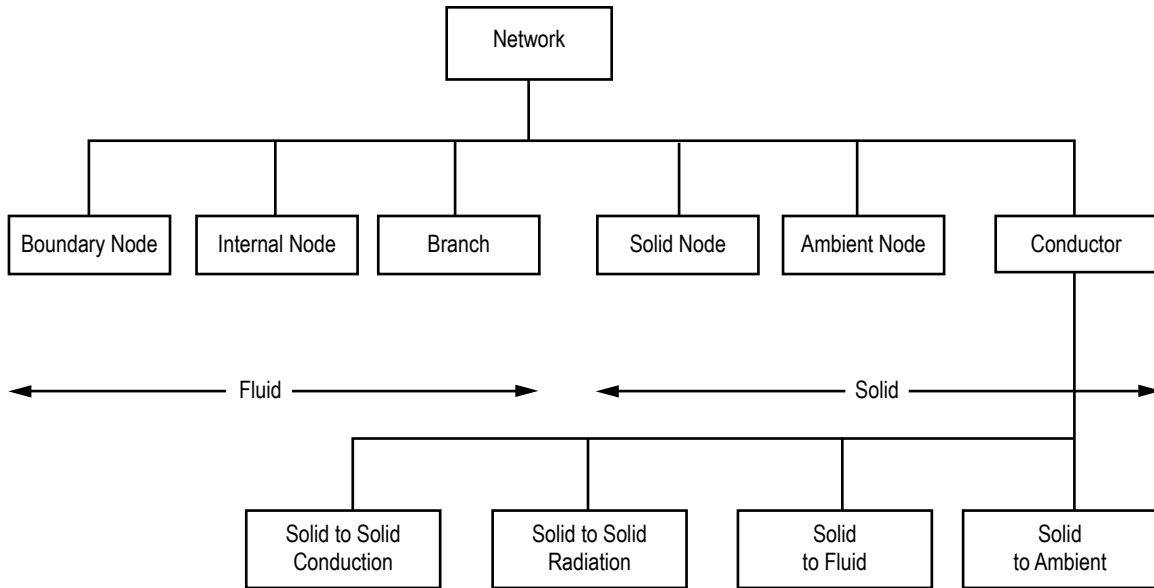
Figure 2. Data structure of the fluid-solid network has six major elements.

structure of the network as it progresses through every junction of the network. The positive or negative flow direction is also defined locally. Unlike the structured coordinate system, there is no global definition of flow direction and origin. The development of a flow network can start from any point and can proceed in any direction.

All elements of a network have properties. The properties can be classified into two categories—geometric and thermofluid. Geometric properties are again classified into two subcategories—relational and quantitative. Relational properties define the relationship of the element with the neighboring elements. Quantitative properties include geometric parameters such as area, length, and volume.

1.4 Mathematical Formulation

GFSSP solves the conservation equations of mass and momentum in internal nodes and branches to calculate fluid properties. It also solves for energy conservation equations to calculate temperatures of solid nodes. Table 2 shows the mathematical closure that describes the unknown variables and the available equations to solve the variables. Pressure, temperature, specie concentration, and resident mass in a control volume are calculated at the internal nodes, whereas the flow rate is calculated at the branch. The equations are coupled and nonlinear; therefore, they are solved by an iterative numerical scheme. GFSSP employs a unique numerical scheme known as simultaneous adjustment with successive substitution (SASS), which is a combination of Newton-Raphson and successive substitution methods. The coupling of equations is shown in figure 3. The mass and momentum conservation equations and the equation of state are solved by the Newton-Raphson method while the conservation of energy and species are solved by the successive substitution method.

Table 2. Mathematical closure.

Unknown Variables	Available Equations to Solve
Pressure	Mass conservation equation
Flow rate	Momentum conservation equation
Fluid temperature	Energy conservation equation of fluid
Solid temperature	Energy conservation equation of solid
Specie concentrations	Conservation equations for species
Fluid mass (unsteady flow)	Thermodynamic equation of state
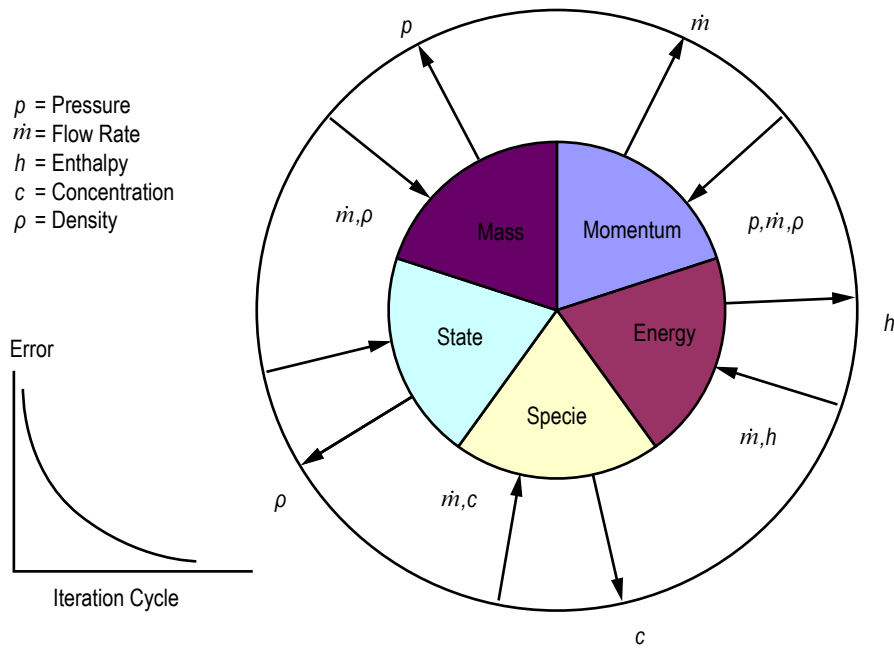
Figure 3. Schematic of mathematical closure of GFSSP.

The total number of equations to be solved is determined from the number of internal nodes and branches. Figure 4 shows a typical interpropellant flow circuit in a rocket engine turbopump. In this circuit there are five boundary nodes and seven internal nodes. These nodes are connected by 12 branches. There are three inlet boundary nodes (48, 66, and 22) where oxygen, helium, and hydrogen enter into the fluid circuit. Mixtures of helium-hydrogen and helium-oxygen exit the circuit through boundary nodes numbered 50 and 16, respectively. At each internal node, four equations are solved to calculate pressure, temperature, and two concentrations. It should be noted that in a mixture of three components, concentrations of two components are solved. The concentration of the third component is determined from the fact that the sum of all concentrations must be unity. Flow rates are calculated in 12 branches. Therefore, GFSSP solves for 40 ($=7\times4+12$) equations to calculate all required variables in the circuit. Since the example problem is at steady state, resident mass in the control volume was not calculated. The transient model of the same fluid circuit would require solution of 47 ($=7\times5+12$) equations at each time step of the simulation. The mathematical formulation has been described in detail in section 2.
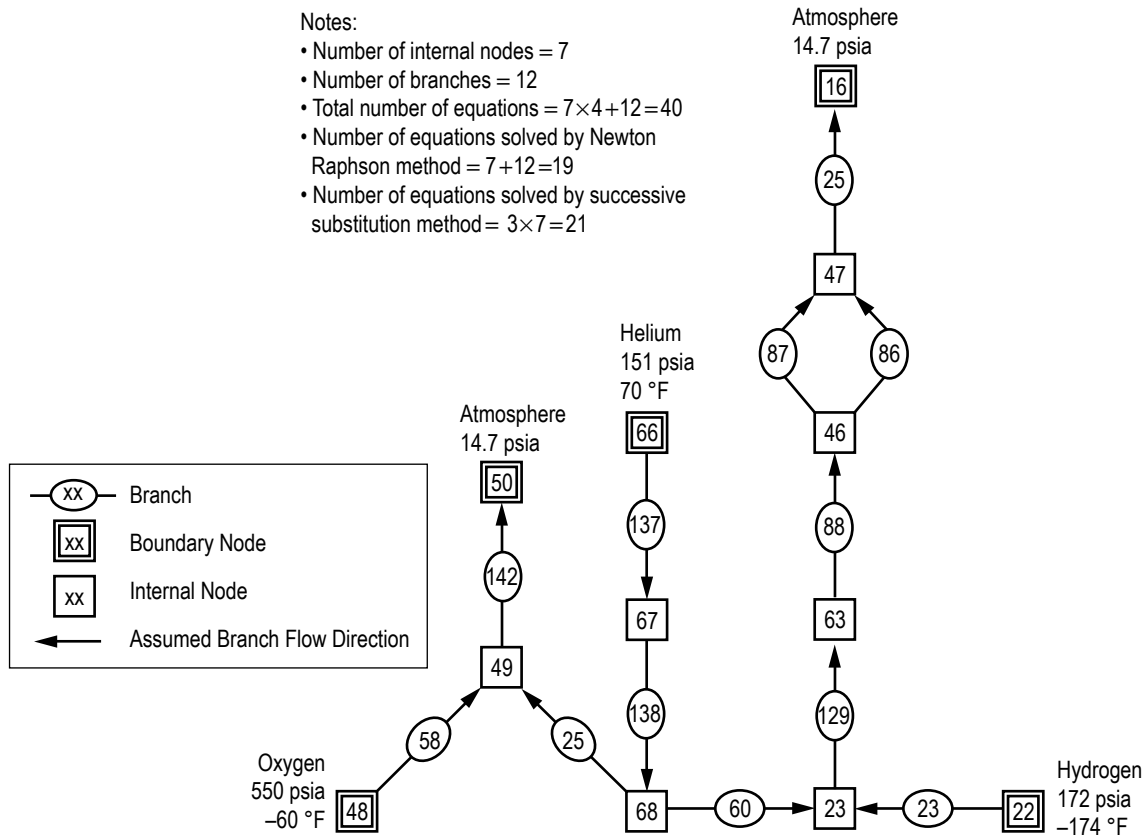
Figure 4. Interpropellant seal flow circuit in a rocket engine turbopump.

1.5 Fluid Properties

GFSSP is linked with two thermodynamic property programs, GASP[10] and WASP[11] and GASPAK,[12] that provide thermodynamic and thermophysical properties of selected fluids. Both programs cover a range of pressure and temperature that allow fluid properties to be evaluated for liquid, liquid-vapor (saturation), and vapor region. GASP and WASP provide properties of 12 fluids (table 3). GASPAK includes a library of 35 fluids (table 4).

Table 3. Fluids available in GASP and WASP.

Index	Fluid
1	Helium
2	Methane
3	Neon
4	Nitrogen
5	Carbon Monoxide
6	Oxygen
7	Argon
8	Carbon Dioxide
9	Fluoride
10	Hydrogen
11	Water
12	RP-1

Table 4. Fluids available in GASPAK.

Index	Fluid	Index	Fluid
1	Helium	19	Krypton
2	Methane	20	Propane
3	Neon	21	Xenon
4	Nitrogen	22	R-1
5	Carbon Monoxide	23	R1
6	Oxygen	24	R2
7	Argon	25	R3
8	Carbon Dioxide	26	R12
9	Parahydrogen	27	R12
10	Hydrogen	28	R12
11	Water	29	R134
12	R-1	30	R152
13	ISO Utane	31	Nitrogen
14	Butane	32	Ammonia
15	Deuterium	33	Ideal
16	Ethane	34	Hydrogen Peroxide
17	Ethylene	35	Air
18	Hydrogen Sulfide		

1.6 Flow Resistances

In network flow analysis code, flow resistances are modeled by empirical laws. These empirical laws have been incorporated to model flow resistances for pipe flow, orifices, valves, and various pipe fittings. GFSSP models these flow resistances in the momentum conservation equation as friction term. There are 20 different resistance options available to users to choose from. There is also a provision for introducing new resistance options through user subroutines. The available resistance options are shown in table 5.

Table 5. Resistance options in GFSSP.

Option	Type of Resistance	Input Parameters	Option	Type of Resistance	Input Parameters
1	Pipe flow	L (in), D (in), ε/D	12	Flow between parallel plates	r_i (in), c (in), L (in)
2	Flow through restriction	C_L, A (in^2)	13	Common fittings and valves (two K method)	D (in), K_1, K_2
3	Non-circular duct	a (in), b (in)	14	Pump characteristics*	A_0, B_0, A (in^2)
4	Pipe with entrance and exit loss	L (in), D (in), ε/D, K_i, K_e	15	Pump power	P (hp), η, A (in^2)
5	Thin, sharp orifice	D_1 (in), D_2 (in)	16	Valve with given C_v	C_v, A
6	Thick orifice	L (in), D_1 (in), D_2 (in)	17	Joule-Thompson device	L_Ω, V_f, k_v, A
7	Square reduction	D_1 (in), D_2 (in)	18	Control valve	See example 12 data file
8	Square expansion	D_1 (in), D_2 (in)	19	User defined	A (in^2)
9	Rotating annular duct	L (in), r_o (in), r_i (in), N (rpm)	20	Heat exchanger core	A_f (in^2), A_s (in^2), A_c (in^2), L (in), K_c, K_e
10	Rotating radial duct	L (in), D (in), N (rpm)	21	Parallel tube	L (in), D (in), ε/D, n
11	Labyrinth seal	r_i (in), c (in), m (in), n, α	22	Compressible orifice	C_L, A (in^2)

* Pump characteristics are expressed as $\Delta p = A_0 + B_0\,\dot{m}^2$, Δp = pressure rise, lbf/ft^2, and $\dot{m}$ = flow rate, lbm/s.

1.7 Program Structure

GFSSP has three major parts (fig. 5). The first part is the GUI visual thermofluid dynamic analyzer for systems and components (VTASC). VTASC allows users to create a flow circuit by a 'point and click' paradigm. It creates the GFSSP input file after the completion of the model building process. It can also create a customized GFSSP executable by compiling and linking user subroutines with the solver module of the code. Users can run GFSSP from VTASC and post process the results in the same environment. The second major part of the program is the solver and property module. This is the heart of the program that reads the input data file and generates the required conservation equations for all internal nodes and branches with the help of thermodynamic property data. It also interfaces with user subroutines to receive any specific inputs from users. Finally, output files are created for VTASC to read and display results. The user subroutine is the third major part of the program. This consists of several blank subroutines that are called by the solver module. These subroutines allow the users to incorporate any new physical model, resistance option, fluid, etc. in the model. The computer program is discussed in detail in section 4.
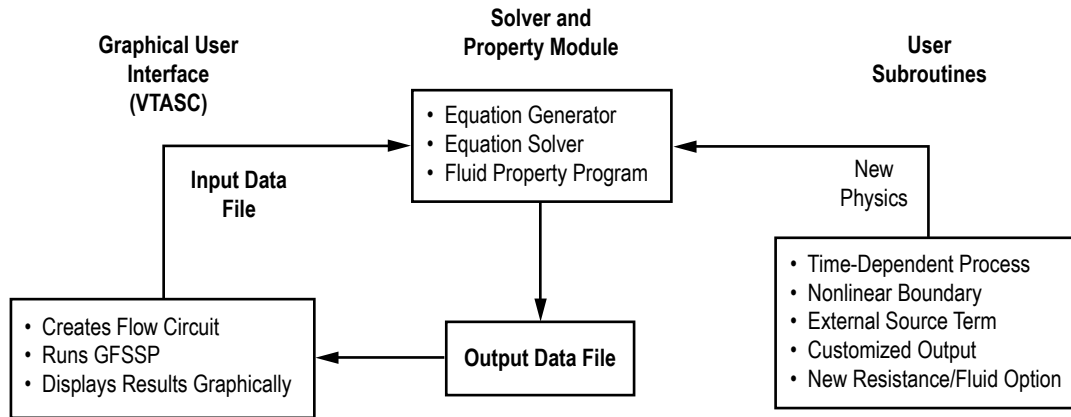
Figure 5. GFSSP's program structure showing the interaction of three major modules.

1.8 Graphical User Interface

GFSSP's GUI (fig. 6) provides the users a platform to build and run their models. It also allows post-processing of results. The network flow circuit is first built using three basic elements—boundary node, internal node, and branch. Then the properties of the individual elements are assigned. Users are also required to define global options of the model that includes input/output files, fluid specification, and any special options such as rotation, heat exchanger, etc. During execution of the program, a run manager window opens up and users can monitor the progress of the numerical solution. On the completion of the run, it allows users to visualize the results in tabular form for steady state solutions and in graphical form for unsteady solutions. It also provides an interface to activate and import data to the plotting program, Winplot[13] for post-processing. The GUI is discussed in detail in section 5.
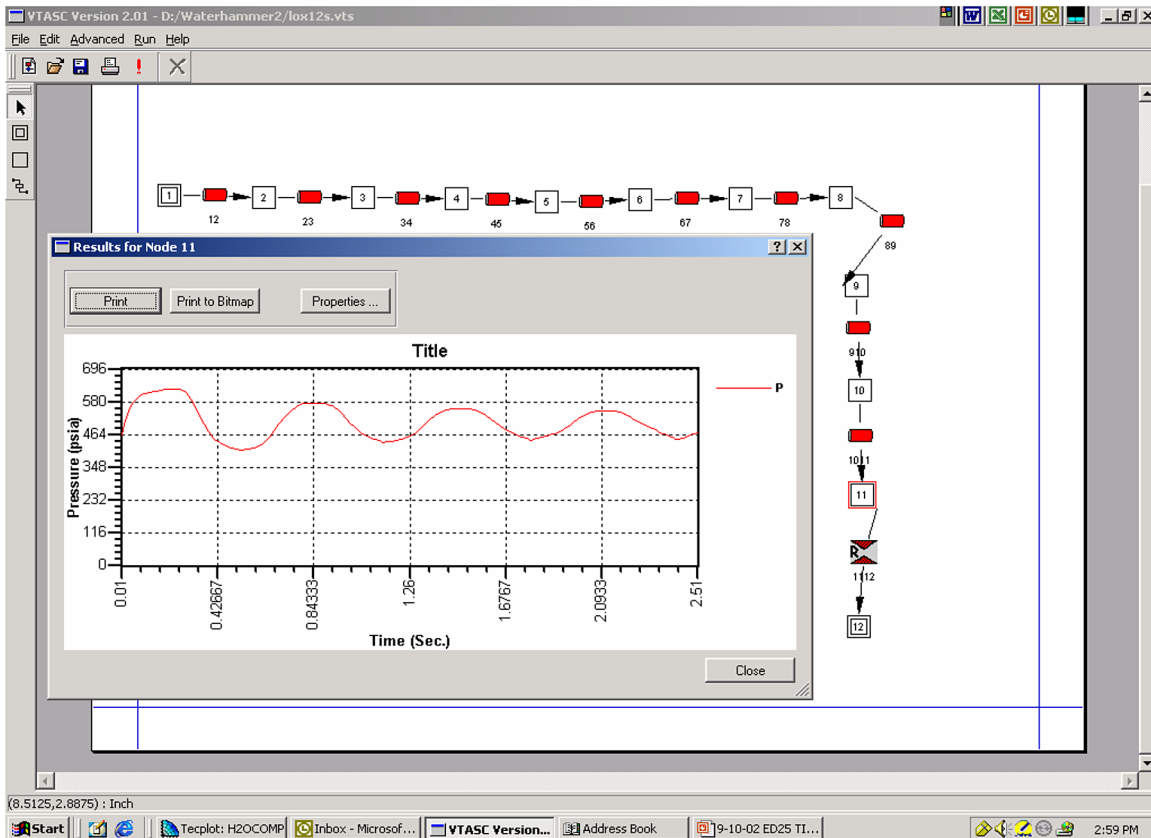
Figure 6. GFSSP's graphical user interface, VTASC allows creating, running, and viewing results in one environment.

1.9 Example Problems

Several example problems have been included to aid users in becoming familiar with different options of the code. The example problems also provide the verification and validation of the code by comparing the code's predictions with analytical solution and experimental data. These examples include: (1) Simulation of a flow system containing a pump, valve, and pipeline, (2) flow network for a water distribution system, (3) compressible flow in a converging-diverging nozzle, (4) mixing of combustion gases and a cold gas stream, (5) flow in a counterflow heat exchanger, (6) radial flow in a rotating radial disk, (7) flow in a squeeze film damper, (8) blowdown of a pressurized tank, (9) a reciprocating-piston cylinder, (10) power balancing of a turbopump assembly, (11) steady state conduction through a circular rod, and (12) fluid transient (waterhammer) due to sudden valve closure. These example problems are discussed in detail in section 5.

11

2. MATHEMATICAL FORMULATION

GFSSP assumes a Newtonian, nonreacting and one-dimensional flow in the flow circuit. The flow can be steady or unsteady, laminar or turbulent, incompressible or compressible, with or without heat transfer, phase change, mixing, and rotation. The analysis of thermofluid dynamics in a complex network requires resolution of the system into fluid nodes and branches, and solid nodes and conductors. GFSSP calculates scalar properties such as pressure, temperature, and density at the nodes, and vector properties such as flow rates, heat fluxes at fluid branches, and conductors, respectively. Fluid nodes can be either internal nodes where properties are calculated or boundary nodes where properties are specified. Temperatures are calculated at the solid nodes and specified at the ambient nodes. This section describes all governing equations and the solution procedure.

2.1 Governing Equations

Figure 7 displays a schematic showing adjacent nodes, their connecting branches, and the indexing system. In order to solve for the unknown variables, mass, energy, and fluid specie conservation equations are written for each internal node and flow rate equations are written for each branch.
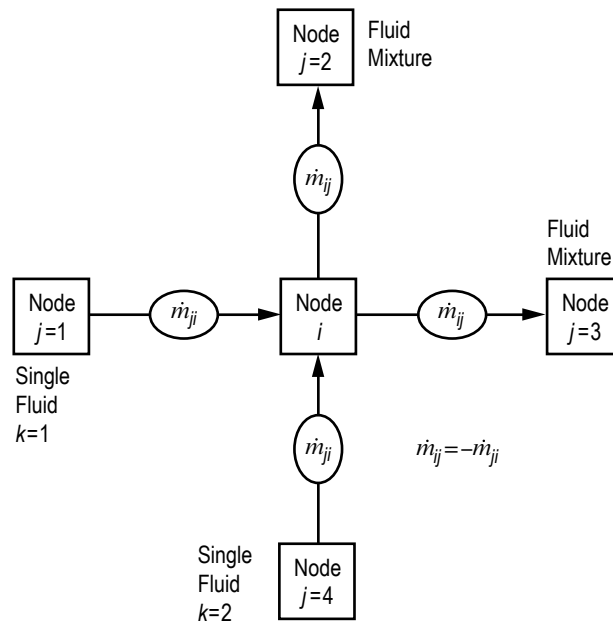
Figure 7. Schematic of GFSSP nodes, branches, and indexing practice.

2.1.1 Mass Conservation Equation

Following is the mass conservation equation:

$$\frac{m_{\tau+\Delta\tau} - m_{\tau}}{\Delta\tau} = -\sum_{j=1}^{j=n} \dot{m}_{ij} \ . \tag{1}$$

Equation (1) requires that for the unsteady formulation, the net mass flow from a given node must equate to the rate of change of mass in the control volume. In the steady state formulation, the left side of the equation is zero. This implies that the total mass flow rate into a node is equal to the total mass flow rate out of the node. Each term in equation (1) has the unit of lb/s.

2.1.2 Momentum Conservation Equation

The flow rate in a branch is calculated from the momentum conservation equation (eq. (2)), which represents the balance of fluid forces acting on a given branch. A typical branch configuration is shown in figure 8. Inertia, pressure, gravity, friction, and centrifugal forces are considered in the conservation equation. In addition to these five forces, a source term, S, has been provided in the equation to input pump characteristics or to input power to a pump in a given branch. If a pump is located in a given branch, all other forces except pressure are set to zero. The source term, S, is set to zero in all branches without a pump or other external momentum source.

$$\frac{(mu)_{\tau+\Delta\tau} - (mu)_{\tau}}{g_c \Delta\tau} + \text{MAX}\left|\dot{m}_{ij}, 0\right|\left(u_{ij} - u_u\right) - \text{MAX}\left|-\dot{m}_{ij}, 0\right|\left(u_{ij} - u_u\right)$$

-----Unsteady-----   ------------------Longitudinal Inertia--------------------

$$\left.\begin{matrix} + \text{MAX}\left|\dot{m}_{\text{trans}}, 0\right|\left(u_{ij} - u_p\right) - \text{MAX}\left|-\dot{m}_{\text{trans}}, 0\right|\left(u_{ij} - u_p\right) \\ \text{------------------------Transverse Inertia------------------------} \end{matrix}\right\} \frac{1}{g_c}$$

$$= \left(p_i - p_j\right)A_{ij} + \frac{\rho g V \cos\theta}{g_c} - K_f \dot{m}_{ij}\left|\dot{m}_{ij}\right|A_{ij} + \frac{\rho K_{\text{rot}}^2 \omega^2 A}{g_c} + \mu \frac{u_p - u_{ij}}{g_c \delta_{ij,p}} A_s$$

--Pressure--   --Gravity--   ----Friction----   -Centrifugal-   ----Shear----

$$-\rho A_{norm} u_{norm} u_{ij} / g_c + \left(\mu_d \frac{u_d - u_{ij}}{\delta_{ij,d}} - \mu_u \frac{u_{ij} - u_u}{\delta_{ij,u}}\right)\frac{A_{ij}}{g_c} + S \ . \tag{2}$$

-Moving Boundary-   ----------Normal Stress---------   -Source-
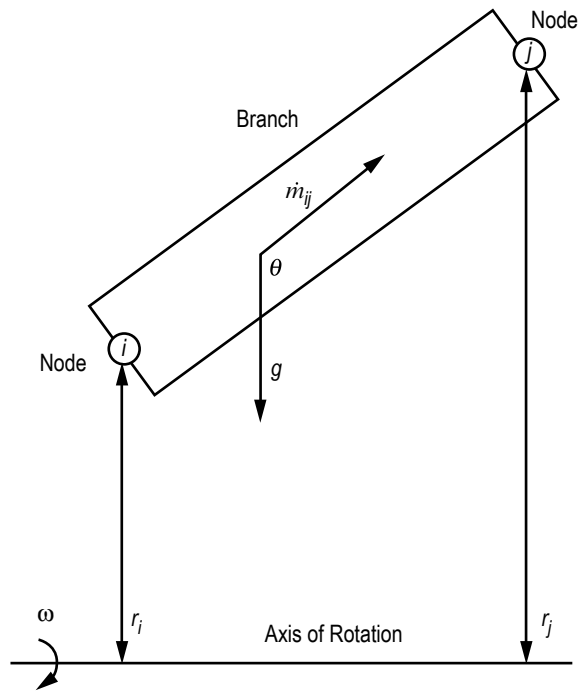
Figure 8. Schematic of a branch showing gravity and rotation.

The momentum equation consists of 11 terms. There will be no occasion when all 11 terms will be present in a control volume. Users have the ability to include or exclude all terms except the pressure term. For example, the friction and shear term will never be active at the same branch. The shear term will be activated for multidimensional flow modeling when the friction term must be set to zero. The pressure term will be active under all circumstances. The left-hand side of the momentum equation represents the inertia of the fluid. The surface and body forces applied in the control volume are assembled in the right-hand side of the equation. Each term of equation (2) has the unit of lb_f. Following are descriptions of the 11 terms:

(1) Unsteady—This term represents rate of change of momentum with time. For steady state flow, time step is set to an arbitrary large value and this term is reduced to zero.

(2) Longitudinal inertia—This term is important when there is a significant change in velocity in the longitudinal direction due to change in area and density. An upwind differencing scheme is used to compute the velocity differential. Flow in a converging-diverging nozzle is an example where this term must be active.

(3) Transverse inertia—This term is important for multidimensional flow. It accounts for any longitudinal momentum being transported by a transverse velocity component. Once again, an upwind differencing scheme is used to compute the velocity differential.

(4) Pressure—This term represents the pressure gradient in the branch. The pressures are located at the upstream and downstream face of a branch.

14

(5) Gravity—This term represents the effect of gravity. The gravity vector makes an angle (θ) with the assumed flow direction vector. At $\theta = 180°$, fluid is flowing against gravity; at $\theta = 90°$, fluid is flowing horizontally and gravity has no effect on the flow.

    (6) Friction—This term represents the frictional effect. Friction was modeled as a product of K_f and the square of the flow rate and area. K_f is a function of the fluid density in the branch and the nature of the flow passage being modeled by the branch. The calculation of K_f for different types of flow passages is described in section 2.1.7.

    (7) Centrifugal—This term in the momentum equation represents the effect of the centrifugal force. This term will be present only when the branch is rotating as shown in figure 8. K_{rot} is the factor representing the fluid rotation. K_{rot} is unity when the fluid and the surrounding solid surface rotate with the same speed. This term also requires knowledge of the distances from the axis of rotation between the upstream and downstream faces of the branch.

    (8) Shear—This term represents shear force exerted on the control volume by a neighboring branch. This term is active only for multidimensional flow. The friction term is deactivated when this term is present. This term requires knowledge of distances between branches to compute the shear stress.

    (9) Moving boundary—This term represents force exerted on the control volume by a moving boundary. This term is not active for multidimensional calculations.

    (10) Normal stress—This term represents normal viscous force. This term is important for highly viscous flows.

    (11) Source—This term represents a generic source term. Any additional force acting on the control volume can be modeled through the source term. In a system level model, a pump can be modeled by this term. A detailed description of modeling a pump by this source term, S, appears in sections 2.1.7.14 and 2.1.7.15.

    A simplified form of the momentum equation has also been provided to compute choked flow rate for compressible flow in an orifice.

$$\dot{m}_{ij} = C_{L_{ij}} A \sqrt{ p_i \rho_i g_c \frac{2\gamma}{\gamma - 1} \left(p_{ratio} \right)^{\frac{2}{\gamma}} \left[1 - \left(p_{ratio} \right)^{\frac{\gamma - 1}{\gamma}} \right] } , \tag{3a}$$

where

$$p_{ratio} = \frac{p_j}{p_i} \tag{3b}$$

if

$$\frac{p_j}{p_i} < p_{c\gamma} \ ,$$

where

$$p_{c\gamma} = \left(\frac{2}{\gamma+1}\right)^{\frac{\gamma}{\gamma-1}}$$

(3c)

and

$$\frac{p_j}{p_i} = p_{c\gamma} \ .$$

(3d)

2.1.3 Energy Conservation Equations

GFSSP solves for energy conservation equations for both fluid and solid at internal fluid nodes and solid nodes. Energy conservation equation for fluid is solved for all real fluids with or without heat transfer. For conjugate heat transfer, the energy conservation equation for solid node is solved in conjunction with the energy equation of fluid node. The heat transfer between solid and fluid node is calculated at the interface and used in both equations as source and sink terms.

2.1.3.1 Energy Conservation Equation of Fluid. The energy conservation equation for node i, shown in figure 7, can be expressed following first or second law of thermodynamics. The first law formulation uses enthalpy as the dependent variable while second law formulation uses entropy. The energy conservation equation based on enthalpy is shown in equation (4a):

$$\frac{m\left(h - \dfrac{p}{\rho J}\right)_{\tau+\Delta\tau} - m\left(h - \dfrac{p}{\rho J}\right)_{\tau}}{\Delta\tau} = \sum_{j=1}^{j=n}\left\{\mathrm{MAX}\left[-\dot{m}_{ij},0\right]h_j - \mathrm{MAX}\left[\dot{m}_{ij},0\right]h_i\right\}$$

$$+ \frac{\mathrm{MAX}\left[-\dot{m}_{ij},0\right]}{\left|\dot{m}_{ij}\right|}\left[\left(p_i - p_j\right) + K_{ij}\dot{m}_{ij}^2\right]\left(v_{ij}A\right) + Q_i \ .$$

(4a)

Equation (4a) shows that for transient flow, the rate of increase of internal energy in the control volume is equal to the rate of energy transport into the control volume minus the rate of energy transport from the control volume plus the rate of work done on the fluid by the pressure force plus the rate of work done on the fluid by the viscous force plus the rate of heat transfer into the control volume.

For a steady state situation, the energy conservation equation, equation (4a), states that the net energy flow from a given node must equate to zero. In other words, the total energy leaving a node is equal to the total energy coming into the node from neighboring nodes and from any

external heat sources (Q_i) coming into the node and work done on the fluid by pressure and viscous forces. The MAX operator used in equation (4a) is known as an upwind differencing scheme and has been extensively employed in the numerical solution of Navier-Stokes equations in convective heat transfer and fluid flow applications.[9] When the flow direction is not known, this operator allows the transport of energy only from its upstream neighbor. In other words, the upstream neighbor influences its downstream neighbor but not vice versa. The second term on the right-hand side represents the work done on the fluid by the pressure and viscous force. The difference between the steady and unsteady formulation lies in the left side of the equation. For a steady state situation, the left side of equation (4a) is zero, where as in unsteady cases, the left side of the equation must be evaluated.

The energy conservation equation based on entropy is shown in equation (4b):

$$\frac{(ms)_{\tau+\Delta\tau}-(ms)_{\tau}}{\Delta\tau} = \sum_{j=1}^{j=n}\left\{\text{MAX}\left[-\dot{m}_{ij},0\right]s_j - \text{MAX}\left[\dot{m}_{ij},0\right]s_i\right\}$$

$$+ \sum_{j=1}^{j=n}\left\{\frac{\text{MAX}\left[-\dot{m}_{ij},0\right]}{\left|\dot{m}_{ij}\right|}\right\}\dot{S}_{ij,gen} + \frac{Q_i}{T_i} \quad .$$

(4b)

The entropy generation rate due to fluid friction in a branch is expressed as

$$\dot{S}_{ij,gen} = \frac{\dot{m}_{ij}\Delta p_{ij,viscous}}{\rho_u T_u J} = \frac{K_f\left(\left|\dot{m}_{ij}\right|\right)^3}{\rho_u T_u J} \quad .$$

(4c)

Equation (4b) shows that for unsteady flow, the rate of increase of entropy in the control volume is equal to the rate of entropy transport into the control volume plus the rate of entropy generation in all upstream branches due to fluid friction plus the rate of entropy added to the control volume due to heat transfer. The first term on the right-hand side of the equation represents the convective transport of entropy from neighboring nodes. The second term represents the rate of entropy generation in branches connected to the ith node. The third term represents entropy change due to heat transfer. Each term in equation (4b) has the unit of Btu/R-s.

2.1.3.2 Energy Conservation Equation of Solid. Typically, a solid node can be connected with other solid nodes, fluid nodes, and ambient nodes. Figure 9 shows a typical arrangement where a solid node is connected with other solid nodes, fluid nodes, and ambient nodes. The energy conservation equation for solid node i can be expressed as:

$$\frac{\partial}{\partial\tau}\left(mC_pT_s^i\right) = \sum_{j_s=1}^{n_{ss}}\dot{q}_{ss} + \sum_{j_f=1}^{n_{sf}}\dot{q}_{sf} + \sum_{j_a=1}^{n_{sa}}\dot{q}_{sa} + \dot{S}_i \quad .$$

(5)

17
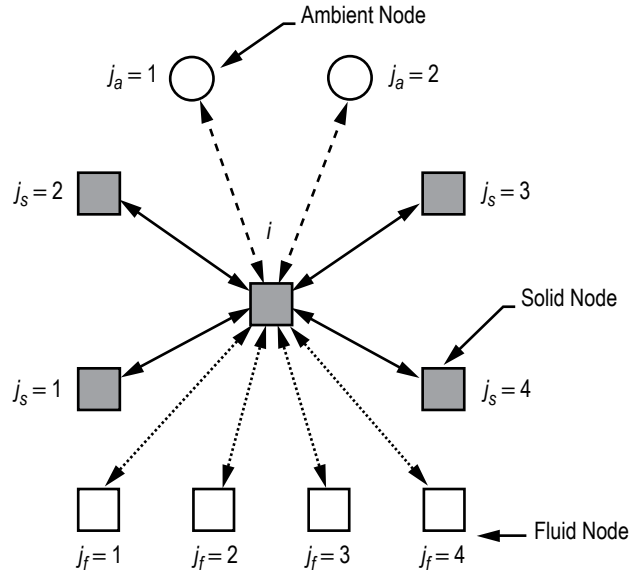
Figure 9. A schematic showing the connection of a solid node with neighboring solid, fluid, and ambient nodes.

The left-hand side of the equation represents rate of change of temperature of the solid node, i. The right-hand side of the equation represents the heat transfer from the neighboring node and heat source or sink. The heat transfer from neighboring solid, fluid and ambient nodes can be expressed as

$$\dot{q}_{ss} = k_{ij_s} A_{ij_s} / \delta_{ij_s} \left(T_s^{j_s} - T_s^i \right) , \qquad (5a)$$

$$\dot{q}_{sf} = h_{ij_f} A_{ij_f} \left(T_f^{j_f} - T_s^i \right) , \qquad (5b)$$

$$\dot{q}_{sa} = h_{ij_a} A_{ij_a} \left(T_a^{j_a} - T_s^i \right) . \qquad (5c)$$

The heat transfer rate can be expressed as a product of conductance and temperature differential. The conductance for equations (5a)–(5c) are as follows:

$$C_{ij_s} = \frac{k_{ij_s} A_{ij_s}}{\delta_{ij_s}}, \quad C_{ij_f} = h_{ij_f} A_{ij_f}, \text{ and } C_{ij_f} = h_{ij_a} A_{ij_a} , \qquad (5d)$$

respectively, where effective heat transfer coefficients for solid to fluid and solid to ambient nodes are expressed as:

18

$$h_{ij_f} = h_{c,ij_f} + h_{r,ij_f}$$

$$h_{ij_a} = h_{c,ij_a} + h_{r,ij_a} \qquad (5e)$$

and

$$h_{r,ij_f} = \frac{\sigma\left[\left(T_f^{j_f}\right)^2 + \left(T_s^i\right)^2\right]\left[T_f^{j_f} + T_s^i\right]}{1/\varepsilon_{ij,f} + 1/\varepsilon_{ij,s} - 1}$$

$$h_{r,ij_a} = \frac{\sigma\left[\left(T_a^{j_a}\right)^2 + \left(T_s^i\right)^2\right]\left[T_a^{j_a} + T_s^i\right]}{1/\varepsilon_{ij,a} + 1/\varepsilon_{ij,s} - 1} \quad . \qquad (5f)$$

GFSSP provides users with three different options for specifying heat transfer coefficient:

(1) User can provide a constant heat transfer coefficient.

(2) User can specify Dittus-Boelter equation[14] for single phase flow where the Nusselt number is expressed as:

$$\frac{h_c D}{k_f} = 0.023(\text{Re})^{0.8}(\text{Pr})^{0.33} \quad , \qquad (5g)$$

where $\text{Re} = \rho u D / \mu_f$ and $\text{Pr} = C_p \mu_f / k_f$.

(3) User can specify modified Miropolosky's correlation[15] for two-phase flow:

$$\text{Nu} = 0.023\left(\text{Re}_{mix}\right)^{0.8}\left(\text{Pr}_v\right)^{0.4}(Y)$$

$$\text{Re}_{mix} = \left(\frac{\rho u D}{\mu_v}\right)\left[x + \left(\frac{\rho_v}{\rho_l}\right)(1-x)\right]$$

$$\text{Pr}_v = \left(\frac{C_p \mu_v}{k_v}\right)$$

$$Y = 1 - 0.1\left(\frac{\rho_v}{\rho_l} - 1\right)^{0.4}(1-x)^{0.4} \quad . \qquad (5h)$$

Equation (5h) can be rearranged to determine T_s^i:

$$T_s^i = \frac{\displaystyle\sum_{j_s=1}^{n_{ss}} C_{ij_s} T_s^{j_s} + \sum_{j_f=1}^{n_{sf}} C_{ij_f} T_f^{j_f} + \sum_{j_a=1}^{n_{sa}} C_{ij_a} T_a^{j_a} + \frac{\left(mC_p\right)_m}{\Delta\tau} T_{s,m}^i + \dot{S}}{\dfrac{mC_p}{\Delta\tau} + \displaystyle\sum_{j_s=1}^{n_{ss}} C_{ij_s} + \sum_{j_f=1}^{n_{sf}} C_{ij_f} + \sum_{j_a=1}^{n_{sa}} C_{ij_a}} \quad . \tag{6}$$

2.1.4 Fluid Specie Conservation Equation

For a fluid mixture, density is a function of mass fraction of fluid species. In order to calculate the density of the mixture, the concentration of the individual fluid species within the branch must be determined. The concentration for the kth specie can be written as

$$\frac{\left(m_i c_{i,k}\right)_{\tau+\Delta\tau} - \left(m_i c_{i,k}\right)_\tau}{\Delta\tau} = \sum_{j=1}^{j=n}\left\{\text{MAX}\left[-\dot{m}_{ij},0\right] c_{j,k} - \text{MAX}\left[\dot{m}_{ij},0\right] c_{i,k}\right\} + \dot{S}_{i,k} \quad . \tag{7}$$

For a transient flow, equation (7) states that the rate of increase of the concentration of kth specie in the control volume equals the rate of transport of the kth specie into the control volume minus the rate of transport of the kth specie out of the control volume plus the generation rate of the kth specie in the control volume.

Like equation (4a), for steady state conditions, equation (7) requires that the net mass flow of the kth specie from a given node must equate to zero. In other words, the total mass flow rate of the given specie into a node is equal to the total mass flow rate of the same specie out of that node. For steady state, the left side of equation (7) is zero. For the unsteady formulation, the resident mass in the control volume is changing and therefore the left side must be computed. Each term in equation (5) has the unit of lb/s.

2.1.5 Thermodynamic and Thermophysical Properties

The momentum conservation equation, equation (2), requires knowledge of the density and the viscosity of the fluid within the branch. These properties are functions of the temperatures, pressures, and concentrations of fluid species for a mixture. Three thermodynamic property routines have been integrated into the program to provide the required fluid property data. GASP[10] provides the thermodynamic and transport properties for 10 fluids. These fluids include hydrogen, oxygen, helium, nitrogen, methane, carbon dioxide, carbon monoxide, argon, neon, and fluorine. WASP[11] provides the thermodynamic and transport properties for water and steam. For RP-1 fuel, a lookup table of properties has been generated by a modified version of GASP. An interpolation routine has been developed to extract the required properties from the tabulated data. GASPAK[12] provides thermodynamic properties for helium, methane, neon, nitrogen, carbon monoxide,

oxygen, argon, carbon dioxide, hydrogen, parahydrogen, water, RP-1, isobutane, butane, deuterium, ethane, ethylene, hydrogen sulfide, krypton, propane, xenon, R-11, R-12, R-22, R-32, R-123, R-124, R-125, R-134A, R-152A, nitrogen trifluoride, ammonia, hydrogen peroxide, and air.

2.1.5.1 Equation of State for a Real Fluid. Transient flow calculations require the knowledge of resident mass in a control volume. The resident mass is calculated from the equation of state for real fluid that can be expressed as

$$m = \frac{pV}{zRT} \ .$$

(8)

It may be noted that equation (8) is valid for liquid, gas, and gas-liquid mixture. For an ideal gas compressibility factor, z is unity. The compressibility factor for real gas is computed from the equation of state of real fluids using the above-mentioned thermodynamic property programs. For two-phase mixture, z is computed from the following relation:

$$z = \frac{p}{\rho_{mix}RT} \ ,$$

(8a)

where

$$\rho_{mix} = \frac{\rho_l \rho_g}{x\rho_l - (1-x)\rho_g}$$

(8b)

and

$$x = \frac{s - s_l}{s_g - s_l} \ .$$

(8c)

2.1.6 Mixture Property Calculations

This section describes a procedure developed for GFSSP to estimate the density and temperature of mixtures of real fluids. Let us assume that n fluids are mixing in the ith node. At node i, pressure (p_i) and molar concentrations (x_k) are known. The problem is to calculate the density (ρ_i), temperature (T_i), specific heat (C_p), specific heat ratio (g), and viscosity (μ) of the mixture at the ith node.

During iterative calculations, GFSSP calculates the mixture properties using the following steps:

(1) Calculate ρ_k, μ_k, $C_{p,k}$ and γ_k from p_i and T_i using the thermodynamic property routines of the program.

(2) Calculate the compressibility factor of each component of the mixture (z_k) from the equation of state for a real gas (eq. (9)):

$$z_k = \frac{p_i}{\rho_k R_k T_k} \ ,$$

(9)

where R_k is the gas constant for kth fluid.

(3) Calculate compressibility factor of the mixture (z_i) as shown in equation (10) by taking the molar average of the component compressibility factors obtained in step (2):

$$z_i = \sum_{k=1}^{k=n} x_k z_k \ . \tag{10}$$

.

(4) Calculate gas constant of the mixture (R_i) by taking the molar average of the component gas constants:

$$R_i = \sum_{k=1}^{k=n} x_k R_k \ . \tag{11}$$

(5) Calculate the density of the mixture (ρ_i) from the equation of state of a real fluid:

$$\rho_i = \frac{p_i}{z_i R_i T_i} \ . \tag{12}$$

(6) Calculate viscosity, specific heat, and specific heat ratio of the mixture by taking the molar average of the component properties μ_k, $C_{p,k}$, and γ_k as shown in equations (13)–(15):

$$\mu_i = \sum_{k=1}^{k=n} x_k \mu_k \ , \tag{13}$$

$$C_{p,i} = \sum_{k=1}^{k=n} \frac{C_{p,k} x_k M_k}{x_k M_k} \ , \tag{14}$$

and

$$\gamma_i \sum_{k=1}^{k=n} x_k \gamma_k \ . \tag{15}$$

(7) Calculate T_i from the energy conservation equation expressed in terms of a product of specific heat and temperature instead of enthalpy:

$$\left(T_i\right)_{\tau+\Delta\tau} = \frac{\displaystyle\sum_{j=1}^{j=n}\sum_{k=1}^{k=nf} C_{p,k,j}\, x_{k,j} T_j \mathrm{MAX}\left[-\dot{m}_{ij},0\right]+\left(C_{p,i}\ m_i T_i\right)_\tau / \Delta\tau + Q_i}{\displaystyle\sum_{j=1}^{j=n}\sum_{k=1}^{k=nf} C_{p,k,j}\, x_{k,j}\mathrm{MAX}\left[\dot{m}_{ij},0\right]+\left(C_{p,i}\, m\right)_\tau / \Delta\tau} \ , \tag{16}$$

where $C_{p,k}$ is the molar specific heat and x_k is the mole-fraction of the kth specie. Note that an unsteady formulation of the energy equation (eq. (4)) was used to compute T_i.

2.1.7 Friction Calculations

It was mentioned earlier in this TM that the friction term in the momentum equation is expressed as a product of K_f, the square of the flow rate and the flow area. Empirical information is necessary to estimate K_f. Several options for flow passage resistance are listed in table 5. In this subsection, the expression of K_f for all resistance options are described.

2.1.7.1 Pipe Flow (Branch Option 1). Figure 10 shows the pipe resistance option parameters that are required by GFSSP. This option considers that the branch is a pipe with length (L), diameter (D), and surface roughness (ε). For this option, K_f can be expressed as:

$$K_f = \frac{8\,fL}{\rho_u \pi^2 D^5 g_c} \ , \tag{17}$$

where ρ_u is the density of the fluid at the upstream node of a given branch. The derivation of K_f for pipe flow is covered in appendix A.

D = Pipe Diameter
L = Pipe Length
ε = Absolute Roughness
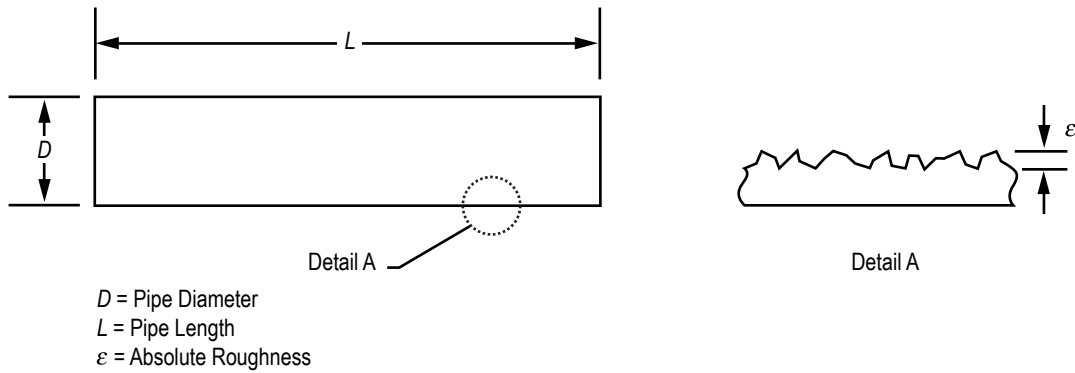
Figure 10. Pipe resistance option parameters.

The Darcy friction factor (f) is determined from the Colebrook equation,[16] which is expressed as:

$$\frac{1}{\sqrt{f}} = -2\log\left[\frac{\varepsilon}{3.7D} + \frac{2.51}{\mathrm{Re}\sqrt{f}}\right] \ , \tag{18}$$

where ε/D and Re are the surface roughness factor and Reynolds number, respectively.

2.1.7.2 Flow Through a Restriction (Branch Option 2). This option regards the branch as a flow restriction with a given flow coefficient (C_L), and area (A). For this option, K_f can be expressed as:

$$K_f = \frac{1}{2g_c \rho_u C_L^2 A^2} \ . \tag{19}$$

23

In classical fluid mechanics, head loss is expressed in terms of a nondimensional 'K factor':

$$\Delta h = K \frac{u^2}{2g} \quad . \tag{20}$$

K and C_L are related as:

$$C_L = \frac{1}{\sqrt{K}} \quad . \tag{21}$$

2.1.7.3 Noncircular Duct (Branch Option 3). This option considers a duct with a non-circular cross section. Four different types of cross sections can be modeled as shown in figure 11.
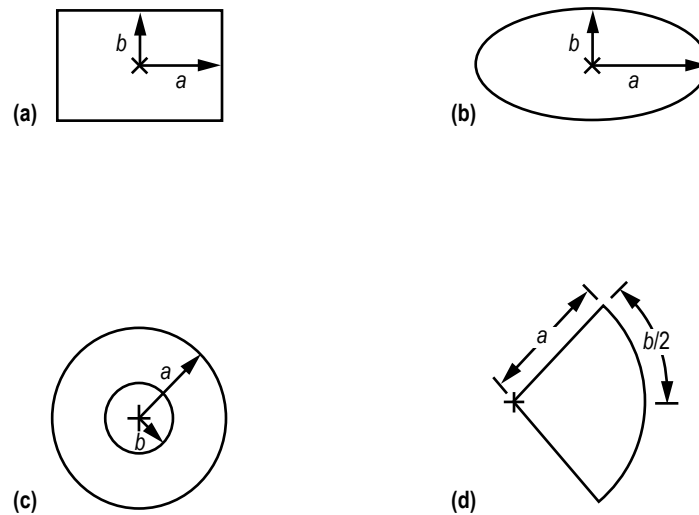
Figure 11. Noncircular duct cross section: (a) Rectangle, (b) ellipse, (c) concentric cylinder, and (d) circular sector.

White describes a procedure to estimate the friction factor in a noncircular duct.[17] This procedure consists of the following steps:

(1) Estimate the hydraulic diameter of the cross section: D_h = (4)(area)/perimeter.

(2) Estimate the Poiseuille number (Po) for a particular cross section. The Poiseuille number can be expressed as a polynomial function of aspect ratio as shown in equation (22). Table 6 provides the coefficients for different geometries.

$$\text{Po} = A_0 + A_1\left(\frac{b}{a}\right) + A_2\left(\frac{b}{a}\right)^2 + A_3\left(\frac{b}{a}\right)^3 + A_4\left(\frac{b}{a}\right)^4 \quad . \tag{22}$$

Table 6. Poiseuille number coefficients for noncircular duct cross sections.

Coefficients	Rectangle	Ellipse	Concentric* Cylinder	Circular Section
A_0	23.9201	19.7669	22.0513	11.9852
A_1	−29.436	−4.53458	6.44473	3.01553
A_2	30.3872	−11.5239	−7.35451	−1.09712
A_3	−10.7128	22.3709	2.78999	–
A_4	–	−10.0874	–	–

* For $b/a < 0.2508$ $P_0 = A_0 \left(\dfrac{b}{a}\right)^{A_1}$, where, $A_0 = 24.8272$, $A_1 = 0.0479888$.

(3) Calculate the friction factor for a noncircular pipe:

• Laminar flow (Re<2,300)

$$f = \frac{4\,\mathrm{Po}}{\mathrm{Re}} \ .$$

(23)

• Turbulent flow

– Compute the effective diameter:

$$D_{eff} = \frac{16 D_h}{\mathrm{Po}} \ .$$

(24)

– Compute the effective Reynolds number:

$$\mathrm{Re}_{eff} = \frac{\dot{m}}{\mu} \frac{D_{eff}}{A} \ .$$

(25)

– Compute the friction factor using the Colebrook equation (eq. (18)).

(4) Compute K_f from the following expression:

$$K_f = \frac{8\,fL}{\rho_u\,\pi^2 D_h^5\, g_c} \ .$$

(26)

2.1.7.4 Pipe With Entrance and Exit Loss (Branch Option 4). Figure 12 shows the pipe with entrance and/or exit loss resistance option parameters that are required by GFSSP. This option is an extension of option 1. In addition to the frictional loss in the pipe, entrance and exit losses are also calculated. For this option, K_f can be expressed as:

25

D = Pipe Diameter K_i = Entrance Loss Coefficient
L = Pipe Length K_e = Exit Loss Coefficient
ε = Absolute Roughness
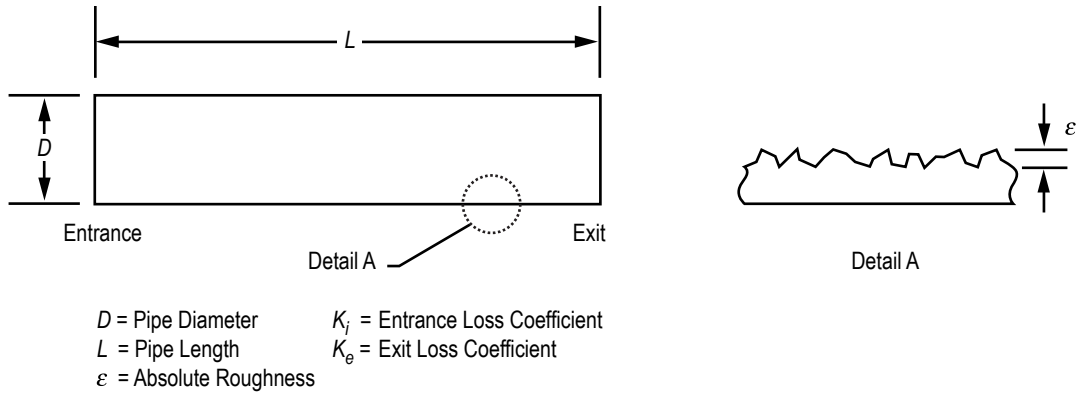
Figure 12. Pipe with entrance and/or exit loss resistance option parameters.

$$K_f = \frac{8K_i}{\rho_u \pi^2 D^4 g_c} + \frac{8fL}{\rho_u \pi^2 D^5 g_c} + \frac{8K_e}{\rho_u \pi^2 D^4 g_c} \quad , \tag{27}$$

where K_i and K_e are the entrance and exit loss coefficients, respectively.

2.1.7.5 Thin, Sharp Orifice (Branch Option 5). Figure 13 shows the thin, sharp orifice resistance option parameters that are required by GFSSP. This option considers the branch as a thin, sharp orifice with a pipe diameter of D_1 and an orifice diameter of D_2. For this option, K_f can be expressed as:[18]

$$K_f = \frac{K_1}{2g_c \rho_u A^2} \quad , \tag{28}$$

where $A = \dfrac{\pi D_1^2}{4}$.

Thin, Sharp Orifice

D_1 = Pipe Diameter
D_2 = Orifice Throat Diameter
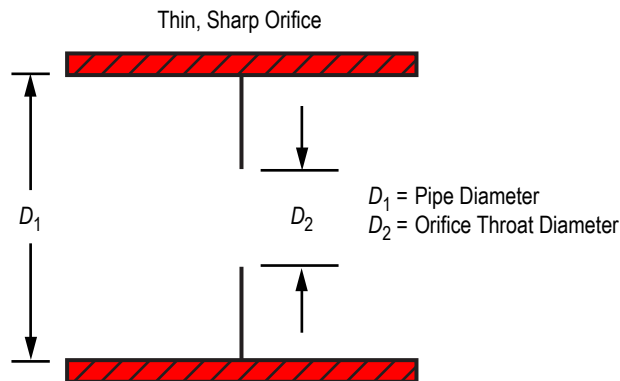
Figure 13. Thin, sharp orifice resistance option parameters.

26

For upstream Re ≤ 2,500,

$$K_1 = \left[2.72 + \left(\frac{D_2}{D_1} \right)^2 \left(\frac{120}{Re} - 1 \right) \right] \left[1 - \left(\frac{D_2}{D_1} \right)^2 \right] \left[\left(\frac{D_1}{D_2} \right)^4 - 1 \right] . \tag{29}$$

For upstream Re > 2,500,

$$K_1 = \left[2.72 - \left(\frac{D_2}{D_1} \right)^2 \left(\frac{4,000}{Re} \right) \right] \left[1 - \left(\frac{D_2}{D_1} \right)^2 \right] \left[\left(\frac{D_1}{D_2} \right)^4 - 1 \right] . \tag{30}$$

This option is recommended for subsonic and incompressible flow.

2.1.7.6 Thick Orifice (Branch Option 6). Figure 14 shows the thick orifice resistance option parameters that are required by GFSSP. This option models the branch as a thick orifice with a pipe diameter of D_1, an orifice diameter of D_2, and orifice length of L_{or}. This option should be used if $L_{or}/D_2 \leq 5$. If $L_{or}/D_2 > 5$, the user should use a square expansion, option 8, or a square reduction, option 7. For option 6, K_f can be expressed as in equation (28). However, the K_1 in equation (28) is calculated[18] from the following expressions:

For upstream Re ≤ 2,500:

$$K_1 = \left[2.72 + \left(\frac{D_2}{D_1} \right)^2 \left(\frac{120}{Re} - 1 \right) \right] \left[1 - \left(\frac{D_2}{D_1} \right)^2 \right] \left[\left(\frac{D_1}{D_2} \right)^4 - 1 \right] \left[0.584 + \frac{0.0936}{\left(L_{or} / D_2 \right)^{1.5} + 0.225} \right] . \tag{31}$$
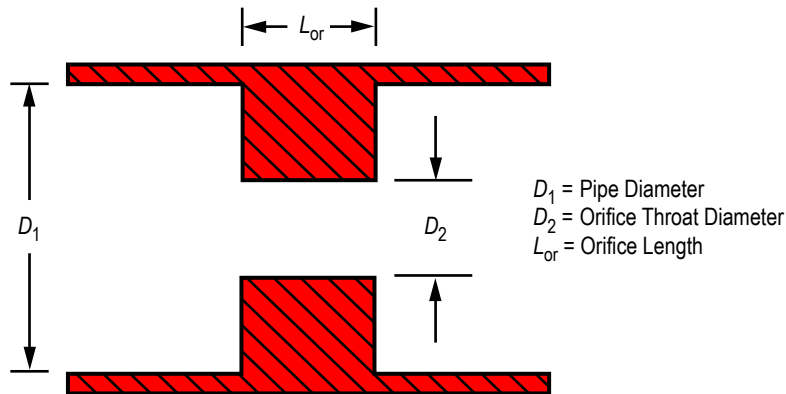
Figure 14. Thick orifice resistance option parameters.

D_1 = Pipe Diameter
D_2 = Orifice Throat Diameter
L_{or} = Orifice Length

For upstream Re > 2,500:

$$K_1 = \left[2.72 - \left(\frac{D_2}{D_1}\right)^2\left(\frac{4,000}{Re}\right)\right]\left[1-\left(\frac{D_2}{D_1}\right)^2\right]\left[\left(\frac{D_1}{D_2}\right)^4 - 1\right]\left[0.584 + \frac{0.0936}{\left(L_{or}/D_2\right)^{1.5}+0.225}\right]. \quad (32)$$

This option is recommended for subsonic and incompressible flow.

2.1.7.7 Square Reduction (Branch Option 7). Figure 15 shows the square reduction resistance option parameters that are required by GFSSP. This option considers the branch as a square reduction. The diameters of the upstream and downstream pipes are D_1 and D_2, respectively. For this option, K_f can be expressed as in equation (28). However, the K_1 in equation (28) is calculated from the following expressions:[18]

For upstream Re ≤ 2,500,

$$K_1 = \left[1.2 + \frac{160}{Re}\right]\left[\left(\frac{D_1}{D_2}\right)^4 - 1\right]. \quad (33)$$

For upstream Re > 2,500,

$$K_1 = \left[0.6 + 0.48f\right]\left(\frac{D_1}{D_2}\right)^2\left[\left(\frac{D_1}{D_2}\right)^2 - 1\right]^2. \quad (34)$$

The Reynolds number and friction factor that are utilized within these expressions are based on the upstream conditions. The user must specify the correct flow direction through this branch. If the model determines that the flow direction is in the reverse direction, the user will have to replace the reduction with an expansion and rerun the model.

D_1 = Upstream Pipe Diameter
D_2 = Downstream Pipe Diameter
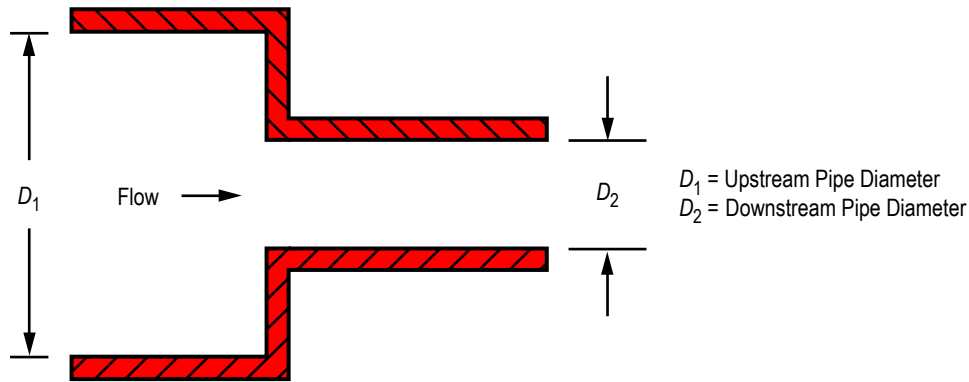
Figure 15. Square reduction resistance option parameters.

2.1.7.8 Square Expansion (Branch Option 8). Figure 16 shows the square expansion resistance option parameters that are required by GFSSP. This option considers the branch as a square expansion. The diameters of the upstream and downstream pipes are D_1 and D_2, respectively. For this option, K_f can be expressed as in equation (28). However, the K_1 in equation (28) is calculated from the following expressions:[18]

For upstream Re ≤ 4,000,

$$K_1 = 2\left[1 - \left(\frac{D_1}{D_2}\right)^4\right]. \tag{35}$$

For upstream Re > 4,000:

$$K_1 = [1 + 0.8f]\left[1 - \left(\frac{D_1}{D_2}\right)^2\right]^2. \tag{36}$$

The Reynolds number and friction factor that are utilized within these expressions are based on the upstream conditions. The user must specify the correct flow direction through this branch. If the model determines that the flow direction is in the reverse direction, the user will have to replace the expansion with a reduction and rerun the model.
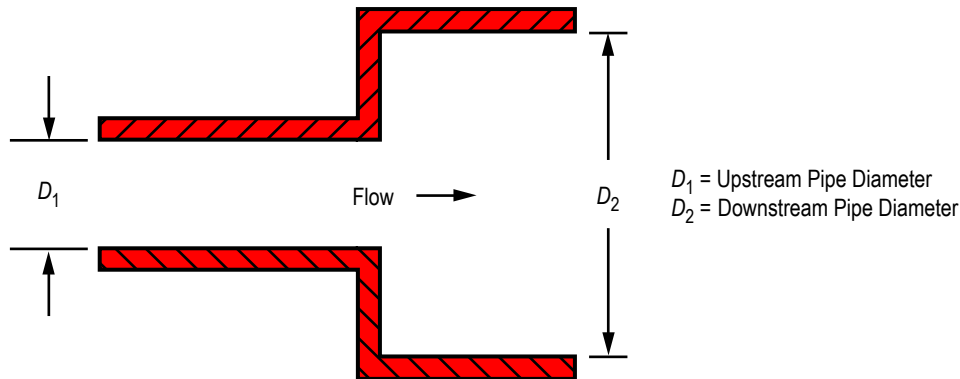
Figure 16. Square expansion resistance option parameters.

This option is recommended for subsonic and incompressible flow.

2.1.7.9 Rotating Annular Duct (Branch Option 9). Figure 17 shows the rotating annular duct resistance option parameters that are required by GFSSP. This option considers the branch as a rotating annular duct. The length, outer radius, and inner radius of the annular passage are L, r_o, and r_i, respectively. The inner surface is rotating at N rpm ($N=30\ w/p$). For this option, K_f can be expressed as:
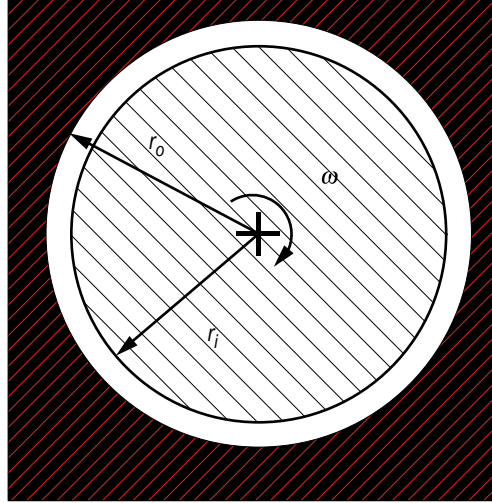
Figure 17. Rotating annular duct resistance option parameters.

$$K_f = \frac{fL}{\rho_u \pi^2 A^2 g_c \left(r_o - r_i \right)} \ . \tag{37}$$

The friction factor (f) in equation (37) was calculated from the following expressions:[19]

$$f_{0T} = 0.077 (Ru)^{-0.24} \ , \tag{38}$$

where

$$Ru = \frac{\rho_u u \, 2 \left(r_0 r_i \right)}{\mu} \tag{39}$$

and u is the mean axial velocity, therefore:

$$\frac{f}{f_{0T}} = \left[1 + 0.7656 \left(\frac{\omega r_i}{2u} \right)^2 \right]^{0.38} \ . \tag{40}$$

2.1.7.10 Rotating Radial Duct (Branch Option 10). Figure 18 shows the rotating radial duct resistance option parameters that are required by GFSSP. This option considers the branch as a rotating radial duct. This option accounts only for the frictional losses encountered with this type of flow. Since centrifugal effects are also important in a rotating radial duct, the user must select this option and activate the rotational term in the momentum conservation equation (2).
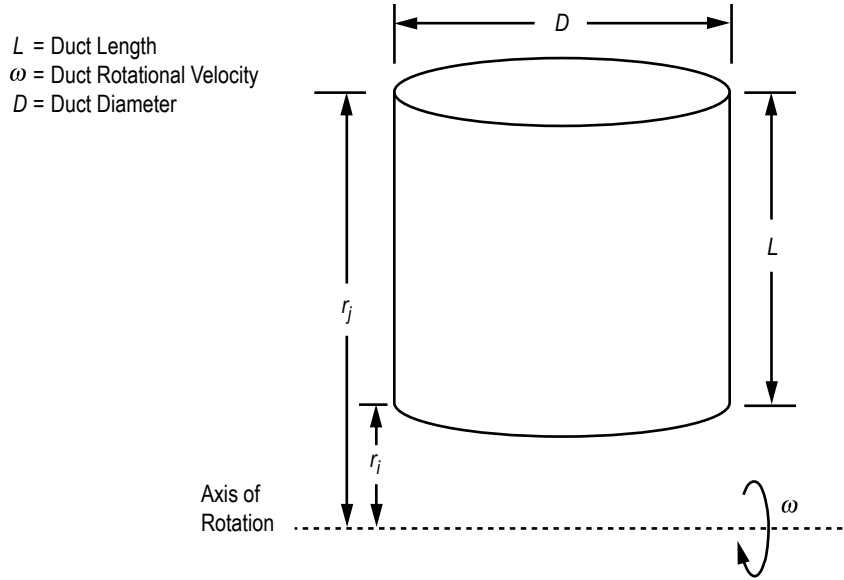
Figure 18. Rotating radial duct resistance option parameters.

The length and diameter of the duct are L and D, respectively. The rotational speed is ω rad/s. For this option, K_f can be expressed as:

$$K_f = \frac{8 f L}{\rho_u \pi^2 D^5 g_c} \;.$$
(41)

The friction factor (f) in equation (41) was calculated from the following equations:[20]

$$f_{0T} = 0.0791 (\text{Re})^{-0.25}$$
(42)

and

$$\frac{f}{f_{0T}} = 0.942 + 0.058 \left[\left(\frac{\omega D}{u} \right) \left(\frac{\omega D^2}{v} \right) \right]^{0.282} \;.$$
(43)

2.1.7.11 Labyrinth Seal (Branch Option 11). Figure 19 shows the labyrinth seal resistance option parameters that are required by GFSSP. This option considers the branch as a labyrinth seal. The number of teeth, clearance, and pitch are n, c, and m respectively. For this option, K_f can be expressed as:
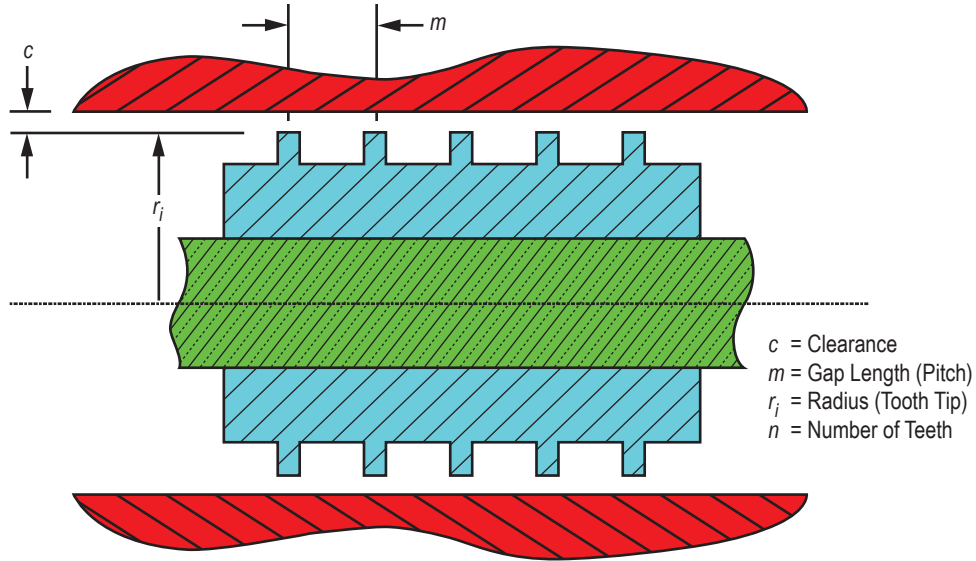
Figure 19. Labyrinth seal resistance option parameters.

$$K_f = \frac{\left(1/\varepsilon^2 + 0.5\right) n + 1.5}{2 g_c\, \rho_u \alpha^2 A^2} \quad , \tag{44}$$

where the carryover factor, ε, is expressed as:

$$\varepsilon = \sqrt{\frac{1}{1 - \dfrac{(n-1)\; c\,/\,m_p}{n(c\,/\,m + 0.02)}}} \quad . \tag{45}$$

For a straight labyrinth seal, α should be set to unity. For a stepped labyrinth seal, α should be less than unity. A value of 0.9 has been recommended for many rocket engine turbopump applications.

2.1.7.12 Flow Between Parallel Plates (Branch Option 12). Figure 20 shows the parallel flat plate resistance option parameters that are required by GFSSP. This option considers the branch as having laminar flow between parallel flat plates. A face seal can be modeled using this option. The flow is assumed to occur between two parallel plates separated by a distance equal to the clearance between the shaft and the housing. The effect of curvature is neglected. The length, inner diameter, and clearance of the seal are L, D, and c, respectively. For this option, K_f can be expressed as:[21]
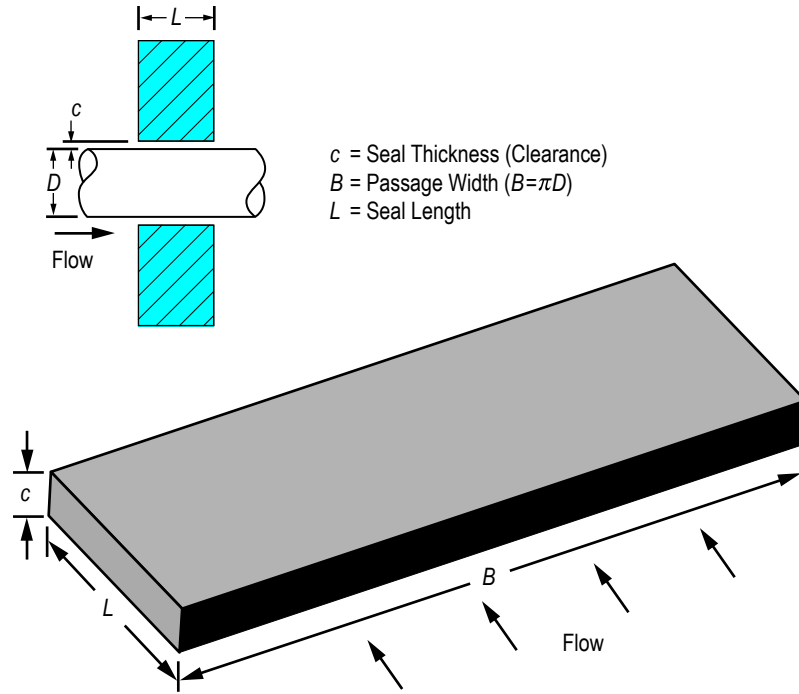
Figure 20. Parallel flat plate resistance option parameters.

$$K_f = \frac{12\mu \, L\rho}{\pi g_c D_c^3 |\dot{m}|} \; . \tag{46}$$

2.1.7.13 Common Fittings and Valves (Branch Option 13). This option considers the branch as common fittings or valves. The resistance in common fittings and valves can be computed by the two-K method.[22] For this option, K_f can be expressed as:

$$K_f = \frac{K_1 / \mathrm{Re} + K_\infty (1 + 1/D)}{2 g_c \rho_u A^2} \; , \tag{47}$$

where

K_1 $= K$ for the fitting at Re $=1$.
K_∞ $= K$ for the fitting at Re $= \infty$.
D $=$ internal diameter of attached pipe (in).

The constants K_1 and K_∞ for common fittings and valves are listed in table 7.

33

Table 7. Constants for two-K method of hooper for fittings/valves (GFSSP resistance option 13).

Fitting Type			K_1	K_∞
90° elbows	Standard (R/D = 1), screwed		800	0.40
	Standard (R/D = 1), flanged or welded		800	0.25
	Long radius (R/D = 1.5), all types		800	0.20
	Mitered (R/D = 1.5)	1 weld (90° angle)	1,000	1.15
		2 welds (45° angle)	800	0.35
		3 welds (30° angle)	800	0.30
		4 welds (22.5° angle)	800	0.27
		5 welds (18° angle)	800	0.25
45° elbows	Standard (R/D = 1), all types		500	0.20
	Long radius (R/D = 1.5), all types		500	0.15
	Mitered, 1 weld, 45° angle		500	0.25
	Mitered, 2 weld, 22.5° angle		500	0.15
180° elbows	Standard (R/D = 1), screwed		1,000	0.60
	Standard (R/D = 1), flanged or welded		1,000	0.35
	Long radius (R/D = 1.5), all types		1,000	0.30
Tee, used as elbow	Standard, screwed		500	0.70
	Long radius, screwed		800	0.40
	Standard, flanged or welded		800	0.80
	Stub-in-type branch		1,000	1.00
Tee, flow through	Screwed		200	0.10
	Flanged or welded		150	0.50
	Stub-in-type branch		100	0.0
Valves	Gate, ball, plug ($\beta = d_{orifice}/d_{pipe}$)	Full line size, $\beta = 1.0$	300	0.10
		Reduced trim, $\beta = 0.9$	500	0.15
		Reduced trim, $\beta = 0.8$	1,000	0.25
	Globe, standard		1,500	4.0
	Globe, angle or Y-type		1,000	2.0
	Diaphragm, dam type		1,000	2.0
	Butterfly		800	0.25
	Check	Lift	2,000	10.0
		Swing	1,500	1.5
		Tilting Disk	1,000	0.5

2.1.7.14 Pump Characteristics (Branch Option 14). This option considers the branch as a pump with given characteristics. The pump characteristics must be expressed as:

$$\Delta p = A_0 + B_0 \dot{m}^2 \, , \tag{48}$$

where

Δp = pressure rise (lbf/ft^2).
$\dot{m}$ = flow rate (lbm/s).

The momentum source (S) in equation (2) is then expressed as:

$$S = \Delta p \, A \, . \tag{49}$$

34

2.1.7.15 Pump Horsepower (Branch Option 15). This option considers the branch as a pump with a given horsepower (P) and efficiency (η). The momentum source (S) in equation (2) is then expressed as:

$$S = \frac{550\rho_u P\eta\ A}{\dot{m}}\ .$$

(50)

2.1.7.16 Valve With a Given Loss Coefficient (Branch Option 16). This option considers the branch as a valve with a given flow coefficient (C_v). The flow coefficient is the volume (in gallons) of water at 60 °F that will flow per minute through a valve with a pressure drop of 1 psi across the valve. The recommended formula for C_v determination with water is:

$$C_v = Q\sqrt{\frac{1}{\Delta p}}\ ,$$

(51)

where Q is the volumetric flow rate in gallons per minute of water at 60° F and Δp is the pressure drop in psia. For this option, K_f can be expressed as:

$$K_f = \frac{4.68 \times 10^5}{\rho_u C_v^2}\ .$$

(52)

2.1.7.17 Joule-Thompson Device (Branch Option 17). This option considers the branch as a Viscojet,[23] which is a specific type of flow resistance with relatively large flow passages with very high pressure drops. The flow rate through the Viscojet is given by:

$$w = 10,000\ k_v\ \frac{V_f}{L_\Omega}\sqrt{\Delta p\ S}\ (1-x)\ ,$$

(53)

where w is the flow rate in lbm/hr, L_Ω is the resistance of the fluid device, k_v is an empirical factor, and V_f is the viscosity correction factor.

For this option, K_f can be expressed as:

$$K_f = \frac{18.6624}{S}\left(\frac{L_\Omega}{V_f k_v (1-x)}\right)^2\ .$$

(54)

2.1.7.18 Control Valve (Branch Option 18). This is an exclusively transient option that considers the branch as a control valve that monitors the pressure at some arbitrary point downstream of the valve and opens and closes to maintain that pressure within a prescribed tolerance. This option was originally developed for use with the pressurization option to model on/off, or 'bang-bang,' pressurization systems as shown in figure 21. The valve is regarded as a flow restriction with a given flow coefficient (C_L) and area (A), and uses equation (18) to calculate K_f for the valve.
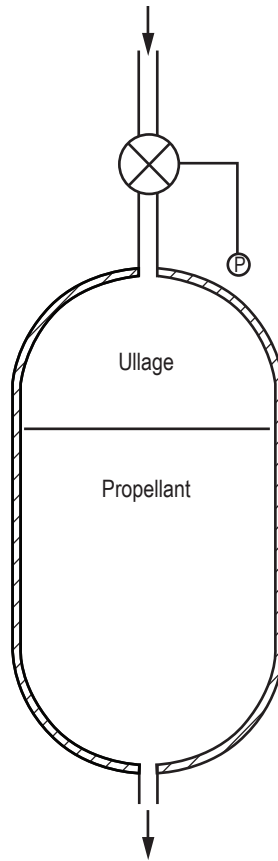
Figure 21. Control valve in a pressurization system.

The remaining inputs for the control valve option define its open/close characteristics. The suboption determines the type of open/close response of the valve (instantaneous, linear, or nonlinear) and the valve initial position describes whether the valve is initially open or closed. The control node defines the location in the model where the control valve option is to monitor and maintain the pressure while the pressure tolerance file name provides the code with the name of the file containing the pressure tolerance data for the control valve. For a linear open/close response, the time to open/close and the number of time steps needed to complete that response are provided as additional inputs. Finally, for a nonlinear open/close response, the file names for the open and close characteristics of the valve are required as additional inputs.

2.1.7.19 User-Defined Resistance (Branch Option 19). This option allows users to create a new resistance option that is not available in GFSSP library. Once this option is chosen, the user is required to supply the coding for calculating K_f for this option in the user subroutine to be described in the following section. In the preprocessor, the user is required to supply the cross-sectional area of the branch.

2.1.7.20 Heat Exchanger Core (Branch Option 20). This option considers branch as a heat exchanger core. In a typical heat exchanger core (fig. 22), the fluid goes past a tube bank to allow heat transfer between fluids in the main duct and fluids within the tubes. Free flow area is reduced
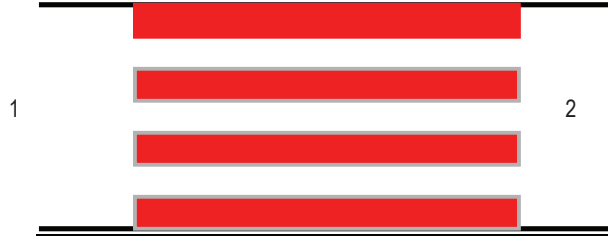
Figure 22. Heat exchanger core.

and there is larger surface area of contact between fluid and solid walls. Sections 1 and 2 in figure 22 represent inlet and outlet of the heat exchanger core, respectively. The pressure drop through the heat exchanger core can be expressed as:[24]

$$\Delta p = \frac{G^2}{2g_c} v_1 \left[\left(K_c + 1 - \sigma^2 \right) + 2 \left(\frac{v_2}{v_1} - 1 \right) + f \frac{A_s}{A_c} \frac{v_m}{v_1} - \left(1 - \sigma^2 - K_e \right) \frac{v_2}{v_1} \right] . \tag{55}$$

Equation (55) can be rewritten as:

$$\Delta p = \frac{1}{2\rho_1 g_c A_c^2} \left[\left(K_c + 1 - \sigma^2 \right) + 2 \left(\frac{\rho_1}{\rho_2} - 1 \right) + f \frac{A_s}{A_c} \frac{\rho_1}{\rho_{avg}} - \left(1 - \sigma^2 - K_e \right) \frac{\rho_1}{\rho_2} \right] \dot{m}^2 . \tag{56}$$

Therefore, K_f can be expressed as:

$$K_f = \frac{\left(K_c + 1 - \sigma^2 \right) + 2 \left(\frac{\rho_1}{\rho_2} - 1 \right) + f \frac{A_s}{A_c} \frac{\rho_1}{\rho_{avg}} - \left(1 - \sigma^2 - K_e \right) \frac{\rho_1}{\rho_2}}{2\rho_1 g_c A_c^2} . \tag{57}$$

2.1.7.21 Parallel Tube (Branch Option 21). This option considers branch as a parallel tube where fluid flows through n number of tubes (fig. 23). The flow is assumed to be distributed uniformly in all tubes. This resistance option calculates the pressure drop in the parallel tube. For this option, K_f can be expressed as:

$$K_f = \frac{8 f L}{\rho_u \pi^2 D^5 g_c n^2} . \tag{58}$$

2.1.7.22 Compressible Orifice (Branch Option 22). This option considers branch as an orifice for compressible flow. In this option, unlike other options, flow rate is calculated from a simplified momentum equation (eq. (3c)). There is no need to calculate K_f for this option. The input to this option is identical to option 2 (flow-through restriction).
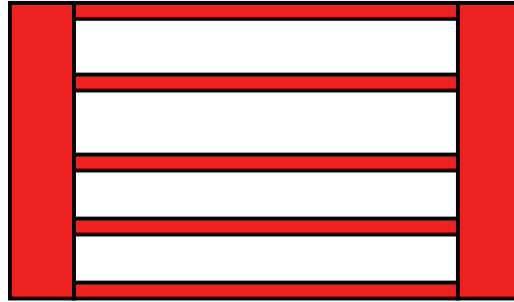
Figure 23. Parallel tube.

2.2 Solution Procedure

GFSSP numerically solves the governing equations described in the previous section to compute pressure, temperature, flow rate, and other fluid properties in a given flow circuit. The mathematical closure is described in table 8 where each variable and the designated governing equation to solve that variable are listed. It may be noted that the pressure is calculated from the mass conservation equation although pressure does not explicitly appear in equation (1). This is, however, possible in the iterative scheme where pressures are corrected to reduce the residual error in mass conservation equation. This practice was first implemented in a semi-implicit pressure linked equation (SIMPLE) algorithm proposed by Patankar and Spalding[25] and commonly referred to as 'pressure based' algorithm in computational fluid dynamics literature. The momentum conservation equation (eq. (2)) which contains both pressure and flow rate is solved to calculate the flow rate. The strong coupling of pressure and flow rate requires that mass and momentum conservation equations are solved simultaneously.

Table 8. Mathematical closure.

Variable Number	Variable Name	Designated Equation to Solve the Variable
1	Pressure	Mass conservation
2	Flow rate	Momentum conservation
3	Fluid enthalpy or entropy	Energy conservation of fluid
4	Solid temperature	Energy conservation of solid
5	Specie concentration	Species conservation
6	Fluid mass	Thermodynamic state

The energy conservation equation can either be expressed in terms of enthalpy or entropy. The temperature, density, and other thermophysical properties, such as viscosity, specific heats are computed either from pressure and enthalpy or from pressure and entropy using thermodynamic property programs, GASP[10]/WASP[11] or GASPAK.[12] In flow circuits where solid to fluid heat transfer is present, the energy conservation equation for solid is solved to calculate the solid temperature. The rate of heat transfer between solid to fluid appears as source or sink term in the energy conservation equations of fluid and solid.

For a mixture, the conservation equations of species are solved to compute the mass fraction of species. Unlike single fluid, the energy equation is solved in terms of temperature (eq. (15)) instead of enthalpy or entropy. For each specie density and other thermophysical properties such as viscosity, specific heats are computed from pressure and temperature using the above-mentioned thermodynamic property programs.

For a transient problem, fluid mass is required in mass and momentum conservation equations (eqs. (1) and (2)). GFSSP uses the thermodynamic equation of state (eq. (8)) to calculate resident mass in an internal node where density, compressibility factor, and temperature are computed.

There are two types of numerical methods available to solve a set of nonlinear coupled algebraic equations: (1) the successive substitution method and (2) the Newton-Raphson method. In the successive substitution method, each equation is expressed explicitly to calculate one variable. The previously calculated variable is then substituted into the other equations to calculate another variable. In one iterative cycle, each equation is visited. The iterative cycle is continued until the difference in the values of the variables in successive iterations becomes negligible. The advantages of the successive substitution method are its simplicity to program and its low code overhead. The main limitation, however, is finding an optimum order for visiting each equation in the model. This visiting order, which is called the information flow diagram, is crucial for convergence. Under-relaxation (partial substitution) of variables is often required to obtain numerical stability. Details of the successive substitution method appear in appendix B.

In the Newton-Raphson method, the simultaneous solution of a set of nonlinear equations is achieved through an iterative guess and correction procedure. Instead of solving for the variables directly, correction equations are constructed for all of the variables. The intent of the correction equations is to eliminate the error in each equation. The correction equations are constructed in two steps: (1) The residual errors in all of the equations are estimated and (2) the partial derivatives of all of the equations, with respect to each variable, are calculated. The correction equations are then solved by the Gaussian elimination method. These corrections are then applied to each variable, which completes one iteration cycle. These iterative cycles of calculations are repeated until the residual error in all of the equations is reduced to a specified limit. The Newton-Raphson method does not require an information flow diagram. Therefore, it has improved convergence characteristics. The main limitation to the Newton-Raphson method is its requirement for a large amount of computer memory. Details of the Newton-Raphson method appear in appendix C.

In GFSSP, a combination of the successive substitution method and the Newton-Raphson method is used to solve the set of equations. This method is called SASS (simultaneous adjustment with successive substitution) (fig. 24). In this scheme, the mass and momentum conservation equations are solved by the Newton-Raphson method. The energy and specie conservation equations are solved by the successive substitution method. The underlying principle for making such a division was that the equations that are more strongly coupled are solved by the Newton-Raphson method. The equations that are not strongly coupled with the other set of equations are solved by the successive substitution method. Thus, the computer memory requirement can be significantly reduced while maintaining superior numerical convergence characteristics.

Iteration Loop	Governing Equations	Variables
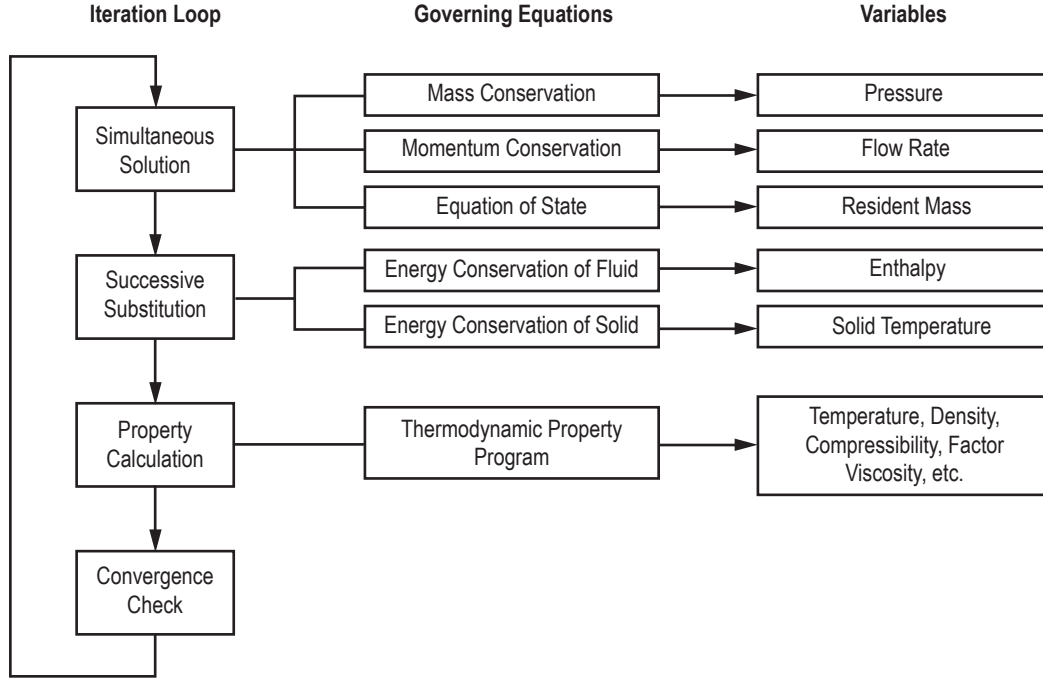
Figure 24. SASS (simultaneous adjustment with successive substitution) scheme for solving governing equations.

SASS has two options available. In one option, there are two iterative loops—inner and outer. In the inner iterative loop, mass and momentum conservation equations are solved by the Newton-Raphson scheme. For unsteady formulation, the equation of state is also solved by the Newton-Raphson scheme in addition to mass and momentum conservation equations. In the outer loop, the energy and specie conservation equations are solved by the successive substitution method. The outer loop also calculates the density and other thermodynamic and thermophysical properties and the flow resistance coefficient (K_f) which is a function of density. This option is called nonsimultaneous option. The total number of iterations in this option can be expressed as:

$$N_{total} = \sum_{i=1}^{n_0} n_i \ , \tag{59}$$

where n_0 is the number of outer iterations and n_i is the number of inner iterations. The inner iterative cycle is terminated when the normalized maximum correction (Δ_{max}), is less than the convergence criterion (C_c). Δ_{max} is determined from

$$\Delta_{max} = \text{MAX} \left| \sum_{i=1}^{N_E} \frac{\Phi'_i}{\Phi_i} \right| \ , \tag{60}$$

where N_E is the total number of equations solved by the Newton-Raphson scheme

40

N_E = Number of nodes + number of branches (steady flow)

N_E = Number of nodes $\times$ 2 + number of branches (unsteady flow).

The outer iteration is terminated when Δ^o_{max} is less than the convergence criterion (C_c). Δ^o_{max} is determined from

$$\Delta^o_{max} = \text{MAX} \left| \Delta K_f, \Delta_\rho, \Delta_h, \text{ or } \Delta_s \right| , \tag{61}$$

where

$$\Delta K_f = \text{MAX} \left| \sum_{i=1}^{N_B} \frac{K'_f}{K_f} \right|$$

$$\Delta_\rho = \text{MAX} \left| \sum_{i=1}^{N_N} \frac{\rho'}{\rho} \right|$$

$$\Delta_h = \text{MAX} \left| \sum_{i=1}^{N_N} \frac{h'}{h} \right|$$

$$\Delta_s = \text{MAX} \left| \sum_{i=1}^{N_N} \frac{s'}{s} \right| . \tag{62}$$

N_B and N_N are the number of branches and nodes, respectively, in a flow circuit.

In the second option, there is only one iterative loop. During the iterative cycle mass, momentum and the equation of state are first solved by the Newton-Raphson scheme. Then the energy and specie conservation equations are solved by the successive substitution method. The iterative cycle is terminated when the normalized maximum correction, Δ_{max}, is less than the convergence criterion (C_c).

This option is called simultaneous option and is more efficient than nonsimultaneous option. The nonsimultaneous option, however, is more numerically stable. With the help of a logical variable.

3. COMPUTER PROGRAM

The purpose of this section is to describe the structure and major functions of the program. The main objective of the computer program is to implement the numerical algorithm described in the previous section in a way that is easy to follow, modular to allow for future extension, robust, and free of errors. There are seven major functions of the computer program:

(1) Development of a flow circuit with fluid and solid nodes with branches and conductors.

(2) Development of an indexing system or data structure to define a network of fluid and solid nodes with branches and conductors.

(3) Generation of conservation equations of fluid mass, momentum, energy and species, and solid temperatures in respective nodes and branches.

(4) Calculation of thermodynamic and thermophysical properties of the fluid and solid in nodes.

(5) Numerical solution of conservation equations.

(6) Input/output.

(7) User-defined modules.

GFSSP consists of three major modules:

(1) GUI.

(2) Solver and property (SP) module.

(3) User subroutine (US) module (fig. 25).

Functions (1) and (6) are done in the GUI, functions (2)–(6) are done in the SP module, and function (7) is done in the US module. A distinct boundary is maintained among GUI, SP, and US modules. The GUI and US modules supply the information to the SP module through an input data file and USs. The SP module returns output data file and plot files for graphical and text display of results. The maintenance of a strict boundary among three modules is a key feature of GFSSP that makes the code easy to use, maintain, and upgrade. Users are not required to know the details of the computational method to become a proficient user of the code. The modularity also helps the developer to add new capabilities with minimum impact to the existing code. This section describes the SP and US modules. The GUI module is described in section 4.
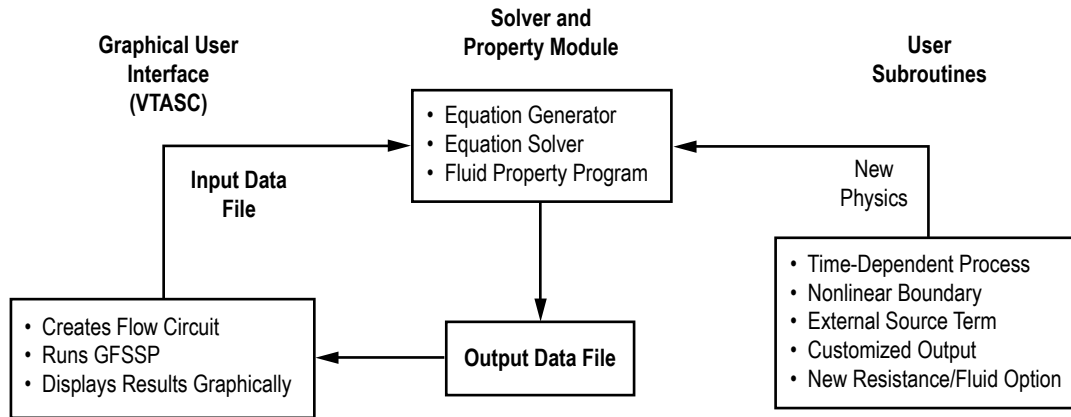
Figure 25. GFSSP process flow diagram showing interaction among three modules.

3.1 Process Flow Diagram

Figure 25 shows GFSSP's process flow diagram to describe the interaction among GUI, SP, and US modules. Users create a flow circuit in the GUI VTASC by a 'point, drag, and click' method. VTASC creates an input data file that is read by the SP module. The user runs the SP module from VTASC, which also reads the output data file generated by the SP module to display the results in the GUI. The VTASC also allows users to plot time-dependent results in Winplot.[13] Specialized input to the model can be supplied through user subroutines that also interact with the SP module. Such specialized input includes time-dependent processes; nonlinear boundary conditions; external mass, momentum, and energy sources; customized output; and new resistance and fluid options.

3.2 Solver and Property Module

The main routine and the associated set of subroutines perform seven major functions that include the following:

(1) Reading the input data file generated by VTASC, GFSSP's graphical user interface.

(2) Generation of trial solution based on the initial guess.

(3) Supply time-dependent boundary conditions for unsteady flow.

(4) Numerical solution of conservation equations by SASS scheme.

(5) Interaction with thermodynamic property programs to calculate properties at nodes.

(6) Calculation of flow resistances in the branches.

(7) Create text output and plot files.

The flow charts of the SP module for nonsimultaneous and simultaneous schemes are shown in figures 26 and 27, respectively.
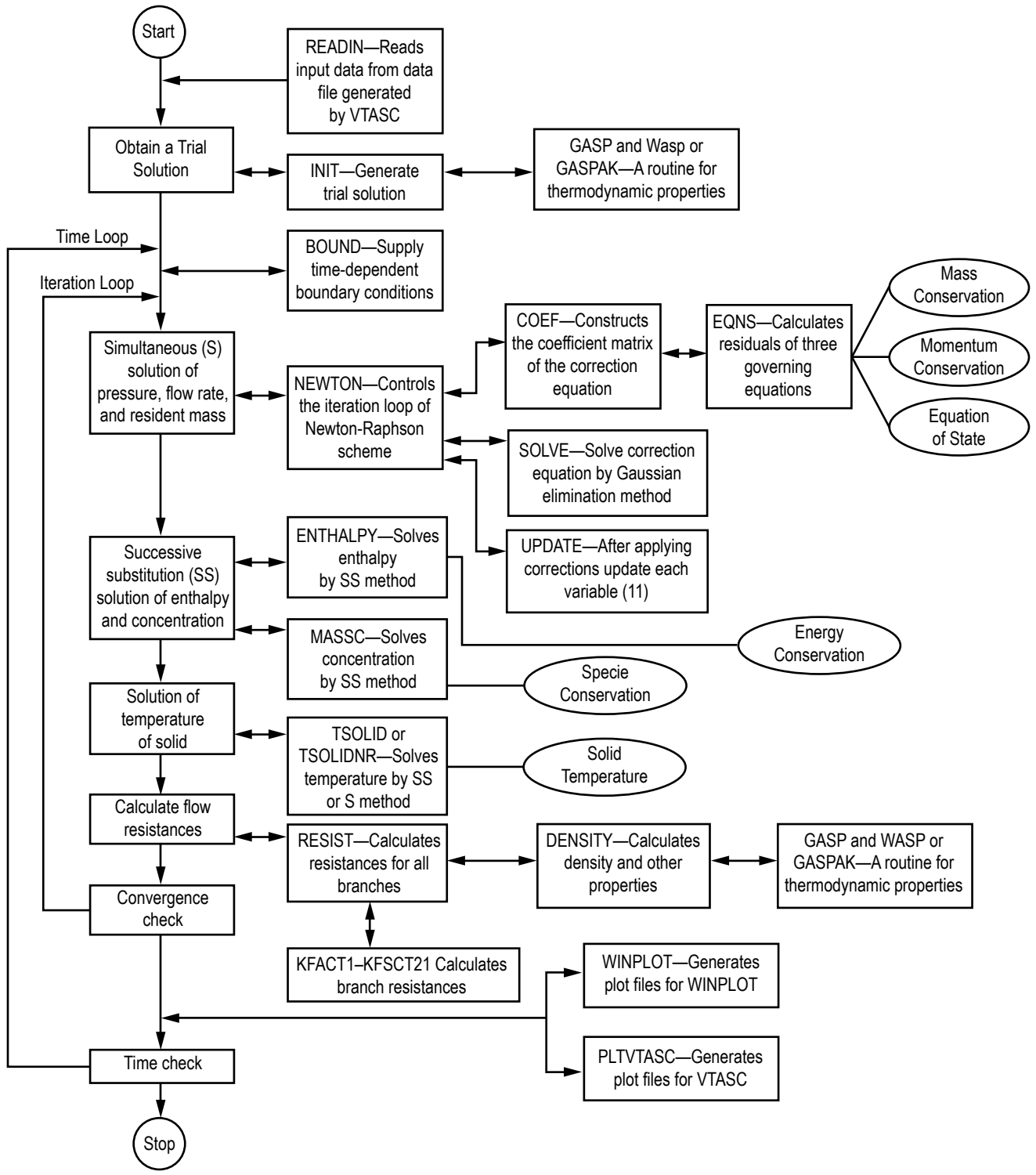
Figure 26. Flowchart of nonsimultaneous solution algorithm in solver and property module.
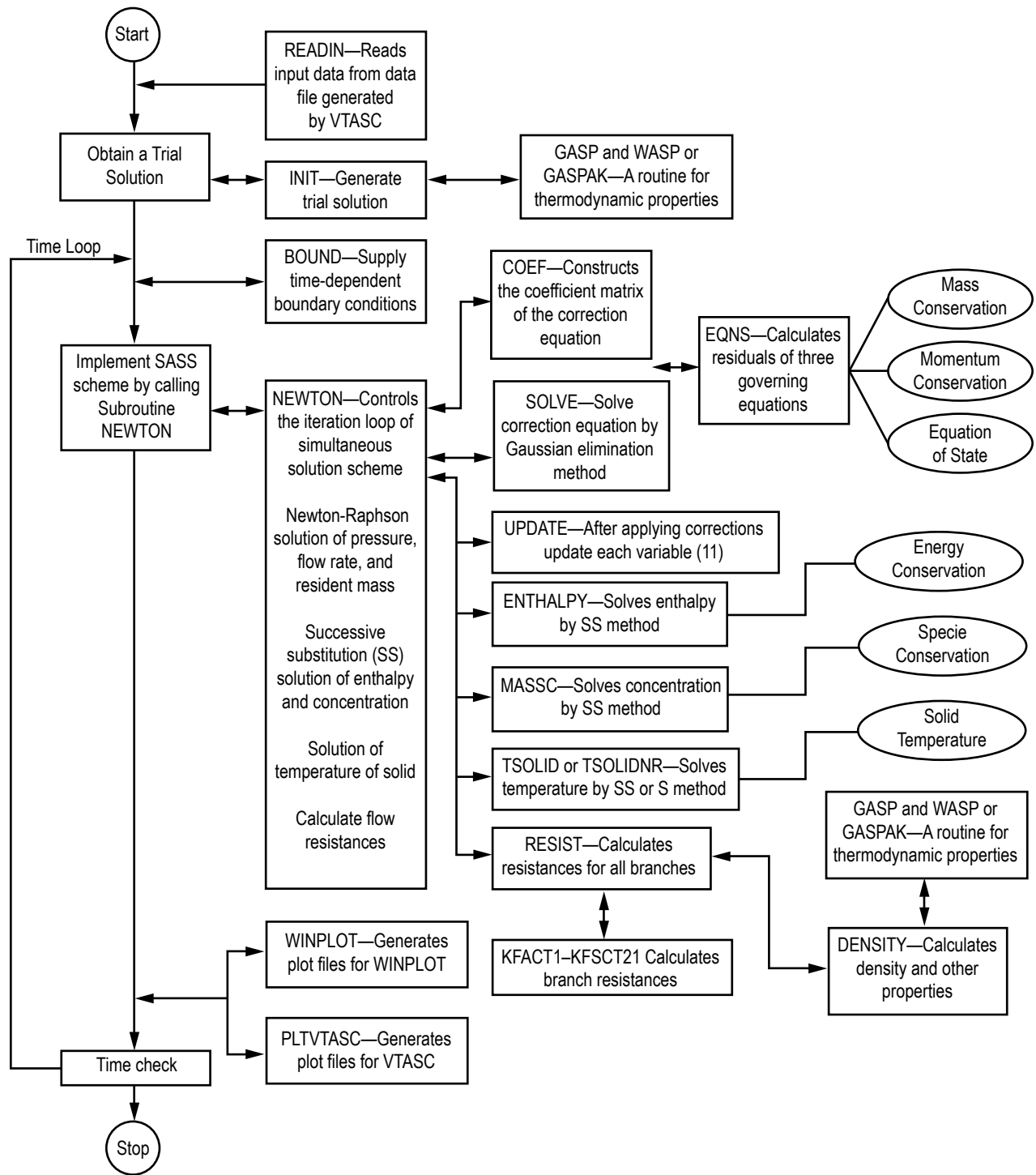
Figure 27. Flowchart of simultaneous solution algorithm in solver and property module.

3.2.1 Nonsimultaneous Solution Scheme

The flowchart of nonsimultaneous solution algorithm is shown in figure 26. In this scheme, there are two iteration cycles—outer and inner. In the inner iteration cycle, the mass and momentum conservation equation and resident equation of state are solved by the Newton-Raphson scheme until convergence. During this iteration cycle, property and resistance coefficients are not updated. In the outer iteration cycle, the energy and concentration equations are solved and density and resistance coefficients are updated and a new set of Newton-Raphson iteration is started. The outer iteration loop is repeated until the fractional change in density, resistance coefficient, and enthalpy is negligible.

The subroutine READIN reads the input data file. The subroutine INIT generates a trial solution by interacting with the thermodynamic property codes GASP, WASP, and GASPAK, or the property tables. Subroutine BOUND reads any applicable time-dependent boundary conditions from the model history files. Subroutine NEWTON conducts the Newton-Raphson solution of the mass conservation, flow rate, and energy conservation equations with the help of the subroutines EQNS, COEF, SOLVE, and UPDATE. The subroutine EQNS generates the equations. The coefficients of the correction equations are calculated in COEF. The correction equations are solved by the Gaussian elimination method in SOLVE. After applying the corrections, the variables are updated in subroutine UPDATE. This cycle of calculations is repeated until the corrections are negligible. The energy conservation equation is then solved in subroutine ENTHALPY or ENTROPY by the successive substitution scheme. For problems involving fluid mixture subroutine, MASSC is called to solve specie conservation equations. For conjugate heat transfer problems, the energy conservation equations for solid nodes are solved in subroutine TSOLID or TSOLIDNR. The resistance for each branch is calculated in RESIST following the calculation of fluid densities at each node in the subroutine DENSITY. The flow resistance coefficients (K_f) for each branch are computed in subroutines KFACT1 through KFACT18, depending upon the resistance option selected for a particular branch. The convergence of the numerical scheme is checked to determine if the cycle of calculation needs to be repeated. The solver module also calls 15 user subroutines from various subroutines.

3.2.2 Simultaneous Solution Scheme

The flowchart of the simultaneous solution algorithm is shown in figure 27. The functionality of subroutine READIN, INIT, and BOUND is identical to the nonsimultaneous scheme. In this scheme, there is only one iteration loop. The enthalpy (or entropy), concentrations, density, and resistance coefficient are updated in each Newton-Raphson iteration. Therefore, in each Newton-Raphson iteration, subroutine ENTHALPY or ENTROPY, MASSC, TSOLID or TSOLIDNR, RESIST, and DENSITY are called to compute and update all variables. The iteration loop is controlled in subroutine NEWTON. The interaction of SP and user subroutine module is identical to the nonsimultaneous scheme.

3.2.3 Conjugate Heat Transfer

GFSSP can model solid to fluid heat transfer which is commonly known as conjugate heat transfer. There are two solution options for solving the conservation equation for solid nodes—

successive substitution and Newton-Raphson. The successive substitution scheme is implemented in subroutine TSOLID and the flowchart of the subroutine is shown in figure 28. Subroutine TSOLID calls STCOND, CONVHC, RADHCF, RADHCSA, RADHCSSR, and SLDCP to estimate different terms of the conservation equation. STCOND determines the thermal conductivity from the property table. CONVHC determines the heat transfer coefficient from GFSSP's built-in correlation. CONVHC also calls subroutine USRHCF to allow the user to provide a problem-specific heat transfer coefficient. RADHCF, RADHCSA, and RADHCSSR are three subroutines called from TSOLID to compute radiation heat transfer from solid to fluid, solid to ambient, and solid to solid, respectively. SLDCP determines the specific heat from property table for computing the transient term. Subroutine QDOTSSCR calculates solid to solid conduction and radiation heat transfer.

The Newton-Raphson scheme is implemented in subroutine TSOLIDNR. The flowchart of this subroutine is shown in figure 29. TSEQNS, TSCOEF, and GAUSSY are three subroutines that perform the major functions of Newton-Raphson scheme. The residuals are calculated in TSEQNS. The flowchart of subroutine TSEQNS is shown in figure 30. TSCOEF calculates the coefficient matrix. The correction equations are solved in GAUSSY. After convergence of the numerical scheme, subroutine QDOTSSCR calculates solid to solid conduction and radiation heat transfer.
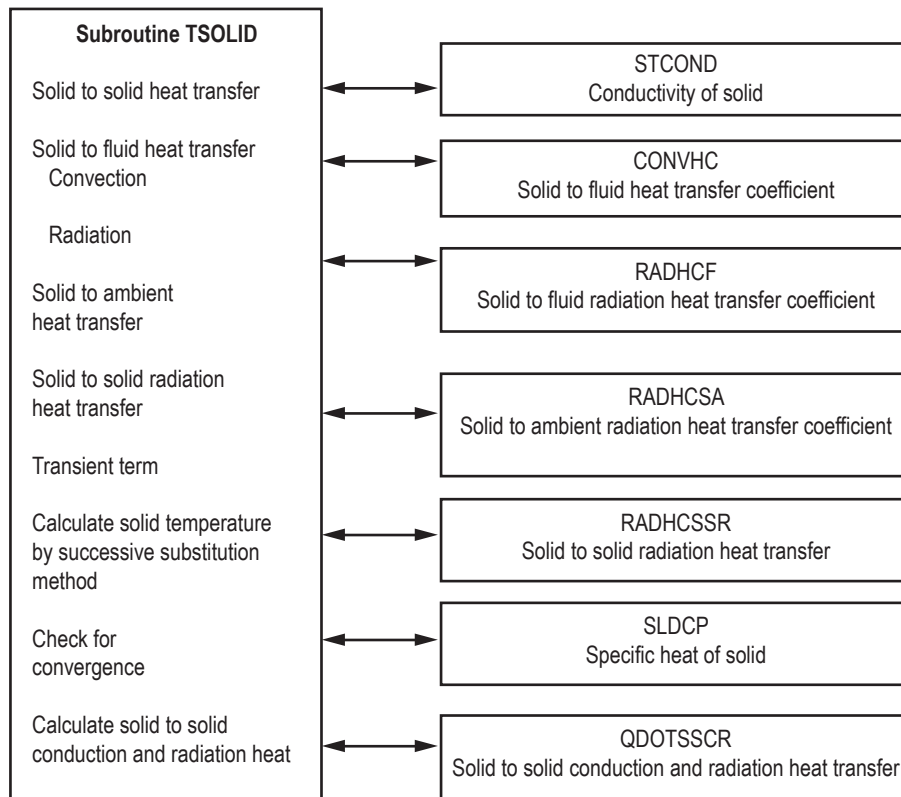
Figure 28. Solid temperature calculation by successive substitution method.
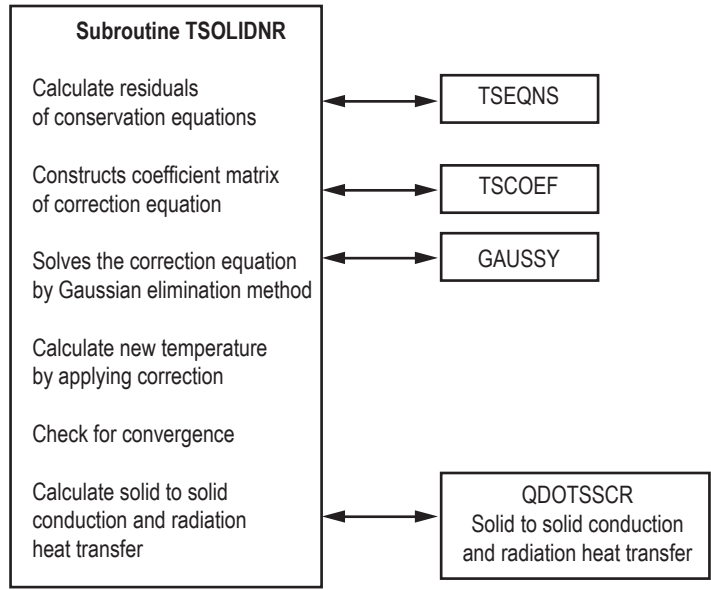
Figure 29. Solid temperature calculation by Newton-Raphson method.
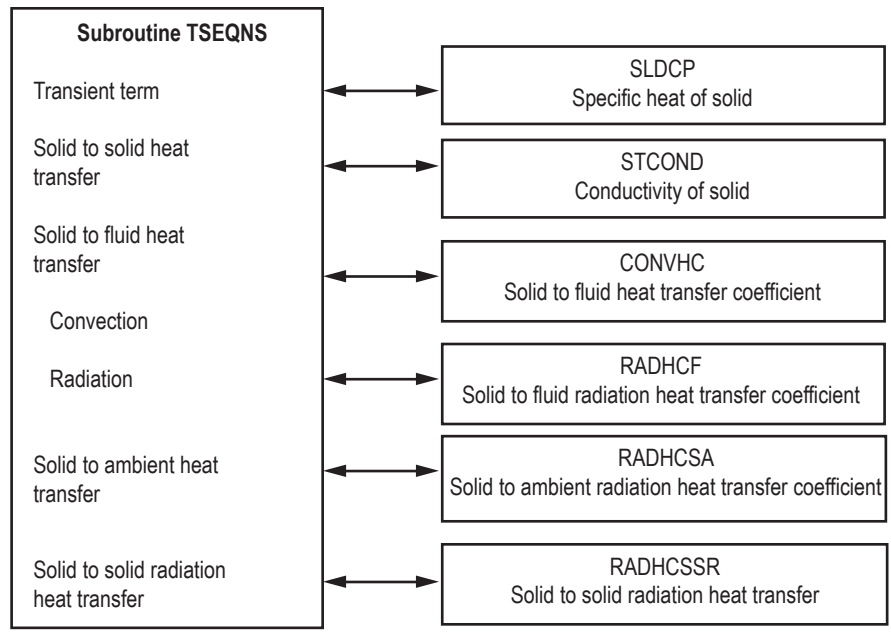
Figure 30. Calculation of residuals of energy conservation equation
for Newton-Raphson method.

3.2.4 Thermodynamic Property Package

The thermodynamic property packages included in GFSSP consist of three separate programs—GASP,[10] WASP,[11] and GASPAK.[12] It also includes tabulated data for RP-1. The GASP and WASP programs consist of a number of subroutines. GASP provides the thermodynamic properties for 10 fluids: helium, methane, neon, nitrogen, carbon monoxide, oxygen, argon, carbon dioxide, fluorine, and hydrogen. WASP provides the thermodynamic properties of water. RP-1 properties are provided in the form of tables. Subroutine RP-1 searches for the required property values from these tables. GASPAK provides thermodynamic properties for helium, methane, neon, nitrogen, carbon monoxide, oxygen, argon, carbon dioxide, hydrogen, parahydrogen, water, isobutane, butane, deuterium, ethane, ethylene, hydrogen sulfide, krypton, propane, xenon, R-11, R-12, R-22, R-32, R-123, R-124, R-125, R-134A, R-152A, nitrogen trifluoride, and ammonia.

The thermodynamic property subroutines are called from two GFSSP subroutines—INIT and DENSITY. In subroutine INIT, enthalpies and densities are computed from given pressures and temperatures at the boundary and internal nodes. In subroutine DENSITY, density, temperatures, specific heats, and specific heat ratios are calculated from given pressures and enthalpies at each node.

4. GRAPHICAL USER INTERFACE

This section introduces the VTASC, a unique GUI designed to simplify the model building process for GFSSP. VTASC allows the user to design GFSSP models using an interactive 'point and click' paradigm. The program seeks to eliminate some of the more tedious, error prone, and time-consuming operations associated with the model building process such as the selection of unique numbers for nodes, branches, and the explicit specification of the upstream and down-stream nodes for every branch. The models may be easily modified both in terms of additional nodes, branches, and the model-specific data. Figure 31 shows the main VTASC window, which consists of menu and toolbar options and a blank canvas.
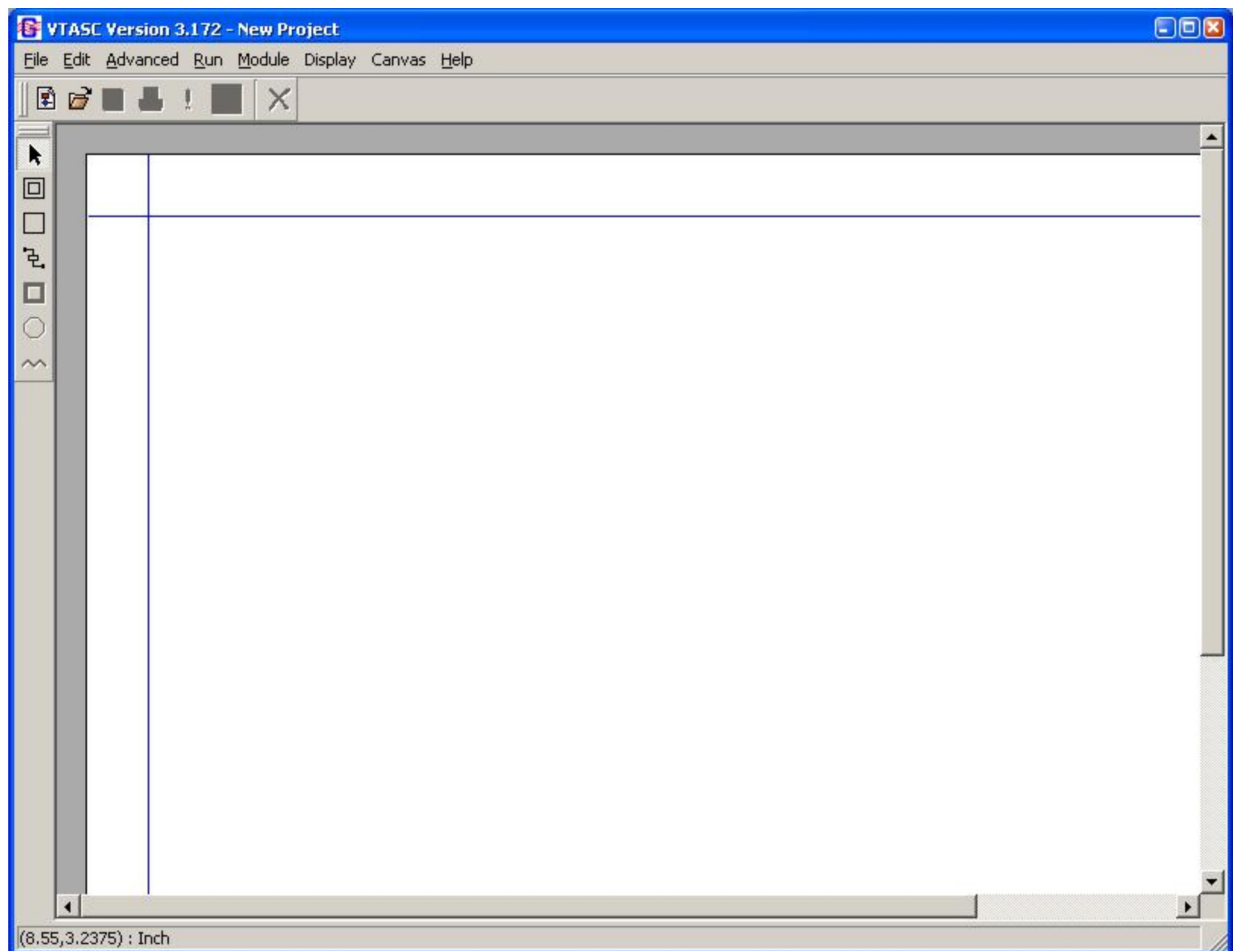
Figure 31. Main VTASC window.

4.1 Menus

4.1.1 File Menu

The file pull-down menu, shown in figure 32, contains the functions to begin a new model, open an existing model, save the model, save the model with an alternate location and name, print the model to a printer, print an image of the model to a bitmap (.bmp extension) file, write an input file for GFSSP based on the current model, and exit the application. The most commonly used of these functions are available, as shortcuts, from the file input/output toolbar. In addition, the File menu contains a listing of the nine most recently saved models.

New		Ctrl+N
Open		Ctrl+O
Save		Ctrl+S
Save As		
Print...		Ctrl+P
Print Image		
Write GFSSP file		
Exit		Ctrl+Q
1 C:\Program Files\GFSSP\Examples\Ex1\Ex1.vts		
2 C:\Program Files\GFSSP\Examples\Ex2\Ex2.vts		
3 C:\Program Files\GFSSP\Examples\Ex3\Ex3.vts		
4 C:\Program Files\GFSSP\Examples\Ex4\Ex4.vts		
5 C:\Program Files\GFSSP\Examples\Ex5\Ex5.vts		
6 C:\Program Files\GFSSP\Examples\Ex6\Ex6.vts		
7 C:\Program Files\GFSSP\Examples\Ex7\Ex7.vts		
8 C:\Program Files\GFSSP\Examples\Ex8\Ex8.vts		
9 C:\Program Files\GFSSP\Examples\Ex9\Ex9.vts		
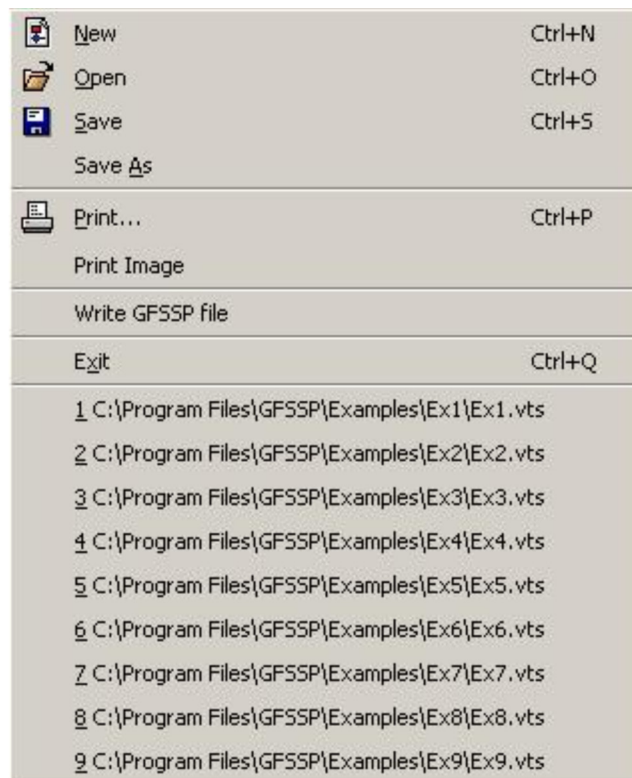
Figure 32. VTASC file menu.

The new model function will reinitialize the application to a clean state without having to exit and then restart the application. If model data are present, then the user will be prompted to continue the operation. The open model function will present a file dialog to allow the user to select a previous model; note that all model files have a '.vts' extension. The VTASC model files are not synonymous with the GFSSP input files. GFSSP compatible input files may be generated, based on the current model, as described below. The save function allows the user to save the current model to a desired location. In the case where the model has not been previously read or saved, a file dialog will appear and allow the user to save the current model to a given location. The 'save as' function works identically except that a file dialog will appear in all instances. The print function

produces a postscript file, which allows the user to print the current circuit to a printer or to a file. The print image function will save an image of the circuit in a bitmap file. The write GFSSP file function will become active once the user has input the required data; this is covered in the following section. The save and print functions are not available until at least one node is present.

4.1.2 Edit Menu

The edit pull-down menu, shown in figure 33, contains the functions to delete a selected item(s), activate the Global Options dialog, open an existing GFSSP output file using Notepad, and select all elements on the canvas. The delete function, which is not available until at least one node is present, also appears as a shortcut from the file input/output toolbar. The Global Options dialog is discussed in detail in section 4.2.
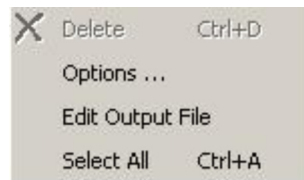
Figure 33. VTASC edit menu.

4.1.3 Advanced Menu

The advanced pull-down menu, shown in figure 34, contains the functions to activate dialogs for GFSSP's advanced options such as Transient Heat, Heat Exchanger, Tank Pressurization, Turbopump, Valve Open/Close, Fluid Conduction, and Conjugate Heat Transfer. With the exception of Conjugate Heat Transfer, these functions are not available unless the advanced option has been activated through the Global Options dialog. The advanced option dialogs are discussed in detail in section 4.4.

Figure 34. VTASC advanced menu.

4.1.4 Run and Module Menus

The run pull-down menu contains the functions to call and run GFSSP and Winplot. Both of these functions also appear as shortcuts from the file input/output toolbar. Note that Winplot is not part of the GFSSP installation package and must be obtained separately. Also note that Winplot is not made available by VTASC unless a model is defined as an unsteady model. The module menu contains the function to activate the user executable Build dialog. The user executable Build dialog is discussed in detail in section 4.6.

4.1.5 Display, Canvas, and Help Menus

The display pull-down menu contains the functions to activate the Display Results/Properties dialog and clear any results/properties displayed on the canvas. The Display Results/Properties dialog is discussed in detail in section 4.8.2. The canvas pull-down menu contains the functions to toggle between a single- or a double-page canvas. The double-page canvas configuration is useful for larger models that will not easily fit on a single-page canvas. Note that in this configuration, a print margin is defined between the two canvas pages. The area within the print margin will not appear when a model hard copy is printed, so the user should avoid placing model elements in this area. The help pull-down menu contains the function to activate a pop-up window with additional information about that particular version of VTASC.

4.2 Global Options

From the Edit menu, select the menu option labeled Options… to display the Global Options dialog shown in figure 35. A left mouse click on items listed to the extreme left allows access to the desired information within the right pane. As shown, selecting the Instructions option gives general instructions on the use of this dialog.

4.2.1 General Information

Selecting the General Information item displays the following dialog (fig. 36) to access User Information, Solution Control, and Output Control. The User Information tab shown in figure 36(a) allows specification of the title, name of the analyst, working directory, GFSSP compatible input file, the output file to be generated by GFSSP, and the name and location of the GFSSP executable that will be used to run the model. The working directory, which is the directory where VTASC will write the GFSSP input and output files associated with the model, is assigned by specifying a file path for the GFSSP input file. The installation version of GFSSP is the default executable defined for any new model. Note that the file menu option 'Write GFSSP File' will become active only when the input and output GFSSP files have been specified.

The Solution Control tab shown in figure 36(b) allows specification of certain characteristics of the solution procedure of a particular model. The user can choose either a simultaneous solution procedure or the original hybrid solution scheme. The user can also choose between the first law and second law of thermodynamics-based solution procedures for the energy equation. For the solid energy equation, the user can select either a Newton-Raphson or Successive Substitution
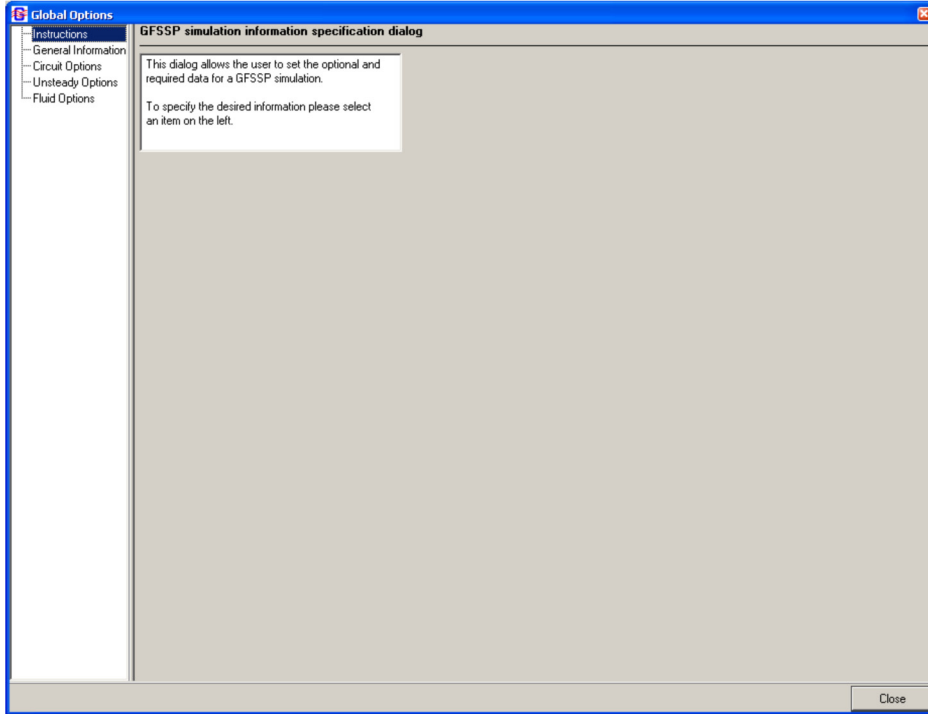
Figure 35. Global Options dialog.
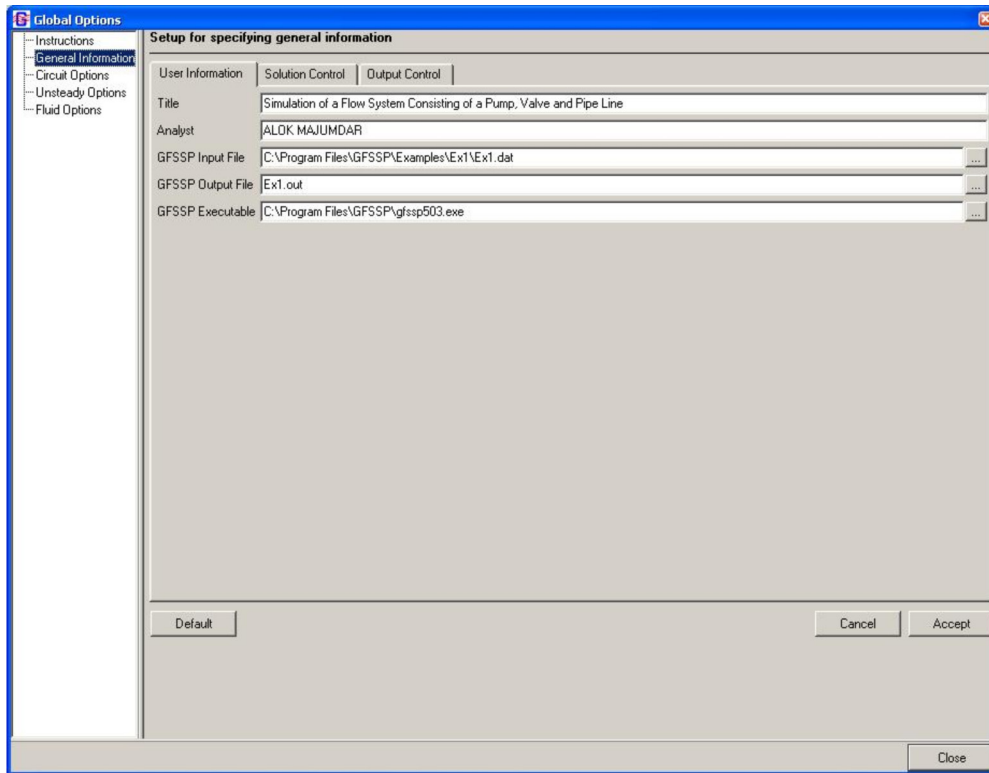
(a)
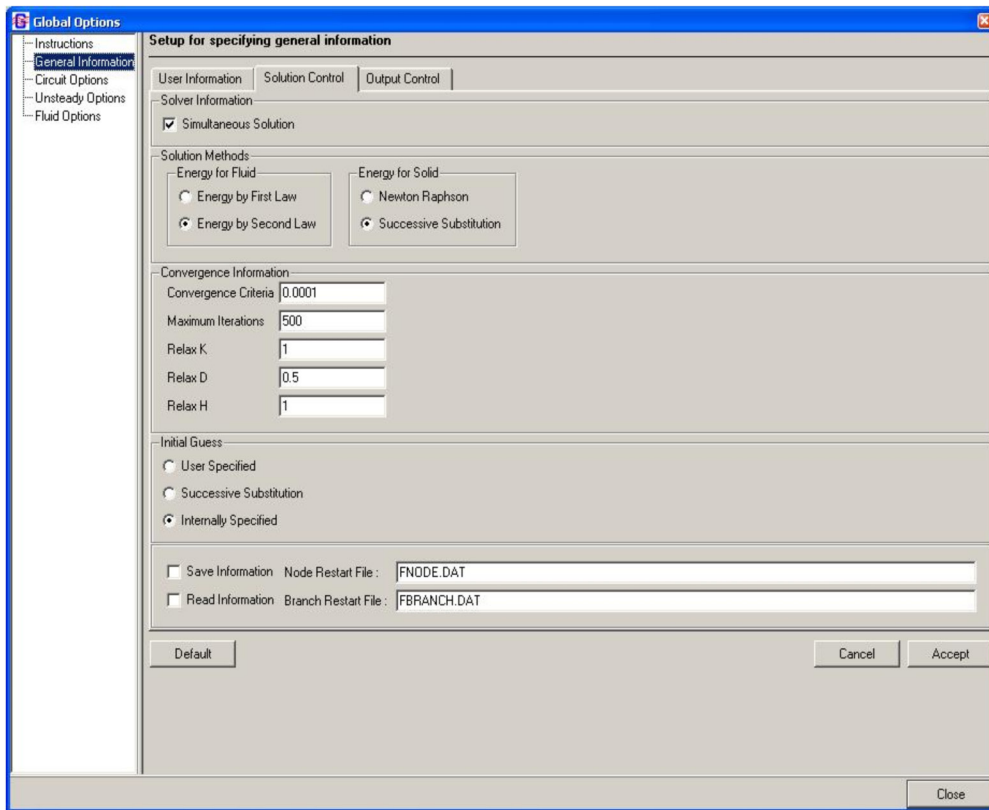
(b)
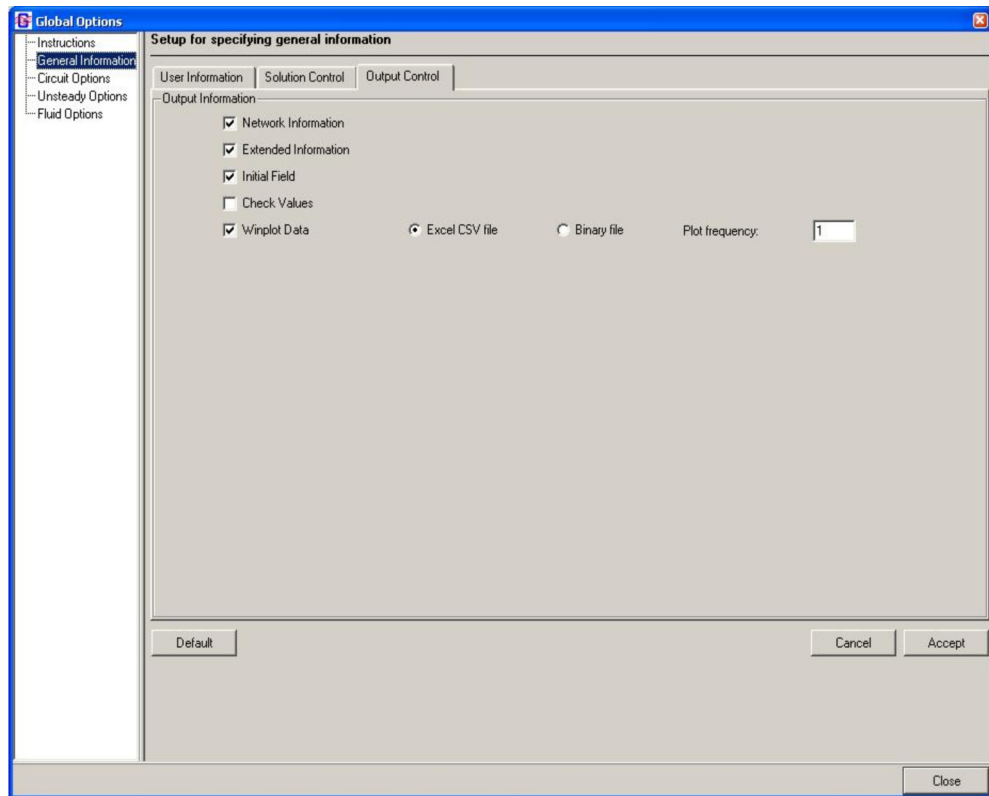
(c)

Figure 36. General Information dialogs: (a) User Information tab,
(b) Solution Control tab, and (c) Output Control tab.

solution scheme. In addition, the user can specify the convergence criteria, relaxation parameters, and choose the method by which the initial guess is made. Note that while there is an input box where the maximum number of iterations can be changed, this value is not currently being used by GFSSP. The user can also specify if they wish to use restart files by checking the appropriate box. Checking the Save Information box indicates that the user wishes to save the final solution to use as an initial guess in another model. Checking the Read Information box indicates that the user wishes to read in a previously saved solution as an initial guess. Note that if both boxes are checked, GFSSP will overwrite the initial restart files during the simulation. Two restart files are used by GFSSP for both saving and reading information. One file is used for node information and one for branch information. The user may name the restart files using the designated text boxes.

The Output Control tab shown in figure 36(c) allows specification of the type of data to output during the GFSSP simulation as well as offering the user the option to perform a sanity check on the GFSSP solution and flag any unreasonable values to the user. The solution check can be activated by choosing Check Values. The output options consist of inclusion (default) or suppression of (1) network information, (2) extended thermodynamic and thermophysical information at the nodes, (3) the initial flow field, and (4) Winplot data. For Winplot data, the user can define how often GFSSP writes output to the Winplot data files. (The default is 1, which writes output at every time step) as well as the type of file that is generated (comma separated value files or binary files.)

Note that the Accept button must be pressed to accept modifications to the data in any of the tabs. To reset the data to default on all three tabs press Default and then the Accept buttons. The Cancel button closes the General Information item without accepting any changes.

4.2.2 Circuit Options

Selecting the Circuit Options item displays the pane in figure 37, allowing access to Circuit Options and Initial Values. The Circuit tab shown in figure 37(a) allows specification of the options that will be activated for this circuit. These options include Inertia. (Note that while this option allows you to choose to supply relative angles between adjacent branches, no mechanism currently exists to define those angles using VTASC.) The user must manually edit the GFSSP input file to supply those angles. This is also discussed in section 4.5.13: Rotation, Gravity, Buoyancy (requires Gravity to be activated), Fluid Conduction (activates Fluid Conduction advanced option), Fluid Mass Injection, Heat Exchangers (activates Heat Exchanger advanced option), Turbopumps (activates Turbopump advanced option), Moving Boundary, Momentum Source, Axial Thrust, Normal Stress, Heat Source (with optional units), Cyclic Boundary, Solid-Fluid Heat Transfer Coefficient with the ability to choose method of calculation (only active for models using conjugate heat transfer), and Dalton's Law of Partial Pressure (only active for multiple fluid models). Note that activating these options may require additional inputs in other areas of VTASC.

The Initial Values tab shown in figure 37(b) allows the user to set initial values of Pressure, Temperature, etc. for both boundary and interior nodes as well as solid nodes. The initial guess for all nodes may be changed, after the model has been built, by modifying the desired data and pressing the Apply to All button.
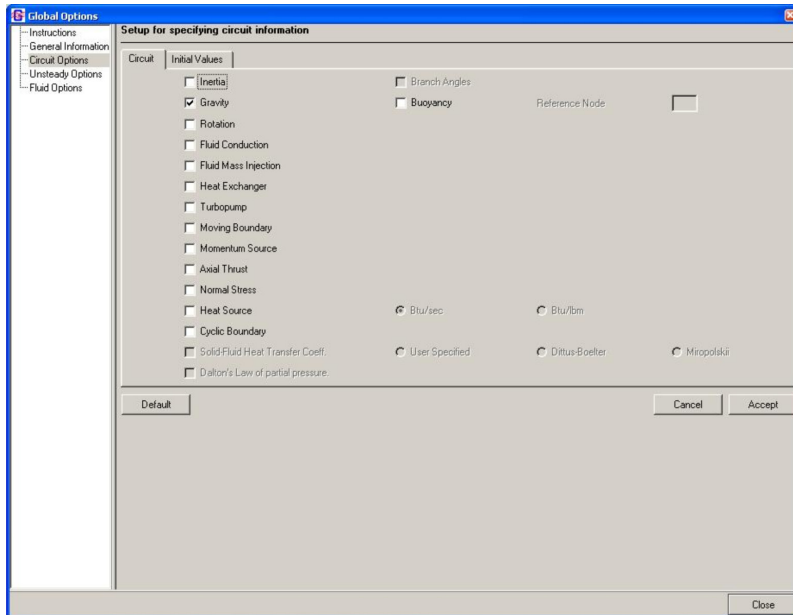
(a)
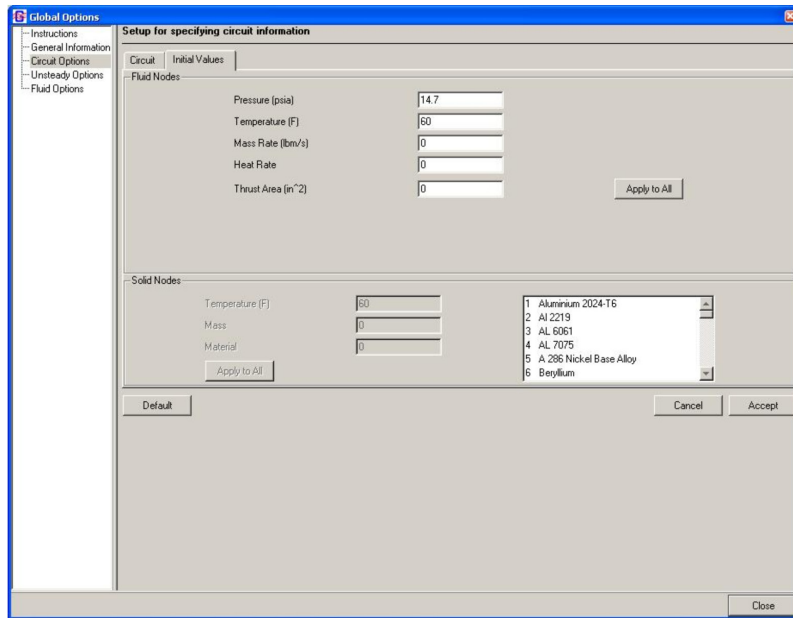
(b)

Figure 37. Circuit options dialogs: (a) Circuit tab and (b) Initial Values tab.

4.2.3 Unsteady Options

Selecting Unsteady Options displays the dialog shown in figure 38. The Unsteady Options dialog allows users to choose from various levels of unsteady modeling. The options in this window include: Steady (default), Quasi-Steady, Time Step, Start Time (a relative time—does not have to be zero), End Time, Print Interval (controls print interval to all output files except Winplot files), Unsteady, Variable Rotation (user specifies variable rotation file name), Variable Heat Load (activates Transient Heat advanced option), Variable Geometry (user specifies the variable geometry file name), Tank Pressurization (activates Tank Pressurization advanced option), and Valve Open/Close (activates Valve Open/Close advanced option). Note that activating the unsteady options may require additional inputs in other areas of VTASC.
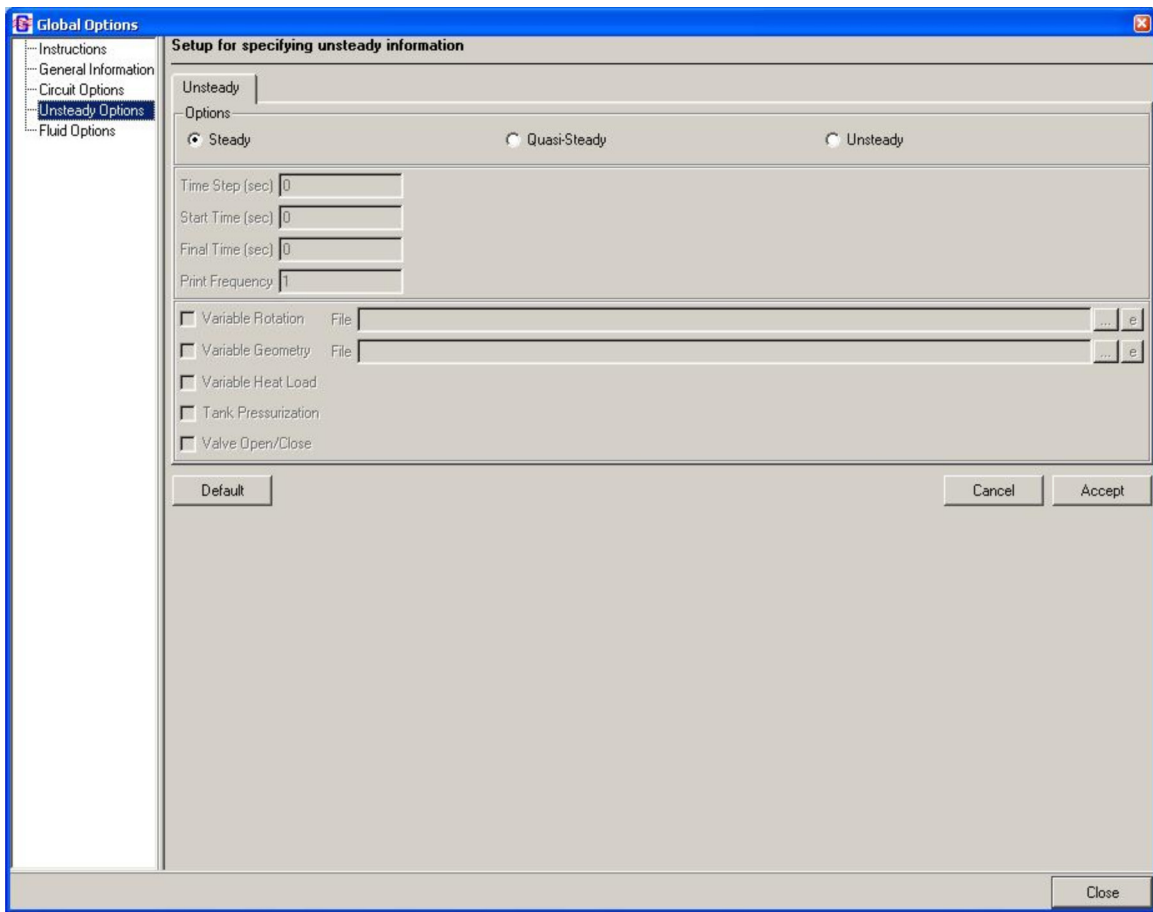
Figure 38. Unsteady Options dialog.

4.2.4 Fluid Options

Finally, selecting Fluid Options displays the dialog shown in figure 39. The Fluid Options dialog allows users to choose the thermodynamic property approach used in the model. The user can choose from the embedded thermodynamic property packages (1) GASP and WASP or (2) GASPAK. Additionally, the user can choose a constant density fluid (the energy equation is not
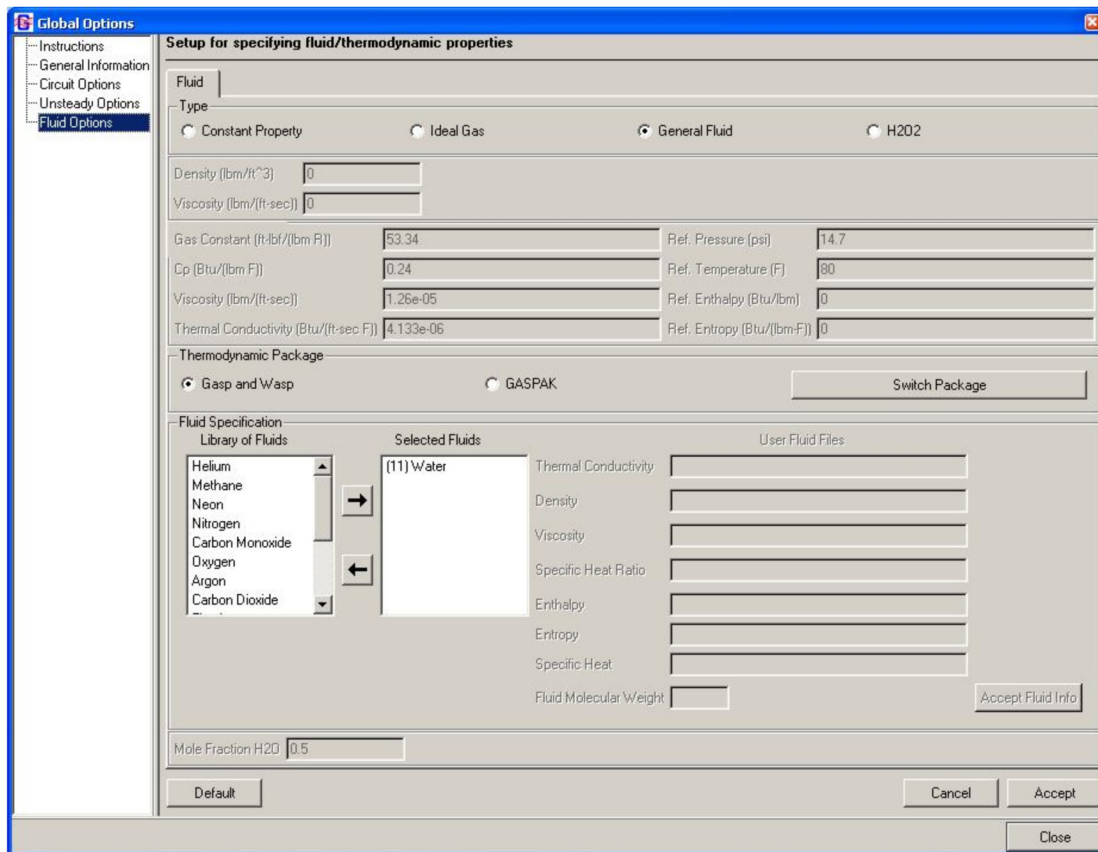
Figure 39. Fluid Options dialog.

calculated with this option and this option cannot be used with fully unsteady modeling); an ideal gas by specifying the fluid gas constant, specific heat, viscosity, thermal conductivity, reference pressure, reference temperature, reference enthalpy, and reference entropy; hydrogen peroxide, with the capability to define the mole fraction of water present in the fluid; and user-defined fluids through user-defined property files. Note that choosing the constant density fluid option causes the program to set the flow to steady and all unsteady options to be turned off.

Desired fluids from the library of fluids may be selected and added to the Selected Fluids list by pressing the ➡ button. Fluids may be deleted from the Selected Fluids list by selecting the unwanted fluids and pressing the ⬅ button. Note that a number enclosed in parentheses appears by each selected fluid. This is the GFSSP index number for that fluid. If a user fluid is selected, VTASC will prompt the user to double-click the fluid name to supply the fluid property file names and fluid molecular weight. Note that all user-defined property files must reside in the model's working directory. The Switch Package button allows the user to switch between the two available thermodynamic property packages. The Switch Package button will only work when all selected fluids are common to both fluid libraries. Note that manually switching between the two thermodynamic property packages will delete all fluids from the selected fluids list.

4.3 Fluid Circuit Design

4.3.1 Boundary and Internal Node Properties

The boundary node addition tool ▣ located on the left border of VTASC is used to place boundary nodes on the drawing area, henceforth called the canvas. Upon selection of this tool the user may add boundary nodes by moving the mouse to the canvas and pressing the left mouse button. Placing a node will activate the delete function in the toolbar, edit menu, or by typing CTRL+D. Similarly, interior nodes may be added by selecting the interior node addition tool ▢. Note that the nodes are automatically given unique numeric identifiers. Figure 40 shows a canvas with a number of boundary and interior nodes.
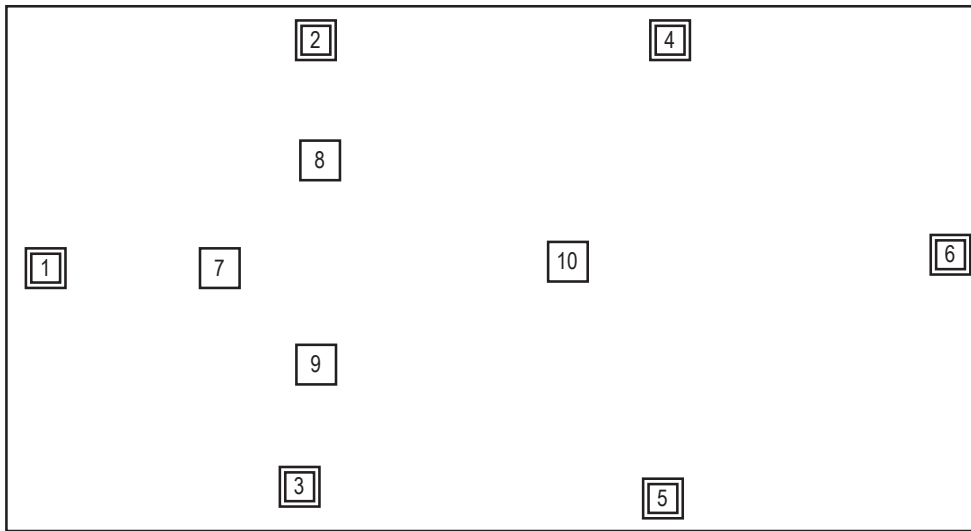
Figure 40. Boundary and internal nodes on canvas.

The selection tool ▣ is used to select the desired node and either modify its location or enable its deletion. Positioning the mouse and pressing the left button performs the selection; upon selection, the selected node will be shown with a red border. Repositioning a node is simply performed by pressing and holding the left mouse button over a node, moving the mouse to the desired location, and releasing the left mouse button. Multiple nodes may be selected for deletion by using the Ctrl keyboard button in conjunction with the mouse. The nodes may then be deleted using the Delete toolbar button as long as they are not attached to any branches. A press of the left mouse button, within the canvas, away from any nodes, will deselect any previously selected nodes.

A right mouse button press upon a node will select the node and present a pop-up menu (fig. 41), allowing the user to delete the node (will not work on multiple node selections and is not available if the node is connected to any branch), set the properties for the indicated node, or align the node either horizontally or vertically with its neighboring elements (horizontal alignment aligns

(a)

(b)
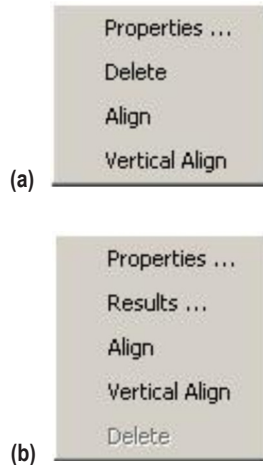
Figure 41. Node pop-up menus: (a) Boundary node and (b) internal node.

all elements to the right of the selected node, while vertical alignment aligns all elements below the selected node). Once a model has been run, the internal node pop-up menu also allows the user to activate the results dialogs, which will be discussed in section 4.8.

Choosing the Properties … option will present the dialog shown in figure 42. The appropriate inputs will be activated dependent upon the choices present within the Global Options dialog and the type of the selected node, whether boundary or interior. The user may modify the desired data within this dialog. To modify the concentration of a given fluid, select the desired fluid and type in the desired concentration. Note that directly upon selecting a fluid, the user may type without having to reposition the mouse. If the user wants to change the numeric identifier for a node, simply type in the desired numeric identifier (maximum of five numbers). The user may enter any desired descriptive text into the Node Description input box. Pressing the OK button will accept and adjust the revised data and the cancel button will reject the revised data. Also, in the case of an unsteady flow, each boundary node will be automatically assigned a unique Node History File name that is subject to user modification.

4.3.2 Branch Properties

The branch addition tool is used to specify the branches between the nodes. Selection of this tool immediately causes each interior and boundary node to be drawn with a series of 'handles' as denoted by the green squares in figure 43.

The 'handles' serve to clearly identify eight possible locations on a node where the initial (upstream) or terminal (downstream) points of a branch may be located. Note that an unlimited number of branches may initiate or terminate at each 'handle.' There are two different types of branches that may be created: the first being a directed line segment between any two nodes while the second type is two possibly discontinuous line segments. In either case, a left mouse button click on a 'handle' will initiate a branch. Once an initial 'handle' (specifies the upstream node) has been selected, further movement of the mouse will draw a directed line segment from that 'handle' to the
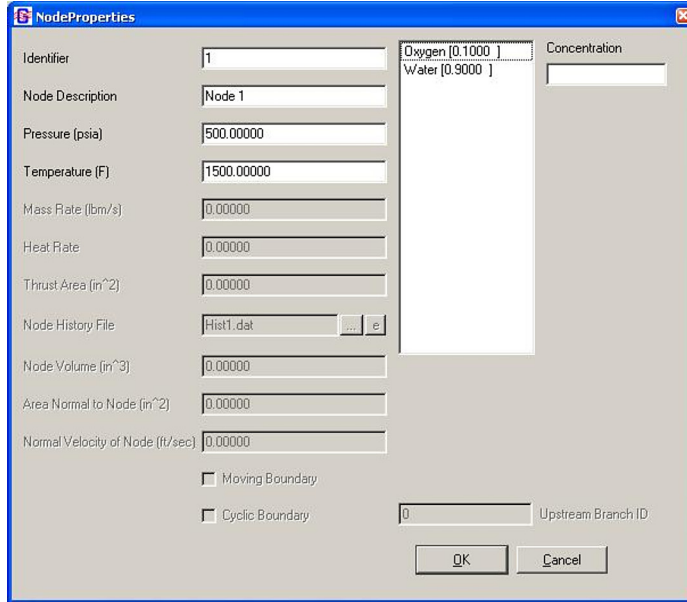
Figure 42. Node Properties dialog.
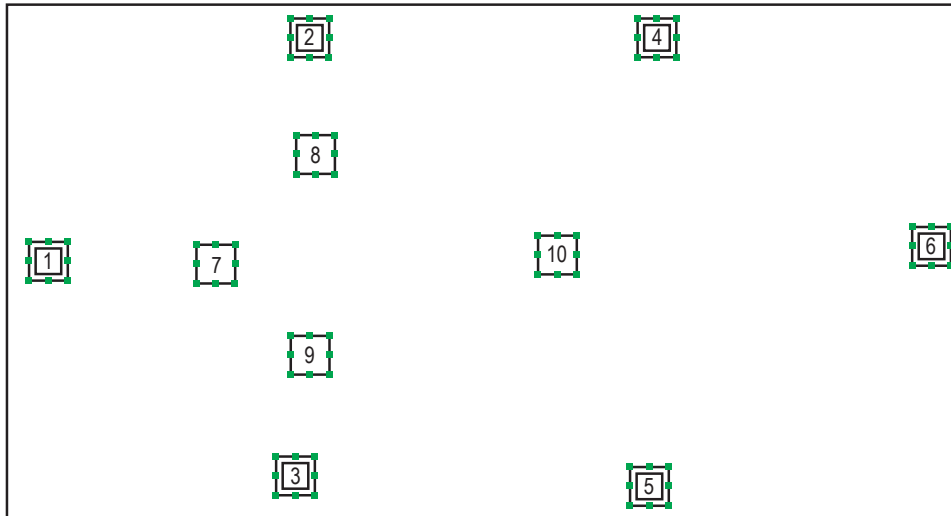
Figure 43. Nodes with branch 'handles.'

current location of the mouse, as shown in figure 44(a). For the first type of branch, selecting another 'handle' completes the branch, as this second 'handle' effectively specifies the downstream node (fig. 44(b)).

(a)

(b)

17
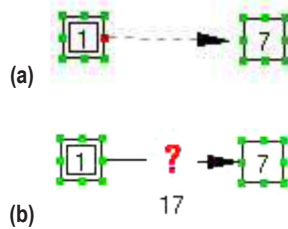
Figure 44. Direct line segment branch: (a) Step 1 and (b) step 2.

The second type of branch is initiated identically; however, after selecting an initial 'handle,' an additional anchor point may be set at any location on the canvas by a press of the left mouse button at the desired location. The branch is then completed as usual by selecting another 'handle.' This series of steps is shown in figure 45(a) and (b).

(a)

(b)

12
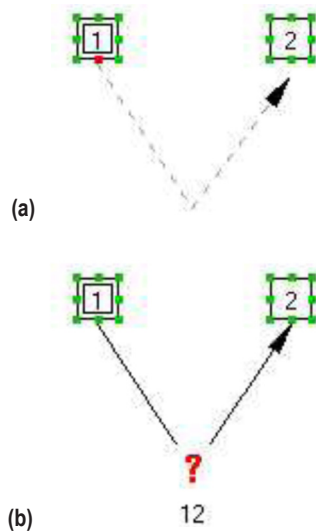
Figure 45. Two-line segment branch: (a) Step 1 and (b) step 2.

Completing a branch will activate the delete function in the toolbar, edit menu, or by typing CTRL+D. As shown in figures 44(b) and 45(b), a unique numeric branch identifier formed by concatenating adjacent node numbers is automatically generated and the directed arrowhead visually defines the branch upstream and downstream node relationship. A click on the branch addition tool may be used to clear a branch currently under design and reinitialize the process. The selection tool may be used to select the desired branch and either modify its location or enable its deletion. The Ctrl button may be used in conjunction with the mouse to select multiple branches and nodes for deletion using the Delete toolbar button. Note that a node can only be deleted using this method if all branches attached to it are deleted as well.

Figure 46 shows an example fluid circuit complete with nodes and branches.

63

Specification of a new branch shows an **?** image, which visually indicates that the resistance for this branch has not been specified. A right mouse click on the image will present the pop-up menu shown in figure 47, which allows the user to specify the Component; i.e., the resistance for the branch; align the branch either horizontally or vertically with its neighboring elements (horizontal alignment aligns all elements to the right of the selected branch, while vertical alignment aligns all elements below the selected branch); activate the Relocate ID dialog; activate the Change Branch Connection dialog; or delete the branch. The Properties option will be activated once a resistance has been selected for the branch and the Rotation/Momentum Data option will be activated in the case where either Rotation or Momentum is selected in the Global Options and
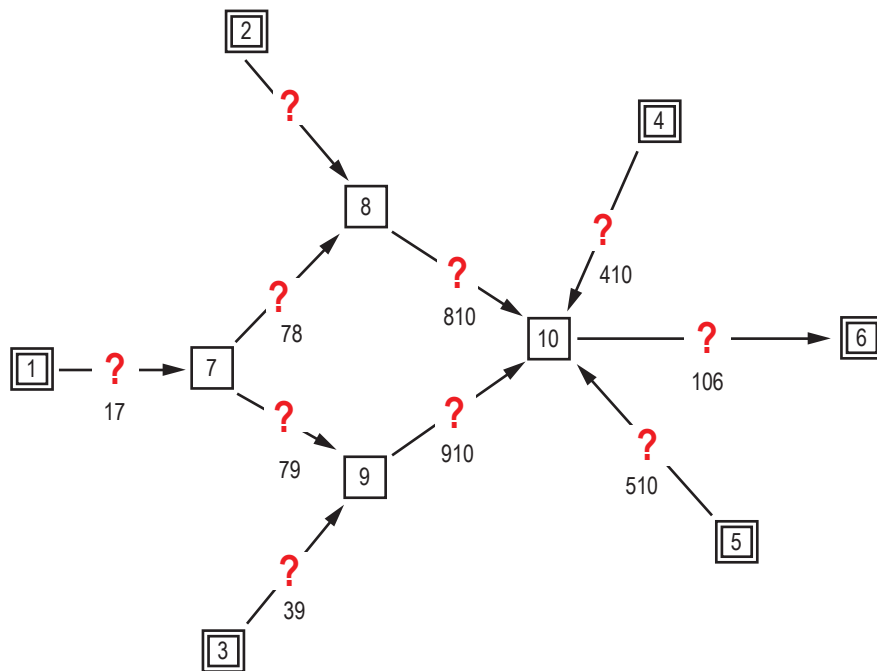
Figure 46. Example fluid circuit with complete branch connections.
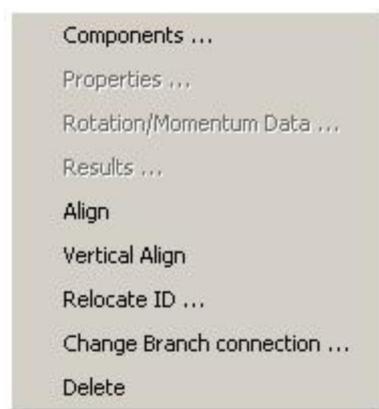
Figure 47. Branch pop-up menu.

for the specific branch under consideration. Once a model has been run, the branch pop-up menu also allows the user to activate the results dialogs, which will be discussed in section 4.8.

Figure 48 shows the Relocate Branch ID dialog. This dialog gives the user a choice of eight locations where the branch identifier can be placed in relation to the branch element on the canvas.

Figure 49 shows the change Branch Connections dialog. This dialog allows the user to change the nodes that the branch connects and/or the 'handles' where the branch attaches to each node. Note that changing the nodes connected to a branch does not automatically change the branch identifier.

Figure 48. Relocate Branch ID dialog.
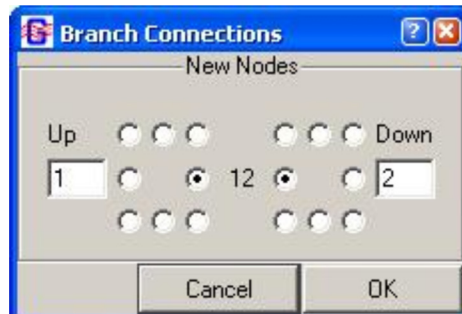
Figure 49. Change Branch Connections dialog.

Choosing the 'Component …' option will present the Resistance Options dialog shown in figure 50. This dialog shows pictorial representations for each of the 22 branch Resistance Options currently allowed in GFSSP. Note that the Control Valve option will not be available for steady flows. The available resistance options are discussed in section 2.1.7. To assign a resistance option, left click on the desired component and press the Accept button. Figure 51 shows an example where each of the branches has been assigned a resistance option. The user may change the resistance option for a branch at any time without deleting the branch.
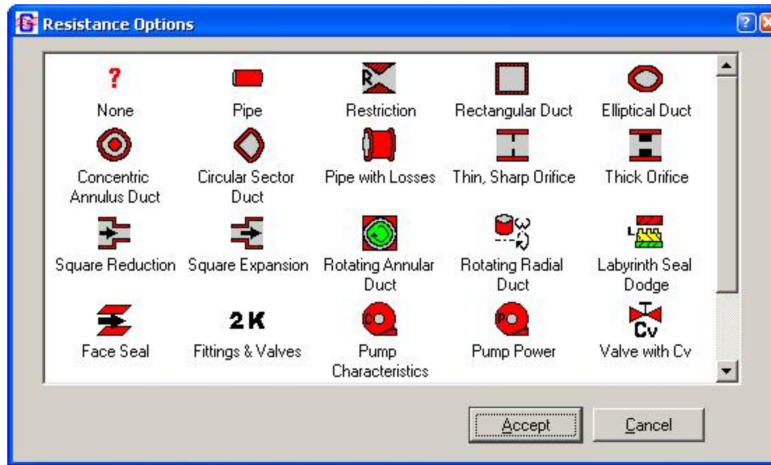
Figure 50. Branch Resistance Options dialog.
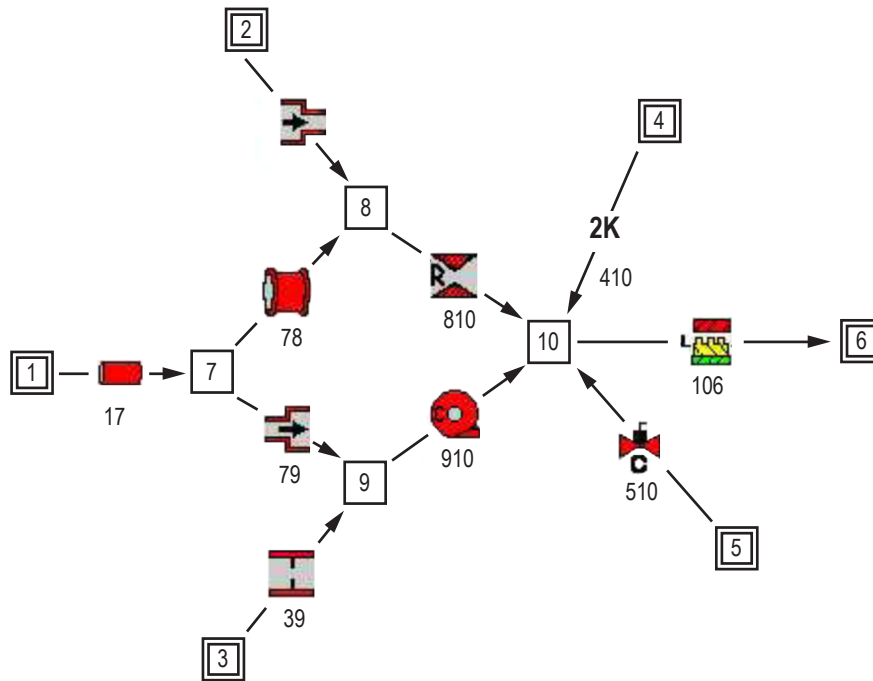
Figure 51. Example fluid circuit with resistance options.

A right click of the mouse on a branch where the resistance has been specified will present the pop-up menu (fig. 47) with the Properties… option activated. Choosing the Properties… option will present a dialog that is specifically tailored to receive input for that resistance option. In all instances, the properties specification dialogs behave in an identical fashion; however, the Fitting & Valves - **2K** dialog is somewhat different and will be shown as an example. Choosing the Properties… option, for a fitting and valve, will present the dialog shown in figure 52. The user can input the desired data or use the tree structure to the right to select a desired fitting or valve. Selection of a fitting or valve, from the tree, will load its specific data into the fields to the left; these data may then be edited as desired. The Accept button must be pressed to apply the data.
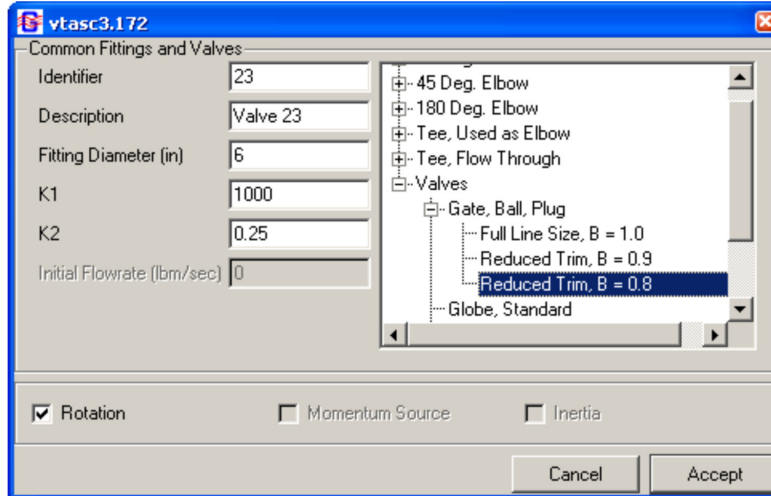
Figure 52. Fittings and valve resistance option properties dialog.

In general, the following applies to every resistance option. If the user wants to change the numeric identifier for a branch, simply type in the desired numeric identifier (maximum of five numbers). For the unsteady case, the initial flow rate may be specified, and depending upon the selected Global options, the Rotation, Momentum Source, and Inertia checkboxes may be active. Notice, in this case, that the Rotation checkbox is active and has been selected. If Rotation has been checked, a right click of the mouse button will present the pop-up menu with the Rotation/ Momentum Source option active and selecting this option will present the dialog shown in figure 53 to allow input of the relevant information.
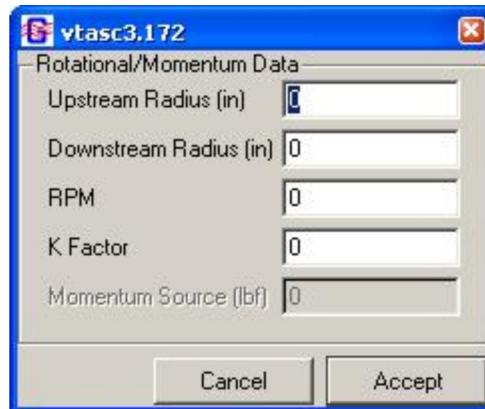
Figure 53. Rotation/Momentum dialog.

4.3.3 Conjugate Heat Transfer

The Solid Node ▣ , Ambient Node ◯ , and Conductor ∿ addition tools are used to specify the conjugate heat transfer portion of a GFSSP model. These tools are inactive until the

user activates Conjugate Heat Transfer by selecting it from the Advanced menu. In practice, adding solid and ambient nodes to the VTASC canvas is analogous to adding fluid boundary and internal nodes, while adding conductors is an identical process to adding fluid resistance branches.

A right mouse click on an ambient node reveals a pop-up menu identical to the fluid boundary node pop-up menu shown in figure 41(a), while the solid node pop-up menu is identical to the fluid internal node pop-up menu shown in figure 41(b). The Properties... dialog for a solid node is shown in figure 54. For a solid node, all inputs are required at each node. A list of available materials is shown at the right of the dialog. When the user left mouse clicks the desired material from the list, the GFSSP index number for that material is automatically written to the Material input box. The ambient node properties dialog, shown in figure 55, requires only temperature as a modeling input.

The conductor pop-up menu, shown in figure 56, is very similar to the fluid branch pop-up menu (fig. 47). The only differences are that a Conductors option replaces the Components option—there is no need for a Rotation/Momentum option, and the Change Branch Connection
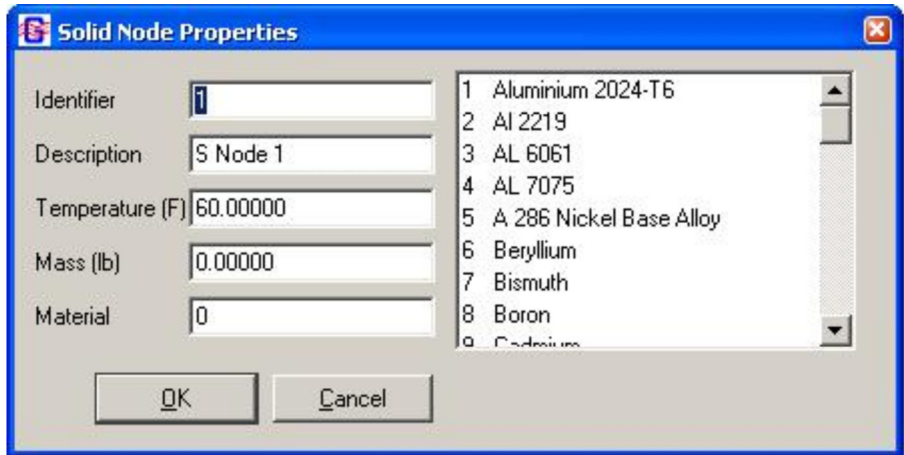
Figure 54. Solid Node Properties dialog.
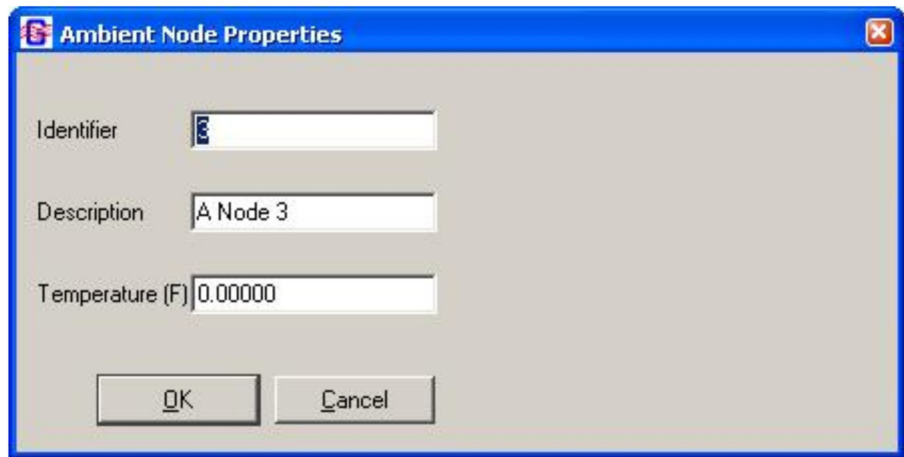
Figure 55. Ambient Node Properties dialog.

Figure 56. Conductor pop-up menu.
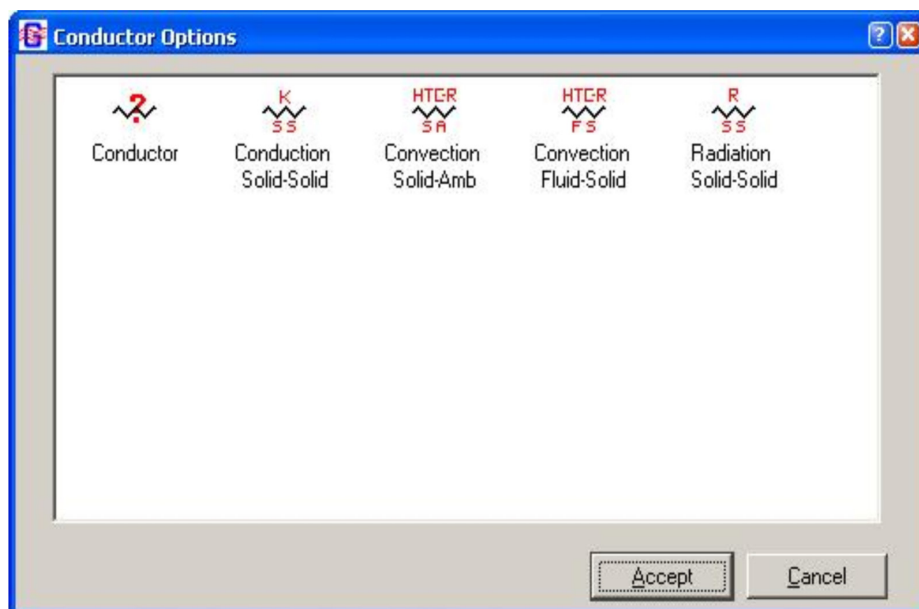
Figure 57. Conductors dialog.

option is here named the Change Conductor Connection option. (The Functionality is identical to the Change Branch Connection option.)

When the user first adds a conductor to the canvas, VTASC indicates that the conductor type is undefined using this symbol . The user defines the type of conductor by selecting the Conductors option from the conductor pop-up menu. This opens the Conductors dialog shown in figure 57. The user must select the appropriate type of conductor and click the Accept button. Note that VTASC will not allow the user to select a conductor type that is inconsistent with the types of nodes attached to that particular conductor; i.e., a solid-ambient convection conductor type cannot be applied to a conductor connecting two solid nodes. As with fluid resistance branches, once the conductor type has been defined, the Properties option becomes active in the conductor pop-up menu. Selecting the Properties option activates a Properties dialog where the user supplies characteristics that are specific to that conductor type.

4.4 Advanced Options

GFSSP contains many advanced features. These advanced features include: Transient Heat Load, Heat Exchanger, Tank Pressurization, Turbopump, Valve Open/Close, and Fluid Conduction. If any or all of the advanced features are selected, the user can input the appropriate information by selecting the option corresponding to the feature from the Advanced pull-down menu (see fig. 34).

The dialogs for each of the advanced options operate in an identical fashion. The user may add any number of components to that option by pressing the Add button. To modify the data for a particular component, the user must select the component of interest, modify the data, and press the Accept button. To delete a component, press the Delete button after a component has been selected.

4.4.1 Transient Heat

The Transient Heat Load option dialog is shown in figure 58. This option is activated from the Unsteady Options pane on the Global Options menu (see sec. 4.2.3). The user provides the fluid node where the heat load is applied and the name and location of a history file containing the heat load as a function of time.

Figure 58. Transient Heat Load option dialog.

4.4.2 Heat Exchanger

The Heat Exchanger option dialog is shown in figure 59. This option is activated from the Circuit Options pane on the Global Options menu (see sec. 4.2.2). The user has the option of modeling a counterflow or parallel flow heat exchanger. The user supplies the branch numbers that will be identified as the 'hot' and 'cold' branches as well as a value for heat exchanger effectiveness. If the user enters a heat exchanger effectiveness value between zero and 1, GFSSP will perform calculations based on that effectiveness. If the user enters a value >1, this prompts GFSSP to internally calculate the effectiveness. In the latter case, the user must also supply a value of UA (the product of the overall conductance for heat transfer and the surface area on which that conductance is based).

70
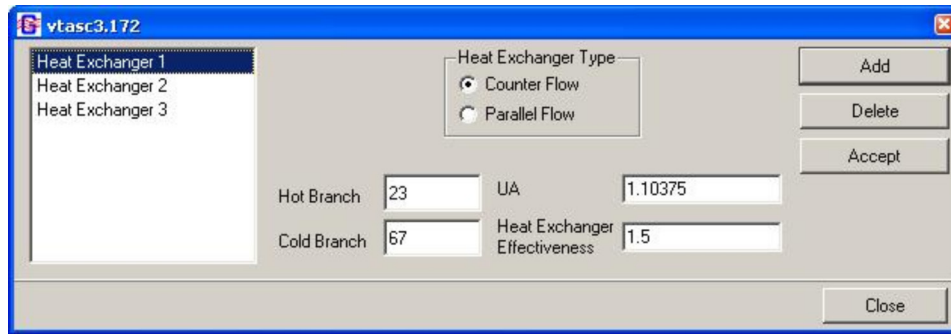
Figure 59. Heat Exchanger option dialog.

4.4.3 Tank Pressurization

The Tank Pressurization option dialog is shown in figure 60. This option is activated from the Unsteady Options pane on the Global Options menu (see sec. 4.2.3). The user has the option of modeling a vertically oriented cylindrical tank or a spherical tank. The user identifies the fluid nodes and fluid resistance branches in the model that represent the tank's ullage and propellant. The user is also asked to provide the initial surface areas where the ullage is interacting with (a) the propellant and (b) the tank wall. The user must also supply relevant tank characteristics (density, specific heat, and thermal conductivity of the tank wall material; tank wall thickness; and initial tank wall temperature). Finally, VTASC provides default values for the constants used in GFSSP's tank pressurization heat transfer calculations, but the user may modify these constants through this dialog if desired.
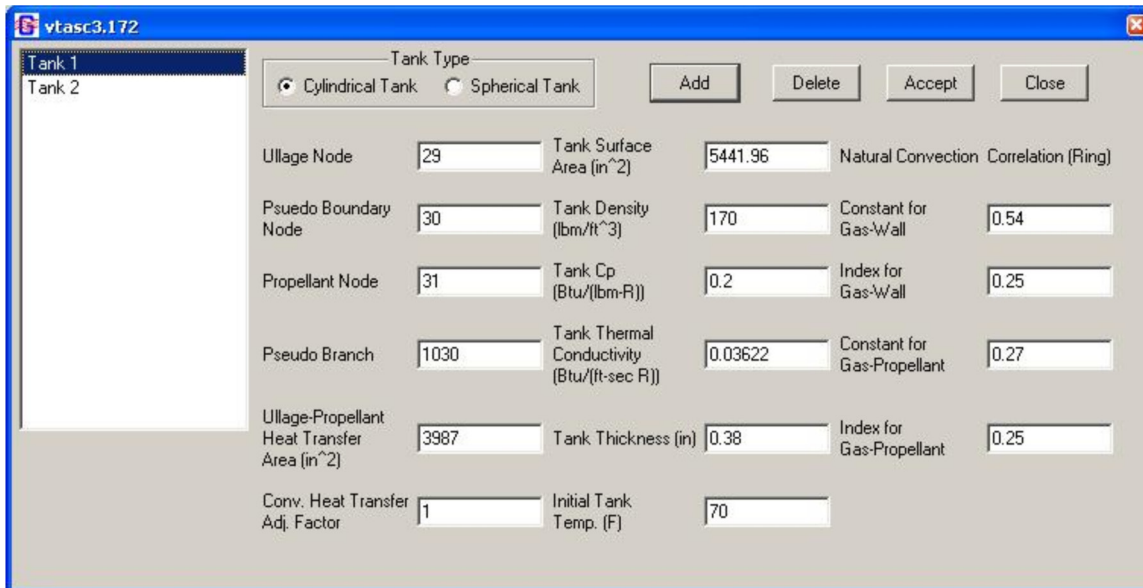
Figure 60. Tank Pressurization option dialog.

4.4.4 Turbopump

The Turbopump option dialog is shown in figure 61. This option is activated from the Circuit Options pane on the Global Options menu (see sec. 4.2.2). The user supplies the fluid resistance branches that will represent the pump and the turbine. The user also supplies some characteristics of the turbine (speed, efficiency, diameter, and design point velocity ratio) as well as the name and location of a history file containing the pump characteristics (the quantities (Head/Speed^2) and (Torque/(Density*Speed^2)) as a function of (Flow Rate/Speed)).
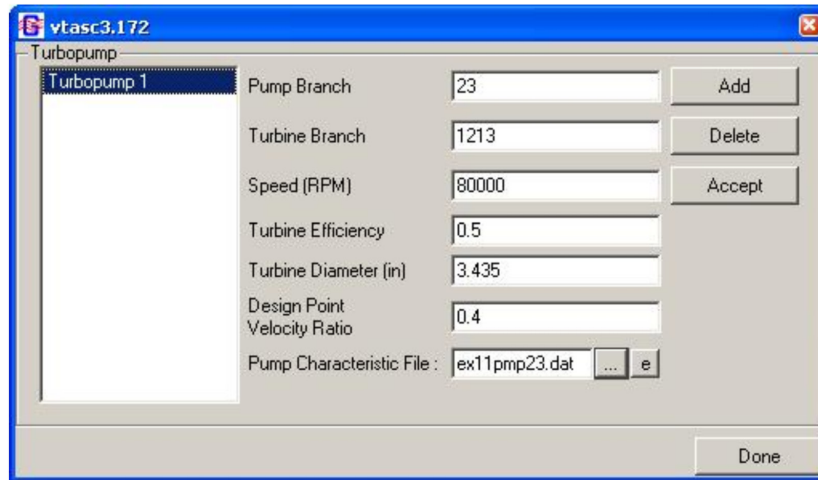
Figure 61. Turbopump option dialog.

4.4.5 Valve Open/Close

The Valve Open/Close option dialog is shown in figure 62. This option is activated from the Unsteady Options pane on the Global Options menu (see sec. 4.2.3). The user provides the fluid resistance branch that represents the valve and the name and location of a history file containing the cross-sectional flow area of the valve as a function of time.
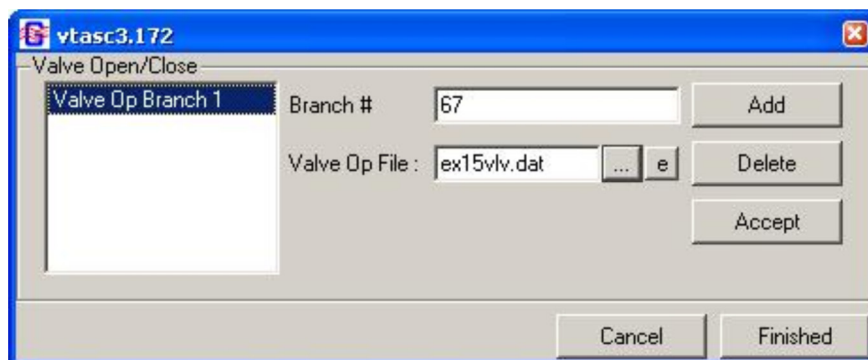
Figure 62. Valve Open/Close option dialog.

4.4.6 Fluid Conduction

The Fluid Conduction option dialog is shown in figure 63. This option is activated from the Circuit Options pane on the Global Options menu (see sec. 4.2.2). The user may populate the list of internal nodes in two ways. First, left mouse clicking the Load Nodes button will automatically populate the list with each internal node. Second, an individual internal node may be added to the list by typing the node identifier into the New Node input box and left mouse clicking the Add button. If the user wants to remove an internal node from the list, select that node from the list and left mouse click the Delete button. Selecting an internal node from the list reveals the list of upstream and downstream neighbors for that node. The user supplies the area and distance for each neighbor node by selecting that node from the neighbor nodes list.
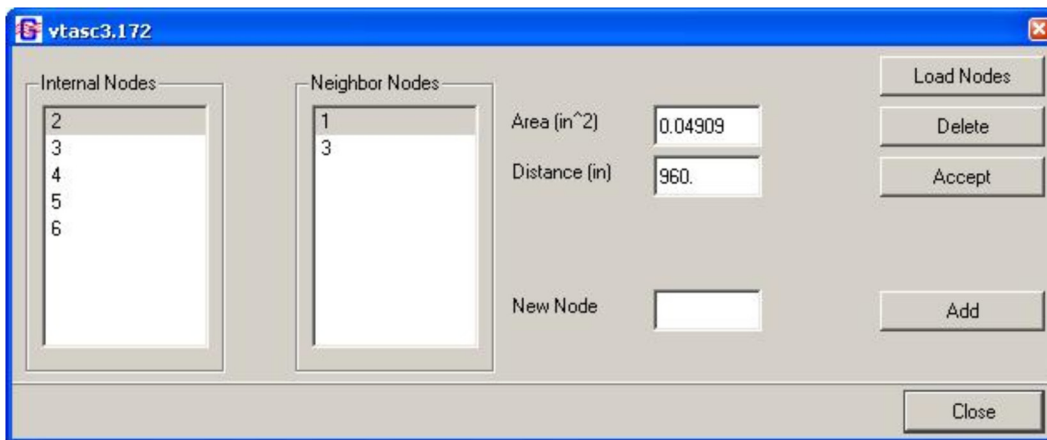
Figure 63. Fluid conduction dialog.

4.5 GFSSP Input File

The primary interface between VTASC and GFSSP is the GFSSP input data file generated by VTASC. While it should not be necessary for the user to directly access the GFSSP input file for most modeling activities, knowledge of the content and format of the GFSSP input data file may be helpful in some circumstances. This section is intended to provide the user with a helpful reference for better understanding the GFSSP input data file.

4.5.1 Title Information

The GFSSP input data file always begins with the title and documentary information for the model, which are shown below. The first two entries are internally defined by VTASC. The first, the GFSSP version, tells GFSSP what features and formatting to expect while reading the input data file. The second entry defines where the user has installed GFSSP. The user defines the remaining four entries in VTASC. They include the analyst's name, the working directory path and input data file name, output data file name, and a descriptive title for the model.

```
GFSSP VERSION
503
GFSSP INSTALLATION PATH
C:\Program Files\GFSSP\
ANALYST
ALOK MAJUMDAR
INPUT DATA FILE NAME
C:\Program Files\GFSSP\Examples\Ex1\Ex1.dat
OUTPUT FILE NAME
Ex1.out
TITLE
Simulation of a Flow System Consisting of a Pump, Valve and Pipe Line
```

4.5.2 Logical Variables

The GFSSP input data file includes all 44 of the logical variable definitions based on the user's choices in VTASC. The user is referred to appendix D (on CD inside back cover) for a specific definition of each logical variable.

```
USETUP
F
DENCON     GRAVITY    ENERGY     MIXTURE    THRUST     STEADY     TRANSV     SAVER
F          T          T          F          F          T          F          F
HEX        HCOEF      REACTING   INERTIA    CONDX      ADDPROP    PRINTI     ROTATION
F          F          F          F          F          F          T          F
BUOYANCY   HRATE      INVAL      MSORCE     MOVBND     TPA        VARGEO     TVM
F          T          F          F          F          F          F          F
SHEAR      PRNTIN     PRNTADD    OPVALVE    TRANSQ     CONJUG     RADIAT     WINPLOT
F          T          T          F          F          F          F          T
PRESS      INSUC      VARROT     CYCLIC     CHKVALS    WINFILE    DALTON
F          F          F          F          F          T          F
NORMAL     SIMUL      SECONDL    NRSOLVT
F          T          T          F
```

4.5.3 Node, Branch, and Fluid Information

This section of the GFSSP input data file defines the basic scope of the model, including (1) the total number of nodes, (2) the number of internal nodes, (3) the number of branches, and (4) the number of fluids.

```
NNODES   NINT   NBR    NF
4        2      3      1
```

4.5.4 Solution Control Variables

The next section of the GFSSP input data file defines the numerical parameters chosen by the user, including the three under-relaxation parameters, the convergence criteria, and the maximum number of iterations.

```
RELAXK   RELAXD   RELAXH   CC        NITER
1        0.5      1        0.0001    500
```

4.5.5 Time Control Variables

This section of the GFSSP input data file is applicable only for unsteady models. It defines the time step, initial time, final time, output file print step, and the Winplot file print step.

```
DTAU    TIMEF    TIMEL    NPSTEP    NPWSTEP
1       0        200      25        1
```

4.5.6 Fluid Designation

This section of the GFSSP input data file lists the appropriate fluid definition information based on the user's selections in VTASC.

For a general fluid (GASP/WASP or GASPAK), the fluid designation lists the GFSSP index number for each selected fluid.

```
NFLUID(I), I=1, NF
1       6       12
```

For a constant property fluid, the fluid designation lists the reference density and viscosity.

```
RHOREF     EMUREF
62.4       0.00066
```

For an ideal gas fluid, the fluid designation lists the index number for an ideal gas and the reference properties associated with the ideal gas fluid.

```
NFLUID(I), I = 1, NF
  33
RREF      CPREF    GAMREF    EMUREF      AKREF       PREF    TREF    HREF    SREF
  53.34   0.24     1.3999    1.26e-05    4.133e-06   14.7    -459    0       0
```

For hydrogen peroxide, the fluid designation lists the index number and the mole fraction of water for the fluid.

```
NFLUID(I), I = 1, NF
  34
MFRAC
  0.5
```

Finally, for a user-defined fluid, the fluid designation lists the molecular weight of the fluid and the property table file names supplied by the user.

```
FLUID 1 PROPERTY FILES
28.0
AKFL1.DAT
RHOFL1.DAT
EMUFL1.DAT
GAMFL1.DAT
HFL1.DAT
SFL1.DAT
CPFL1.DAT
```

4.5.7 Node Numbering and Designation

The next section of the GFSSP input data file lists each node, designates whether that node is a boundary node (INDEX=2) or an internal node (INDEX=1), and includes a user-supplied text description of the node. Nodes are listed in the order that they are created in VTASC, which may not be numerical order.

```
NODE   INDEX    DESCRIPTION
 1     2         "Node 1"
 2     1         "Node 2"
 3     1         "Node 3"
 4     2         "Node 4"
```

If the user has chosen to activate buoyancy, the reference node will be defined in this section right below the node listing.

```
REFERENCE NODE FOR DENSITY
2
```

4.5.8 Node Variables

The next section of the GFSSP input data file lists the initial properties at each node based on the user's selections in VTASC.

For a steady state model, the model boundary conditions are listed along with the internal node initial guesses. Concentrations are listed at each node in the same order the fluids are listed (see sec. 4.5.6). If the user has chosen the Constant Property Fluid option, the temperature will not appear in this listing.

```
NODE   PRES   (PSI)   TEMP(DEGF)   MASS SOURC   HEAT SOURC   THRST AREA   CONCENTRATION
 1     500    1500    0            0            0            0.1          0.9
 2     500    80      0            0            0            1            0
 3     338.2  1500    0            0            0            0.1          0.9
 4     14.7   80      0            0            0            0.5          0.5
```

For an unsteady model, the internal node initial solution values are listed first in the same order they were created. These properties include the node volume property, which does not appear in a steady state model. After all of the internal nodes have been listed, each boundary node history file is listed (again, in the order they were created). Each boundary node requires a separate history file.

```
NODE   PRES (PSI)   TEMP(DEGF)   MASS SOURC   HEAT SOURC   THRST AREA   NODE-VOLUME   CONCENTRATION
 1     100          80           0            0            0            17280
 ex8hs2.dat
```

4.5.9 Transient Heat/Variable Geometry Information

This section of the GFSSP input data file is applicable only for unsteady models where the user has activated either the Transient Heat or Variable Geometry options.

If the user has elected to use the Variable Geometry option, the Variable Geometry file name will appear right below the last boundary node history file name. There is no description line associated with the variable geometry listing in the input data file.

The transient heat section of the GFSSP input data file first lists the number of nodes identified by the user as having a transient heat load. Each identified node is then listed along with the corresponding heat load file name in the order the user added their information in the Transient Heat dialog (see sec. 4.4.1).

```
Transient Heat Load Information
Number of Nodes with Transient Heat Loads
1
Transient Heat Node Number
2
Corresponding Heat Load History File Name
qdot.dat
```

4.5.10 Node-Branch Connections

The next section of the GFSSP input data file identifies which branches are attached to each internal node. Each internal node (variable INODE) is listed in the same order they were created. The variable NUMBR defines how many branches are attached to that node. The array NAMEBR identifies which branches are attached to that node in the order they were created.

```
INODE   NUMBR   NAMEBR
2       2       12 23
3       2       23 34
```

4.5.11 Branch Flow Designation and Resistance Options

The next section of the GFSSP input data file describes the characteristics of each fluid branch. This section consists of two subsections. The first subsection identifies the upstream node, downstream node, and branch resistance option chosen by the user. This subsection also includes any text description of that branch supplied by the user.

```
BRANCH   UPNODE   DNNODE   OPTION   DESCRIPTION
12       1        2        14       "Pump 12"
23       2        3        13       "Valve 23"
34       3        4        1        "Pipe 34"
```

The second subsection lists the properties of each fluid branch as defined by the user. The branch properties are specific to each branch resistance option. They are discussed in detail in section 2.1.7.

```
BRANCH      OPTION-14   PUMP CONST1   PUMPCONST2    PUMPCONST3    AREA
12          30888       0             -0.0008067    201.06
BRANCH      OPTION-13   DIA           K1            K2            AREA
23          6           1000          0.1           28.274
BRANCH      OPTION-1    LENGTH        DIA           EPSD          ANGLE       AREA
34          18000       6             0.005         95.74         28.274
```

4.5.12 Unsteady Information

The 12th section of the GFSSP input data file is applicable only for unsteady models. This section defines the initial mass flow rates in each fluid branch in the order the branches were created.

```
INITIAL FLOWRATES IN BRANCHES FOR UNSTEADY FLOW
1001  0.803
1002  0.803
1003  0.423
1004  0.423
```

4.5.13 Inertia Information

This section of the GFSSP input data file is applicable only for models where the user has activated the Inertia option. This section is divided into four subsections. The first subsection defines a fluid branch's relationship with any upstream branches. Branches are listed in the order they were created. The variable NOUBR defines the number of upstream branches connected to a particular branch. The array NMUBR identifies which branches are attached upstream of that branch in the order they were created.

The second subsection defines a fluid branch's relationship with any downstream branches. Each branch is listed in the order they were created. The variable NODBR defines the number of downstream branches connected to a particular branch. The array NMDBR identifies which branches are attached downstream of that branch in the order they were created.

```
BRANCH      NOUBR       NMUBR
12          0
23          1           12
34          1           23
BRANCH      NODBR       NMDBR
12          123
23          1           34
```

The third subsection allows the user to define relative angles between branches if desired. As discussed in section 5.2.2, the user must edit this section of the input data file manually. VTASC supplies a template for each branch in the order they were created. The template lists each upstream branch and corresponding angle first, then each downstream branch and corresponding angle. VTASC defines each angle as a placeholder value of zero degrees, which the user must replace with the appropriate angles.

```
BRANCH
12
   UPSTRM BR.  ANGLE
   DNSTRM BR.  ANGLE
   23          0.00000
BRANCH
23
   UPSTRM BR.  ANGLE
   12          0.00000
   DNSTRM BR.  ANGLE
   34          0.00000
```

The fourth subsection identifies the fluid branches where the user has activated inertia. The first number (16 in the example below) defines the number of branches where the user has activated inertia. The subsequent lines list each branch where the user has activated inertia in the order they were created.

```
NUMBER OF BRANCHES WITH INERTIA
16
12
23
34
45
56
67
78
89
910
1011
1112
1213
1314
1415
1516
1617
```

4.5.14 Fluid Conduction Information

This section of the GFSSP input data file is applicable only for models where the user has activated the Fluid Conduction option. This section is divided into two subsections. The first sub-section identifies how many fluid conduction nodes the user has selected. For each of these fluid nodes, the number of upstream and downstream nodes connected to that node (identified here as neighbors) is defined and each neighbor node is listed.

```
NUMBER OF FLUID CONDUCTION NODES
2
NODE   NO. OF NEIGHBORS   NEIGHBOR NODES
2      2                  1 3
3      2                  2 4
```

The second subsection defines the fluid conduction properties (area and internode distance) for the interaction between a particular node and each of its neighbors. For each node, the property of interest between that node and each neighbor is listed in the order the neighbor nodes are listed in the first subsection.

```
NODE    CONDUCTION AREAS
2       0.04909   0.04909
3       0.04909   0.04909
NODE    INTERNODE DISTANCES
2       960       960
3       960       960
```

4.5.15 Rotation Information

This section of the GFSSP input data file is applicable only for models where the user has activated the Rotation option. This section first defines the number of branches where the user has activated rotation. Then, each branch is identified along with the rotational information for that branch (upstream and downstream node radii from center of rotation, rotational speed, and the rotational 'slip' factor).

```
NUMBER OF ROTATING BRANCHES
9
BRANCH    UPST RAD    DNST RAD    RPM      K ROT
23        1.25        2.25        5000     0.8671
34        2.25        3.625       5000     0.8158
45        3.625       4.6875      5000     0.763
56        4.6875      5.375       5000     0.7252
67        5.375       5.5         5000     0.7076
89        5.5         5.375       5000     0.7129
910       5.375       4.6875      5000     0.7349
1011      4.6875      3.625       5000     0.7824
1112      3.625       2.65        5000     0.8376
```

4.5.16 Valve Open/Close Information

This section of the GFSSP input data file is applicable only for models where the user has activated the Valve Open/Close option. This section first defines the number of fluid branches where the user will be modeling a valve transient. Next, for each valve, the branch that will represent the valve and the valve history file name are listed.

```
NUMBER OF CLOSING/OPENING VALVES IN THE CIRCUIT
1
BRANCH
67
FILE NAME
ex15vlv.dat
```

4.5.17 Momentum Source Information

This section of the GFSSP input data file is applicable only for models where the user has activated the Momentum Source option. This section first defines the number of fluid branches where the user wishes to add a momentum source. Next, each branch where the user has defined a momentum source is listed along with the momentum source.

```
NUMBER OF BRANCHES WITH MOMENTUM SOURCE
1
BRANCH   MOMENTUM SOURCE
12       100
```

4.5.18 Heat Exchanger Information

This section of the GFSSP input data file is applicable only for models where the user has activated the Heat Exchanger option. First, the number of heat exchangers identified by the user is defined. Then, the characteristics of each heat exchanger are listed as defined by the user, including the 'hot' and 'cold' branches, the type of heat exchanger (Counterflow=1, Parallel Flow=2), the 'hot' and 'cold' surface areas, UA, and the heat exchanger effectiveness. Note that the 'hot' and 'cold' surface areas are not currently recommended for use in GFSSP and cannot be modified using VTASC.

```
NUMBER OF HEAT EXCHANGERS
1
IBRHOT   IBRCLD   ITYPHX   ARHOT   ARCOLD   UA       HEXEFF
23       67       1        0       0        1.1038   1.5
```

4.5.19 Moving Boundary Information

This section of the GFSSP input data file is applicable only for models where the user has activated the Moving Boundary option. This section defines the number of nodes identified as having moving boundary, and lists each identified node.

```
NUMBER OF NODES WITH MOVING BOUNDARY
2
NODE
1
2
```

4.5.20 Turbopump Information

This section of the GFSSP input data file is applicable only for models where the user has activated the Turbopump option. First, the number of turbopumps in the model is listed. Then, the characteristics for each turbopump (fluid branch representing the pump, fluid branch representing the turbine, speed, turbine efficiency, turbine diameter, design point velocity ratio, and the pump characteristics curve file name) are listed.

```
NUMBER OF TURBOPUMP ASSEMBLY IN THE CIRCUIT
1
IBRPMP   IBRTRB   SPEED(RPM)   EFFTURB   DIATRB   PSITRD
23     1213        80000        0.5       3.435    0.4
PUMP CHARACTERISTICS CURVE DATA FILE
ex11pmp23.dat
```

4.5.21 Tank Pressurization Information

This section of the GFSSP input file is applicable only for models where the user has activated the Tank Pressurization option. First, the number of pressurized propellant tanks in the model is defined. Next, the characteristics of each tank are listed including the tank type (spherical=0, cylindrical=1); fluid node representing the ullage; ullage-propellant interface pseudo boundary node; fluid node representing the propellant; fluid branch representing the propellant surface; the initial tank wall surface area exposed to the ullage; the tank wall thickness; the tank wall material density, specific heat, and thermal conductivity; the ullage-propellant interface surface area; the heat transfer coefficient adjustment factor; the initial tank wall temperature; the heat transfer correlation ullage-propellant constants; and the heat transfer correlation ullage-tank wall constants.

```
NUMBER OF PRESSURIZATION PROPELLANT TANKS IN CIRCUIT
1
TNKTYPE  NODUL   NODULB   NODPRP   IBRPRP   TNKAR    TNKTH   TNKRHO   TNKCP
1       2   3       4        34       6431.9   0.375    170     0.2


TNKCON   ARHC   FCTHC   TNKTM   CIP    FNIP    CIW     FNIW
0.0362   4015   1       -264    0.27   0.25    0.54    0.25
```

4.5.22 Variable Rotation Information

This section of the GFSSP input file is applicable only for models where the user has activated the Variable Rotation option. The variable rotation history file name is listed in this section.

```
ROTATION DATA FILE
varrot.dat
```

4.5.23 Restart Information

This section of the GFSSP input file is applicable only for models where the user has elected to read from and/or write to restart files. The section lists the node and branch restart file names.

```
RESTART NODE INFORMATION FILE
FNDEX15.DAT
RESTART BRANCH INFORMATION FILE
FBREX15.DAT
```

4.5.24 Cyclic Boundary Information

This section of the GFSSP input file is applicable only for models where the user has activated the cyclic boundary option. The section lists the boundary node where the cyclic boundary option has been activated and the node that is upstream of the cyclic boundary node.

```
CYCLIC BNDARY NODE    UPSTREAM NODE
1                     22
```

4.5.25 Conjugate Heat Transfer Information

This section of the GFSSP input file is applicable only for models where the user has activated Conjugate Heat Transfer. The section is divided into seven subsections.

The first subsection identifies how many solid and ambient nodes are present in the model as well as how many conductors of each type (solid-solid conduction, solid-fluid, solid-ambient, and solid-solid radiation) are present in the model.

```
NSOLID  NAMB   NSSC   NSFC   NSAC   NSSR
8       2      7      8      2      1
```

The second subsection defines the characteristics of each solid node in the order they were created. The properties of each solid node (material, mass, and initial temperature) are listed first. Then, the number of conductors of each type attached to the solid node is listed along with a text description of the solid node provided by the user. Finally, for each type of conductor, every conductor attached to that solid node is listed.

```
NODESL  MATRL  SMASS   TS       NUMSS  NUMSF  NUMSA  NUMSSR  DESCRIPTION
2       41     1.00000 70.00000 1      1      1      1       "S Node 2"
NAMESS
23
NAMESF
122
NAMESA
12
NAMESSR
24
```

The third subsection lists each ambient node in the order they were created and lists the temperature at that node along with a text description of the ambient node provided by the user.

```
NODEAM  TAMB      DESCRIPTION
1       32.00000  "A Node 1"
```

The fourth subsection lists each solid-solid conduction conductor along with its characteristics ('upstream' solid node, 'downstream' solid node, surface area, distance, and a user-supplied text description) in the order they were created.

```
ICONSS   ICNSI   ICNSJ   ARCSIJ    DISTSIJ    DESCRIPTION
23       2       3       3.14159   3.00000    "Conductor 23"
```

The fifth subsection lists each solid-fluid conductor along with its characteristics including: solid node; fluid node; heat transfer coefficient model (User Supplied=0, Dittus-Boelter=1, and Miropolskii=2); surface area, user-supplied heat transfer coefficient (if Model=0); emissivity of the solid; emissivity of the fluid; and user-supplied text description.

```
ICONSF   ICS   ICF    MODEL   ARSF         HCSF          EMSFS
122      2     12     0       1.88500e+01  3.17000e-04   0.00000e+00
EMSFF            DESCRIPTION
0.00000e+00      "Convection 122"
```

The sixth subsection lists each solid-ambient conductor along with it characteristics (solid node, ambient node, surface area, heat transfer coefficient, emissivity of the solid, emissivity of the ambient, and a user-supplied text description).

```
ICONSA   ICSAS   ICSAA   ARSA         HCSA          EMSAS
12       2       1       3.14159e+00  2.00000e-02   0.00000e+00
EMSAA            DESCRIPTION
0.00000e+00      "Convection 12"
```

The seventh subsection lists each solid-solid radiation conductor along with its characteristics ('upstream' solid node, 'downstream' solid node, 'upstream' surface area, 'downstream' surface area, view factor, 'upstream' emissivity, 'downstream' emissivity, and a user-supplied text description).

```
ICONSSR   ICNSRI   ICNSRJ   ARRSI     ARRSJ     VFSIJ     EMSSI
24        2        3        3.14159   3.14159   1.00000   0.70000
EMSSJ     DESCRIPTION
0.70000   "Conductor 24"
```

4.6 GFSSP Execution

As noted in section 4.1.4, GFSSP can be executed directly from the VTASC environment using either the Run menu or the shortcut on the file Input/Output toolbar. When the user activates the Run GFSSP command, VTASC automatically writes the GFSSP text input file before executing GFSSP. If the text file already exists, VTASC will ask if the user wishes to overwrite the file. VTASC then executes GFSSP and opens the GFSSP Run Manager window. The appearance and function of the Run Manager depends on whether the model is a steady state or transient model.

4.6.1 Steady State Run Manager

Figure 64 shows the GFSSP Run Manager appearance for a steady state simulation. If the user wishes to stop the GFSSP simulation for any reason, the button in the upper left corner of the Run Manager will stop GFSSP execution. During execution, the Run Manager will display GFSSP-generated messages in the GFSSP display pane. After execution is complete, the GFSSP

messages may be printed by clicking the Print button in the lower right corner of the Run Manager. The GFSSP-generated text output file may also be viewed after execution is complete by clicking the Edit Output button in the lower left corner of the Run Manager. Clicking the Close button will exit the Run Manager and return the user to the VTASC window.

Figure 64. GFSSP steady state run manager.

4.6.2 Unsteady Run Manager

Figure 65 shows the GFSSP Run Manager appearance for an unsteady simulation. The only difference between the unsteady and steady Run Managers is that the GFSSP display pane appears in the top half of the Run Manager and a real-time updated plot of GFSSP's convergence behavior as a function of time appears in the bottom half of the Run Manager.
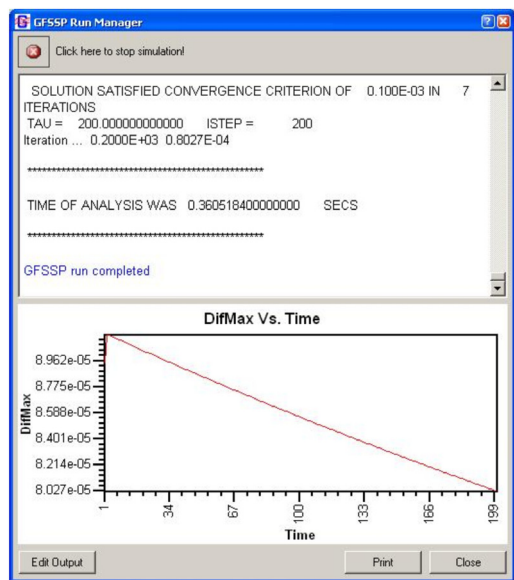
Figure 65. GFSSP unsteady run manager.

4.7 GFSSP Output File

The basic GFSSP output for any simulation is the text output file. As mentioned in the previous section, once a simulation is complete the Run Manager gives the user the option of viewing the output file in a text editor. The content of the output file is dependent on the options selected by the user during VTASC model development. This section is intended to give the user an understanding of the format and general layout of the text output file.

4.7.1 Title and Data Files

Each GFSSP output file begins with the header shown below, which identifies the version of GFSSP that was used for the model simulation.

```
G F S S P (Version 5.0)
Generalized Fluid System Simulation Program
September, 2006
Developed by NASA/Marshall Space Flight Center
Copyright © by Marshall Space Flight Center

A generalized computer program to calculate flow
rates, pressures, temperatures, and concentrations
in a flow network.
```

Directly below the GFSSP header, the model title, analyst name, model working directory and text input file name, and text output file name as defined by the user are supplied.

```
TITLE:Simulation of a Flow System Consisting of a Pump, Valve and Pipe Line
ANALYST:ALOK MAJUMDAR
FILEIN:C:\Program Files\GFSSP\Examples\Ex1\Ex1.dat
FILEOUT:Ex1.out
```

4.7.2 Logical Variables

This section of the GFSSP output file lists the logical variable definitions as used in the simulation.

```
LOGICAL VARIABLES
DENCON   = F
GRAVITY  = T
ENERGY   = T
MIXTURE  = F
THRUST   = F
STEADY   = T
TRANSV   = F
SAVER    = F
HEX      = F
HCOEF    = F
REACTING = F
```

```
INERTIA   = F
CONDX     = F
TWOD      = F
PRINTI    = T
ROTATION  = F
BUOYANCY  = F
HRATE     = T
INVAL     = F
MSORCE    = F
MOVBND    = F
TPA       = F
VARGEO    = F
TVM       = F
SHEAR     = F
PRNTIN    = T
PRNTADD   = T
ADDPROP   = F
PRESS     = F
INSUC     = F
VARROT    = F
NORMAL    = F
SECONDL   = T
CONJUG    = F
NRSOLVT   = F
```

4.7.3 Node and Branch Information

This section of the output file documents the size and scope of the model. It lists the total number of nodes as well as the number of internal nodes, the number of branches, the number of fluids, the number of variables (or equations) in the model (this is the sum of NBR and NINT), and finally the enthalpy reference node, which is hard-coded in GFSSP as the second node.

```
NNODES = 4
NINT   = 2
NBR    = 3
NF     = 1
NVAR   = 5
NHREF  = 2
```

4.7.4 Fluid Information

This section of the output file documents the fluids that were used in the simulation.

For a constant property fluid, the fluid information lists the reference density and viscosity.

```
RHOREF = 62.4000     LBM/FT**3
EMUREF = 0.6600E-03  LBM/FT-SEC
```

For all other fluid options, the fluid information lists each fluid in the order they were entered by the user.

```
FLUIDS:     O2    H2O
```

4.7.5 Boundary Conditions

This section of the output file documents the boundary conditions of the model, which were supplied at each boundary node by the user. For a model with multiple fluids, the pressure, temperature, density, thrust surface area of the node, and concentration of each fluid at that node are listed. A single-fluid model provides the same listing with the exception of the fluid concentrations. A constant property fluid model lists only the pressure and surface area.

```
BOUNDARY NODES
   NODE  P            T            RHO          AREA              CONCENTRATIONS
         (PSI)        (F)          (LBM/FT^3)   (IN^2)        O2             H2O
    1    0.5000E+03   0.1500E+04   0.3931E+00   0.0000E+00   0.1000E+00   0.9000E+00
    2    0.5000E+03   0.8000E+02   0.2819E+01   0.0000E+00   0.1000E+01   0.0000E+00
    4    0.1470E+02   0.8000E+02   0.4725E+02   0.0000E+00   0.5000E+00   0.5000E+00
```

4.7.6 Fluid Network Information

This section of the output file is only active if the user has selected to print network information from the Global Options dialog (see sec. 4.2.1). For each internal node, it lists the thrust surface area, mass source, and heat source designated by the user. For each branch, it reprints the branch flow designation and resistance option information from the input text file (see sec. 4.5.11).

```
INPUT SPECIFICATIONS FOR INTERNAL NODES
NODE    AREA         MASS         HEAT
        (IN^2)       (LBM/S)      (BTU/S)
2       0.0000E+00   0.0000E+00   0.0000E+00
3       0.0000E+00   0.0000E+00   0.0000E+00


BRANCH    UPNODE   DNNODE   OPTION
12        1        2        14
23        2        3        13
34        3        4         1


BRANCH    OPTION -14:   PUMP CONST1     PUMP CONST2     PUMP CONST3 AREA
12        0.309E+05     0.000E+00       -0.807E-03     0.201E+03
BRANCH    OPTION -13:   DIA, K1, K2,  AREA
23        0.600E+01     0.100E+04       0.100E+00      0.283E+02
BRANCH    OPTION -1:    LENGTH, DIA, EPSD, ANGLE, AREA
34        0.180E+05     0.600E+01       0.500E-02      0.957E+02     0.283E+02
```

4.7.7 Initial Field Information

This section of the output file is only active if the user has selected to print the initial field from the Global Options dialog (see sec. 4.2.1).

For each internal node of a single-fluid model, it lists the initial guesses for pressure and temperature as well as the resulting compressibility, density, and quality from the thermodynamic property calculations. For a multiple fluid model, the list is the same except that the quality is replaced with the initial guesses for the mass concentration of each fluid. For a constant property fluid model, only the initial guess for pressure is listed.

```
INITIAL GUESS FOR INTERNAL NODES
   NODE  P(PSI)       TF(F)        Z(COMP)      RHO          QUALITY
                                                (LBM/FT^3)
    2     0.1470E+02   0.6000E+02   0.7616E-03   0.6237E+02   0.0000E+00
    3     0.1470E+02   0.6000E+02   0.7616E-03   0.6237E+02   0.0000E+00
```

For each branch, the trial solution for the pressure drop across the branch and the mass flow rate in the branch is listed.

```
TRIAL SOLUTION
   BRANCH   DELP(PSI)   FLOWRATE(LBM/SEC)
   12       0.0000      0.0100
   23       0.0000      0.0100
   34       0.0000      0.0100
```

4.7.8 Conjugate Heat Transfer Network Information

This section of the output file is only active for models where the user has activated conjugate heat transfer and selected to print network information from the Global Options dialog (see sec. 4.2.1). For each solid node and conductor, the conjugate heat transfer information from the input text file is printed (see sec. 4.5.25).

```
CONJUGATE HEAT TRANSFER
   NSOLIDX = 8
   NAMB    = 2
   NSSC    = 7
   NSFC    = 8
   NSAC    = 2
   NSSR    = 0
NODESL  MATRL  SMASS   TS         NUMSS   NUMSF   NUMSA
2       41     1.0000  70.0000    1       1       1
NAMESS
23
NAMESF
122
NAMESA
12
NODEAM  TAMB
 1         32.0000
10        212.0000
ICONSS   ICNSI   ICNSJ   ARCSIJ     DISTSIJ
23       2       3       3.1416     3.0000
34       3       4       3.1416     3.0000
```

```
ICONSF   ICS     ICF     ARSF       EMSFS
122      2       12      18.8500    0.0000    0.0000
123      3       12      18.8500    0.0000    0.0000
ICONSA   ICSAS   ICSAA   ARSA       HCSA        EMSAS        EMSAA
12       2       1       0.3142E+01  0.2000E-01  0.0000E+00   0.0000E+00
910      9       10      0.3142E+01  0.2000E-01  0.0000E+00   0.0000E+00
```

4.7.9 Solution Results

This section of the output file documents the solution results of the GFSSP model. If the model is unsteady, a solution will be output at each time step the user has chosen to print (defined by the Print Frequency as discussed in sec. 4.2.3). The first line in the solution will list the current time step and the time at this step.

```
ISTEP = 25   TAU =  0.25000E+02
```

Next, the unsteady model will print out the boundary conditions at each boundary node for that time step. The format is identical to that discussed in section 4.8.5.

```
BOUNDARY NODES
   NODE  P(PSI)      TF(F)        Z(COMP)     RHO         QUALITY
                                              (LBM/FT^3)
   2     0.1470E+02  0.8000E+02   0.1000E+01  0.7355E-01  0.0000E+00
```

After this line, the solution will be output in the same format for a steady model or the time step of interest in an unsteady model. For each internal node in a single fluid model, the calculated pressure, temperature, compressibility, density, resident mass, and fluid quality are listed. The listing is identical for a multiple fluid model except that the quality is replaced with the calculated mass concentration of each fluid at that node. For a constant property fluid model, only the calculated pressure and resident mass are listed. Note that for a steady model, the resident mass will always be zero.

```
SOLUTION
INTERNAL NODES
   NODE  P(PSI)      TF(F)        Z           RHO         EM(LBM)     QUALITY
                                                          (LBM/FT^3)
   2     0.2290E+03  0.6003E+02   0.1186E-01  0.6241E+02  0.0000E+00  0.0000E+00
   3     0.2288E+03  0.6003E+02   0.1185E-01  0.6241E+02  0.0000E+00  0.0000E+00
```

If the user elects to print extended information in the Global Options dialog (see sec. 4.2.1), the output file will next list the calculated enthalpy, entropy, viscosity, thermal conductivity, specific heat, and specific heat ratio for each internal node. Note that this information will not be printed for constant property fluid models.

```
NODE    H            ENTROPY      EMU          COND        CP          GAMA
        BTU/LB       BTU/LB-R     LBM/FT-SEC   BTU/FT-S-R  BTU/LB-R
   2    0.2869E+02   0.5542E-01   0.7542E-03   0.9523E-04  0.1000E+01  0.1003E+01
   3    0.2869E+02   0.5542E-01   0.7542E-03   0.9523E-04  0.1000E+01  0.1003E+01
```

For each branch, the calculated resistance factor, pressure drop, mass flow rate, velocity, Reynolds number, Mach number, entropy generation, and lost work are listed.

```
BRANCHES
   BRANCH   KFACTOR       DELP         FLOW RATE    VELOCITY     REYN. NO.   MACH NO.
            (LBF-S^2/     (PSI)        (LBM/SEC)    (FT/SEC)
            (LBM-FT)^2)
   12       0.000E+00    -0.214E+03    0.191E+03    0.219E+01    0.241E+06   0.183E-02
   23       0.764E-03     0.193E+00    0.191E+03    0.156E+02    0.644E+06   0.130E-01
   34       0.591E+00     0.214E+03    0.191E+03    0.156E+02    0.644E+06   0.130E-01


   ENTROPY GEN.   LOST WORK
   BTU/(R-SEC)    LBF-FT/SEC
   0.000E+00      0.000E+00
   0.210E-03      0.848E+02
   0.162E+00      0.657E+05
```

If the second law is used to solve the energy equation, the total entropy generation and work lost will be listed directly below the branch solution information.

```
     ***** TOTAL ENTROPY GENERATION = 0.163E+00 BTU/(R-SEC) *****
     ***** TOTAL WORK LOST = 0.120E+03 HP *****
```

If the user has activated conjugate heat transfer for a model, the conjugate heat transfer results will be listed next in the output file.

For each solid node, the specific heat that was used is listed along with the calculated solid temperature. Note that the specific heat will be zero for steady models.

```
SOLID NODES
   NODESL   CPSLD        TS
            BTU/LB       F F
   2        0.000E+00    0.423E+02
   3        0.000E+00    0.569E+02
```

For each solid-to-solid conductor, the thermal conductivity that was used is listed along with the calculated heat transfer rate.

```
SOLID TO SOLID CONDUCTOR
   ICONSS   CONDKIJ      QDOTSS
            BTU/S FT F   BTU/S
   23       0.261E-02    -0.333E-02
   34       0.261E-02    -0.279E-02
```

For each solid-to-fluid conductor, the calculated heat transfer rate is listed along with the convection and radiation heat transfer coefficients that were used.

```
SOLID TO FLUID CONDUCTOR
   ICONSF   QDOTSF       HCSF             HCSFR
            BTU/S        BTU/S FT**2 F    BTU/S FT**2 F
   122      -0.115E-02   0.317E-03        0.000E+00
   123      -0.544E-03   0.317E-03        0.000E+00
```

For each solid-to-ambient conductor, the calculated heat transfer rate is listed along with the convection and radiation heat transfer coefficients that were used.

```
SOLID TO AMBIENT CONDUCTOR
   ICONSA   QDOTSA        HCSA            HCSAR

            BTU/S         BTU/S FT**2 F   BTU/S FT**2 F
   12        0.448E-02    0.200E-01       0.000E+00
   910      -0.136E-01    0.200E-01       0.000E+00
```

For each solid-to-solid radiation conductor, the calculated heat transfer rate is listed along with the effective conductivity that was used.

```
SOLID TO SOLID RADIATION CONDUCTOR
   ICONSSR   QDOTSSR       EFCSSR

             BTU/S         BTU/S F
   79        -0.113E-06    0.421E-08
```

If the user has requested that axial thrust be calculated in the Global Options dialog (see sec. 5.2.2), the calculated axial thrust will be listed next in the output file.

```
AXIAL THRUST = -527.30169 LBF
```

If the user has activated the turbopump advanced option (see sec. 4.4.4), the turbopump output will be listed next in the output file. First, the number of turbopumps in the model is listed. (Note that this value is not labeled in the output file.) Then, the pump branch, turbine branch, speed, the turbine efficiency at the design point, the turbine velocity ratio at the design point, the required torque, and the horsepower are listed for each turbopump in the model.

```
1
IBRPMP  IBRTRB  SPEED(RPM)  ETATRB      PSITR       TORQUE(LB-IN)  HPOWER
23      1213    0.800E+05   0.578E+00   0.269E+00   0.511E+02      0.649E+02
```

If the user has activated the pressurization advanced option (see sec. 4.4.3), the pressurization output will be listed next in the output file. First, the number of pressurization tanks in the model is listed. Then, the ullage node, propellant node, ullage to propellant heat transfer rate, ullage to tank wall heat transfer rate, tank wall conduction heat transfer rate, tank wall temperature, propellant volume and ullage volume are listed for each pressurization tank. Note that the labels for this output do not include the units. The units are Btu/s for the heat transfer rates, degrees Rankine for the tank wall temperature, and cubic feet for the volumes.

```
NUMBER OF PRESSURIZATION SYSTEMS = 1
   NODUL   NODPRP  QULPRP  QULWAL  QCOND   TNKTM     VOLPROP   VOLULG
   2       4       0.6644  2.1888  0.0000  195.6238  473.0886  26.9114
```

4.7.10 Convergence Information

The final section of the output file contains information on the convergence of the solution. It is important to remember that GASP/WASP allows extrapolation outside the stated limits of its fluid property relationships. While this allows for flexibility during the iterative process, it can occasionally lead to a final solution based on extrapolated properties. For models where the user has selected GASP/WASP, GFSSP checks the pressure and temperature at each node and prints a warning in the output file if they are outside of GASP/WASP's stated limits so that the user can verify that the results are reasonable.

```
WARNING! CHKGASP: T out of fluid property range at node 1
WARNING! CHKGASP: T out of fluid property range at node 3
```

GFSSP also prints a statement indicating whether or not the solution converged. For an unsteady model, this statement is printed at each time step. If the solution converges, the statement lists the convergence criteria and the number of iterations needed to reach convergence.

```
SOLUTION SATISFIED CONVERGENCE CRITERION    0.100E-03 IN    5 ITERATIONS
```

If the solution does not converge, the statement lists the convergence criteria, the number of iterations that were performed, and the maximum difference after the last iteration.

```
SOLUTION DID NOT SATISFY CONVERGENCE CRITERION    0.100E-02 IN    541 ITERATIONS
DIFMAX IN SUCCESSIVE ITERATION = 0.175E-02
```

If the model includes the cyclic boundary option (see sec. 4.2.2), the number of adjustment iterations and the final temperature difference are listed next in the output file.

```
ITERADJC = 3    DIFTEM = 1.634E-16
```

This section of the output file is only active if the user has selected to print the initial field from the Global Options dialog (see sec. 4.2.1). The time and time step will be listed after the convergence information. For a steady model, the time will read 100,000,000 s and the time step will be 1.

```
TAU = 100000000.000000    ISTEP = 1
```

The final section of the output file lists the CPU time to complete the model simulation.

```
TIME OF ANALYSIS WAS 1.001440000000000E-002 SECS
```

4.8 Post-Processing Simulation Data

While the GFSSP output file provides a comprehensive summary of model simulation results, it is not always a practical source of information to meet the user's needs. Therefore, VTASC provides alternative methods of viewing GFSSP output for both steady and unsteady simulations.

4.8.1 Steady State Simulation Results

As mentioned in section 4.3, each GFSSP solution model element (fluid internal nodes and branches, conjugate heat transfer solid nodes and conductors) has a Results… dialog option located on their respective pop-up menus. After running a steady state simulation, if the user selects the Results option for a particular element, a table of results at that location will be displayed.

Figure 66 shows the internal fluid node results table for a steady state simulation with multiple fluids. For this case, the table includes the calculated pressure, temperature, compressibility, density, resident mass, and the mass concentration of each fluid at that node. The internal fluid node table contents will vary just like the fluid node solution results discussed in section 4.8.9 based on the user's selections (multiple fluid, single fluid, constant property fluid, print extended information). Clicking the OK button will close the Results option and return the user to VTASC.

The results tables for the fluid branches, solid nodes, and conductors are the same in appearance and function as the internal fluid node table discussed above. The parameters that are listed in each table are the same parameters discussed in section 4.8.9 for each respective element.

4.8.2 Unsteady Simulation Results

There are two options available in VTASC for generating plots of unsteady simulations, depending on the user's needs—VTASC Plot and Winplot.

4.8.2.1 VTASC Plot. VTASC Plot is a built-in plotting capability within VTASC. As with the steady state results tables, it is accessed by selecting the Results… dialog from the desired model element's pop-up menu. The appearance and function of VTASC Plot is the same for each model element. The only difference will be the parameters available to plot, which are the same parameters discussed for each element in section 4.7.9.

Figure 67 shows the Results dialog for an unsteady simulation. Initially, the plot canvas space will be blank. The user can generate a hard copy or a bitmap of the desired plot by clicking the Print or Print to Bitmap button, respectively. The user creates the desired plot using the Properties dialog, which is activated by clicking the Properties… button. Once the user has finished, clicking the Close button will end the Results dialog and return the user to VTASC.

Figure 68 shows the Properties dialog used to create a plot of unsteady results. The dialog consists of three tabs, as well as Apply, OK, and Cancel buttons. Clicking the Apply button accepts any changes that have been made. The OK button closes the Properties dialog and returns to the Results dialog. The Cancel button fulfills the same function as the OK button.

The first tab (fig. 68(a)) allows the user to define the data they wish to plot. The user may select parameters for plotting using the Data Selection list at the top of the tab. The user selects plot parameters by highlighting the desired parameters in the Available Data list and clicking the ➡ button. These parameters will then be added to the Selected Data list. If the user wishes to remove parameters from the Selected Data list, highlight those parameters and click the ⬅ button.

Figure 66. GFSSP steady state simulation results internal fluid node table.
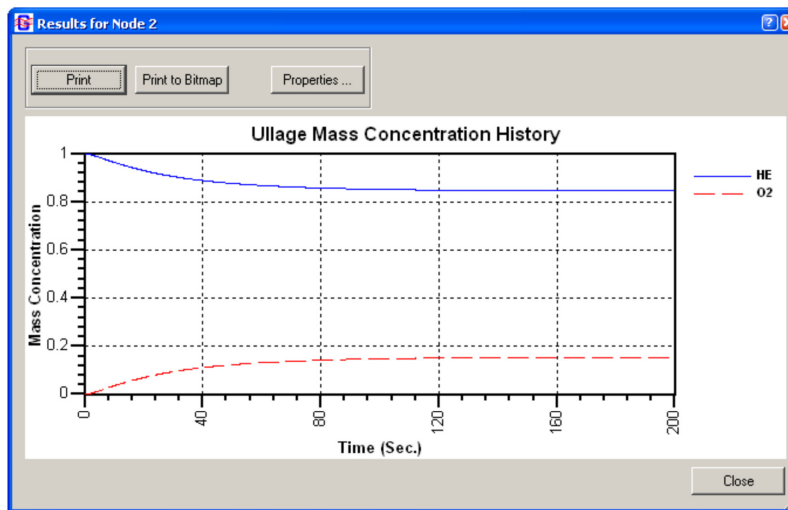
Figure 67. GFSSP results dialog for unsteady simulation.

Note that VTASC Plot does not have Multi-Y axis plotting capability so scale should be considered when plotting multiple parameters on a single plot. The Data Properties list at the bottom of the tab can be used to design the line style of each plot parameter. The user highlights the parameter whose line style they wish to design and then selects the line type, width, and color from the available selections on the right. Once all changes have been made to a particular parameter, click the Apply button to accept the changes.

The second tab (fig. 68(b)) allows the user to define the labeling parameters. Titles may be written or modified for the X and Y axes as well as the overall plot. The user may select whether or not they wish to include a grid or a legend on the plot by clicking the appropriate check box. The user may also define the number of minor tick marks they wish to see for each axis. Once all changes have been made, click the Apply button to accept the changes.

95
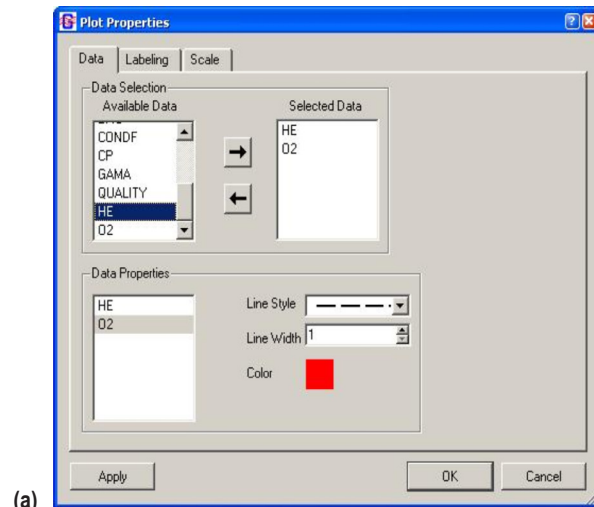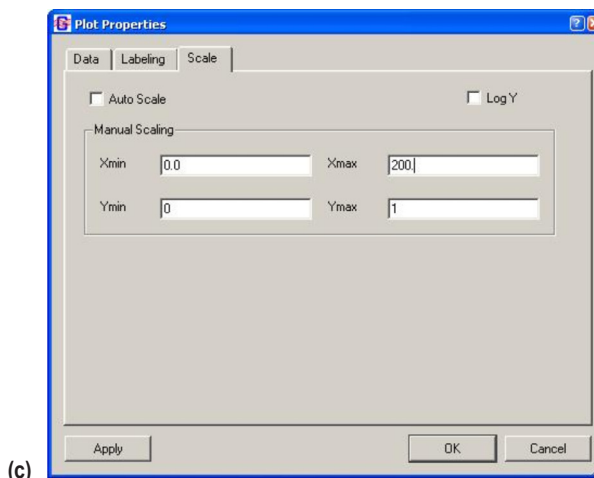
Figure 68. GFSSP VTASC plot properties dialog: (a) Data tab, (b) labeling tab,
and (c) scale tab.

The third tab (fig. 68(c)) allows the user to modify the scale of each axis. By default, VTASC will auto scale a plot for the user. Deselecting the Auto Scale check box allows the user to define the minimum and maximum values for each axis. The user also has the option of converting the Y axis to a log scale. Once all changes have been made, click the Apply button to accept the changes.

4.8.2.2 Winplot. If the user selects the Winplot plotting option from the Global Options dialog (see sec. 5.2.1), unsteady plot files will be generated in either comma delimited or binary formats. If the user selects the comma delimited option, several files are generated. The naming convention, description, and available parameters for each file are listed in table 9. Note that the conjugate heat transfer related output files are only written if a node or conductor of that type is present in the model. If the user selects the binary format, a single file with the name convention '*filename*.WPL' will be generated. This file will contain all of the available parameters for each model element as discussed in section 4.7.9 as well as DIFMAX, RSDMAX, and ITER.

Table 9. Winplot comma delimited unsteady output files.

| Naming Convention	Description	Parameters
*filename*FN.CSV	Fluid node results	P (psia), T (°F), Z, ρ (lbm/ft^3), x of fluid or c of each fluid, μ (lbm/ft-s), k (Btu/ft-s-R), V (ft^3), DIFMAX, RSDMAX, ITER
*filename*B.CSV	Fluid branch results	v (ft/s), DP (psid), $\dot{m}$ (lbm/s), $\dot{S}_{gen}$ (Btu/R-s)
*filename*SN.CSV	Solid node results	$C_{p,s}$ (Btu/lbm-°F), T_s (°F)
*filename*SF.CSV	Solid-fluid conductor results	h_{csf} (Btu/s-ft^2-°F), $h_{csf,rad}$ (Btu/s-ft^2-°F) if needed, $\dot{Q}_{sf}$ (Btu/s)
*filename*SS.CSV	Solid-solid conductor results	k_{ss} (Btu/ft-s-R), $\dot{Q}_{ss}$ (Btu/s)
*filename*SA.CSV	Solid-ambient conductor results	h_{csa} (Btu/s-ft^2-°F), $h_{csa,rad}$ (Btu/s-ft^2-°F) if needed, $\dot{Q}_{sa}$ (Btu/s)
*filename*SSR.CSV	Solid-solid radiation results	$k_{eff,ssr}$ (Btu/ft-s-R), $\dot{Q}_{ssr}$ (Btu/s)

As mentioned in section 4.1.4, Winplot must be obtained separately by the user. If Winplot is installed on the user's computer, the user may open Winplot using the Run Menu's Winplot selection or the Run Winplot button on the VTASC toolbar. If the unsteady plot files already exist, they will automatically be loaded into Winplot. Otherwise, the user must reselect the Run Menu Winplot selection or toolbar Winplot button to load the plot files into Winplot. For plotting and manipulating data in Winplot, the user is referred to the Winplot user's manual.[13]

4.8.3 Display in Flow Circuit

An option exists within VTASC to display results for a particular model element on the VTASC canvas itself. The user can then observe how certain solution parameters change as adjustments are made to the model. This also allows the user to print the model with the results of interest as a hard copy or bitmap for reports or presentations. The user activates this option by first selecting the model element(s) using the selection tool. Then, as discussed in section 4.1.5, the user activates the Display Results/Properties dialog from the Display menu. Figure 69 shows an example of displaying the results on the VTASC canvas.
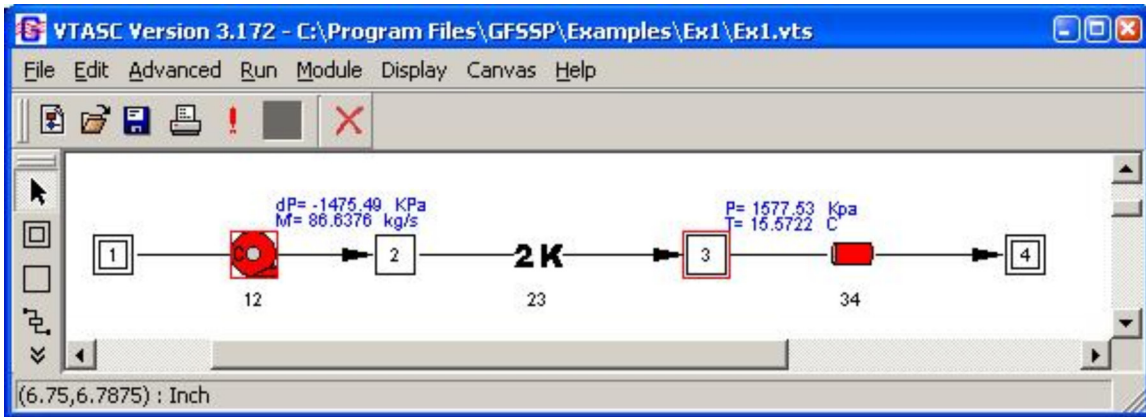
Figure 69. Display Results in flow circuit example.

Figure 70 shows the Display Results/Properties dialog. The user can select a maximum of three different parameters to display for each model element. Note that display parameters cannot be varied between like model elements (i.e., the user cannot display the pressure at one fluid node and the temperature at another fluid node). The selected parameters are displayed at all selected elements of that type. Also note that the conjugate heat transfer parameter selections are not active unless the user has activated conjugate heat transfer. Once the user has selected all desired display parameters, the Apply button is used to accept the changes. The OK button closes the Display Results/Properties dialog and returns the user to VTASC. The Cancel button fulfills the same function as the OK button.

The display units may be changed through the Display Property Units dialog, which is activated by clicking the Change button. Figure 71 shows the Display Property Units dialog. Alternative display units are available here for certain display parameters. The user toggles between the available units choices for each parameter. The OK button closes the Display Property Units dialog and returns the user to the Display Results/Properties dialog. The Cancel button fulfills the same function as the OK button.
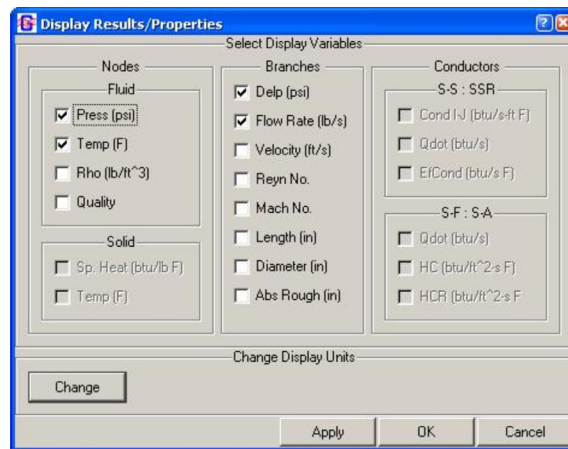
Figure 70. Display Results/Properties dialog.
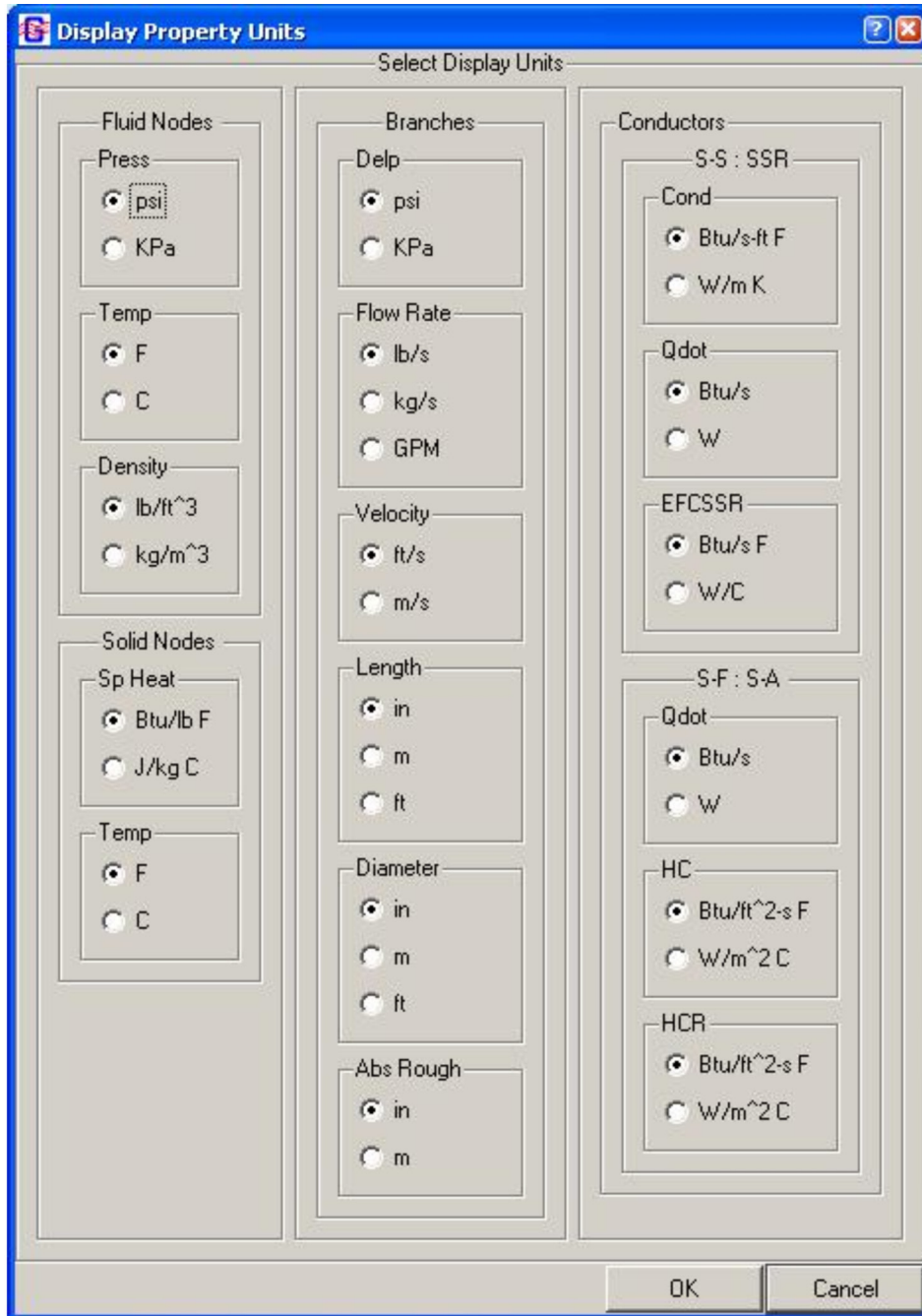
Figure 71. Display Property Units dialog.

5. EXAMPLES

This section demonstrates the major features of the code through 12 example problems, selected to serve two purposes. First, these problems will instruct the user on how to use the various options available in the code to analyze different fluid engineering problems. The other purpose of the examples contained within this section is to verify the code's predictions. This verification was accomplished by comparing the GFSSP solutions with analytical solutions, other numerical solutions, or with test data. The included demonstration problems are:

(1) Simulation of a flow system consisting of a pump, valve, and pipe line.
(2) Simulation of a water distribution network.
(3) Simulation of compressible flow in a converging-diverging nozzle.
(4) Simulation of the mixing of combustion gases and a cold gas stream.
(5) Simulation of a flow system involving a heat exchanger.
(6) Radial flow on a rotating radial disk.
(7) Flow in a long-bearing squeeze film damper.
(8) Simulation of the blowdown of a pressurized tank.
(9) A reciprocating piston-cylinder.
(10) Power balancing of a turbopump assembly.
(11) Steady state and transient conduction through a circular rod, with convection.
(12) Simulation of fluid transient following sudden valve closure.

The selection of the order for these problems is primarily determined by their complexities. The first seven problems consider steady state flows and use relatively simple flow networks. Each example demonstrates use of a special option. Example 8 is a two-node model to demonstrate the use of the unsteady option. More complex unsteady flow examples are illustrated in examples 9, 10, and 12. Options for time-dependent geometry and moving boundary are shown in example 9. The application of the turbopump and heat exchanger options in a typical gas turbine system is illustrated in example 10. Example 11 introduces GFSSP's conjugate heat transfer capability. Example 11 is an adaptation of a classical heat transfer problem into GFSSP. Example 12 emphasizes GFSSP's ability to predict fluid transient phenomena. Table 10 describes a matrix of the example problems and their use of various options to model the necessary physical processes. Several technical papers[37–39] also illustrate the application of GFSSP in computing secondary flow and axial thrust in rocket engine turbopumps for both steady and unsteady flow.

5.1 Example 1—Simulation of a Flow System Consisting of a Pump, Valve, and Pipe Line

5.1.1 Problem Considered

A problem commonly encountered in fluid engineering is to match a pump's characteristics with the operating system's characteristics. The designer needs to know the flow rate in the system and the power consumed by the pump. The following example problem demonstrates how GFSSP can be used to simulate such problems.

Table 10. Use of various options in example problems.

Example	Conjugate Heat Transfer	Constant Property	Gravity	Heat Exchanger	Ideal Gas	Long Inertia	Mixture	Moving Boundary	Non Circular Duct	Phase Change	Pump	Rotation	Turbopump	Unsteady	Variable Geom	Water Hammer
1			1								1					
2		2														
3						3										
4							4									
5				5												
6						6						6				
7		7						7	7							
8					8									8		
9								9						9	9	
10				10									10			
11	11															
12														12		12

The system considered for this example is shown in figure 72. It consists of two reservoirs connected by 1,500 ft of 6-in-diameter pipe with a roughness factor (ε/D) of 0.005. The receiving reservoir is located at an elevation that is 150 ft higher than the supply reservoir. The head-flow characteristics of the pump considered in this problem are shown in figure 73. This pump should be used to transport water, at 60 °F, from the supply reservoir to the receiving reservoir. GFSSP will be used to determine the system flow rate and required pump horsepower.

5.1.2 GFSSP Model

The fluid system shown in figure 72 can be simulated with a GFSSP model consisting of four nodes and three branches as shown in figure 74(a). Nodes 1 and 4 are the boundary nodes representing the supply and receiving reservoirs that are both at 14.7 psia and 60 °F. Node 2 is an internal node representing the pump exit and the inlet to the gate valve. Node 3 is an internal node representing the exit from the gate valve and the inlet to the pipeline that connects the valve to the receiving reservoir. Branches 12, 23, and 34 represent the pump, gate valve, and pipeline, respectively. Figure 74(b) shows how this model appears in VTASC.

Once the boundary conditions have been established, the next step is to obtain the necessary information required to model the resistances and the momentum source located in the branches.

5.1.2.1 Branch 12 (Pump). Option 14 was selected to represent the pump because this option allows the user to model a pump with a given characteristics curve using either two or three constants. For this problem, two constants, A_0 and B_0, were input as well as the pump area (area
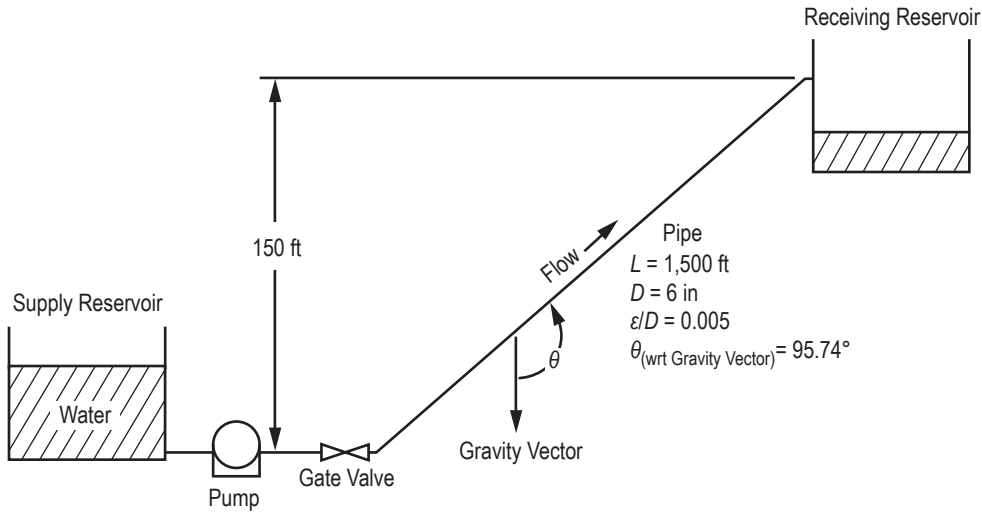
Figure 72. Schematic of pumping system and reservoirs (Example 1).
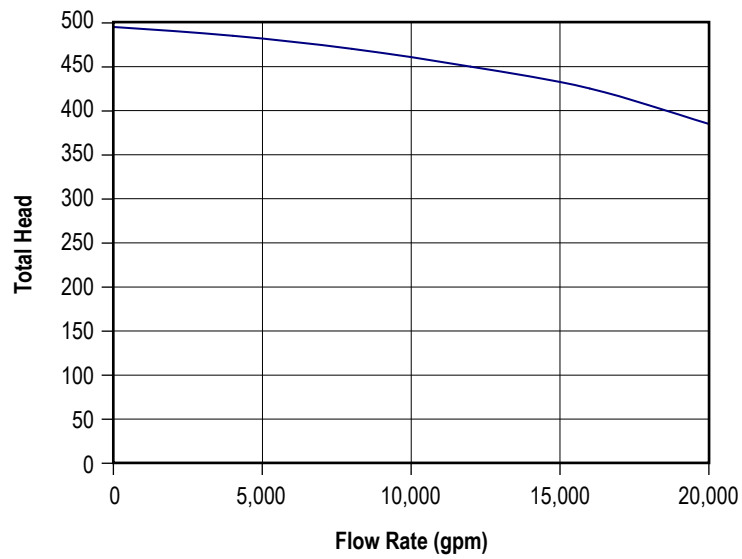
Figure 73. Manufacturer supplied pump head-flow characteristics.
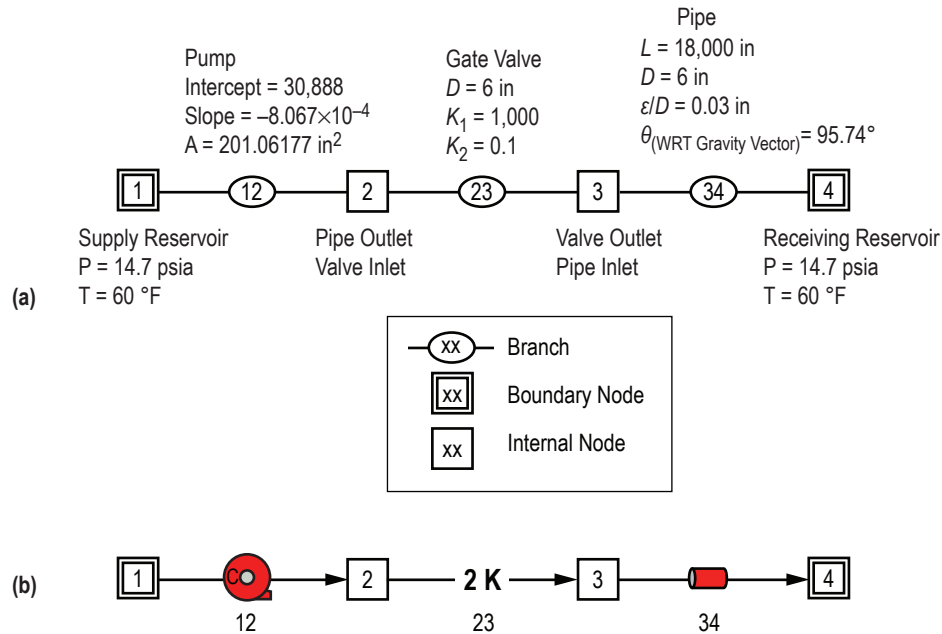
Figure 74. GFSSP model of pumping system and reservoirs: (a) Detailed schematic and (b) VTASC model.

is only required for the velocity calculation). These constants represent the slope and the intercept of the $\dot{m}^2$ versus Δp curve. The following procedure is used to obtain these constants:

(1) Construct a table, based on user-selected points, from the pump characteristics curve shown in figure 73 to develop a relationship between $\dot{m}^2$ and Δp. These data are shown in table 11, where $\dot{m} = \rho Q$ and $\Delta p = \dfrac{\rho g}{g_c} H$.

(2) Plot the Δp and $\dot{m}^2$ data from table 11 as shown in figure 75. Note that the relationship is linear (i.e., $\Delta p = A_0 + B_0\, \dot{m}^2$). Therefore, the pump characteristic curve can be prescribed with two constants, A_0 and B_0, and the optional third constant is not necessary.

(3) Determine the constants A_0 and B_0 from figure 75.

The intercept (Δp at $\dot{m}^2 = 0$) is:

$$A_0 = 30{,}888. \tag{63}$$

The slope (taken about $Q = 10{,}000$ gpm) is:

$$B_0 = \frac{28{,}080 - 29{,}328}{(2.784E+6) - (1.2372E+6)} = -(8.067E-4) \ . \tag{64}$$

103

Table 11. Tabulated pump characteristics data.

Q (gpm)	$\dot{m}$ (lb/s)	Head (ft)	Δp (psf)	$\dot{m}^2$ (lb/s)^2
–	–	495	30,888	–
4,000	556.13	485	30,264	3.093×10^5
8,000	1,112.3	470	29,328	1.2372×10^6
12,000	1,668.4	450	28,080	2.784×10^6
16,000	2,224.5	425	26,520	4.9484×10^6
20,000	2,781	385	24,024	7.734×10^6
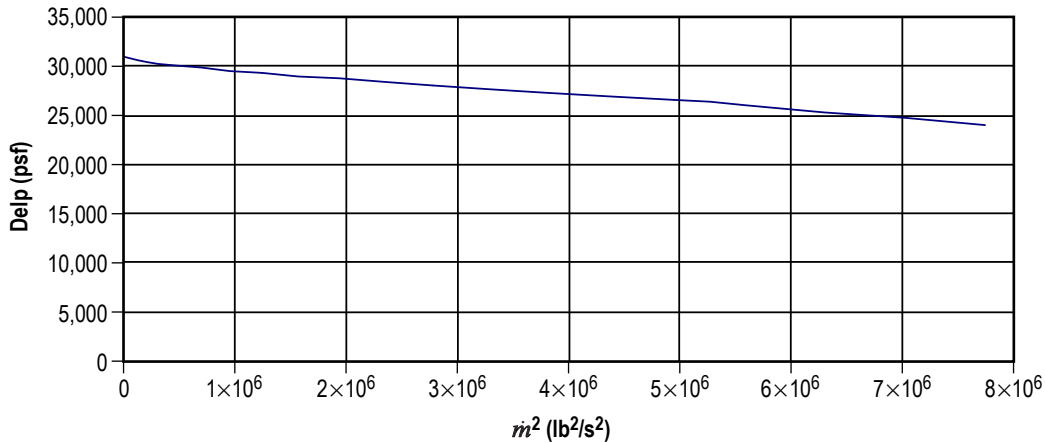
Figure 75. Pump characteristics curve in GFSSP format.

Since the curve is linear, the slope can be determined at any point without sacrificing accuracy. In VTASC, A_0 is entered in the intercept input box and B_0 is entered in the second order input box.

5.1.2.2 Branch 23 (Gate Valve). Option 13 was used to represent the gate valve. Option 13 requires two constants, K_1 and K_∞ (two-K method), and the internal diameter to model various pipe fittings. The two required constants were obtained from table 7, assuming a reduced trim ($\beta=0.8$) gate valve.

5.1.2.3 Branch 34 (Pipeline). Option 1 was used to represent the pipeline. This branch resistance option requires the user to supply the length, diameter, roughness factor (ε/D), and the angle between the gravity vector and the pipeline.

5.1.3 Results

The example 1 GFSSP input and output data files (ex1.dat and ex1.out) are included in appendix D (on CD inside back cover). The example 1 GFSSP model predicts a flow rate of 191 lb/s and the pressure rise across the pump is 214 psi. Interpolation in the table 11 data shows that the pump pressure rise for the GFSSP predicted flow rate is 213 psi, which indicates

that the model is working as expected. This example demonstrates that GFSSP can accurately predict the operating point of a fluid system consisting of a pump and a pipeline with a valve.

When selecting a pump, the mass flow rate in the attached fluid system is generally unknown. By generating a system characteristic curve and plotting this curve against the pump characteristic curve, the operating point of the system can be determined. Using the example 1 GFSSP model, the system characteristic curve can be generated in the following manner:

(1) Eliminate the pump by setting A_0 and B_0 to zero.
(2) Set boundary pressures P_1 and P_4 to desired values.
(3) Run the model.
(4) Repeat steps (2) and (3) to cover the desired range.

Table 12 shows typical system characteristics generated by performing the parametric study described above. The inlet pressures were arbitrarily selected to cover the expected operating range. The GFSSP predicted mass flow rates are shown in the third column. The flow resistance coefficients for the valve and the pipe are shown in the next two columns. The method of calculating these values is discussed in section 2. The next three columns of table 12 show hand-calculated pressure drops over the gate valve and the pipe and the pressure difference that is associated with the elevation change that exists in the example 1 model. The sum of these three losses is tabulated in the next column. The last column shows the overall pressure drop for the system for the given mass flow rate. A comparison of the values contained in the last two columns shows good agreement.

Table 12. Predicted system characteristics.

P_1 (psia)	P_4 (psia)	$\dot{m}$ (lbm/s)	K_f, gate lbf–s²/ (lb–ft)²	K_f, pipe lbf–s²/ (lb–ft)²	Δp, gate (psia)	Δp, pipe (psia)	Δp, gate (psia)	Δp, cal (psia)	Δp, pres (psia)
150	14.7	131	0.0019	0.593	0.225	70.67	65.00	135.89	135.3
200	14.7	171	0.0019	0.592	0.385	120.21	65.00	185.59	185.3
250	14.7	203	0.0019	0.591	0.544	169.13	65.00	234.67	235.3
300	14.7	231	0.0019	0.591	0.704	219.00	65.00	284.71	285.3

To determine the operating point of the system with a given pump, the system characteristics can be plotted together with the pump characteristics. The system operating point will be determined by the intersection of these two curves. Figure 76 shows the example 1 fluid system characteristics, generated previously, plotted along with the pump characteristics data that are shown in table 11. As seen from this figure, the operating point predicted by this method occurs at a pressure drop of approximately 214 psid and a mass flow rate of 190 lbm/s, which compares well with the predicted results from the GFSSP model containing the pump.
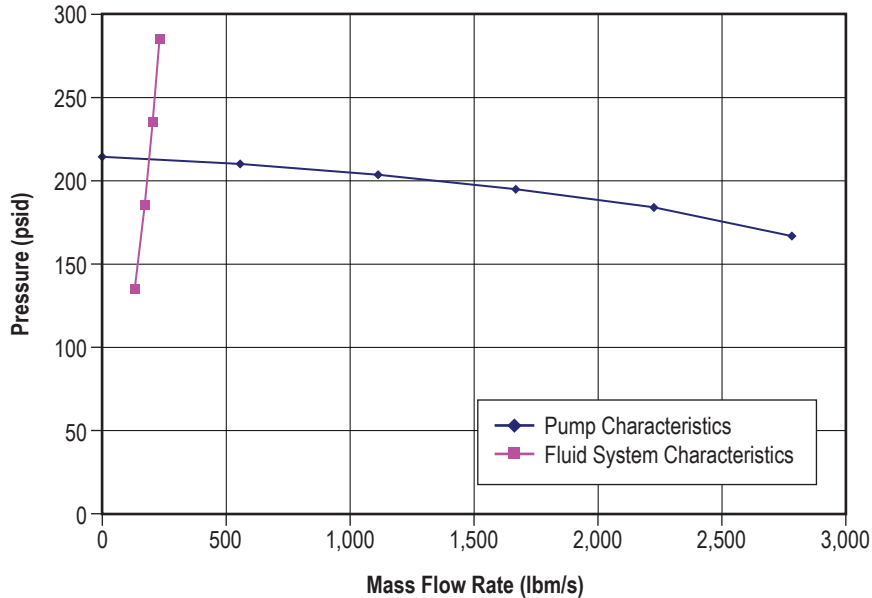
Figure 76. Fluid system operating point.

Finally, the power input to the pump can be calculated from the following relationship:

$$\text{Horse power} = \frac{\dot{m}}{\rho}\Delta p = \frac{(191\,\text{lbm/s})}{(62.4\,\text{lbm/ft}^3)}\frac{(214\,\text{lbf/in}^2)(144\,\text{in}^2/\text{ft}^2)}{(550\,\text{ft-lbf/hp})} = 171\,\text{hp} \ . \tag{65}$$

5.2 Example 2—Simulation of a Water Distribution Network

5.2.1 Problem Considered

In Example 1, a single line pipe flow problem commonly encountered by pipeline design-ers is analyzed. In this example, an example associated with multipath systems, commonly known as flow networks, is considered. In general, water supply systems are considered as flow networks, since nearly all such systems consist of many interconnecting pipes. A 10-pipe (commercial steel) distribution system is shown in figure 77. Water at 50 psia enters the circuit at boundary node 1. Water is removed from the circuit at boundary nodes 3, 4, and 9 where pressures are also known. Use GFSSP to determine pressures at all of the remaining nodes and the flow rates in all of the pipes. The length, diameter, and roughness factors for each pipe are given in table 13. Note that pipes are designated as branches in the subsequent discussions.

5.2.2 GFSSP Model

The system shown in figure 77 is modeled by GFSSP in VTASC using 9 nodes and 10 branches as shown in figure 78. The fluid was assumed incompressible and therefore a constant

106
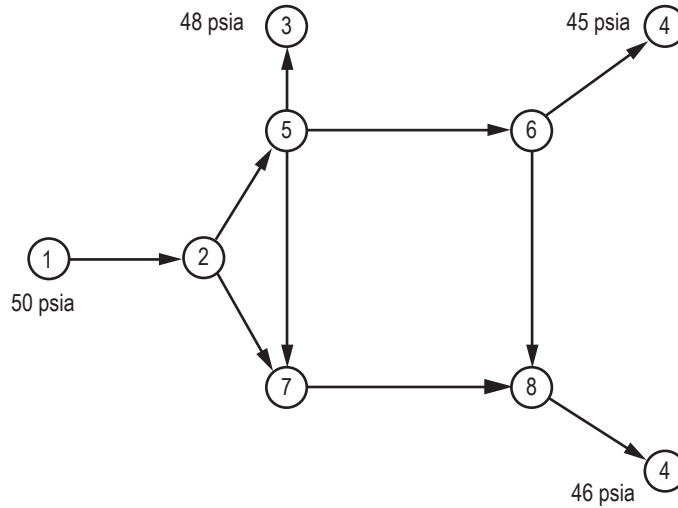
Figure 77. Water distribution network schematic (Example 2).

Table 13. Water distribution network branch data.

Branch	Length (in)	Diameter (in)	Roughness Factor
12	120	6	0.0018
25	2,400	6	0.0018
27	2,400	5	0.0018
57	1,440	4	0.0018
53	120	5	0.0018
56	2,400	4	0.0018
64	120	4	0.0018
68	1,440	4	0.0018
78	2,400	4	0.0018
89	120	5	0.0018
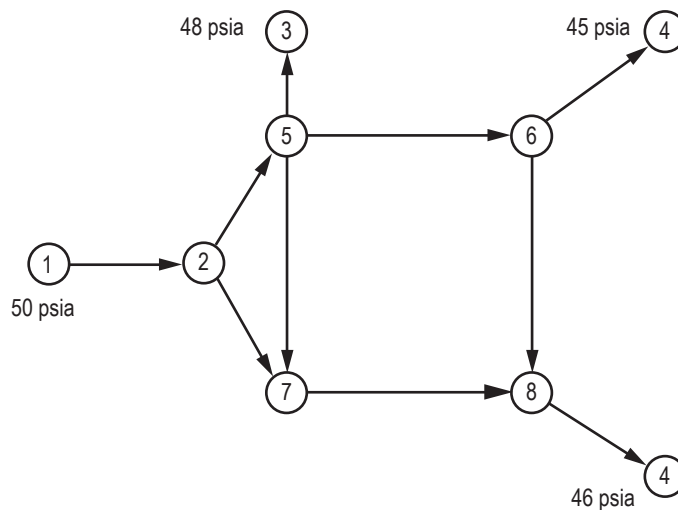
Figure 78. GFSSP model of the water distribution network.

density (DENCON = .TRUE.) option was used. Nodes 1, 3, 4, and 9 are boundary nodes where the pressures are prescribed. Node 1 represents the inlet boundary node. Nodes 3, 4, and 9 are outlet boundary nodes. All of the remaining nodes (2, 5, 6, 8, and 7) are internal nodes where the pressures are calculated. All of the branches in this circuit simulate pipes. Therefore, each branch uses branch resistance option 1. The length, diameter, and roughness factors of all branches are given in table 13.

5.2.3 Results

The input and output data files (ex2.dat and ex2.out) are shown in appendix E (on CD inside back cover). The GFSSP-predicted results are shown in tables 14 and 15. Table 15 lists the predicted pressures at the internal nodes in psia and feet of water. Table 15 lists the predicted flow rates in lbm/s and ft^3/s. Table 15 also provides a comparison between the GFSSP predicted results and values predicted by the Hardy Cross[2,26] method.

Table 14. GFSSP predicted pressure distribution at the internal nodes.

P_2		P_5		P_6		P_7		P_8	
psia	ft	psia	ft	psia	ft	psia	ft	psia	ft
49.80	114.92	48.11	111.02	45.34	104.63	48.35	111.58	46.01	106.18

Table 15. GFSSP and Hardy Cross method predicted branch flow rates.

Flow Rate	GFSSP		Hardy Cross	
	lb/s	ft^3/s	lb/s	ft^3/s
$\dot{m}_{12}$	100.16	1.605	100.16*	1.605*
$\dot{m}_{25}$	63.1	1.011	63.59	1.019
$\dot{m}_{27}$	37.0	0.593	36.58	0.5862
$\dot{m}_{53}$	44.43	0.7115	44.43*	0.7115*
$\dot{m}_{56}$	29.1	0.466	29.11	0.4665
$\dot{m}_{57}$	−10.4	−0.167	−9.93	−0.1592
$\dot{m}_{64}$	47.07	0.7548	47.07*	0.7548*
$\dot{m}_{68}$	−18.0	−0.288	−17.99	−0.2883
$\dot{m}_{78}$	26.7	0.428	26.64	0.4270
$\dot{m}_{89}$	8.66	0.1387	8.66*	0.1387*

* Boundary flow rates are prescribed from GFSSP predictions.

Figure 79 shows a comparison between GFSSP and Hardy Cross predicted flow rates. The comparison appears reasonable considering the fact that the Hardy Cross method assumes a constant friction factor in the branch while GFSSP computes the friction factor for all branches. Therefore, as the flow rates change, the friction factor also changes.
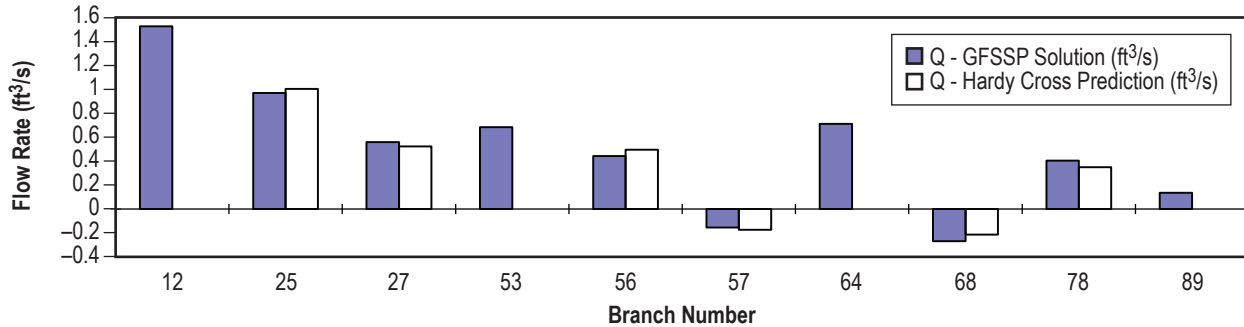
Figure 79. A flow rate comparison between GFSSP and hardy cross method predictions.

5.3 Example 3—Simulation of Compressible Flow in a Converging-Diverging Nozzle

5.3.1 Problem Considered

In the previous examples, incompressible flows in fluid systems were considered. In this example, compressible flow in a converging-diverging nozzle demonstrating GFSSP's capability to handle compressibility will be considered. One of the characteristics of the compressible flow in a duct is that the flow rate becomes independent of exit pressure after reaching a threshold flow rate. This threshold value is known as the choked flow rate and it is a function of inlet pressure and temperature. Flow in a confined duct becomes choked when the flow velocity equals the local velocity of sound. The purpose of this example is to investigate how accurately GFSSP can predict the choked flow rate in a converging-diverging nozzle.

The converging-diverging nozzle considered for this example is shown in figure 80. The nozzle is 6.3 in long with a 0.492-in-diameter throat. The inlet diameter of the nozzle is 0.6758 in and throat of the nozzle is located 0.158 in downstream of the inlet. The fluid considered was steam at 150 psia and 1,000 °F. The nozzle backpressure was varied from 134 to 45 psia. GFSSP is required to predict the flow rate and the pressure distribution for different exit pressures. The predicted flow rate will also be compared with the isentropic solution.

5.3.2 GFSSP Model

The fluid system shown in figure 80 can be simulated with a GFSSP model consisting of 17 nodes and 16 branches as shown in figure 81(a). Nodes 1 and 17 are the boundary nodes representing the inlet and outlet of the nozzle. All of the remaining nodes are internal nodes connected in series. GFSSP can be used to construct an isentropic model by selecting branch resistance option 2 (flow through a restriction), using a flow coefficient, C_L set equal to zero and by setting the logical flag INERTIA = .TRUE. This option eliminates friction from the momentum equation, which represents a balance between the inertia and pressure force with the inclusion of the inertia term. Each branch assumes a constant flow area that was determined from the nozzle geometry at the midpoint of the branch location. The branch information is listed in table 16. Figure 81(b) shows how this model appears in VTASC. It may also be noted that the energy equation has been solved using the second law option.
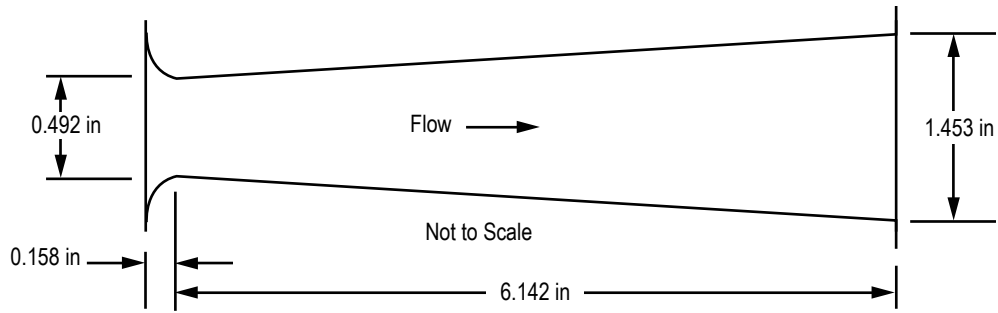
Figure 80. Converging-diverging steam nozzle schematic (Example 3).
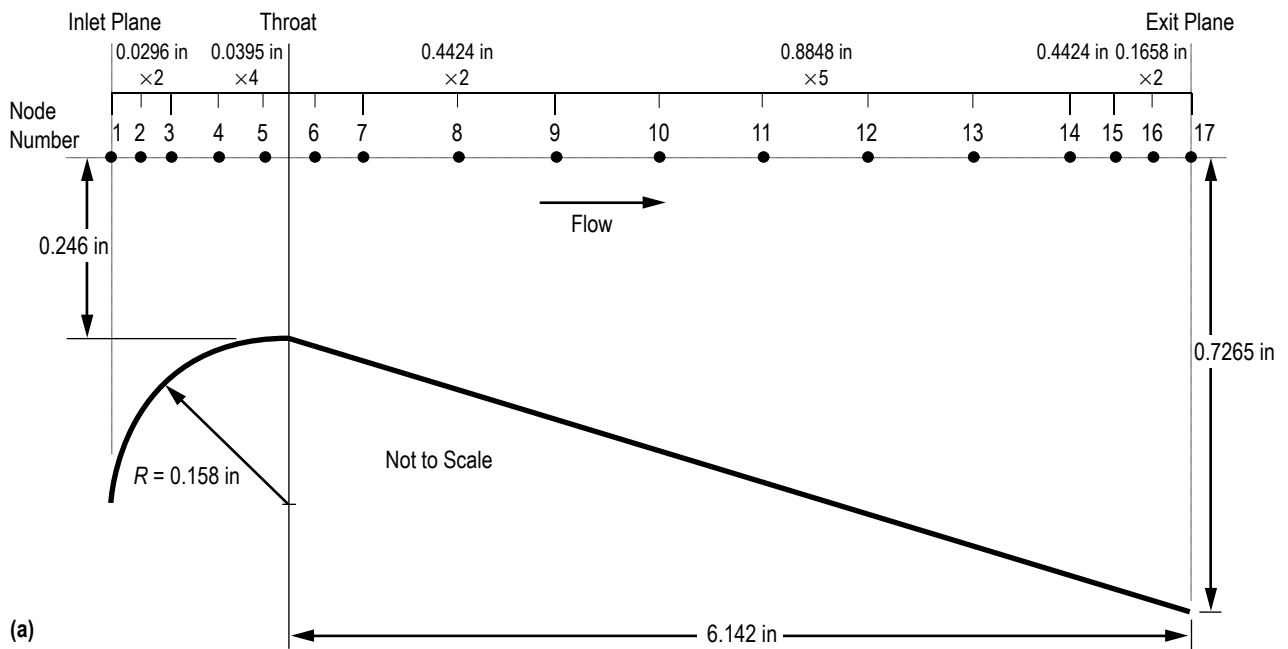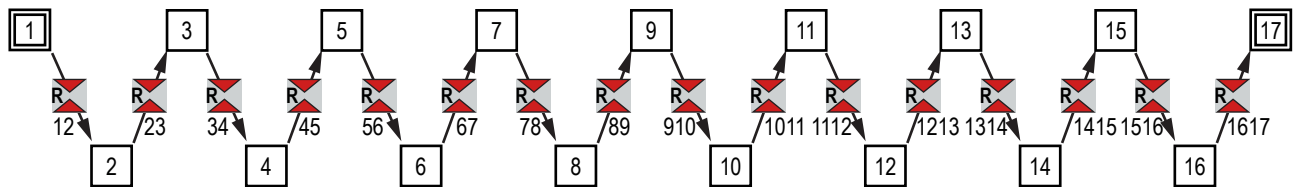
Figure 81. Converging-diverging steam nozzle model: (a) Detailed schematic
and (b) VTASC model.

Table 16. Converging-diverging nozzle branch information.

Branches	Option	Area (in^2)
12	2	0.3587
23	2	0.2717
34	2	0.2243
45	2	0.2083
56	2	0.1901
67	2	0.1949
78	2	0.2255
89	2	0.2875
910	2	0.3948
1,011	2	0.5640
1,112	2	0.7633
1,213	2	0.9927
1,314	2	1.2520
1,415	2	1.4668
1,516	2	1.5703
1,617	2	1.6286

It may be mentioned here that the temperature at the outlet boundary node has no influence on the solution. However, the code must be supplied with a value to satisfy the input requirements for a boundary node. In this example the temperature was specified arbitrarily to 1,000 °F at node 17. The boundary conditions are specified in table 17.

Table 17. Converging-diverging nozzle boundary conditions.

P_1 (psia)	T_1 (°F)	P_{17} (psia)	T_{17} (°F)
150	1,000	134	1,000
150	1,000	100	1,000
150	1,000	60	1,000
150	1,000	50	1,000
150	1,000	45	1,000

5.3.3 Results

The outlet boundary node pressures were varied to include 134, 100, 60, 50, and 45 psia. The input and output files (ex3.dat and ex3.out) from the example case using an exit pressure of 60 psia are included in appendix F (see CD inside back cover). The predicted pressure distributions for five test cases are shown in figure 82. Figure 83 shows the predicted temperature distributions for the same cases.

Table 18 lists the model predicted mass flow rates with varying exit pressures. As expected, the mass flow rate increased as the exit pressure was decreased until the pressure ratio decreased below the critical pressure ratio. At this point and below, the mass flow rate remained constant due to choking of the flow at the nozzle throat.
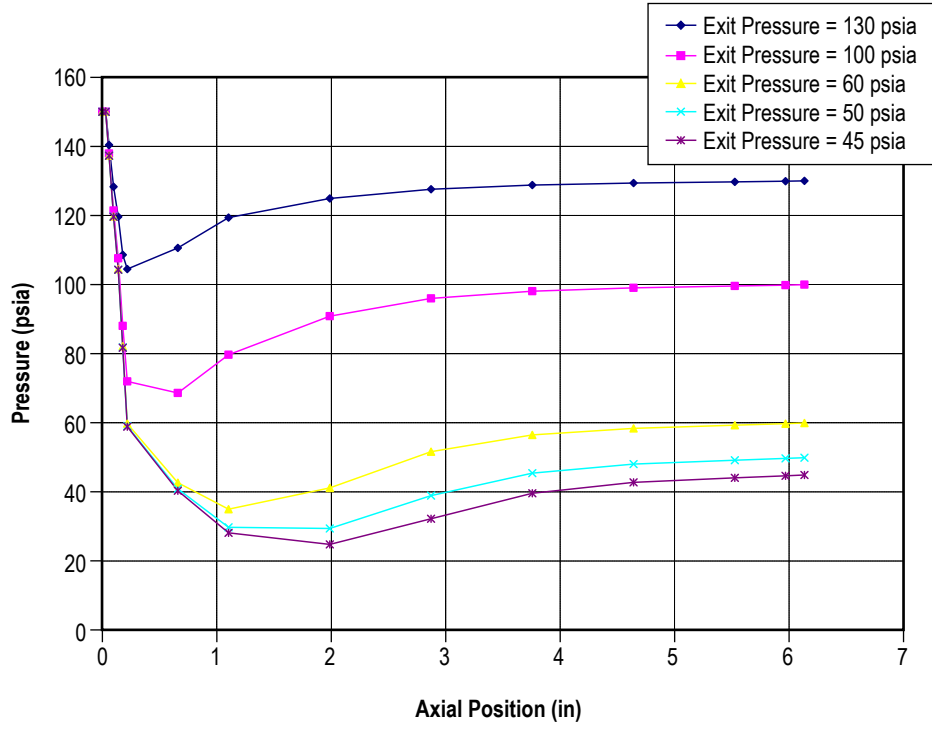
Figure 82. Predicted pressures for the isentropic steam nozzle.
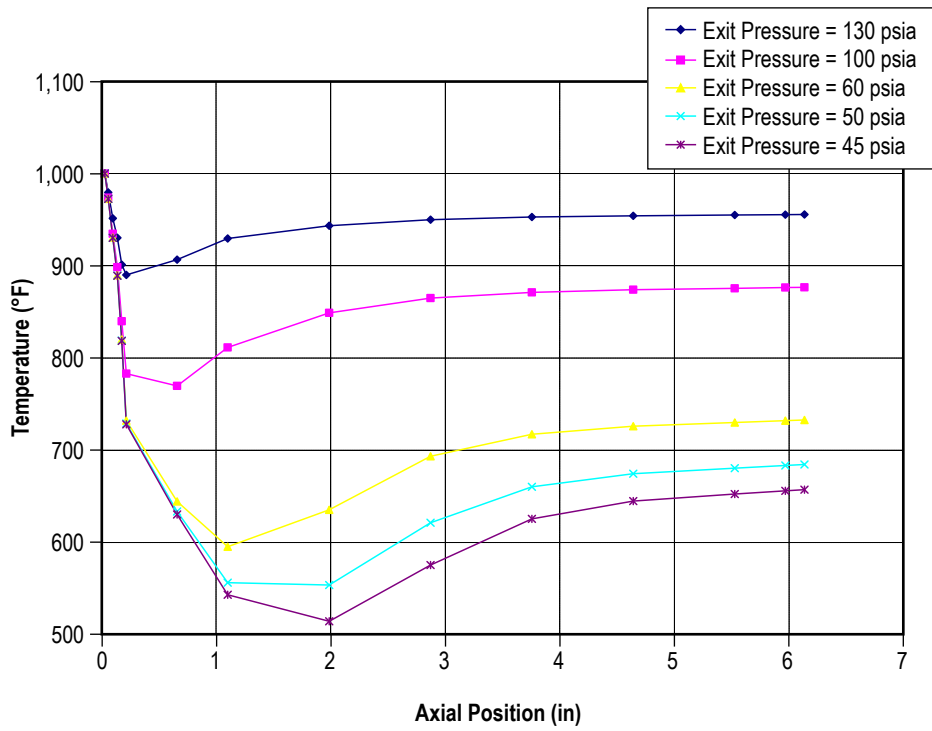
Figure 83. Predicted temperatures for the isentropic steam nozzle.

112

Table 18. Predicted mass flow rate with varying exit pressure.

P_{exit} (psia)	$\dot{m}$ (lbm/s)
134	0.279
100	0.329
60	0.336
50	0.337
45	0.337

The isentropic flow rate was calculated from equation (66). This equation assumes that the inlet pressure is a stagnation pressure. GFSSP's formulation assumes that the prescribed boundary conditions are taken at a static condition. The nozzle inlet velocity head component must be added to the GFSSP static inlet boundary pressure to obtain the correct nozzle inlet stagnation pressure to use in equation (66) as shown in equation (67):

$$\dot{m} = A_{\text{throat}} P_{\text{inlet}} \sqrt{\frac{g_c \, \gamma}{R \, T_{\text{inlet}}} \left(\frac{2}{\gamma + 1} \right)^{\left(\frac{\gamma + 1}{\gamma - 1} \right)}} \tag{66}$$

and

$$P_{\text{inlet}} = P_{\text{static}} \left(1 + \left(\frac{\gamma - 1}{2} \right) M^2 \right)^{\frac{\gamma}{\gamma - 1}} . \tag{67}$$

A value of the specific heat ratio at the nozzle inlet boundary node was obtained from GASP. Then, using the case where the exit pressure is 60 psia (the model output data file contained in appendix F (on CD inside back cover)), the inlet Mach number is obtained from the first branch connected to the inlet node. Substituting these values into equation (67) gives the following total pressure at the nozzle inlet:

$$P_{\text{inlet}} = (150 \text{ psia}) \left(1 + \left(\frac{1.2809 - 1}{2} \right) (0.342)^2 \right)^{\frac{1.2809}{1.2809 - 1}} = 161.6 \text{ psia} . \tag{68}$$

Substituting the calculated total inlet pressure from equation (68) into equation (66) and solving for the choked mass flow rate gives a calculated isentropic choked mass flow rate of 0.327 lbm/s as shown:

$$\dot{m} = \left(0.19012 \text{ in}^2 \right) \left(161.6 \frac{\text{lbf}}{\text{in}^2} \right) \sqrt{\frac{32.174 \frac{\text{lbm-ft}}{\text{lbf-s}^2} (1.281)}{85.83 \frac{\text{lbf-ft}}{\text{lbm-}^\circ\text{R}} 1,460 \text{ }^\circ\text{R}} \left(\frac{2}{1.281 + 1} \right)^{\frac{2.281}{0.281}}} = 0.327 \frac{\text{lbm}}{\text{s}} . \tag{69}$$

As the reader can see by comparing the results shown in table 18 and equation (69), there is good agreement (approximately a 3% difference) between the GFSSP predicted choked flow rate and the calculated isentropic choked flow rate. The prediction from the first law-based formulation has also been compared with the second law formulation. In the first law formulation, enthalpy was used as the dependent variable and equation 4(a) was used instead of equation 4(b). Unlike the second law formulation where density is computed from pressure and entropy, the first law formulation calculates density from pressure and enthalpy. The comparison of choked mass flow rate for both formulations with the isentropic solution is shown in table 19. It may be noted that the entropy-based formulation more accurately predicts the mass flow rate than the enthalpy-based formulation.

Table 19. Comparison of choked mass flow rates.

Parameter	Second Law Formulation	First Law Formulation
GFSSP predicted isentropic mass flow rate	0.337 lbm/s	.308 lbm/s
Calculated stagnation inlet pressure	161.6 psia	159.71 psia
Calculated isentropic mass flow rate	0.323 lbm/s	0.323 lbm/s
Percent difference between GFSSP predicted and calculated isentropic mass flow rates	3.06%	−4.64%

To validate GFSSP's ability to predict temperatures, the GFSSP predicted temperature at the nozzle throat was also compared with a hand-calculated temperature using equation (70). This equation assumes an isentropic process. In equation (70), the pressure P_1 was assumed to be the total pressure at the nozzle inlet that was calculated from equation (68) and the throat pressure was taken from the GFSSP output:

$$T_2 = T_1\left(\frac{P_2}{P_1}\right)^{\frac{\gamma-1}{\gamma}} = (1,460\ °R)\left(\frac{82.13\ \text{psia}}{161.6\ \text{psia}}\right)^{\frac{1.2809-1}{1.2809}} = 1,258.6\ °R = 798.6\ °F\ . \tag{70}$$

The GFSSP predicted nozzle throat temperature is 819.9 °F. This temperature compares well, within 3%, with the value calculated from equation (70).

The isentropic steam nozzle model represents a reversible process in which no entropy is generated. In an actual steam nozzle there will be frictional losses that result in an increase in entropy. To demonstrate GFSSP's ability to predict the irreversibility (entropy generation) of a process, the isentropic steam nozzle model was modified to allow for frictional losses. The branch resistance option for each model branch was changed from Option 2 with a C_L =0, to Option 1 using the branch lengths and diameters shown in figure 81 and assuming an absolute roughness of 0.01 in.

Figure 84 shows a temperature/entropy comparison between the GFSSP isentropic steam nozzle model and the GFSSP steam nozzle model with frictional losses. As one can see in figure 84,
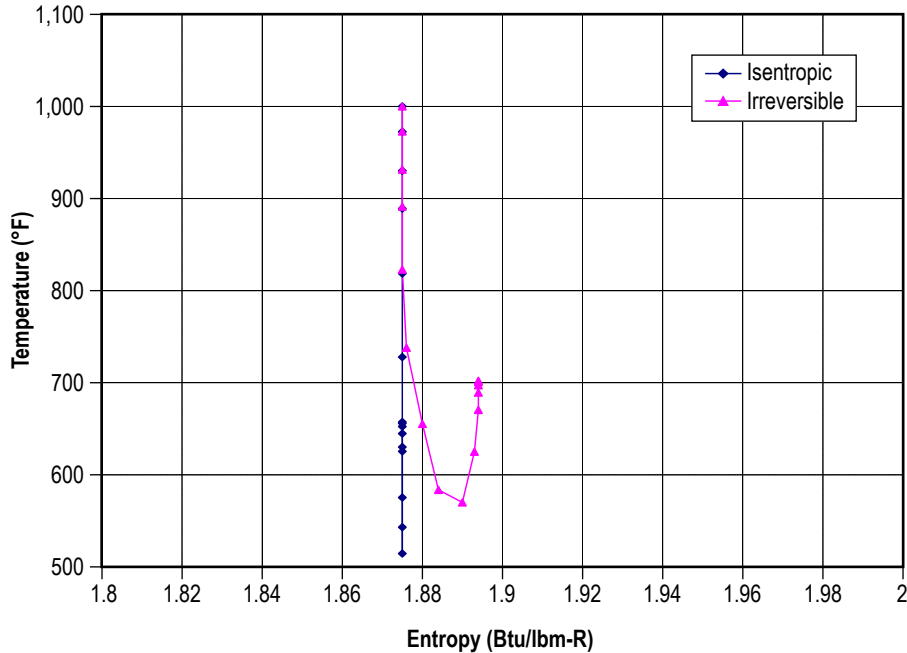
Figure 84. Temperature/entropy plot comparing the isentropic steam nozzle
with an irreversible process.

the isentropic model predicts no change in entropy through the nozzle while the irreversible process predicts a increase in entropy of 0.019 Btu/(lbm °R).

5.4 Example 4—Simulation of the Mixing of Combustion Gases and a Cold Gas Stream

5.4.1 Problem Considered

In the previous examples, the fluid systems that were considered employed a single fluid. In this example, simulation of multiple fluids in a mixing process are considered. How to use the MIXTURE logical option in the code to simulate the mixing of combustion gases and a cold gas stream by utilizing the flow system shown in figure 85 will be demonstrated. A mixture of hot combustion products, consisting of water vapor and oxygen, is mixed with cooler oxygen gas. The mixture temperature and composition are required to be calculated.

A mixture consisting of 90% water vapor and 10% oxygen (by mass) at 500 psia and 1,500 °F mixes with pure oxygen at 500 psia and 80 °F. GFSSP is required to predict the flow rate, mixture temperature, and composition of the mixture. A hand calculation will also be performed of the mixture temperature and the composition of the mixture to verify GFSSP's predictions.

5.4.2 GFSSP Model

The mixing chamber shown in figure 85 can be simulated with a GFSSP model consisting of four nodes and three branches as shown in figure 86. Nodes 1, 2, and 4 are the boundary nodes
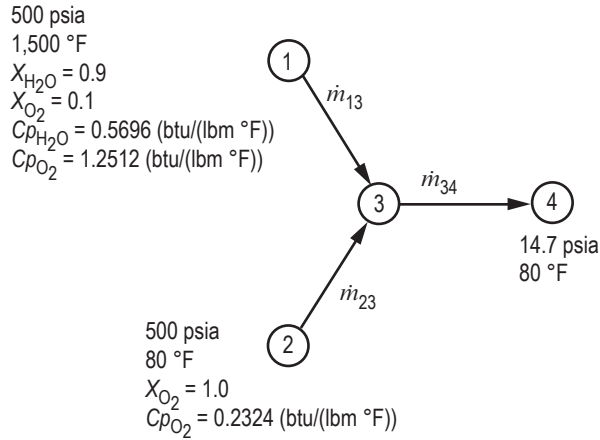
Figure 85. Mixing problem schematic (Example 4).
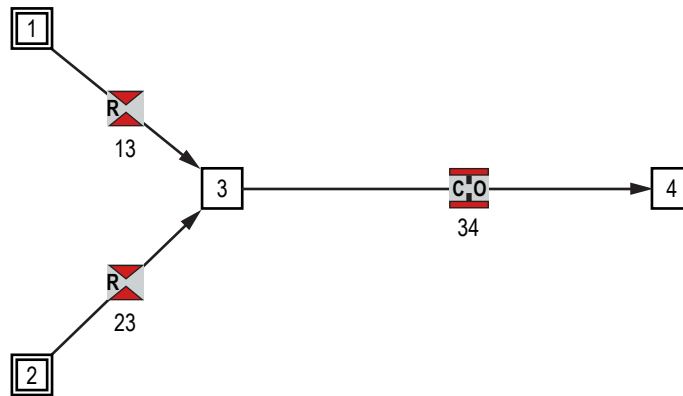
Figure 86. GFSSP model of mixing problem.

representing the inlet and outlet of the mixing chamber and node 3 is the internal node representing the mixing chamber. Branches 13 and 23 are represented by option 2 using a flow coefficient of 0.6 and area of 1 in^2. Branch 34 also uses a flow coefficient of 0.6 and area of 1 in^2, but it is modeled using option 22. The reason option 22 is used for branch 34 is to account for the possibility of choked flow in the branch.

5.4.3 Results

The input and output files of this example are included in appendix G as ex4.dat and ex4.out (see CD inside back cover). The predicted flow rates in branches 13, 23, and 34 are 1.16, 3.10, and 4.26 lbm/s, respectively. The predicted temperature at the outlet of the mixing chamber, node 3, is 689 °F and the composition is 24.47% water vapor and 75.53% oxygen. The mixture will not vary between nodes 3 and 4.

Now verify the predicted results by performing hand calculations of the mixing process. The temperature of the mixture can be calculated from the energy conservation equation written for the mixing chamber. The energy conservation equation for node 3 can be written as:

$$x_{H_2O} \dot{m}_{13} C_{p,H_2O} T_1 + x_{O_2} \dot{m}_{13} C_{p,O_2} T_1 + \dot{m}_{23} C_{p,O_2} T_2 = \dot{m}_{34} C_{p,\text{mix}} T_3 \ . \tag{71}$$

Equation (71) can be rearranged to find T_3:

$$T_3 = \frac{x_{H_2O} \dot{m}_{13} C_{p,H_2O} T_1 + x_{O_2} \dot{m}_{13} C_{p,O_2} T_1 + \dot{m}_{23} C_{p,O_2} T_2}{\dot{m}_{34} c_{p,\text{mix}}}$$

$$= \frac{(0.9)(1.16 \text{ lb/s})(0.5696 \text{ Btu/lb-R})(1{,}960\text{R}) + (0.1)(1.16 \text{ lb/s})(1.2512 \text{ Btu/lb-R})(1{,}960\text{R})}{(4.26 \text{ lb/s})(0.3757 \text{ Btu/lb-R})}$$

$$+ \frac{(3.1 \text{ lb/s})(0.2324 \text{ Btu/lb-R})(540\text{R})}{(4.26 \text{ lb/s})(0.3757 \text{ Btu/lb-R})} = 1149.1 \text{ °R or } 689.5 \text{ °F} \ . \tag{72}$$

Equation (72) calculates the temperature to be 689.5 °F, which compares well with the GFSSP prediction of 688.6 °F.

The mass concentration of the species can be calculated from the species conservation equation for node 3. The concentration of water vapor and oxygen can be expressed as:

$$X_{3,H_2O} = \frac{X_{1,H_2O} \dot{m}_{13}}{\dot{m}_{34}} = \frac{(0.9)(1.16 \text{ lb/s})}{4.26 \text{ lb/s}} = 0.2451 \tag{73}$$

and

$$X_{3,O_2} = \frac{X_{1,O_2} \dot{m}_{13} + \dot{m}_{23}}{\dot{m}_{34}} = \frac{(0.1)(1.16 \text{ lb/s}) + 3.1 \text{ lb/s}}{4.26 \text{ lb/s}} = 0.7549 \ . \tag{74}$$

The concentration of water vapor and oxygen from the above equations are 0.2451 and 0.7549, respectively, which also compare well with the GFSSP predictions.

5.5 Example 5—Simulation of a Flow System Involving a Heat Exchanger

5.5.1 Problem Considered

In dealing with fluid system analysis, engineers often encounter systems that contain a heat exchanger. It is important that the thermal behavior of a heat exchanger is correctly accounted for in any system simulation. Otherwise, temperature discrepancies in the fluid property calculations will result in inaccurate system characteristics being predicted. The following example demonstrates

GFSSP's ability to accurately predict fluid temperatures in a heat exchanger system using effectiveness calculations.

GFSSP has the ability to calculate temperatures downstream of a heat exchanger for three different cases. For the first case, a known heat exchanger effectiveness is used by GFSSP to calculate the flow temperatures downstream from the heat exchanger. The second case involves requiring GFSSP to calculate the effectiveness of the heat exchanger using the counterflow heat exchanger equations. That calculated effectiveness is then used to calculate the heat exchanger downstream temperatures. For the third case, the heat exchanger effectiveness is calculated using the parallel flow heat exchanger equations and the heat exchanger downstream temperatures are calculated from that effectiveness.

A simple counterflow heat exchanger system configuration, as shown in figure 87, was chosen for this example. As shown in figure 87, counterflow occurs when the hot branch of the heat exchanger has flow that is propagating in a direction opposite to the cold branch. This counterflow heat exchanger configuration consists of hot water, at 50 psi and 100 °F, flowing through 10 in of 0.25-in inner diameter pipe, through a 10-in-long heat exchanger and out through another 10-in-long section of 0.25-in inner diameter pipe at 25 psi. Also, cold water, at 50 psi and 60 °F, flows through a 10-in section of 0.5-in inner diameter pipe, through the heat exchanger, and out through another 10-in section of 0.5-in inner diameter pipe at 25 psi. All of the pipes are assumed to have an absolute roughness of zero. At the conditions described above, C_p=0.9978 Btu/lbm-R is calculated for the hot water and C_p=1.0014 Btu/lbm-R is calculated for the cold water.

5.5.2 GFSSP Model

A GFSSP model consisting of eight nodes and six branches can represent the counterflow heat exchanger system shown in figure 87. This model is shown in figure 88(a). Nodes 1, 4, 5, and 8 are boundary nodes. Nodes 1 and 5, the inlet boundary nodes for the hot and cold flow, respectively, both have a pressure of 50 psi. In addition, the boundary temperature at Node 1 is 100 °F while the boundary temperature at Node 5 is 60 °F. Nodes 4 and 8, which are the downstream boundary nodes for the hot and cold flow, both have a boundary pressure of 25 psi. Downstream boundary temperatures are not used in GFSSP calculations so 'dummy' temperature values of 80 and 70 °F, respectively, are used for the hot and cold flow downstream boundary nodes. Nodes 2 and 6 are internal nodes that represent the entrances to the heat exchanger for the hot and cold flow, respectively. In the same manner, nodes 3 and 7 are internal nodes that represent the hot and cold flow heat exchanger exits. Branches 12, 34, 56, and 78 represent the pipes leading into and out of the heat exchanger for both the hot and cold flows. Finally, branches 23 and 67 represent the hot and cold sides of the heat exchanger. Figure 88(b) shows how this model appears in VTASC.

5.5.2.1 Branches 12, 34, 56, and 78 (Pipe Lines). Option 1 was used to represent each of the pipe sections in the heat exchanger model. The user is required to provide the length, inner diameter, and relative roughness factor (ε/D) for this branch resistance option.
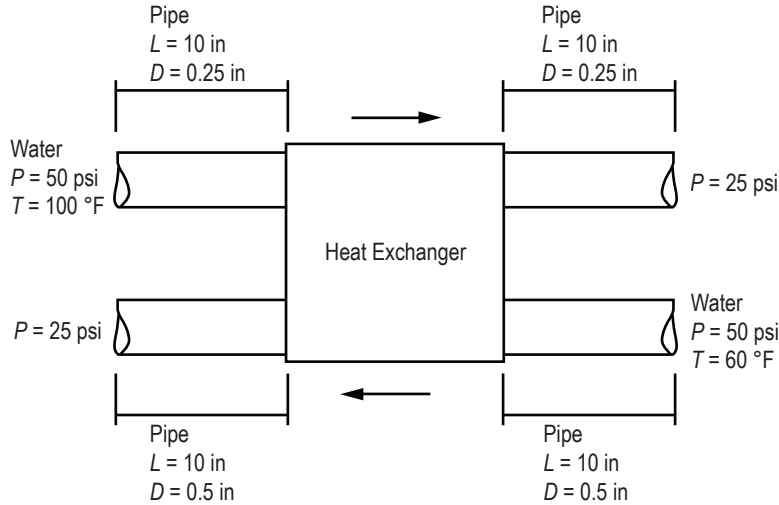
Figure 87. Flow system schematic of a heat exchanger (Example 5).

(a)

(b)
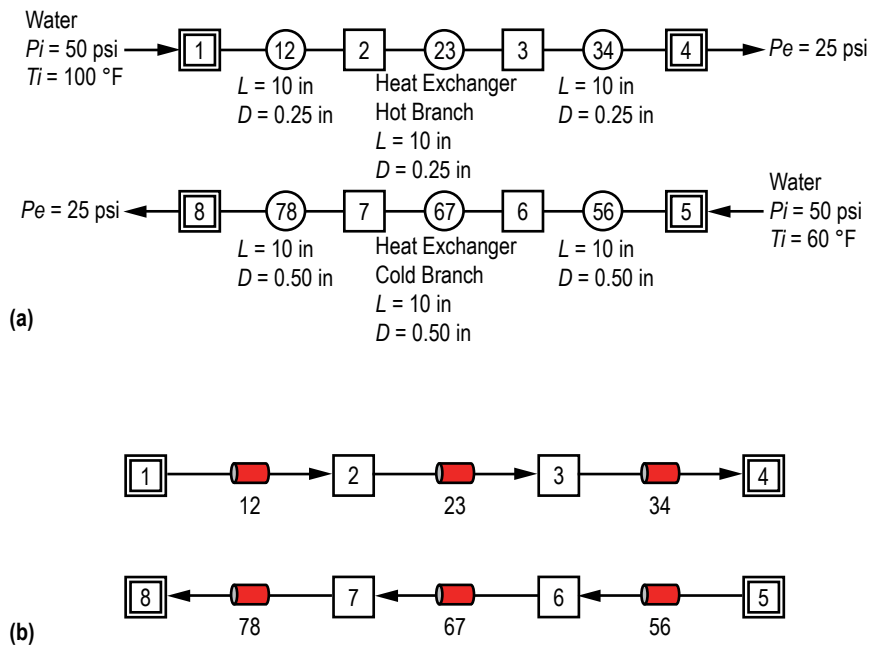
Figure 88. GFSSP model of the heat exchanger: (a) Detailed schematic
and (b) VTASC model.

5.5.2.2 Branches 23 and 67 (Heat Exchanger). Option 1 was also used to simulate the two heat exchanger branches. In addition to providing the length, inner diameter, and ε/D for the two branches, the user must designate additional information in the Heat Exchanger dialog window shown in figure 89. First, the user must add a heat exchanger using the Add button. Next, the user must input which branch represents the hot flow side of the exchanger and which branch represents the cold flow side of the exchanger. Also, the user may either designate an effectiveness between zero and 1 or enter an effectiveness >1 and designate the type of heat exchanger in the system and
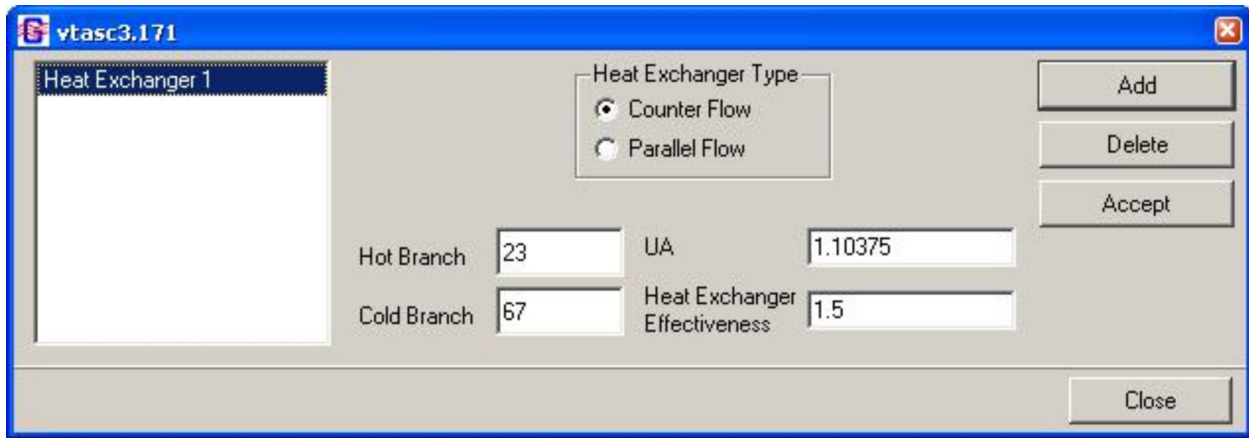
Figure 89. VTASC Heat Exchanger dialog.

a value for UA. UA is the product of the overall conductance for heat transfer and the surface area on which that conductance is based.

5.5.3 Results

The example 5 GFSSP input and output data files (ex5.dat and ex5.out) are included in appendix H (on CD inside back cover). The output file includes all of the input data, the trial solution for the internal nodes, and the final model solution.

The first area of interest is the counterflow heat exchanger effectiveness calculations. During the GFSSP preprocessor input, a value for UA and an effectiveness are input to define the heat exchanger's characteristics. For these verifications, a value for UA was assumed with the following process. It was assumed that the heat exchanger had an effectiveness of $\varepsilon = 0.7$. Then, a GFSSP model was run with that effectiveness to obtain the mass flow rates. The mass flow rate for the cold branch was calculated to be 5.41 lbm/s and the flow rate for the hot branch was calculated to be 0.885 lbm/s. Equations (75) and (76) were used to calculate the hot and cold fluid capacity rates:[24]

$$C_h = \left(\dot{m} \, C_p \right)_{\text{hot branch}} = (0.885 \text{ lbm/s})(0.9978 \text{ Btu/lbm} - {}^\circ\text{R}) = 0.883 \text{ Btu/s-}{}^\circ\text{R} \qquad (75)$$

and

$$C_c = \left(\dot{m} \, C_p \right)_{\text{cold branch}} = (5.41 \text{ lbm/s})(1.0014 \text{ Btu/lbm} - {}^\circ\text{R}) = 5.418 \text{ Btu/s-}{}^\circ\text{R} \ . \qquad (76)$$

Based on the previously calculated values, $C_{\text{max}} = C_c$ and $C_{\text{min}} = C_h$. For the counterflow heat exchanger case, it was assumed that C_{max}, C_{min} and ε would remain the same as the values above. Next, a counterflow exchanger performance table was used, along with the previously calculated values, to estimate the number of heat transfer units, N_{tu}=1.25, for the counterflow exchanger.[24] Then, equation (77) was used to calculate UA in equation (78):[24]

120

$$N_{tu} = \frac{UA}{C_{min}} \tag{77}$$

and

$$UA = N_{tu}C_{min} = (1.25)(0.883 \text{ Btu/s} - °R) = 1.10375 \text{ Btu/s} - °R) \ . \tag{78}$$

A value >1 was used for the effectiveness, which instructed GFSSP to calculate the effectiveness instead of employing a user input value. For this case, the counterflow heat exchanger option was chosen. Figure 90 shows the predicted temperatures and mass flow rates from this model.
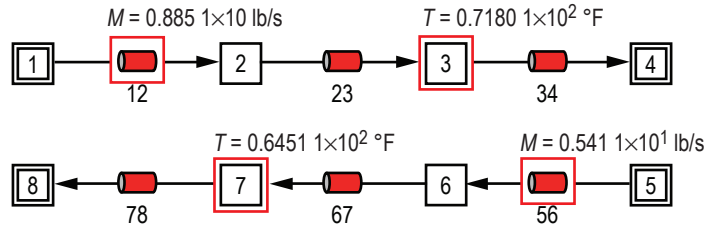
Figure 90. Temperature and flow rate predictions in heat exchanger.

The mass flow rates predicted by this model (0.885 lbm/s at branch 12 and 5.41 lbm/s at branch 56) were the same as predicted for the counterflow exchanger that was used for the assumed case. Therefore, C_c and C_h remained the same. The heat exchanger effectiveness is not included in the data written to the GFSSP output file so it was necessary to calculate the effectiveness that GFSSP used. GFSSP's effectiveness was calculated using equation (79):[24]

$$\varepsilon = \frac{C_h(T_{h,in} - T_{h,out})}{C_{min}(T_{h,in} - T_{c,in})} = \frac{C_c(T_{c,out} - T_{c,in})}{C_{min}(T_{h,in} - T_{c,in})}$$

$$\varepsilon = \frac{(0.883 \text{ Btu/s}-°R)(560 \text{ °R} - 531.8 \text{ °R})}{(0.883 \text{ Btu/s}-°R)(560 \text{ °R} - 520 \text{ °R})} = 0.705 \ . \tag{79}$$

For comparison, a hand-calculated counterflow effectiveness was determined using equation (80):[24]

$$\varepsilon = \frac{1 - e^{-N_{tu}\left(1 - C_{min}/C_{max}\right)}}{1 - \left(C_{min}/C_{max}\right)e^{-N_{tu}\left(1 - C_{min}/C_{max}\right)}}$$

$$\varepsilon = \frac{1 - e^{-1.25\left(1 - \left(\frac{0.883 \text{ Btu/s–°R}}{5.418 \text{ Btu/s–°R}}\right)\right)}}{1 - \left(\frac{0.883 \text{ Btu/s–°R}}{5.418 \text{ Btu/s–°R}}\right)e^{-1.25\left(1 - \frac{0.883 \text{ Btu/s–°R}}{5.418 \text{ Btu/s–°R}}\right)}} = 0.688 \, . \tag{80}$$

Good agreement can be seen in a comparison between the hand-calculated value and the GFSSP value.

The second area of interest is the accuracy of GFSSP's temperature predictions at the nodes downstream of the hot and cold heat exchanger branches. Equation (79) was manipulated to come up with equations (81) and (82) which were used to hand calculate $T_{h,\text{out}}$ and $T_{c,\text{out}}$, respectively:[24]

$$T_{h,\text{out}} = T_{h,\text{in}} - \frac{C_{\min}\left(T_{h,\text{in}} - T_{c,\text{in}}\right)\varepsilon}{C_h}$$

$$T_{h,\text{out}} = 560 \text{ °R} - \frac{(0.883 \text{ Btu/s–°R})(560 \text{ °R–}520 \text{ °R})\,(0.688)}{(0.883 \text{ Btu/s–°R})} = 532.48 \text{ °R} = 72.48 \text{ °F} \, . \tag{81}$$

and

$$T_{c,\text{out}} = T_{c,\text{in}} + \frac{C_{\min}\left(T_{h,\text{in}} - T_{c,\text{in}}\right)\varepsilon}{C_c} \, .$$

$$T_{c,\text{out}} = 520 \text{ °R} - \frac{(0.883 \text{ Btu/s–°R})(560 \text{ °R–}520 \text{ °R})\,(0.688)}{(5.418 \text{ Btu/s–°R})} = 524.49 \text{ °R} = 64.49 \text{ °F} \, . \tag{82}$$

Comparing the hand-calculated values with GFSSP's temperature results of 71.8 °F at node 3 and 64.51 °F at node 7 in figure 90 shows very good agreement, verifying the heat exchanger temperature calculation process used by the GFSSP code.

5.6 Example 6—Radial Flow on a Rotating Radial Disk

5.6.1 Problem Considered

This example illustrates the rotational effect (centrifugal force contribution) capability of GFSSP by modeling the flow of water through a closed impeller.[27] The impeller has a diameter of 11 in, it uses water as the operating fluid, and is running at 5,000 rpm. The 'slip' of the fluid is described by the rotational K-factor (K_{rotation}). K_{rotation} is defined as the ratio of the mean circumferential fluid speed divided by the impeller speed: ($K_{\text{rotation}} = u_\theta/r\omega$). (Higher K_{rotation}

factors translate to a higher pressure rise for radially outward flow.) A $K_{rotation}$ for each side of the impeller has been proposed and it is the purpose of this example to validate these $K_{rotation}$ correlations. The proposed correlations are: $K_{front\ face} = 0.8455 - 0.1403(r - r_i / r_o - r_i)$ for the front face; $K_{back\ face} = 0.8857 - 0.1762(r - r_i / r_o - r_i)$ for the back face. It is desired to compare the results with experimental data. The impeller is schematically shown in figure 91. For this example, the effects of friction will be neglected for the rotating branches.
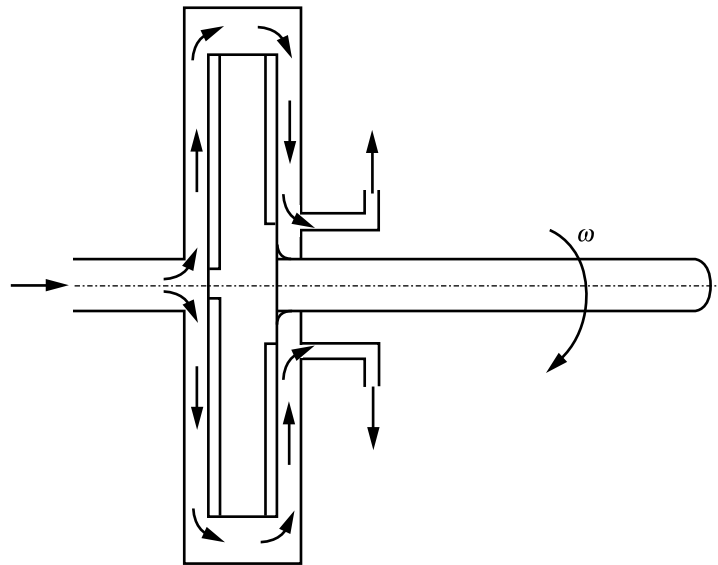
Figure 91. Flow schematic of a rotating radial disk (example 6).

5.6.2 GFSSP Model

The GFSSP model circuit is shown in figure 92(a). All branches are modeled using option 2. In the model, branches 23, 34, 45, 56, 67, 89, 910, 1011, and 1112 are rotating at 5,000 rpm. The inlet and outlet radii are defined in the preprocessor for each of the rotating branches. The area of each of the radial branches is calculated as the average cross-sectional area for each branch. Figure 92(b) shows how this model appears in VTASC.

5.6.3 Results

The example 6 GFSSP input and output data files (ex6.dat and ex6.out) are included in appendix I (on CD inside back cover).

The pressure distribution predicted by GFSSP for the front and back faces of the impeller is shown in figure 93. As is seen in figure 93, the model results show excellent agreement with the experimental data.
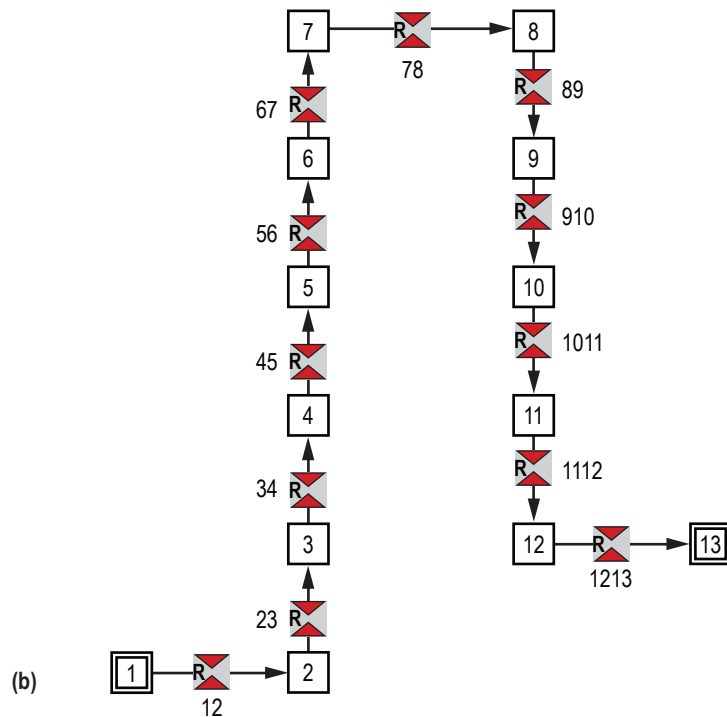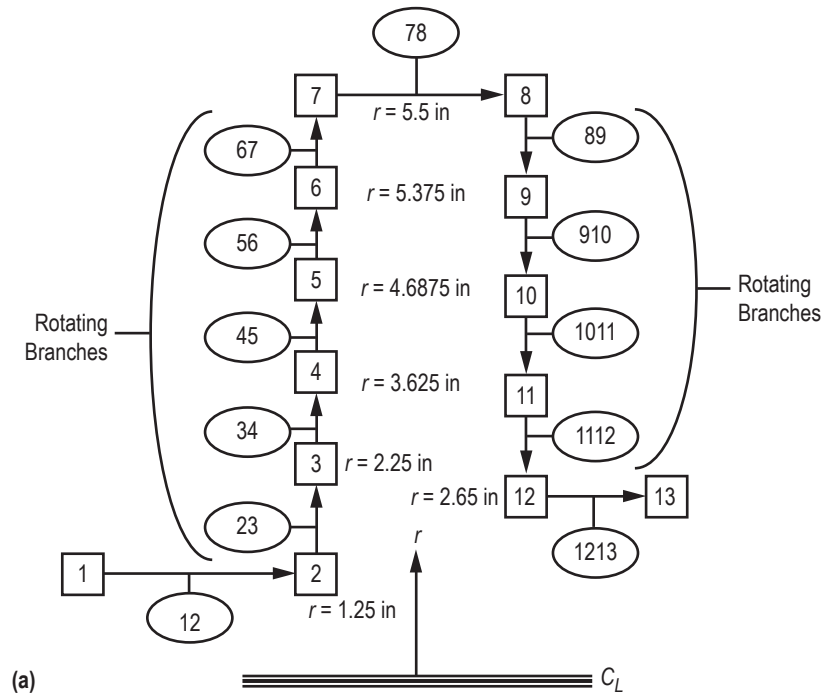
Figure 92. GFSSP model of the rotating radial disk: (a) Detailed schematic and (b) VTASC model.
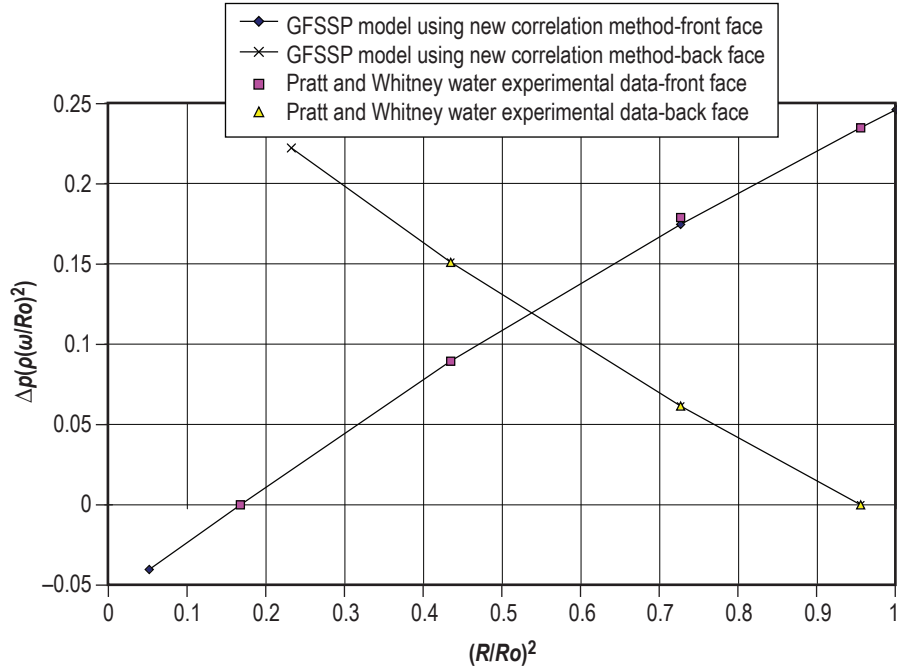
Figure 93. Comparison of GFSSP model results with experimental data.

5.7 Example 7—Flow in a Long-Bearing Squeeze Film Damper

5.7.1 Problem Considered

Squeeze film dampers are used in turbomachinery to dampen out unstable behavior. The damper is installed at the bearing supports of a rotor-stator system on the outer race of a rolling-element bearing. The squeeze film damper consists of inner and outer elements separated by fluid (usually an oil). The inner element is mounted to the outer race of the rolling-element bearing, and the outer element is mounted to the bearing support. The arrangement is similar to a journal bearing except that the inner damper element does not rotate; it only translates. In order to calculate the effect of the squeeze film damper on the system, the forces generated by the squeeze film damper in the radial and tangential directions must be estimated. The forces are estimated by integrating the pressure distribution of the fluid in the damper. The difficulty for the designer/analyst is the estimation of the pressure distribution. The following example problem demonstrates how GFSSP can be used to predict this pressure distribution.

The squeeze film damper considered for this example is shown schematically in figures 94 and 95. Since the damper has sealed ends, the axial flow is neglected. The diameter (d) of the bearing is 5 in, the width (w) of the bearing is 0.94 in, the clearance (c) is 0.0625 in, and the ratio of the dynamic eccentricity (ε, radius of orbit to the clearance) is 0.82. The fluid density (ρ) is 57.806 lbm/ft^3. The fluid viscosity (μ) is 5.932×10^{-3} lbm/(ft•s). The rotational speed is set at 1,770 rpm ($\omega = 185.354$ rad/s). GFSSP will be used to determine the pressure distribution around the damper and the results will be compared with experimental data.[28]
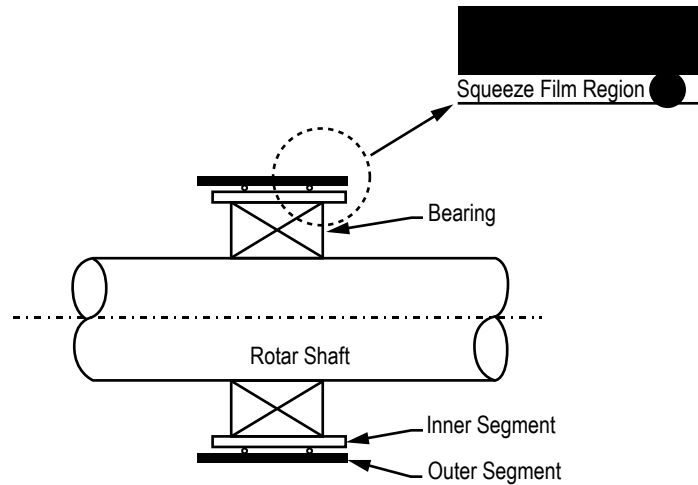
Figure 94. Squeeze film damper schematic (example 7, view 1).
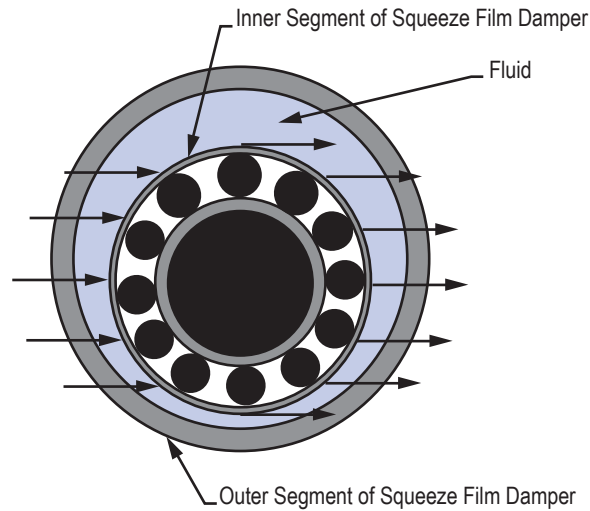
Figure 95. Squeeze film damper schematic (example 7, view 2).

5.7.2 GFSSP Model

A GFSSP model consisting of 20 nodes and 19 branches can approximate the fluid contained within the squeeze film damper system shown in figures 94 and 95. The fluid to be used is not contained in the standard library of fluids and is assumed to be incompressible; therefore, the constant density feature of GFSSP must be used. In order to model the squeeze film damper, the damper will be 'unwrapped.' Figure 96 shows the unwrapping of the damper and the discretization of the flow region. The GFSSP model is shown in figure 97. As is shown in figure 97, nodes 1 and 20 are the boundary nodes. The branches will use branch resistance option 3 - Non Circular Duct,
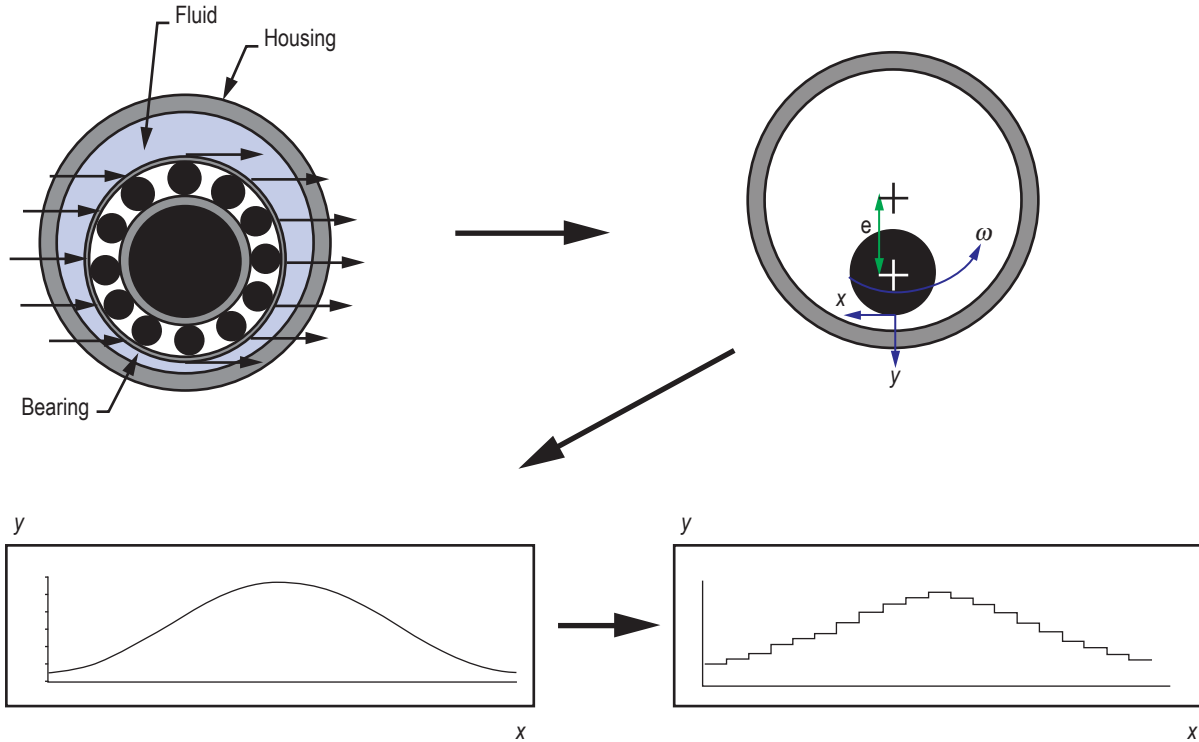
Figure 96. Unwrapping and discretization of squeeze film damper.
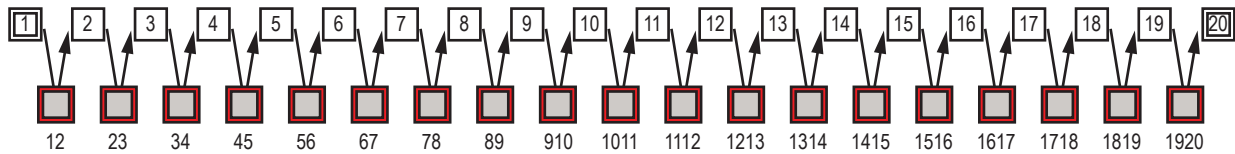
Figure 97. GFSSP model of squeeze film damper.

Sub-option 1 - Rectangular Duct. The heights of the branches are given in table 20. The motion of the inner element will be simulated using the moving boundary option in GFSSP. (Only the motion of the damper normal to the inner element is modeled in this technique.) The velocity of the moving boundary is given in table 21. Setting the boundary nodes at the same pressure will simulate the periodic behavior of the damper. The boundary pressure is set at 0.0 psi.

5.7.3 Results

The Example 7 GFSSP input and output data files (ex7.dat and ex7.out) are included in appendix J (on CD inside back cover).

The pressure distribution predicted by GFSSP is shown in figure 98. The plot of pressure versus angle (i.e., node position) in figure 98 shows that the pressure is symmetric about the boundary pressure of zero psi. The model results are compared to experimental results in figure 99.

Table 20. Branch dimensions of squeeze film damper.

Branch Number	Width (in)	Length (in)	Height (in)
12	0.94	0.82673	0.012578
23	0.94	0.82673	0.017987
34	0.94	0.82673	0.028221
45	0.94	0.82673	0.042169
56	0.94	0.82673	0.058320
67	0.94	0.82673	0.074925
78	0.94	0.82673	0.090183
89	0.94	0.82673	0.102441
910	0.94	0.82673	0.110370
1,011	0.94	0.82673	0.113113
1,112	0.94	0.82673	0.110370
1,213	0.94	0.82673	0.102441
1,314	0.94	0.82673	0.090183
1,415	0.94	0.82673	0.074925
1,516	0.94	0.82673	0.058320
1,617	0.94	0.82673	0.042169
1,718	0.94	0.82673	0.028221
1,819	0.94	0.82673	0.017987
1,920	0.94	0.82673	0.012578

Table 21. Moving boundary information of squeeze film damper.

Node	Normal Area (in^2)	Velocity (ft/s)
2	0.777126	0.256180
3	0.777126	0.484598
4	0.777126	0.660503
5	0.777126	0.764832
6	0.777126	0.786280
7	0.777126	0.722522
8	0.777126	0.580468
9	0.777126	0.375510
10	0.777126	0.129861
11	0.777126	–0.129861
12	0.777126	–0.375510
13	0.777126	–0.580468
14	0.777126	–0.722522
15	0.777126	–0.786280
16	0.777126	–0.764832
17	0.777126	–0.660503
18	0.777126	–0.484598
19	0.777126	–0.256180

In figure 99, the pressure is normalized with a characteristic pressure (CpRe) and the angle has been converted to compare to a dimensionless time (*wt*) for comparison with the experimental data. As seen in figure 99, the pressure profile of the GFSSP model compares favorably with the experimental results in shape and magnitude, the only major difference between the two results is a phase shift.
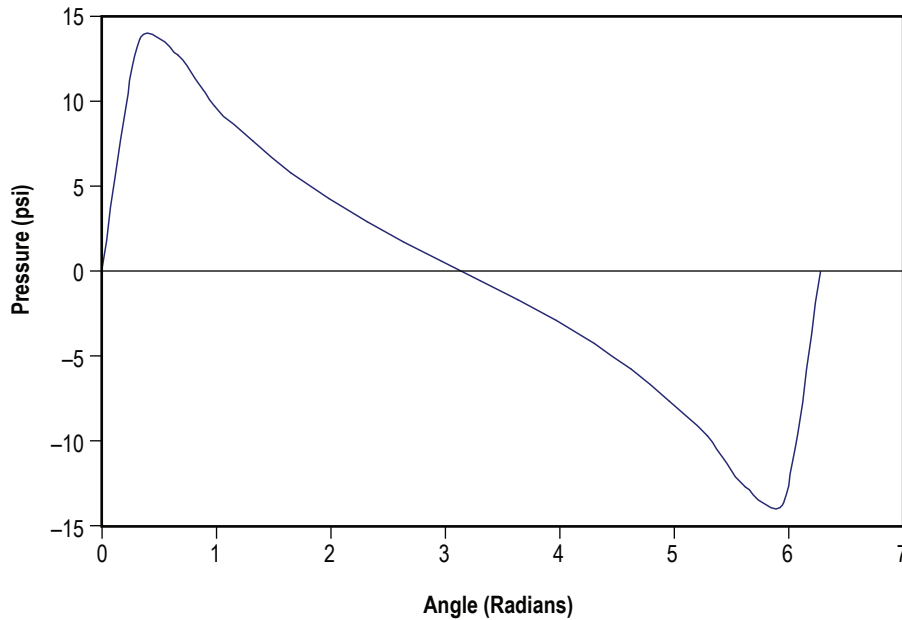

Figure 98. Predicted circumferential pressure distributions in the squeeze film damper.
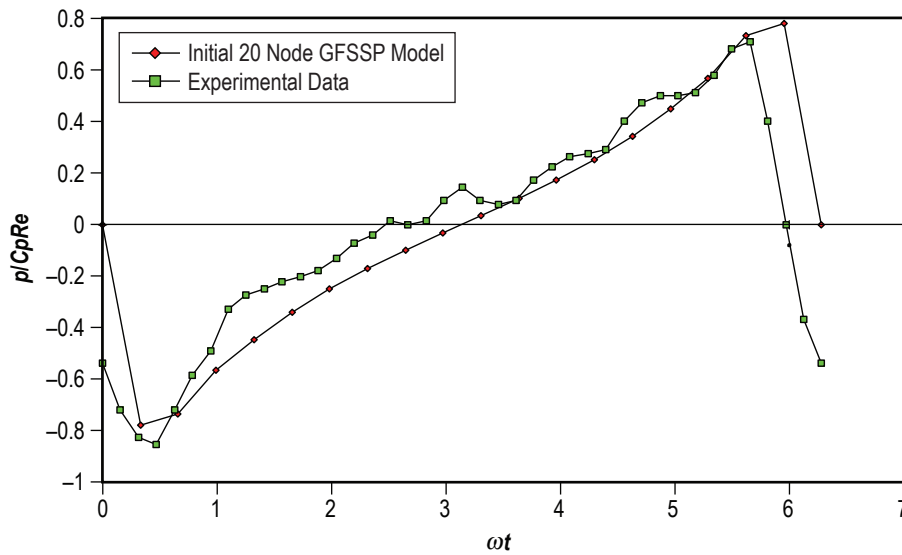

Figure 99. Comparison of GFSSP model results with experimental data for squeeze film damper.

5.8 Example 8—Simulation of the Blowdown of a Pressurized Tank

5.8.1 Problem Considered

In the previous examples, the simulation of steady state flow in a given flow circuit was considered. In this example, the capabilities of the unsteady flow formulation of GFSSP to simulate the process of blowing down a pressurized tank will be employed.

Consider a tank with an internal volume of 10 ft^3, containing air at a pressure and temperature of 100 psia and 80 °F, respectively. Air is discharged into the atmosphere through an orifice of 0.1-in diameter for a period of 200 s. GFSSP will be used to determine the pressure, mass flow rate, and temperature history of the isentropic blowdown process. These predicted values are then compared with the analytical solution.

5.8.2 GFSSP Model

The physical schematic for example 8 is shown in figure 100(a) and a schematic of the corresponding GFSSP model is shown in figure 100(b). Figure 100(c) shows how the model looks in VTASC. The venting process can be modeled with two nodes and one branch. Node 1 is an internal node that represents the tank. For the unsteady formulation, the node volume and the initial conditions must be supplied for each internal node and a history file must be supplied for each boundary node. The history file contains the pressures, temperatures, and concentrations at discrete times. At a minimum, this file should include values at the process start time and at some time corresponding to the expected process stop time. Additional times can be included to account for nonlinear variation in the values if required. The code interpolates in the history file data to determine the values for a particular instant. Shown below is a listing of EX8HS2.DAT, which is the history file of example 8, used to provide the boundary conditions for node 2. The file listing has been annotated to explain the meaning of the entries. In the actual file, column headings and descriptions must not appear.

```
EX8HS2.DAT
  2 - Number of data points
  tau(sec)   p(psia)   T (°F)   Concentration
  0          14.700    80.00    1.00
  1000       14.700    80.00    1.00
```

In addition to supplying the internal node volumes and history data files, the time step (DTAU), start time (TAUF), stop time (TAUL), and print interval (NPSTEP) must also be included within the model input data file when creating an unsteady flow (STEADY = .False.) model.

The initial pressure within the tank (node 1) was 100 psia. Resistance Option 22 was used for branch 12 with a flow coefficient of 1. Air is modeled using the ideal gas option that is available in VTASC.
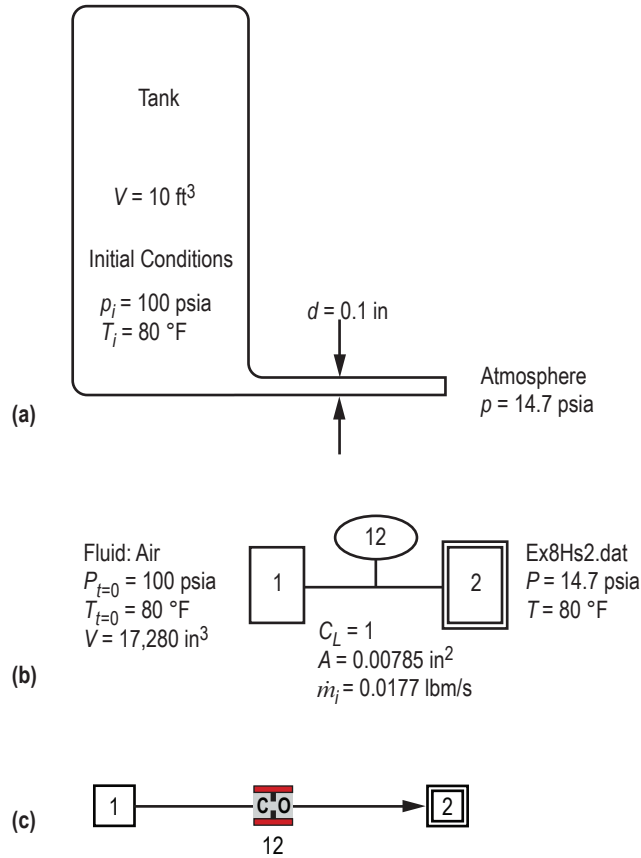
Figure 100. Venting air tank schematics: (a) Physical schematic, (b) detailed
model schematic, and (c) VTASC model.

As an interesting note, this example could be used to model an isothermal process by using the SORCEQ user subroutine. The temperature of the fluid remains constant in an isothermal process. In this example it is presumed that initially the air and tank wall are at the same temperature. During blowdown, the air temperature tends to drop. With heat transfer from the wall, temperature drop would be less compared to an isentropic process. For an isothermal process, there will be no change in temperature. This particular situation (isothermal) can be modeled by setting an infinite heat transfer coefficient between the wall and fluid in SORCEQ.

5.8.3 Results

The input and output files of this example are included in appendix K (see CD inside back cover) as ex8.dat and ex8.out. It may be noted that for each time step, solutions for each node and branch are printed in the output file.

5.8.3.1 Analytical Solution. The differential equation governing an isentropic blowdown process can be written as:

131

$$\left(\frac{p}{p_i}\right)^{(1-3\gamma)/2\gamma} \frac{d(p/p_i)}{d\tau} = \frac{\gamma A}{\rho_i V} \sqrt{\gamma g_c p_i \rho_i} \left(\frac{2}{\gamma+1}\right)^{(\gamma+1)/2(\gamma-1)} . \tag{83}$$

This is an initial value problem and the initial conditions are:

$$\tau = 0, \ \frac{p}{p_i} = 1 . \tag{84}$$

The analytical solution for p/p_i is given by Moody as:[29]

$$\frac{p}{p_i} = \left[1 + \left(\frac{\gamma-1}{2}\right)\left(\frac{2}{\gamma+1}\right)^{(\gamma+1)/2(\gamma-1)} \sqrt{\frac{\gamma g_c p_i}{\rho_i}} \frac{A\tau}{V}\right]^{-2\gamma/(\gamma-1)} . \tag{85}$$

The analytical and GFSSP solutions are compared in figure 101. The figure shows a comparison between the GFSSP solution and the analytical solution of pressures. The difference in pressures is also shown plotted for three different time steps (1, 0.1, and 0.01 s). The discrepancies between analytical and numerical solutions are found to diminish with reduction in time step. This observation is in conformity with expectations.

5.9 Example 9—A Reciprocating Piston-Cylinder

5.9.1 Problem Considered

This example further illustrates GFSSP's capability to model complex unsteady flow. Figure 102 shows the piston-cylinder configuration considered by this example problem. The cylinder has a diameter of 3 in. Within the cylinder is nitrogen gas, sealed in by a piston moving at a rotational speed of 1,200 rpm and a stroke of 3 in. GFSSP will be used to predict the pressure and temperature within the system and the results will be compared with the isentropic solution.

5.9.2 GFSSP Model

In order to model this configuration, a coordinate transformation is utilized. In this new coordinate system, the endplate of the cylinder is modeled as another piston and the origin of the coordinate system is at the midpoint between the two 'pistons.' Figure 103 demonstrates the modified piston-cylinder arrangement.

The GFSSP model of the piston-cylinder arrangement consists of two internal nodes and one branch. (Note: the model does not have any boundary nodes.) Figure 104(a) shows the GFSSP piston-cylinder model. In order to model the motion of the piston, two special options are utilized—the moving boundary option and the variable geometry option. The moving boundary option is required to adequately model the work input by the motion of the pistons. The variable geometry option is required to model the variation of the geometry of branch 12. The initial condition of the nitrogen in the cylinder is 14.7 psia and 75 °F. Figure 104(b) shows how the model looks in VTASC.
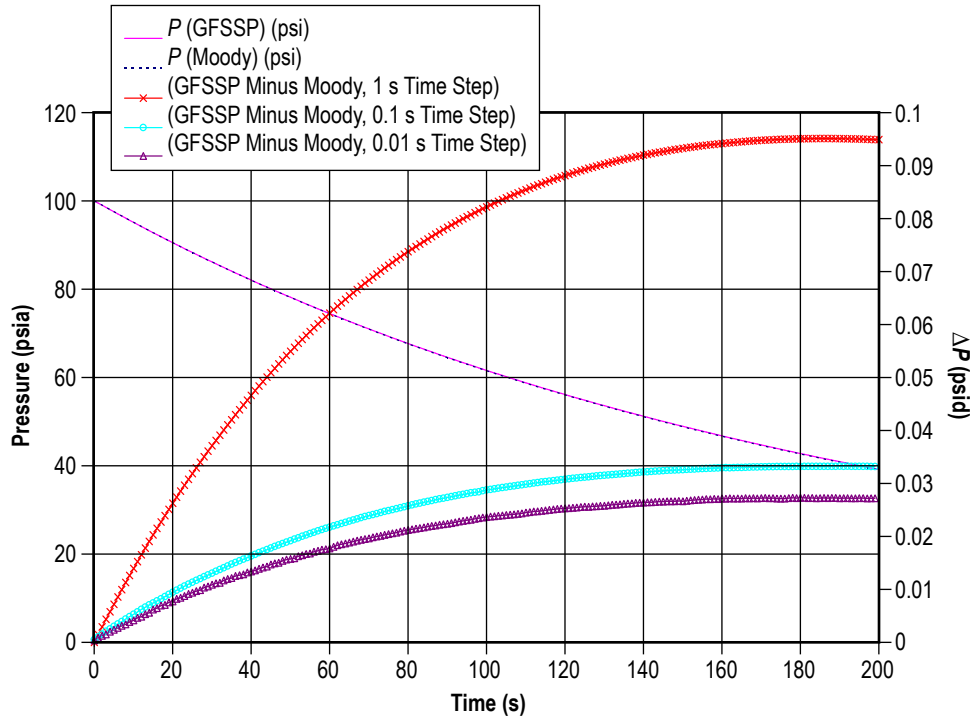
Figure 101. Comparison of the predicted pressure history by GFSSP
and the analytical solution.
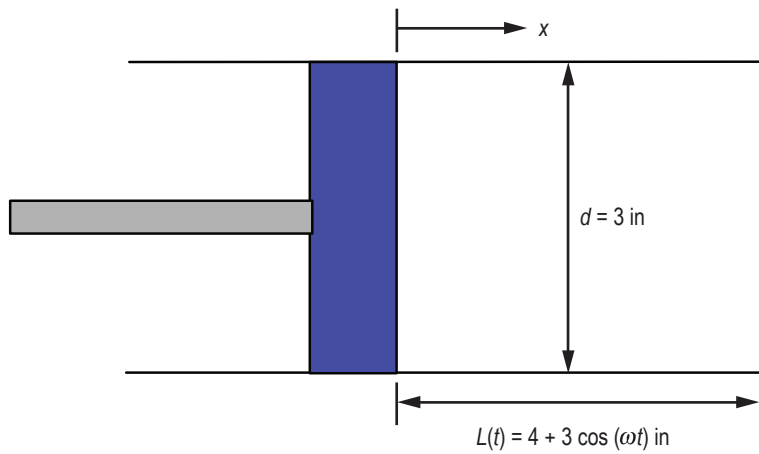
Figure 102. Piston-cylinder configuration.
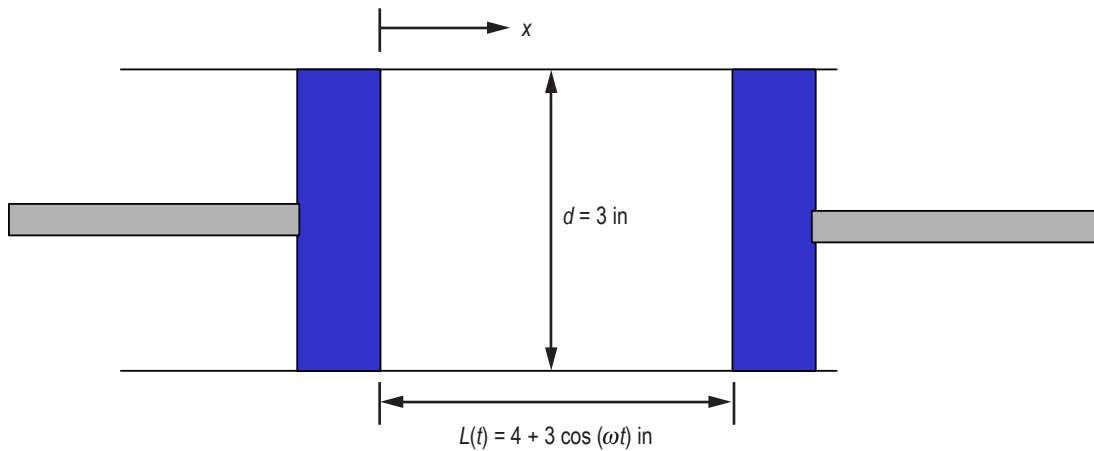
Figure 103. Coordinate transformed piston-cylinder configuration.
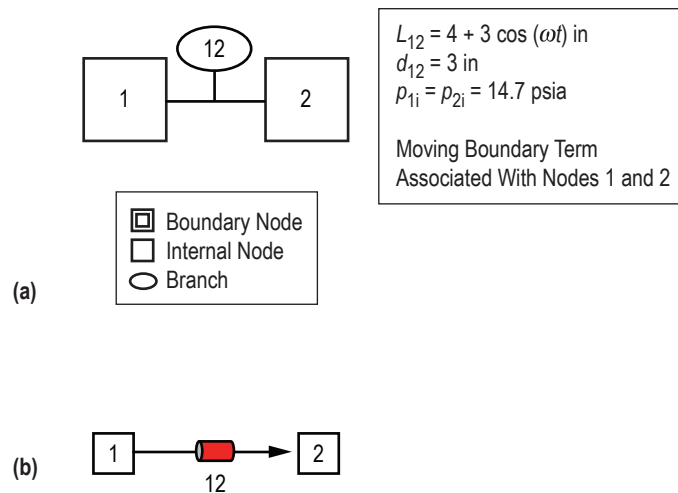
Figure 104. GFSSP model of the piston-cylinder: (a) Detailed model schematic
and (b) VTASC model.

5.9.3 Results

Appendix L (on CD inside back cover) contains the input, variable geometry history, and output files for this example. The results of the study are compared to an analytical solution (for constant ratio of specific heat, γ). Equations (86) and (87) are used to obtain the analytical solution assuming an isentropic process:

$$T(t) = \left\{ (T_0 + 459.6) \left[\frac{\rho(t)}{\rho_0} \right]^{\gamma-1} \right\} - 459.6 \tag{86}$$

and

134

$$p(t) = p_0 \left[\frac{\rho(t)}{\rho_0} \right]^{\gamma} \quad , \tag{87}$$

where T_0, p_0, and ρ_0 are temperature, pressure, and density at time equal zero.

Figures 105 and 106 compare the results of the GFSSP piston-cylinder model with the analytical solution from equations (86) and (87). As these figures illustrate, the GFSSP model compares favorably to the analytical solution. It should be noted that the isentropic solution uses a constant ratio of specific heats (g), whereas GFSSP accounts for the variation of specific heat ratios with changes in temperature and pressure.
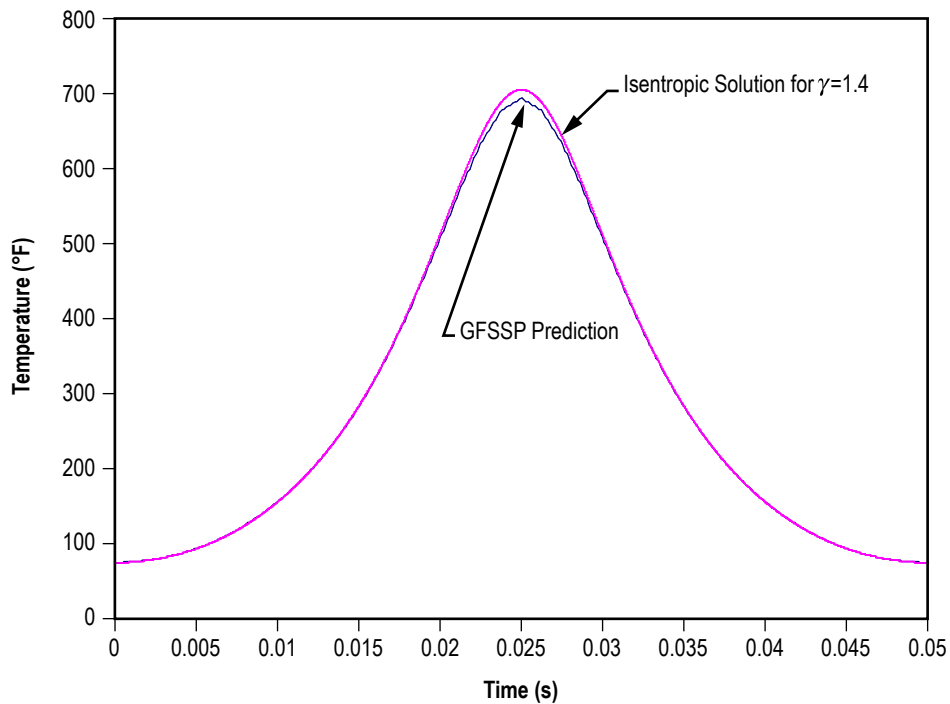
Figure 105. Predicted temperature history of piston-cylinder model.

5.10 Example 10—Power Balancing of a Turbopump Assembly

5.10.1 Problem Considered

This example, Example 10, illustrates the modeling of the mechanical coupling between two flow components. In the turbopump assembly shown in figure 107, a coaxial shaft mechanically connects the pump and turbine. The power required by the pump must be transmitted from the turbine in order for the system to be in balance. The purpose of this example is to demonstrate this power balancing for a turbopump when used in a gas turbine cycle. The physical plausibility of the predicted results was demonstrated by performing parametric studies on shaft speed.
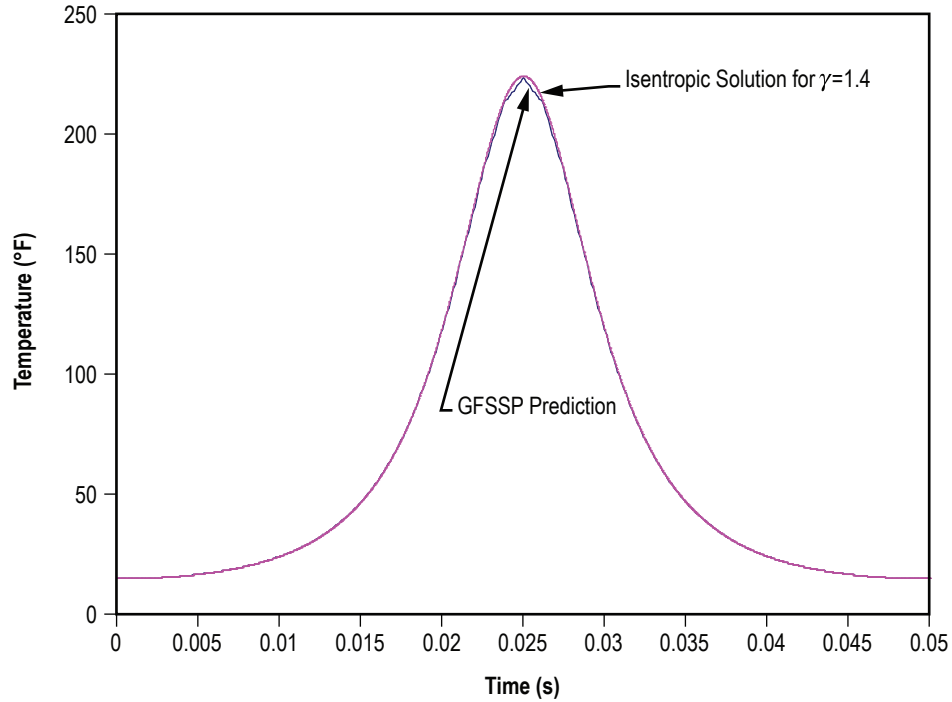
Figure 106. Predicted pressure history of piston-cylinder model.
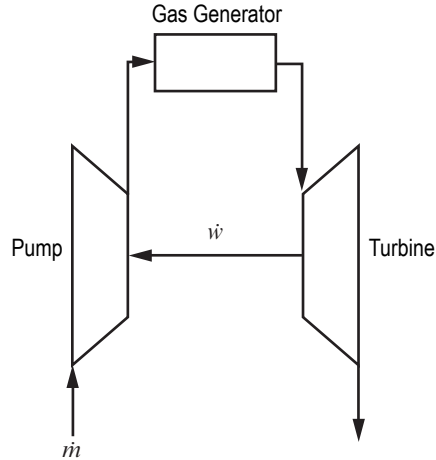
Figure 107. Simplified turbopump assembly.

5.10.2 GFSSP Model

A model of the turbopump portion of a flow circuit is shown in figure 108(a). This model consists of an inlet from a hydrogen tank, a turbopump assembly (pump, turbine, and a connection between them (shaft)), two heat exchangers, a bypass dump outlet, and an outlet to the power turbine. The first of the heat exchangers (denoted on fig. 108(a) as the Regenerator) is used to heat a small portion of the main LH$_2$ flow by using the 'hotter' hydrogen exiting the turbine, while the
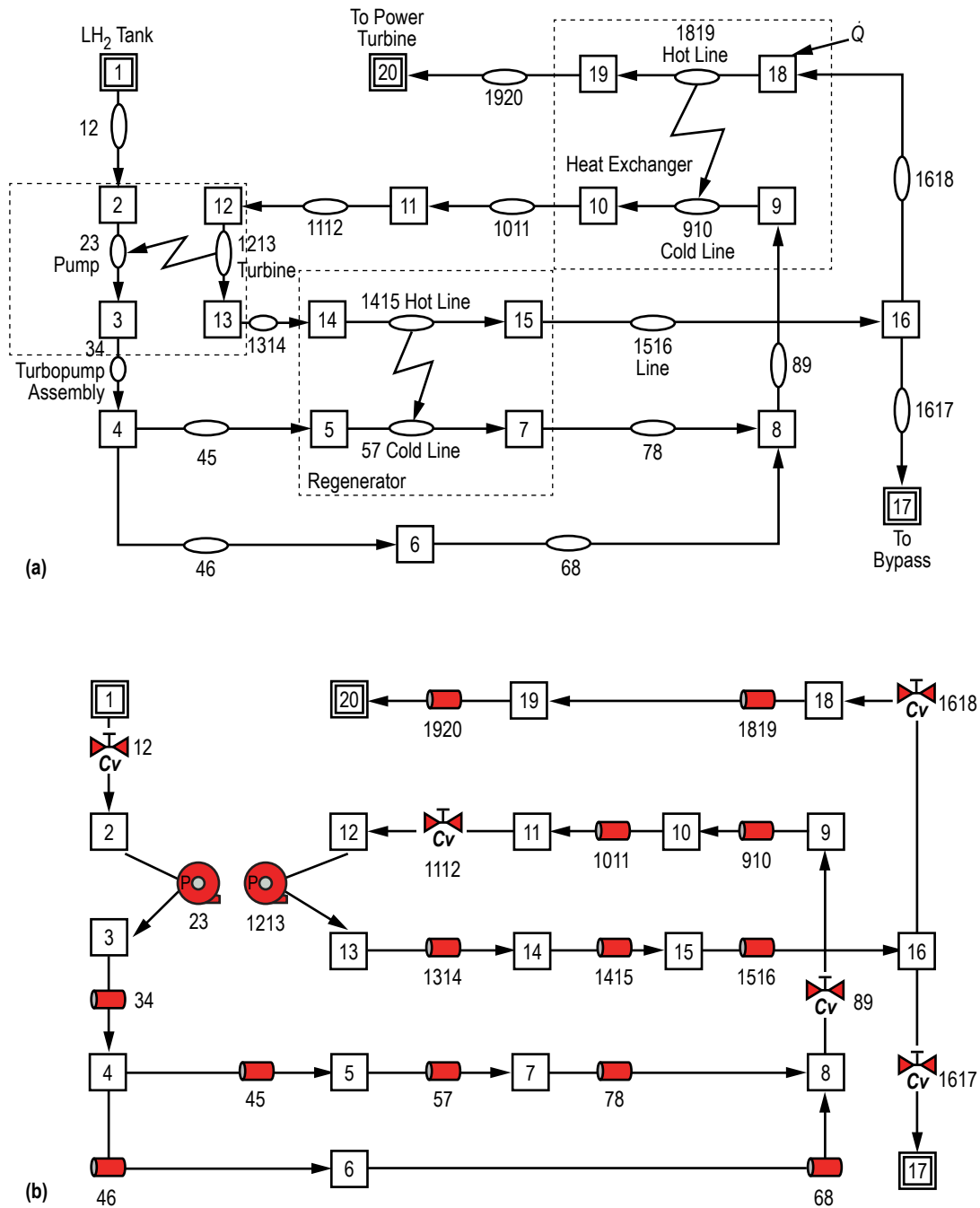
Figure 108. A flow circuit containing turbopump assembly: (a) Detailed model
schematic and (b) VTASC model.

remainder of the LH$_2$ flow bypasses this heat exchanger. The second heat exchanger is used to boil and superheat the hydrogen by means of external heat addition. The shaft speed for this model is set in the input file to 80,000 rpm. Figure 108(b) shows how this model looks in VTASC.

This model uses the following options:

- Branch resistance options:

  (1) Pipe flow (option 1).
  (2) Pump with pump efficiency (option 15).
  (3) Valve with a given C_v (option 16).

- Special options:

  (1) Heat exchangers.
  (2) Turbopump assembly.

Each pipe flow branch has a length of 100 in, an inside diameter of 0.3927 in, and an absolute roughness of 0.00098175 in. Branches 89, 1112, and 1618 each have $C_v = 3.554$ and $A = 0.19635$ in^2. Branch 12 has $C_v = 2.877$ with $A = 0.19635$ in^2 while branch 1617 has $C_v = 0.00354$ with $A = 0.01$ in^2. The branch options chosen to represent the turbine (branch 1213) and the pump (branch 23) have no bearing on the model calculations except for the flow areas that are provided. For this case, option 15 was used for both branches with arbitrary inputs for pump horsepower and efficiency. The flow areas are 0.12112 in^2 for branch 23 and 0.019635 in^2 for Branch 1213. The turbopump characteristics are defined in the turbopump dialog shown in figure 109. The pump characteristic file is also shown below with annotations to explain the meanings of each value. The two heat exchanger dialogs are shown in figure 110(a) and (b).

EX11PMP23.DAT

```
18 - Number of lines of data
Flowrate/Speed    Head/Speed²    Torque/(Density*Speed²)
0.000             8.680E-06      0.000
3.035E-05         8.971E-06      8.8724E-10
6.071E-05         9.190E-06      9.7065E-10
9.106E-05         9.341E-06      1.0804E-09
1.214E-04         9.436E-06      1.2166E-09
1.518E-04         9.486E-06      1.3393E-09
1.821E-04         9.486E-06      1.4570E-09
2.125E-04         9.445E-06      1.5644E-09
2.428E-04         9.372E-06      1.6733E-09
2.732E-04         9.263E-06      1.7872E-09
3.035E-04         9.117E-06      1.9105E-09
3.339E-04         8.935E-06      2.0558E-09
3.643E-04         8.753E-06      2.2161E-09
3.718E-04         8.689E-06      2.2698E-09
3.749E-04         8.625E-06      2.2869E-09
3.794E-04         8.479E-06      2.3215E-09
3.807E-04         8.388E-06      2.3281E-09
3.810E-04         0.000E+00      0.000
```
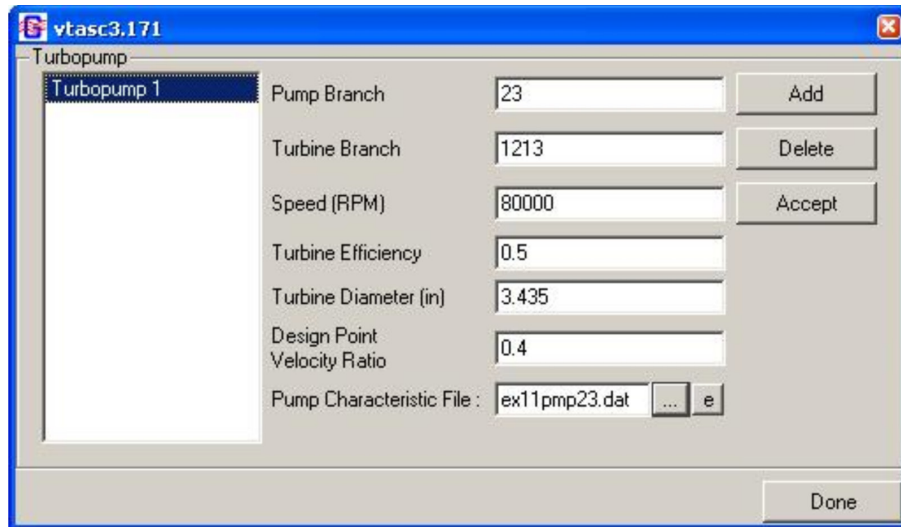
Figure 109. Example 10 turbopump dialog.
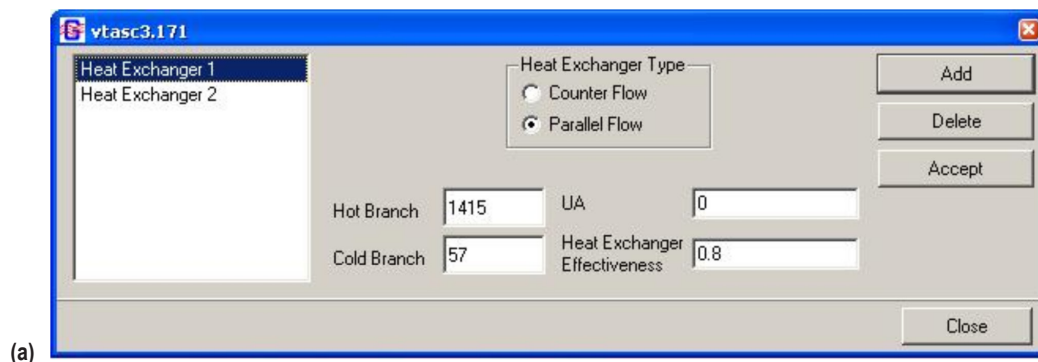
(a)
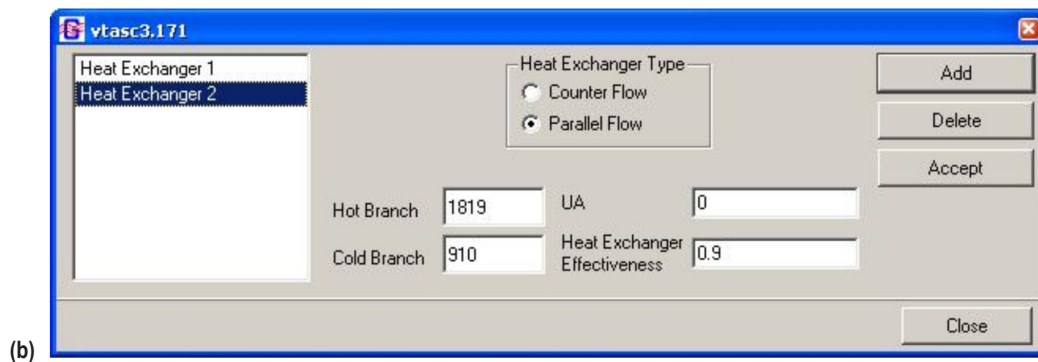
(b)

Figure 110. Example 10 heat exchanger dialog: (a) Heat exchanger 1 and (b) heat exchanger 2.

5.10.3 Results

Appendix M (see CD inside back cover) contains the input, pump characteristics, and output files for this example (ex10.dat, ex10pmp23.dat, and ex10.out). The results of the study are illustrated in figure 111.
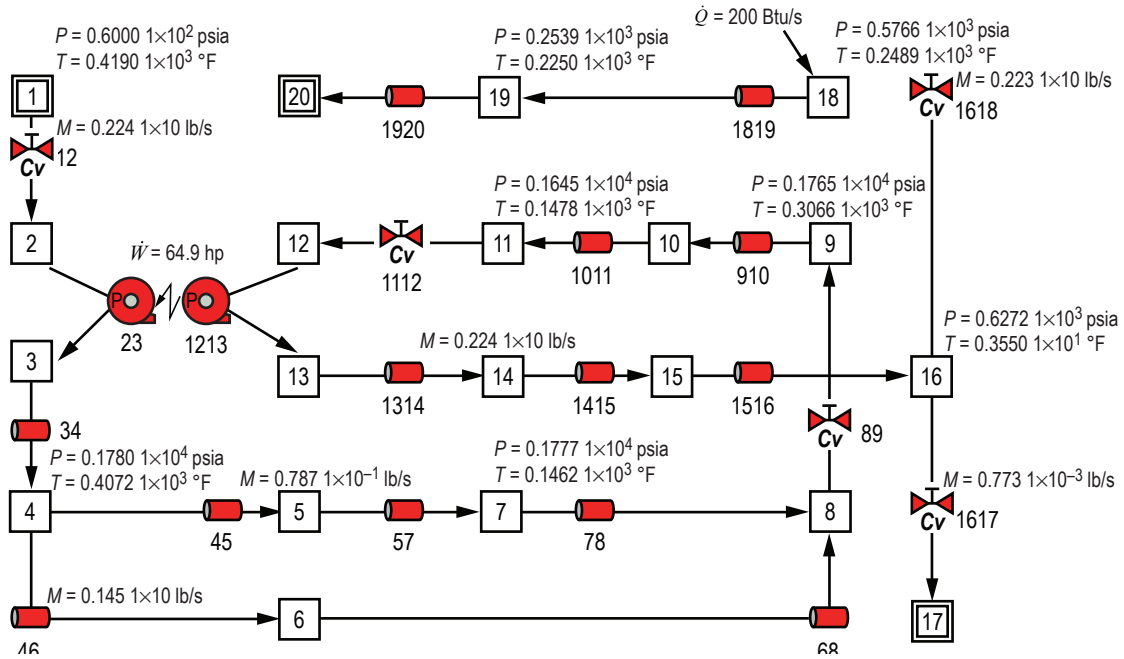
Figure 111. GFSSP RCS model results.

5.10.4 Parametric Study

In order to verify this complicated model, a parametric study on the shaft speed of the tur-bopump was conducted. Figures 112–114 illustrate the results of this model. Figure 112 illustrates the pressure differential across the turbopump for both the pump and the turbine as a function of the shaft speed. Figure 113 illustrates the hydrogen mass flow rate through the turbopump as a function of the shaft speed. Figure 114 illustrates the torque and horsepower transmitted in the turbopump as a function of the shaft speed. As each of these figures illustrates, a functional rela-tionship is identifiable for each predicted variable as a function of shaft speed.
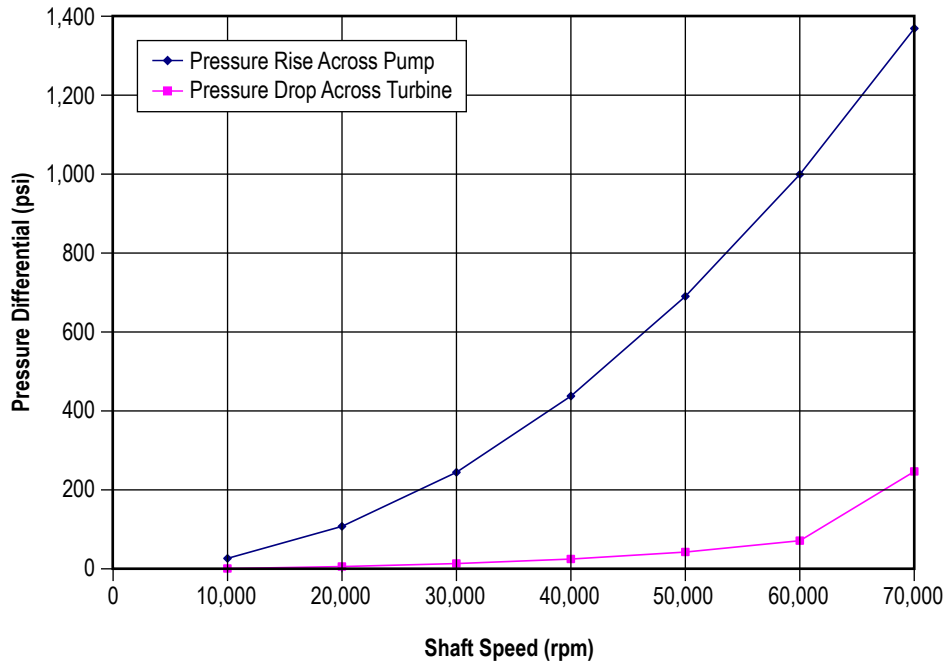
Figure 112. Parametric study results: turbopump pressure differential.
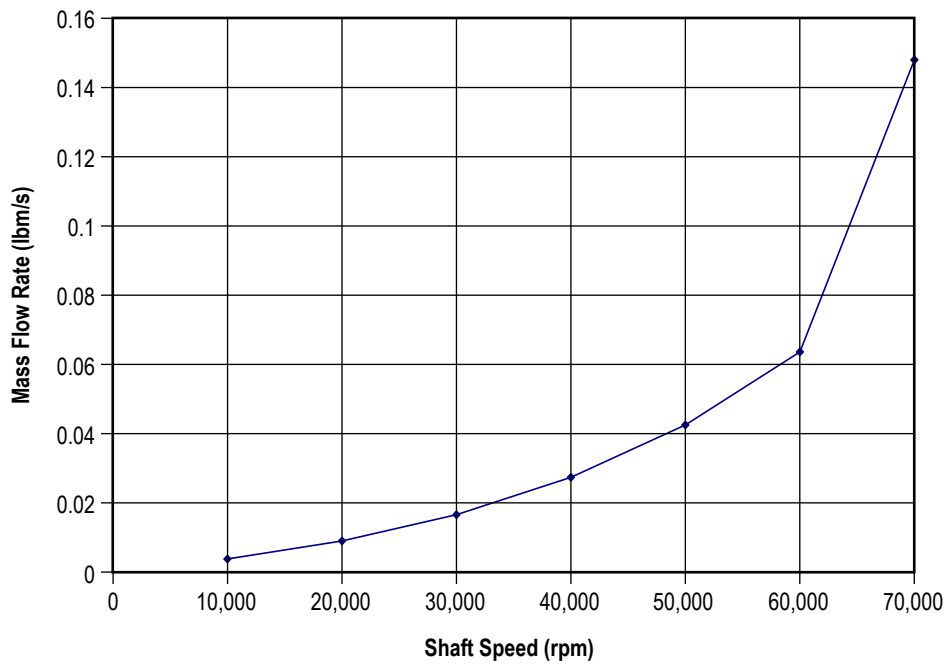
Figure 113. Parametric study results: turbopump hydrogen mass flow rate.
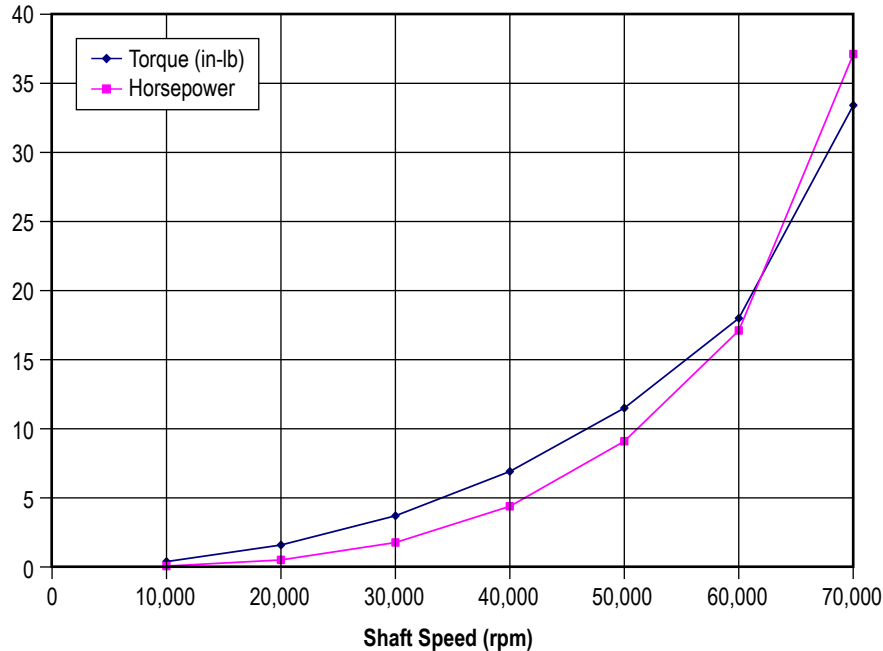
Figure 114. Parametric study results: turbopump torque and horsepower.

5.11 Example 11—Steady State and Transient Conduction Through a Circular Rod, With Convection

5.11.1 Problem Considered

In the previous examples, focus was on GFSSP's fluid modeling capabilities. In this example, GFSSP's ability to model applications with conjugate heat transfer is introduced. The verification and validation of GFSSP's conjugate heat transfer capability was performed by comparing with the known solution of a simple conduction-convection problem.[4] The heat transfer in a homogenous circular rod between two walls was considered (fig. 115). The two walls are held at temperatures of 32 °F and 212 °F, respectively. The 0.167-ft-diameter rod is 2 ft in length and is initially at a temperature of 70 °F. The heat transfer coefficient between the rod and the ambient air is 1.14 Btu/ft^2-hr-R and the thermal conductivity of the rod is 9.4 Btu/ft-hr-R.

5.11.2 GFSSP Model

Figure 116(a) shows a GFSSP schematic of the system described in figure 115. The circular rod is represented by eight solid nodes and seven solid-solid conductors. Even though all of the material properties are not used for a steady state model, GFSSP still requires that placeholder values be input at each solid node. The thermal conductivity and specific heat temperature history files, which are shown below in an annotated form, are based on a user-defined material.

USER1K.PRP
```
  2 - Number of lines of data
  Temperature ®     Thermal Conductivity (Btu/ft-sec-R)
  0                 0.002611
  1000              0.002611
```

USER1CP.PRP
```
  2 - Number of lines of data
  Temperature ®     Specific Heat (Btu/lbm-R)
  0                 0.1981
  1000              0.1981
```

     Two ambient nodes are used to model the hot and cold walls, and their interaction with the rod is modeled using two solid-ambient conductors. Because GFSSP is first and foremost a fluid analysis code, it is necessary to include a fluid flow path in any GFSSP model that is being developed. Therefore, a dummy flow circuit consisting of two boundary nodes, two internal nodes and three pipe flow branches was used to represent the ambient environment of figure 15. The details of the flow path were arbitrarily chosen with the sole intent of maintaining a constant temperature of 70 °F at all points in the flow path to correctly simulate the ambient environment. The two internal flow nodes are connected to the solid rod by eight solid-fluid conductors that represent the heat transfer between the ambient and the rod in figure 115. Figure 116(b) shows how this model looks in VTASC.
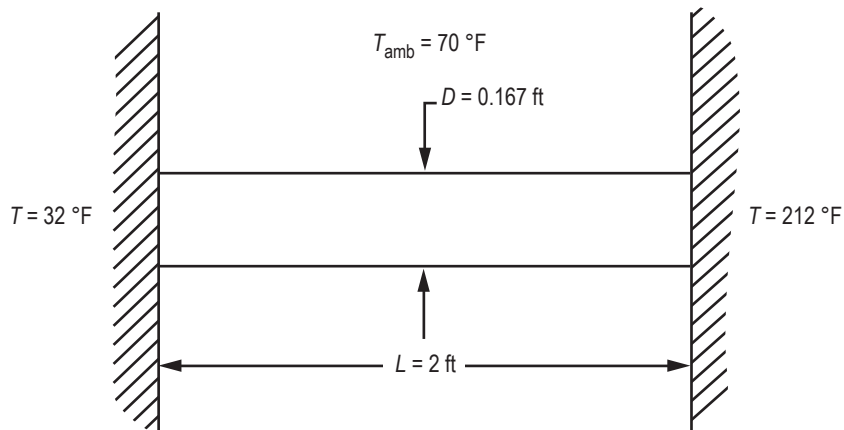
Figure 115. Schematic of circular rod connected to walls at different temperatures.
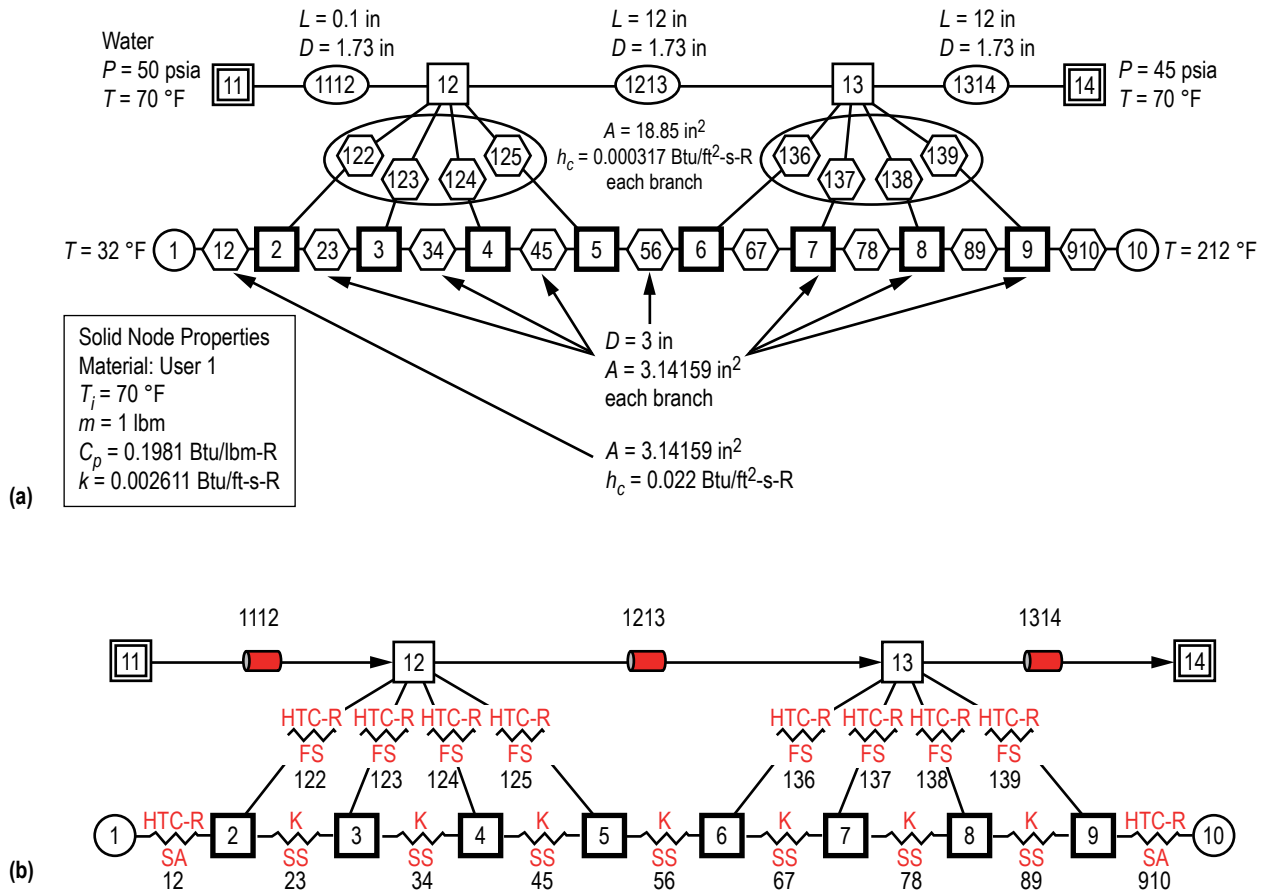
Figure 116. GFSSP model of circular rod for example 11: (a) Detailed model schematic and (b) VTASC model.

5.11.3 Results

The input and output files, including property files, of Example 11 have been attached in appendix N (see CD inside back cover).

5.11.3.1 Analytical Solution

From the Thermal Analysis Workbook,[4] the differential equation of energy transport is given by

$$\frac{d^2T}{dx^2} - \frac{4h}{Dk}\left(T - T_\infty\right) = 0 \tag{88}$$

with boundary conditions of $T(0)=32$ °F and $T(L)=212$ °F. The closed form of the solution is given by

$$T(x) = T_{amb} + 4.653e^{\sqrt{\frac{4h}{Dk}}x} - 42.65e^{-\sqrt{\frac{4h}{Dk}}x} \ . \tag{89}$$

Figure 117 compares GFSSP's predicted temperature distribution along the rod with the closed-form solution. The comparison shows very close agreement between GFSSP and the closed-form solution.
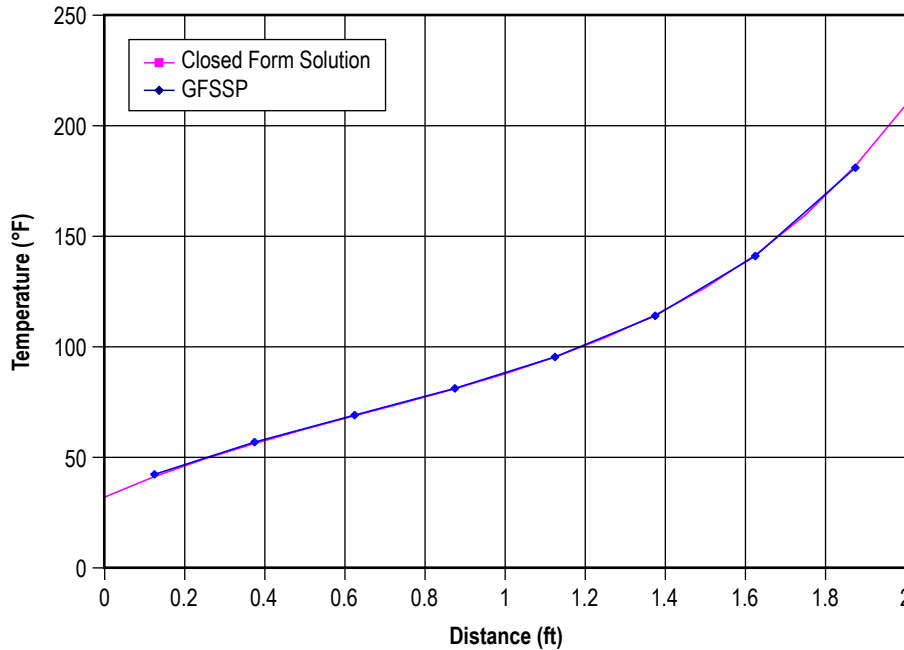
Figure 117. Comparison of GFSSP temperature prediction and closed-form solution.

5.12 Example 12—Simulation of Fluid Transient Following Sudden Valve Closure

5.12.1 Problem Considered

This example takes advantage of GFSSP's capability to model fluid transients. Fluid transients, also known as water hammer, can have a significant impact on the design and operation of both spacecraft and launch vehicle propulsion systems. These transients often occur at system activation and shut down, and they must be predicted accurately to ensure the structural integrity of the propulsion system fluid network.

Consider the system shown in figure 118. Liquid oxygen (LOX) at 500 psia and 200 °R flows through a 400-ft-long, 0.25-in inside diameter pipeline at a mass flow rate of 0.1 lbm/s. The corresponding downstream pressure is 450 psia. At time zero, a valve at the end of the pipe begins a 100-ms rapid closure. This example discusses how to predict the liquid's response to the sudden valve closure, including the maximum expected surge pressure in the line.

5.12.2 GFSSP Model

The GFSSP model of the propellant tank and pipeline schematic of figure 118 is shown in figure 119. The system is represented by seven nodes and six branches. Node 1 represents the propellant tank as a boundary node. Node 7 represents the downstream pressure as a boundary node. Nodes 2 to 6 are internal nodes where pressure, temperature, and density are calculated. Branches 12 to 56 represent 80-ft-long, 0.25-in-diameter pipe segments. Branch 67 represents the valve as a flow through a restriction with a flow area of 0.0491 in^2 and a flow coefficient of 0.6. In addition, GFSSP's unsteady valve open/close option is used to model the rapid valve closure in branch 67. The valve open/close characteristics are defined in the valve open/close dialog shown in figure 120. The valve open/close characteristic file is also shown below with annotations to explain the meanings of each value. GFSSP's restart option is used to set the initial conditions of the model. The model is run as a steady state model, and the solution is saved in files FNDEX12.DAT and FBREX12.DAT. This solution is then read in as the initial solution for the transient model run.

EX12VLV.DAT
```
 7 - Number of lines of data
 Time (sec)      Flow Area (in²)
 0.00            0.0491
 0.02            0.0164
 0.04            0.00545
 0.06            0.00182
 0.08            0.00061
 0.1             1.E-16
 100             1.E-16
```
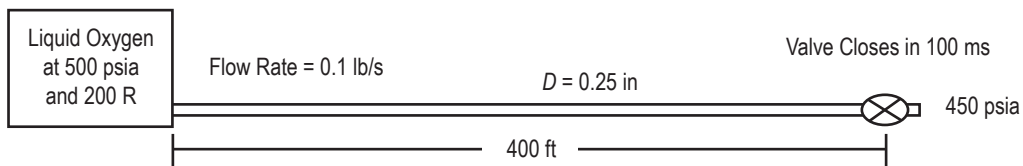

Figure 118. Schematic of a propellant tank, pipeline, and valve.
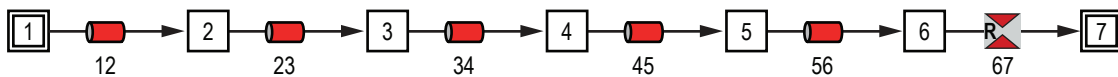

Figure 119. GFSSP model of a propellant tank, pipeline, and valve.
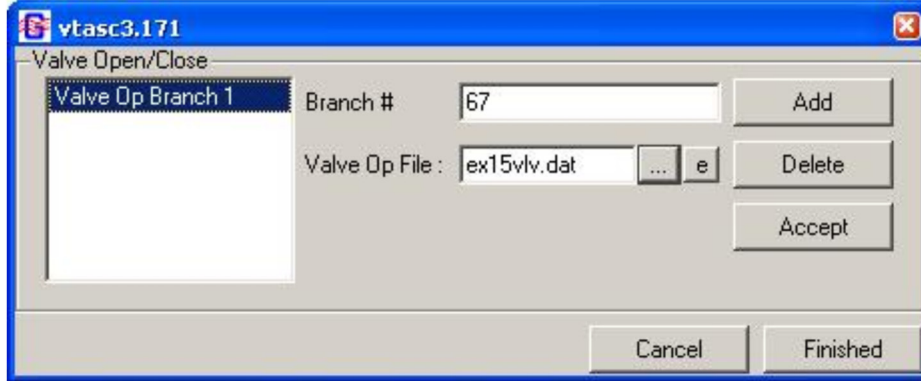
Figure 120. Example 15 Valve Open/Close dialog.

Some consideration should be given to the time step for this model. In order to properly model the fluid transient, a time step must be chosen that is small enough to accommodate the model discretization. This is done by calculating the Courant number, which is the period of oscillation of one branch divided by the time step (eq. (90)). For the model to properly capture the fluid transient phenomena, the Courant number should be greater than unity.

$$\text{Courant number} = \frac{4L_{\text{branch}}}{a_{\text{fluid}}\Delta\tau} \geq 1 \ . \tag{90}$$

The speed of sound (a_{fluid}) for LOX is 2,462 ft/s. Choosing a time step of 0.02 s gives a Courant number of 6.5, which satisfies the criteria for this model.

5.12.3 Results

The input and output files including history and restart files of example 15 have been attached in appendix O (see CD inside back cover). Figure 121 compares GFSSP's predicted pressure at node 6 with a Method of Characteristics (MOC) solution. Both solutions compare very well in the timing and character of the predicted pressure oscillations. The maximum surge pressure predicted by GFSSP is 624 psia compared to a MOC prediction of 636 psia. Additional studies have been performed using varying levels of discretization, different fluids, and even liquid-gas mixtures.[30]
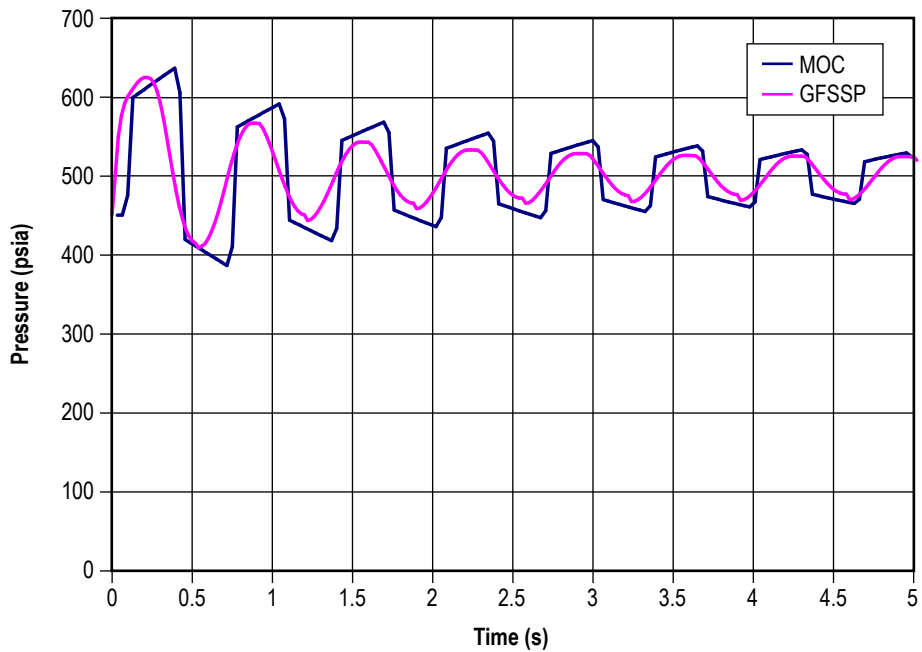
Figure 121. Comparison of GFSSP and MOC predicted pressure oscillations.

5.13 Publications

In addition to the examples described in this section, there are large numbers of GFSSP applications published in journals and presentations at conferences. A list of publications appears in appendix P (see CD inside back cover).

APPENDIX A—DERIVATION OF K_f FOR PIPE FLOW

It is assumed that there is a dynamic equilibrium that exists between the friction and the pressure forces. Therefore, the momentum conservation equation can be expressed as:

$$P_u - P_d = K_f \dot{m}^2 \ ,$$
(91)

where K_f is a function of f, L, D, and r.

For a fully developed pipe flow, the momentum conservation equation can be written as:

$$\tau \ \pi \ DL = \left(P_u - P_d\right)\frac{\pi D^2}{4} \ .$$
(92)

The Darcy friction factor, f, can be expressed as:

$$f = \frac{8 \ \tau \ g_c}{\rho u^2} \ .$$
(93)

From the continuity equation,

$$u = \frac{4\dot{m}}{\rho \ \pi \ D^2} \ .$$
(94)

Substituting equations (93) and (94) into equation (92),

$$P_u - P_d = \frac{8 f L \dot{m}^2}{g_c \rho \pi^2 D^5} \ .$$
(95)

Therefore,

$$K_f = \frac{8 f L}{g_c \rho \pi^2 D^5} \ .$$
(96)

APPENDIX B—SUCCESSIVE SUBSTITUTION METHOD OF SOLVING COUPLED NONLINEAR SYSTEMS OF ALGEBRAIC EQUATIONS

The application of the successive substitution method involves the following steps:

(1) Develop the governing equations:

$$x_1 = f_1\left(x_1, x_2, x_3, \ldots, x_n\right)$$

$$x_2 = f_2\left(x_1, x_2, x_3, \ldots, x_n\right)$$

$$\ldots$$

$$x_n = f_n\left(x_1, x_2, x_3, \ldots, x_n\right) . \tag{97}$$

If there are n number of unknown variables, there are n number of equations.

(2) Guess a solution for the equations:

Guess $x_1^*, x_2^*, x_3^*, \ldots, x_n^*$ as an initial solution for the governing equations.

(3) Compute new values of $x_1, x_2, x_3, \ldots, x_n$ by substituting $x_1^*, x_2^*, x_3^*, \ldots, x_n^*$ in the right-hand side of equation (97).

(4) Under-relax the computed new value:

$x = (1 - \alpha)x + \alpha x$, where α is the under-relaxation parameter.

(5) Replace $x_1^*, x_2^*, x_3^*, \ldots, x_n^*$ with the computed value of $x_1, x_2, x_3, \ldots, x_n$ from step (4).

(6) Repeat steps (3)–(5) until convergence.

APPENDIX C—NEWTON-RAPHSON METHOD OF SOLVING COUPLED NONLINEAR SYSTEMS OF ALGEBRAIC EQUATIONS

The application of the Newton-Raphson method involves the following seven steps:

(1) Develop the governing equations. The equations are expressed in the following form:

$$f_1(x_1, x_2, x_3, ..., x_n) = 0$$

$$f_2(x_1, x_2, x_3, ..., x_n) = 0$$

$$...$$

$$f_n(x_1, x_2, x_3, ..., x_n) = 0 \ . \tag{98}$$

If there are n number of unknown variables, there are n number of equations.

(2) Guess a solution for the equations. Guess $x_1^*, x_2^*, x_3^*, ..., x_n^*$ as an initial solution for the governing equations.

(3) Calculate the residuals of each equation. When the guessed solutions are substituted into equation (98), the right-hand side of the equation is not zero. The nonzero value is the residual.

$$f_1(x_1^*, x_2^*, x_3^*, ..., x_n^*) = R_1$$

$$f_2(x_1^*, x_2^*, x_3^*, ..., x_n^*) = R_2$$

$$...$$

$$f_n(x_1^*, x_2^*, x_3^*, ..., x_n^*) = R_n \ . \tag{99}$$

The intent of the solution scheme is to correct $x_1^*, x_2^*, x_3^*, ..., x_n^*$ with a set of corrections $x_1', x_2', x_3', ..., x_n'$ such that $R_1, R_2, R_3, ..., R_n$ are zero.

(4) Develop a set of correction equations for all variables. First, construct the matrix of influence coefficients:

$$\frac{\partial f_1}{\partial x_1} \quad \frac{\partial f_1}{\partial x_2} \quad \frac{\partial f_1}{\partial x_3} \quad \cdots \quad \frac{\partial f_1}{\partial x_n}$$

$$\frac{\partial f_2}{\partial x_1} \quad \frac{\partial f_2}{\partial x_2} \quad \frac{\partial f_2}{\partial x_3} \quad \cdots \quad \frac{\partial f_2}{\partial x_n}$$

$$\cdots \quad \cdots \quad \cdots \quad \cdots \quad \cdots$$

$$\frac{\partial f_n}{\partial x_1} \quad \frac{\partial f_n}{\partial x_2} \quad \frac{\partial f_n}{\partial x_3} \quad \cdots \quad \frac{\partial f_n}{\partial x_n} \; . \tag{100}$$

Then, construct the set of simultaneous equations for corrections:

$$\begin{bmatrix} \dfrac{\partial f_1}{\partial x_1} & \dfrac{\partial f_1}{\partial x_2} & \dfrac{\partial f_1}{\partial x_3} & \cdots & \dfrac{\partial f_1}{\partial x_n} \\[2mm] \dfrac{\partial f_2}{\partial x_1} & \dfrac{\partial f_2}{\partial x_2} & \dfrac{\partial f_2}{\partial x_3} & \cdots & \dfrac{\partial f_2}{\partial x_n} \\[2mm] \cdots & \cdots & \cdots & \cdots & \cdots \\[2mm] \dfrac{\partial f_n}{\partial x_1} & \dfrac{\partial f_n}{\partial x_2} & \dfrac{\partial f_n}{\partial x_3} & \cdots & \dfrac{\partial f_n}{\partial x_n} \end{bmatrix} \begin{bmatrix} x_1' \\ x_2' \\ \\ x_n' \end{bmatrix} = \begin{bmatrix} R_1 \\ R_2 \\ \\ R_n \end{bmatrix} . \tag{101}$$

(5) Solve for $x_1', x_2', x_3', \ldots, x_n'$ by solving the simultaneous equations.

(6) Apply correction to each variable.

(7) Iterate until the corrections become very small.

REFERENCES

1. Majumdar; A.K.; Bailey, J.W.; Schallhorn, P.A.; and Steadman, T.E.: Generalized Fluid System Simulation Program, U.S. Patent No. 6,748,349, June 8, 2004.

2. Streeter, V.L.: *Fluid Mechanics*, 3rd ed., McGraw-Hill, 1962.

3. Stoecker, W.F.: *Design of Thermal Systems*, 3rd ed., McGraw-Hill, 1989.

4. Owen, J.W.: "Thermal Analysis Workbook," *NASA TM–103568*, Marshall Space Flight Center, AL, January 1992.

5. SINDA/G Thermal Analyzer, Network Analysis Inc., <http://www.sinda.com>, accessed January 2001.

6. SINDA/FLUINT, Heat Transfer and Fluid Flow Design and Analysis Software, C&R Technologies, <http://www.crtech.com/sinda.html>, accessed January 2001.

7. Seymore, D.C.: ROCETS Users Manual, Internal Report, NASA Marshall Space Flight Center, AL, October 1999.

8. Broyden, C.G.: "A Class of Methods for Solving Nonlinear Simultaneous Equations," *Mathematics of Computation*, Vol. 19, No. 92, pp. 577–593, October 1965.

9. Patankar, S.V.: *Numerical Heat Transfer and Fluid Flow*, Hemisphere Publishing Corp., Washington, DC, 1980.

10. Hendricks, R.C.; Baron, A.K.; and Peller, I.C.: "GASP—A Computer Code for Calculating the Thermodynamic and Transport Properties for Ten Fluids: Parahydrogen, Helium, Neon, Methane, Nitrogen, Carbon Monoxide, Oxygen, Fluorine, Argon, and Carbon Dioxide," *NASA TN D-7808*, February 1975.

11. Hendricks, R.C.; Peller, I.C.; and Baron, A.K., "WASP - A Flexible Fortran IV Computer Code for Calculating Water and Steam Properties," *NASA TN D-7391*, Glenn Research Center, OH, November 1973.

12. Cryodata, Inc., *User's Guide to GASPAK*, Version 3.20, November 1994.

13. Winplot Version 4.54 User's Manual, NASA Marshall Space Flight Center, AL, July 16, 2008.

14. Holman, J.P.: *Heat Transfer*, 8th ed., McGraw Hill, 1997.

15. Miropolskii, Z.L.: "Heat Transfer in Film Boiling of a Steam-Water Mixture in Steam Generating Tubes," *Teploenergetika*, Vol. 10, No. 5, pp. 49–52, 1963 (in Russian; translation Atomic Energy Commission, AEC-Tr-6252, 1964).

16. Colebrook, C.F.: "Turbulent Flow in Pipes, with Particular Reference to the Transition Between the Smooth and Rough Pipe Laws," *J. Inst. Civil Eng.,* Vol. 11, pp. 133–156, 1938–1939.

17. White, F.W.: *Viscous Fluid Flow*, McGraw Hill, 1991.

18. Hooper, W.B.: "Calculate Head Loss Caused by Change in Pipe Size," *Chem. Engr.,* Vol. 95, No. 16, pp. 89–92, November 7, 1988.

19. Yamada, Y.: "Resistance to a Flow through an Annulus with an Inner Rotating Cylinder," *Bulletin of the Japan Society of Mechanical Engineers*, Vol. 5, pp. 302–310, 1962.

20. Ito, H.; and Nanbu, K.: "Flow in Rotating Straight Pipes of Circular Cross Section," *Transactions of ASME*, Vol. 93, Series D, No. 3, pp. 383–394, 1971.

21. Howell, G.W.; and Weather, T.M.: "Aerospace Fluid Component Designers Handbook," Vol. 1, Rev. D, TRW Systems Group, RPL-TDR-64-25, February 1970.

22. Hooper, W.B.: "The Two-K Method Predicts Head Losses in Pipe Fittings," *Chem. Engr.*, Vol. 24, pp. 97–100, August 24, 1981.

23. Lebar, J.F.; and Cady, E.C.: "Viscojet Testing at NASA Lewis Research Center CCL-7 Test Facility," Report No. A3-Y953-JFL-9G136, July 1990.

24. Kays, W.M.; and London, A.L.: *Compact Heat Exchangers*, 3rd ed., McGraw-Hill, New York, 1984.

25. Patankar, S.V.; and Spalding, D.B.: "A Calculation Procedure for Heat, Mass and Momentum Transfer in Three Dimensional Parabolic Flows," *Int. J. Heat Mass Transfer*, Vol. 15, pp. 1787–1806, 1972.

26. Hodge, B.K.: *Analysis and Design of Energy Systems*, 2nd ed., Prentice Hall, 1990.

27. Schallhorn, P.A.; and Majumdar, A.K.: "Numerical Prediction of Pressure Distribution Along the Front and Back Face of a Rotating Disc With and Without Blades," AIAA 97-3098, Presented at the 33rd Joint Propulsion Conference, Seattle, WA, July 6–9, 1997.

28. Schallhorn, P.A.; Elrod, D.A.; Goggin, D.G.; and Majumdar, A.K.: "A Novel Approach for Modeling Long Bearing Squeeze Film Damper Performance," Paper No. AIAA 98-3683, Presented at the 34th Joint Propulsion Conference, Cleveland, OH, July 13–15, 1998.

29. Moody, F.J.: *Introduction to Unsteady Thermofluid Mechanics*, John Wiley, 1990.

30. Majumdar, A.K.; and Flachbart, R.H.: "Numerical Modeling of Fluid Transients by a Finite Volume Procedure for Rocket Propulsion Systems," Paper No. FEDSM2003-45275, *Proceedings of ASME FEDSM'03*, 4th ASME/JSME Joint Fluids Engineering Conference, Honolulu, HI, July 6–10, 2003.

37. Majumdar, A.K.; and Van Hooser, K.: "A General Fluid System Simulation Program to Model Secondary Flows in Turbomachinery," Paper No. AIAA 95-2969, 31st AIAA/ASME/SAE/ASEE Joint Propulsion Conference and Exhibit, San Diego, CA, July 10–12, 1995.

38. Schallhorn, P.; Majumdar, A.; Van Hooser, K.; and Marsh, M.: "Flow Simulation in Secondary Flow Passages of a Rocket Engine Turbopump," Paper No. AIAA 98-3684, 34th AIAA/ASME/SAE/ASEE, Joint Propulsion Conference and Exhibit, Cleveland, OH, July 13–15, 1998.

39. Van Hooser, K.; Majumdar, A.; and Bailey, J.: "Numerical Prediction of Transient Axial Thrust and Internal Flows in a Rocket Engine Turbopump," Paper No. AIAA 99-2189, 35th AIAA/ASME/SAE/ASEE, Joint Propulsion Conference and Exhibit, Los Angeles, CA, June 21, 1999.

40. Reid, R.C.; Prausnitz, J.M.; and Poling, B.E.: *The Properties of Gases and Liquids*, 4th ed., McGraw Hill, 1987.

41. Epstein, M.; and Anderson, R.E.: "An Equation for the Prediction of Cryogenic Pressurant Requirements for Axisymmetric Propellant Tanks," *Adv. Cryog. Eng.*, Vol. 13, pp. 207–214, 1968.

42. Van Dresar, N.T.: "Prediction of Pressurant Mass Requirements for Axisymmetric Liquid Hydrogen Tanks," *J. Propul. Power*, Vol. 13, No. 6, pp. 796–799, 1997.

REPORT DOCUMENTATION PAGE

1. REPORT DATE (DD-MM-YYYY)	2. REPORT TYPE	3. DATES COVERED (From - To)
01–08–2011	Technical Memorandum	

4. TITLE AND SUBTITLE

Generalized Fluid System Simulation Program, Version 5.0—Educational

5a. CONTRACT NUMBER

5b. GRANT NUMBER

5c. PROGRAM ELEMENT NUMBER

6. AUTHOR(S)

A.K. Majumdar

5d. PROJECT NUMBER

5e. TASK NUMBER

5f. WORK UNIT NUMBER

7. PERFORMING ORGANIZATION NAME(S) AND ADDRESS(ES)

George C. Marshall Space Flight Center
Huntsville, AL 35812

8. PERFORMING ORGANIZATION REPORT NUMBER

M–1319

9. SPONSORING/MONITORING AGENCY NAME(S) AND ADDRESS(ES)

National Aeronautics and Space Administration
Washington, DC 20546–0001

10. SPONSORING/MONITOR'S ACRONYM(S)

NASA

11. SPONSORING/MONITORING REPORT NUMBER

NASA/TM—2011–216470

12. DISTRIBUTION/AVAILABILITY STATEMENT

Unclassified-Unlimited
Subject Category 34
Availability: NASA CASI (443–757–5802)

13. SUPPLEMENTARY NOTES

Prepared by the Propulsion Systems Department, Engineering Directorate
Supplemental information is available on CD through CASI

14. ABSTRACT

The Generalized Fluid System Simulation Program (GFSSP) is a finite-volume based general-purpose computer program for analyzing steady state and time-dependent flow rates, pressures, temperatures, and concentrations in a complex flow network. The program is capable of modeling real fluids with phase changes, compressibility, mixture thermodynamics, conjugate heat transfer between solid and fluid, fluid transients, pumps, compressors and external body forces such as gravity and centrifugal. The thermofluid system to be analyzed is discretized into nodes, branches, and conductors. The scalar properties such as pressure, temperature, and concentrations are calculated at nodes. Mass flow rates and heat transfer rates are computed in branches and conductors. The graphical user interface allows users to build their models using the 'point, drag and click' method; the users can also run their models and post-process the results in the same environment. The integrated fluid library supplies thermodynamic and thermo-physical properties of 36 fluids and 21 different resistance/source options are provided for modeling momentum sources or sinks in the branches. This Technical Memorandum illustrates the application and verification of the code through 12 demonstrated example problems.

15. SUBJECT TERMS

network flow, finite volume method, thermofluid system, two-phase, conjugate heat transfer

16. SECURITY CLASSIFICATION OF:			17. LIMITATION OF ABSTRACT	18. NUMBER OF PAGES	19a. NAME OF RESPONSIBLE PERSON
a. REPORT	b. ABSTRACT	c. THIS PAGE	UU	180	STI Help Desk at email: help@sti.nasa.gov
U	U	U			19b. TELEPHONE NUMBER (Include area code) STI Help Desk at: 443–757–5802

National Aeronautics and
Space Administration
IS20
George C. Marshall Space Flight Center
Huntsville, Alabama 35812